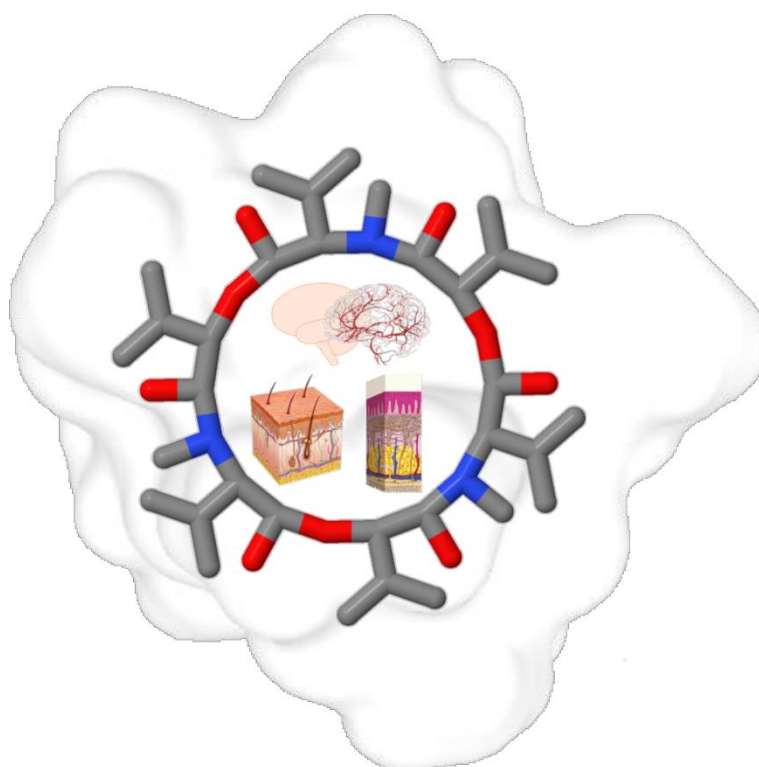


SKIN, MUCOSAL AND BLOOD-BRAIN BARRIER KINETICS OF MODEL CYCLIC DEPSIPEPTIDES: THE MYCOTOXINS BEAUVERICIN AND ENNIATINS



Thesis submitted to obtain the degree of Doctor in Pharmaceutical Sciences

Lien TAEVERNIER

Promoter
Prof. Dr. Bart DE SPIEGELEER

SKIN, MUCOSAL AND BLOOD-BRAIN BARRIER KINETICS OF MODEL CYCLIC DEPSIPEPTIDES: THE MYCOTOXINS BEAUVERICIN AND ENNIATINS

Lien TAEVERNIER

Master of Science in Drug Development

Promoter

Prof. Dr. Bart DE SPIEGELEER

2016

Thesis submitted to obtain the degree of
Doctor in Pharmaceutical Sciences

COPYRIGHT

The author and the promotor give the authorization to consult and to copy parts of this thesis for personal use only. Any other use is limited by the Laws of Copyright, especially the obligation to refer to the source whenever results from this thesis are cited.

Ghent, 9th of September 2016

The promotor

The author

Prof. Dr. Bart De Spiegeleer

Lien Taevernier

ACKNOWLEDGEMENTS

I never could have achieved this work on my own, therefore I wish to thank some very important people and address a few words to them. I consider myself fortunate to know you and I was honoured to be able to work together with you and learn a great deal from all of you.

First of all, a special thank you to my **promoter Prof. Dr. Bart De Spiegeleer**. I am grateful that you gave me the opportunity to pursue my Ph.D. at DruQuaR. Your door was always open for me, even if it did not consider work. I really appreciate your excellent guidance these last four years and I am proud to say that I have learned a lot from you and from your lifelong experience. Thank you for the trust you have put into me and for always challenging me to bring my work to the next level. Working at DruQuaR has definitely contributed to my personal development, it has conquered its special place and I will never forget it.

I also wish to thank the members of the **examination committee, Prof. Dr. Christophe Stove as chairman, Prof. Dr. Sarah De Saeger, Prof. Dr. Serge Van Calenbergh, Prof. Dr. Antoon Bronselaer and Prof. Dr. Jos Hoogmartens**, for critically reviewing this work. The interesting and dynamic discussions certainly improved the quality of this thesis.

I acknowledge **Ghent University**, the **Faculty of Pharmaceutical Sciences** and the **DruQuaR** lab for the use of their facilities and funding. I would also like to thank **Doctoral Schools** for the educational support. This research work could never have been established without the financial support and scientific interest of the **Special Research Fund** (BOF 01D23812) of Ghent University.

Furthermore, I would like to express my gratitude to the people that I worked with during **collaboration projects**. I'm grateful to **Prof. Dr. Stijn Vansteelandt** (Department Applied Mathematics, Computer Science and Statistics, Ghent University) for your help with the statistical analyses and interpretation of the adsorption results, **Prof. Dr. Catherine Delesalle, Prof. Dr. Christian Burvenich** (Department of Comparative Physiology and Biometrics, Ghent University) and **Dr. Kathelijne Peremans** (Department of Veterinary Medical Imaging and Small Animal Orthopaedics, Ghent University) for your scientific contributions and **Dr. Nathalie Roche** and **Evelien Vervaeet** (Department of Plastic and Reconstructive Surgery, UZ Ghent) for your commitment and excellent follow-up on human skin logistics. Also thank you to **Dr. Leen De Vreese** (Centre for Logic and Philosophy of Science, Ghent University) for your interesting philosophic input in our work about the mycotoxin definition. **Sven Detroyer** and **Antoon Daneels**, thank you for all your efforts and help

during your master thesis at DruQuaR. I am also grateful to **Laurent Dehennin** from **Porc Meat Zele NV** for the provision of the porcine buccal mucosa. Lastly, thank you **Prof. Dr. Ralf Hoffmann** and **Dr. Daniela Volke** (Centre for Biotechnology and Biomedicine, University of Leipzig) for providing the experimental framework for the MALDI-MS analyses.

I'm grateful to all my **former and present DruQuaR co-workers**: **Dr. Jente Boonen** for teaching me all about the Franz diffusion cell technique and **Dr. Matthias D'Hondt** for sharing your knowledge about chromatography and introducing me into the world of quality assurance. Thank you **Dr. Sofie Stalmans**, **Dr. Evelien Wynendaele**, **Lieselotte Veryser** and **Nathalie Bracke** for the interesting scientific discussions, for your contributions to many manuscripts, for your help during experiments and most importantly, thank you for being there for me in times of need. **Han Yao**, thank you for the nice atmosphere at our desk; when you return to China I hope to visit you there one day. **Kirsten Vandercruyssen**, **Mathieu Verbeken**, **Dr. Sultan Suleman**, **Bert Gevaert**, **Frederick Verbeke**, **Xiaolong Xu**, **Sileshi Belew Yohannes**, **Yorick Janssens** and **Anne Kosgei**, thank you all for your help and amazing workshop. I really enjoyed our scientific discussions, our laughs and joyful evening activities. With some of you I also had some memorable moments at scientific conferences that will always stick to me. Also our DruQuaR weekends were truly fantastic. I will miss all of you, but I hope this is not a final "goodbye".

Finally, I wish to thank all my **family & friends** for every now and then, puncturing my Ph.D. bubble and therefore providing the necessary distractions. The parties, dinners and trips were always so much fun! Thank you all for your kind words, support and interest, you are really the best! A very special thank you is in place for the four most important people in my life. **Mama, papa & Anja**, for the past 27 years you have been my biggest support. Thank you for everything you always do to help me achieve my goals. I love you. Last, but certainly not least, thank you **Jasper** ♡. Your patience is endless, your love and encouraging and comforting words really helped me get through this last year. I am so much looking forward to our future together. I love you.

Lien

LIST OF ABBREVIATIONS AND SYMBOLS

θ	Exposure time
15-ADON	15-Acetyldeoxynivalenol
3-ADON	3-Acetyldeoxynivalenol
A	Adenylation
A	Area
ABC	ATP binding cassette
ACAT	Acyl-CoA:cholesterol acyltransferase
ACP	Acyl carrier protein
ACN	Acetonitrile
AF	Aflatoxin
Ahp	Amino-hydroxy-piperidone
Ala	Alanine
Ama	Amino-methyl-acid
Am(o)ya	Amino-methyl-(oct)ynoic-acid
Amp	Amino-methoxy-piperidone
AOH	Alternariol
AT	Acyltransferase
AT	Averaging time
ATP	Adenosine triphosphate
BBB	Blood-brain barrier
BEA	Beauvericin
BEH	Ethylene bridged hybrid
BMD	Benchmark dose
BSA	Bovine serum albumin
BW	Body weight

C	Condensation
CART	Classification and regression tree
CB	Cytochalasin B
CD	Capillary depletion
CDP	Cyclic depsipeptide
CHAID	Chi-squared automatic interaction detector
CIT	Citrinin
Cl	Plasma clearance
CMDh	Coordination Group for Mutual Recognition and Decentralised Procedures – Human
CNS	Central nervous system
CONTAM	Contaminants in the Food Chain
CPG	Compliance Policy Guides
$C_{p,ss,buccal}$	Steady-state plasma concentration after buccal application
CSH	Charged surface hybrid
CSF	Cerebrospinal fluid
CT	Condensation-like
C_v	Concentration in vehicle
Cy	Heterocyclisation
Cys	Cysteine
Cyt c	Cytochrome c
D	Derringer desirability
DDE	Daily dermal exposure
DDE_{max}	Maximum daily dermal exposure
DH	Dehydration
DMA	Dimethylacetamide
Dmh(e/y)a	Dimethyl-hydroxy-(e/y)noic-acid
DMSO	Dimethylsulfoxide

DNA	Deoxyribonucleic acid
DON	Deoxynivalenol
DS	Dose solution
E	Epimerisation
ED	Exposure duration
EF	Exposure frequency
EFSA	European Food Safety Authority
EMA	European Medicines Agency
EMAN	European Mycotoxins Awareness Network
ENN	Enniatin
ESI	Electrospray ionisation
EtOH	Ethanol
EU	European Union
EV	Event frequency
F	Formylation
FA	Fatty acid
FA	Formic acid
FAO	Food and Agriculture Organization of the United Nations
FB1	Fumonisin B1
FDA	Food and Drug Administration
FDC	Franz diffusion cell
FID	Flame ionisation detector
FUS	Fusaproliferin
FUS-X	Fusarenon-X
GC	Gas chromatography
GLI	Gliotoxin
Gly	Glycine
H	Heterocyclisation

HCA	Hierarchical cluster analysis
HDAC	Histone deacetylase
HIV	Human immunodeficiency virus
HPBCD	Hydroxypropyl- β -cyclodextrin
Hppa	3-Hydroxy-3-phenylpropanoic acid
Ibu	Amino-dimethyl-oxo-acid
IC ₅₀	Inhibitory concentration, 50%
ICR-CD-1	Institute for Cancer Research, Caesarean derived-1
ICV	Intracerebroventricular
IFN- γ	Interferon-gamma
IPCS	International Programme on Chemical Safety
IPM	Isopropyl myristate
IS	Internal standard
J _{max}	Maximum flux
J _{ss}	Steady-state flux
K	Net brain clearance
K ₁	Unidirectional blood-to-brain clearance
k _{out}	Efflux rate constant
k _p	Permeability coefficient
k _{p,v}	Permeability coefficient in vehicle
k _{p,w}	Permeability coefficient in water
KR	Ketoreduction
KS	Ketosynthase
LD ₅₀	Lethal dose, 50%
LMP	Lysosomal membrane permeabilisation
LOAEL	Lowest observed adverse effect level
LoD	Limit of detection
LoQ	Limit of quantification

LPS	Lipopolysaccharide
M	Methylation
MALDI	Matrix-assisted laser desorption/ionisation
MeOH	Methanol
Mh(e/y)a	Methyl-hydroxy-(e/y)noic-acid
MLR	Multiple linear regression
MOMP	Mitochondrial outer membrane permeabilisation
MON	Moniliformin
MRM	Multiple reaction monitoring
MS	Mass spectrometry
MT	Mycotoxin
MTR	Multiple time regression
MTT	3-(4,5-dimethylthiazol-2-yl)-2,5-diphenyltetrazolium bromide
MW	Molecular weight
NCRI	Negligible cancer risk intake
NGF	Neural growth factor
NIV	Nivalenol
NO	Nitric oxide
NOAEL	No observed adverse effect level
NRPS	Nonribosomal peptide synthase
OTA	Ochratoxin A
Ox	Oxidation
PAT	Patulin
PBS	Phosphate buffered saline
PC	Principal component
PCA	Principal component analysis
PCP	Peptidyl carrier protein
Ph.Eur.	European Pharmacopoeia

PIL	Patient information leaflet
PKS	Polyketide synthase
PRAC	Pharmacovigilance Risk Assessment Committee
Q	Cumulative quantity (expressed as percentage of the effective dose applied)
QbD	Quality-by-design
QC	Quality control
RF	Response factor
ROS	Reactive oxygen species
RRF	Relative response factor
RSD	Relative standard deviation
S	Solubility
SA	Surface area
SC	Stratum corneum
S_v	Solubility in vehicle
S_w	Solubility in water
SEM	Standard error of the mean
SmPC	Summary of product characteristics
$T_{1/2}$	Half-life
TDI	Tolerable daily intake
TE	Thioesterase
TFA	Trifluoroacetic acid
t_{lag}	Lag time
TNF- α	Tumour necrosis factor-alpha
Tyr	Tyrosine
UHPLC	Ultra-high performance liquid chromatography
US	United States
USP	United States Pharmacopoeia
UV	Ultraviolet

V_0	Vascular brain distribution volume
V_g	Brain tissue distribution volume
ZEA	Zearalenone

TABLE OF CONTENTS

Chapter I: Introduction	19
1. Cyclic depsipeptides	21
2. Mycotoxins	23
3. Beauvericin and enniatins	27
4. Biological barriers in the human body	34
5. Study objectives	38
6. Thesis outline	39
7. References	42
Chapter II: Chemical classification of cyclic depsipeptides	55
1. Cyclic depsipeptides: a diverse family	57
2. Methods	60
3. Proposed classification	61
4. Discussion	74
5. Conclusions	78
6. References	79
Supplementary Information	86
Chapter III: The mycotoxin definition reconsidered towards fungal cyclic depsipeptides	103
1. The mycotoxin definition: current status	105
2. Philosophical approach to a 'definition'	109
3. Proposed mycotoxin definition	110
4. Application of definition on fungal cyclic depsipeptides	114
5. Conclusions	121
6. References	122
Supplementary Information	131

Chapter IV: UHPLC-MS/MS method for the determination of beauvericin and enniatins	145
1. The need for a quantitative, sensitive and selective high-throughput bioanalytical method	147
2. Materials and methods	149
3. Results and discussion	157
4. Conclusions	166
5. References	167
Chapter V: Human skin permeation of beauvericin and enniatins	171
1. Introduction	173
2. Materials and methods	175
3. Results	181
4. Discussion	187
5. Conclusions	192
6. References	193
Chapter VI: Blood-brain barrier transport kinetics of beauvericin and enniatins	201
1. Introduction	203
2. Materials	204
3. Methods	205
4. Results	211
5. Discussion	217
6. Conclusions	219
7. References	220
Chapter VII: QbD risk assessment of enniatin-containing solutions for oromucosal use	225
1. Influence of excipients	227
2. Materials and methods	229
3. Results and discussion	234
4. Conclusions	239
5. References	241

Broader international context, relevance and future perspectives	245
Summary and general conclusions	259
Samenvatting en algemene conclusies	265
Curriculum vitae	271

CHAPTER I

INTRODUCTION

“Heard melodies are sweet, but those unheard are sweeter.”

*John Keats
(°1795 - †1821, English poet)*

CHAPTER I

INTRODUCTION

1. CYCLIC DEPSIPEPTIDES

Peptides are becoming an increasingly important group within the current diversity of therapies and health products, which help to meet the current health care needs. The technological advances, making peptides accessible and affordable, as well as our more detailed understanding of their biological roles, have made them fulfil their interest and made them available for use as diagnostic and therapeutic products. Currently, several hundred peptides are already authorised or are undergoing preclinical and clinical development [1].

A subcategory of peptides are the so-called ‘cyclic depsipeptides’ (CDPs) (also known as ‘cyclodepsipeptides’ or ‘peptolides’), a term first introduced in scientific literature in mid-1960s [2,3]. It is used to describe cyclic peptide-related compounds of which the ring is mainly composed of amino- and hydroxy-acid residues joined by amide and ester bonds (at least one is required to refer to a depsipeptide), which are commonly, but not necessarily, regularly alternating [3-5].

Reports on the isolation of these compounds started as early as the 1940s, *i.e.* with the isolation of enniatin A from the fungus *Fusarium orthoceras* var. *enniatinum* [6]; however, it took decades before scientists began to unravel their biosynthesis [7,8], which still today is an active research field [9-15]. Inspection of the structures of diverse CDP members illustrates that many of these compounds are not only synthesized by non-ribosomal peptide synthases (NRPS) [16-18], but actually are hybrids formed by both NRPS and polyketide synthases (PKS), due to similarities in their modular organization and biosynthetic processes [11,19-22] or fatty acid (FA) synthase enzyme systems. The latter, however, is currently under debate, as Ishidoh and colleagues surprisingly demonstrated that for the cyclic lipodepsipeptide verlamelin, there are no genes coding for fatty acid synthase or even polyketide synthase, suggesting that the hydroxytetradecanoic acid moiety of the CDP is supplied via the primary fatty acid metabolism and then loaded onto the NRPS [13].

In both enzyme systems, a so-called thiol template mechanism is followed to catalyse stepwise condensation in a modularly organized way, where each module is responsible for the incorporation of a specific monomer. Both enzyme systems are thus generally described as having a modular organisation, although it was recently revealed by Wang *et al.* that they can have nonmodular compositions as well [23]. The amino acid and carboxylic acid precursors are selected and attached as thioesters to the long phosphopantetheinyl arms of carrier proteins, *i.e.* ACP (acyl carrier protein)

in the case of PKS and PCP (peptidyl carrier protein) in the case of NRPS. In a following step, linkage occurs between the monomer bound to the downstream ACP/PCP domain and the activated thioester of the upstream ACP/PCP domain bound intermediate, via a peptide bond by the condensation (C) domains or through a C–C bond by ketosynthase (KS) domains in respectively NRPS and PKS. This is schematically presented in Figure 1.

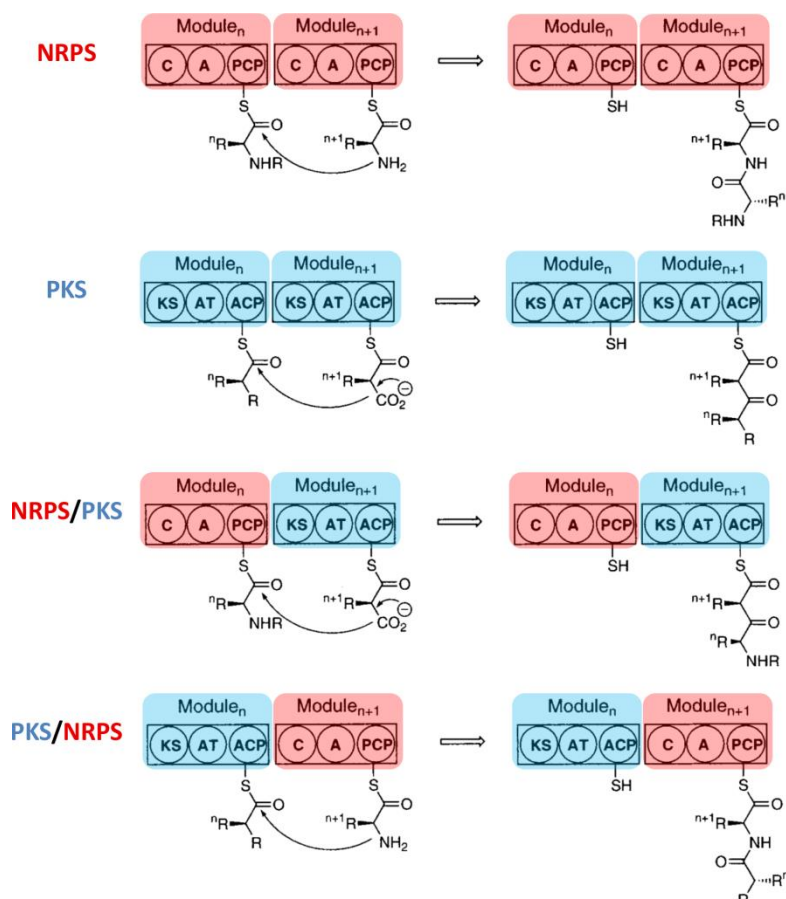


Figure 1: Modular organization of NRPS, PKS and hybrid NRPS-PKS systems, showing the C-N and C-C bond formation between two hypothetical modules. A = adenylation; ACP = acyl carrier protein; AT = acyltransferase; C = condensation; KS = ketosynthase; NRPS = non-ribosomal peptide synthase; PCP = peptidyl carrier protein; PKS = polyketide synthase (adapted from Du *et al.* [20]).

Subsequent modifications by additional secondary domains can also be involved in synthesis, *e.g.* epimerisation (E), heterocyclisation (Cy), oxidation (Ox), methylation (M), ketoreduction (KR), dehydration (DH) and formylation (F), contributing to the immense structural diversity characterising CDPs. Finally, the mature chain is released via cyclization or hydrolysis by a thioesterase (TE) domain, or in the case of fungi a condensation-like (CT) domain, in the terminal modules of the assembly line [16,19-21,23-35]. Hybrid NRPS-PKS systems can combine these PKS and NRPS in two different ways, namely in a non-iterative and iterative manner. The former is predominantly found in bacteria and places different PKS modules and NRPS modules together in a production line, whereas the latter

uses a single PKS module followed by a single NRPS module and is mainly found in fungi. However, complete understanding of CDP biosynthesis and full agreement between researchers working in the field still has a long way to go, especially since only a few enzymes are currently linked to their biosynthetic products and programming of these enzymes is still poorly understood [21].

Considering these natural assembly lines, it is thus not unexpected that different CDPs vary in *i.a.* number and nature of monomeric building blocks, molecular mass, lipophilicity, polarity, side chains and ring size, creating thus a chemically extremely diverse family. As a consequence, these compounds also exert a broad range of biological activities including antitumor, anti-inflammatory, anthelmintic, insecticidal, antibiotic, antifungal, antimalarial and immunosuppressant activities. Due to these unique structural and biological properties, CDPs have emerged as promising drugs and lead structures or are feared as mycotoxins [21,29]. To date, a significant number of original research papers has already been published, presenting the identification and structure elucidation of newfound CDPs, sometimes complemented with some biological activity data. Upon their discovery, these compounds are named very arbitrarily, *e.g.* after the geographic location where they were first found, after the producing organism they were first isolated from or referring to a particular aspect of their chemical structure.

2. MYCOTOXINS

The harmful effect of moulds and fungi have been known to mankind already from ancient times [36]. Famous were the epidemic ergotism outbreaks (“St. Anthony's fire”) during the Middle Ages, caused by eating rye bread contaminated with ergot alkaloids from the fungus *Claviceps purpurea* and clinically characterised by mutilating gangrene, neurological disorders and eventually death [36,37]. However, it was not until the mid-1950s before the terms ‘mycotoxin’ (MT) and ‘mycotoxicosis’, both combinations of the Greek word ‘mykes’ meaning fungus and the Latin word for poison ‘toxicum’, were first introduced. During this time, it was discovered that aflatoxins, which are secondary metabolites from the fungus *Aspergillus*, had caused the death of more than 100,000 turkeys in the England’s poultry industry [38-40]. From then on, scientific research on mycotoxins grew tremendously (Figure 2).

Today, it is widely recognised that dietary, respiratory and dermal exposures to these toxic fungal metabolites can produce diseases collectively called mycotoxicoses. The symptoms and severity of such a mycotoxicosis depend on the age, sex, health and nutritional status of the individual, many poorly understood synergistic effects involving genetics, dietary status and interactions with other chemicals to which the individual is exposed and the toxicity and extent of exposure of the mycotoxin [36,41,42].

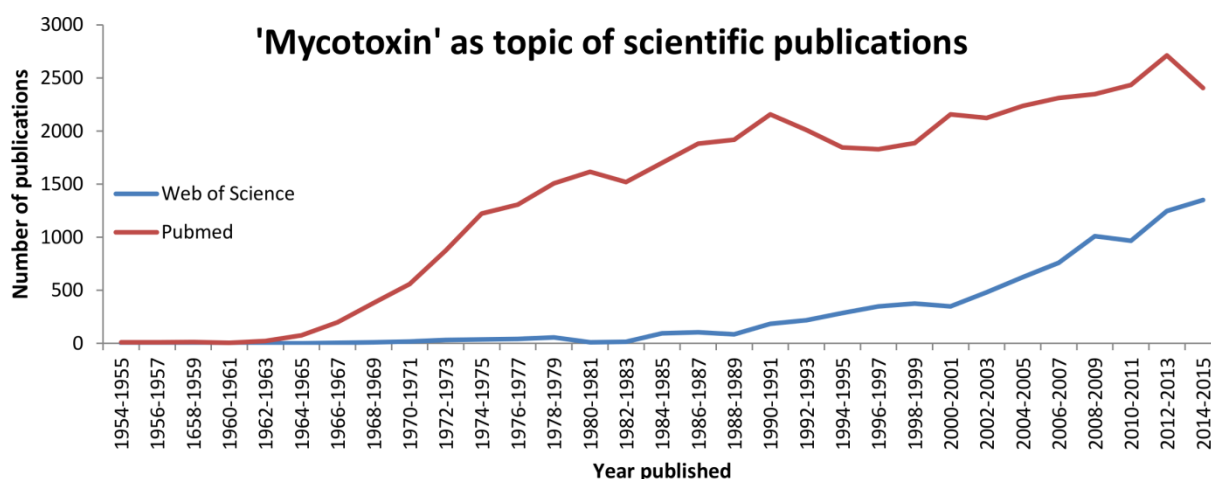


Figure 2: 'Mycotoxin' as topic of scientific publications (consulted on February 25th, 2016).

The chemical structures of mycotoxins vary considerably, some of which are simple, such as patulin, while others are rather complex, *e.g.* penitrem [43]. Moreover, some were initially considered to be beneficial as antibiotics (*e.g.* citrinin); however, were subsequently found to be too toxic for therapeutic use [36,44].

Mycotoxin-producing fungi (*e.g. Fusarium, Aspergillus* and *Penicillium*) can grow on a wide range of substrates and under a wide range of environmental conditions, making infestation very common and ultimately resulting in worldwide mycotoxin occurrence [45-47]. For example, a Dutch study demonstrated that 50% of a total of 11 768 animal feed samples, collected over a period from 2001 to 2009 in the Netherlands, was found to be positive for at least one of the eight major mycotoxins investigated [48]. Moreover, in another study, 72% of a total of 17,316 samples of feed and feed raw materials from all over the world, collected during an 8-year period (2004 – 2011), tested positive for at least one of the five major mycotoxins investigated [49]. Animal and human health are not only exposed to these hazards through contaminated feed and foodstuff, but also through the use of herbal medicinal plant products as well [50-53]. Therefore, in order to protect consumers, several national and international organisations have set up guidelines concerning *i.a.* prevention, reduction, sampling and analysis of mycotoxins. Moreover, regulatory authorities have established legislative regulations [41]. An overview of these regulations is given in Table 1.

The most investigated and regulated mycotoxins, or otherwise called 'major' mycotoxins, are the aflatoxins produced by *Aspergillus*, patulin isolated from *Penicillium* and ochratoxin A synthesised by both *Aspergillus* and *Penicillium* fungi, *Claviceps* ergot alkaloids, the *Fusarium* mycotoxins fumonisins, zearalenone and the trichothecenes deoxynivalenol, T-2 and HT-2 toxin [41,54,55]. However, besides these 'traditional' mycotoxins, *Fusarium* species are also able to produce other 'emerging' mycotoxins, such as beauvericin and enniatins, which only recently became of interest but for which worldwide no legal maximum levels have yet been set [56,57].

Overall, it is stated that over 400 compounds are recognized as mycotoxins [41,55,58-63] although only a few of these have been thoroughly investigated for their potential toxic effects [64,61] and have been addressed by legislation (Table 1) [60]. Moreover, it has been suggested that thousands of these potentially toxic fungal metabolites exist [54,58,65-67]. However, according to Miller and McMullin, on many occasions it seems that nearly any fungal secondary metabolite is casually, but incorrectly referred to as a mycotoxin [68]. It has indeed been recognized that mycotoxins are hard to define [41].

Table 1: Mycotoxin legislation in Europe and the US.

Food/Feed	Europe: European Commission	United States: FDA^{(5),(6),(7)}
<u>Food</u>		<u>Food & Feed</u>
Legislation	<ul style="list-style-type: none"> ▪ 178/2002: general principles + requirements feed/food law ▪ 882/2004: official controls of compliance with feed/food law ▪ 1754/2006: granting financial assistance to laboratories ▪ 96/23: monitor certain substances and residues ▪ 2002/657: analytical methods and interpretation of results ▪ 315/93: procedures for contaminants in food ▪ 401/2006: sampling and analysis methods for official control of mycotoxins ▪ 2008/128: purity criteria colours for use in foodstuffs ▪ 1272/2009: buying-in and selling of agricultural products (1234/2007) ▪ 1152/2009: import of certain foodstuffs from certain third countries due to contamination risk by aflatoxins ▪ 2008/47: pre-export checks carried out by the United States of America on peanuts and derived products thereof as regards the presence of aflatoxins 	<p>FDA has not yet established regulatory limits for mycotoxins in food or feed.</p> <p><i>Action levels (regulatory actions can be taken):</i></p> <ul style="list-style-type: none"> ▪ Aflatoxin B1: 20 – 300 ppb ▪ Aflatoxin M1: 0.5 ppb ▪ Patulin: 50 ppb <p><i>Advisory levels (guidance levels, adequate margin of safety):</i></p> <ul style="list-style-type: none"> ▪ Deoxynivalenol: 1 – 30 ppm ▪ Fumonisin B1, B2, B3: 2-100 ppm
MTs + limits	<p>1881/2006: maximum levels for contaminants in foodstuffs⁽²⁾:</p> <ul style="list-style-type: none"> ▪ Aflatoxin B1: 0.10 – 12.0 µg/kg ▪ Aflatoxins B1, B2, G1, G2: 4.0 – 15.0 µg/kg ▪ Aflatoxin M1: 0.025 – 0.050 µg/kg ▪ Ochratoxin A: 0.50 – 80 µg/kg ▪ Patulin: 10.0 – 50 µg/kg ▪ Deoxynivalenol: 200 – 1750 µg/kg ▪ Zearalenone: 20 – 400 µg/kg ▪ Fumonisin B1, B2: 200 – 4000 µg/kg ▪ Citrinin: 2000 µg/kg ▪ T-2 and HT-2 toxin⁽¹⁾: 15 – 2000 µg/kg ▪ Ergot alkaloids⁽⁴⁾: 1000 mg/kg 	
<u>Feed</u>		
Legislation	178/2002, 882/2004, 1754/2006, 1272/2009, 2008/47 (identical to food law)	
MTs + limits	<p>2002/32: undesirable substances in animal feed⁽²⁾:</p> <ul style="list-style-type: none"> ▪ Aflatoxin B1: 0.005 – 0.02 ppm ▪ Ochratoxin A⁽³⁾: 0.01 – 0.25 mg/kg ▪ Deoxynivalenol⁽³⁾: 0.9 – 12 mg/kg ▪ Zearalenone⁽³⁾: 0.1 – 3 mg/kg ▪ Fumonisin B1, B2⁽³⁾: 5 – 60 mg/kg ▪ T-2 and HT-2 toxin^{(1),(3)}: 0.015 – 2 mg/kg ▪ Ergot alkaloids⁽⁴⁾: 1000 mg/kg 	
Medicines	Europe: Ph.Eur.	United States: USP
Conditions	General monographs on herbal drugs: 2.8.18 and 2.8.22:	General monograph on articles of botanical origin: <561>:
MTs + limits	<ul style="list-style-type: none"> ▪ Routine testing not required: only herbal drugs that are subject to contamination ▪ Appropriate risk assessment ▪ Aflatoxin B1: ≤ 2 ppb ▪ Sum of aflatoxins B1, B2, G1 and G2: ≤ 4 ppb (if required by competent authority) ▪ Ochratoxin A: limits in specific monographs 	<ul style="list-style-type: none"> ▪ Extent of testing considers the likelihood of contamination ▪ Risk-based approach ▪ Aflatoxin B1: ≤ 5 ppb ▪ Sum of aflatoxins B1, B2, G1 and G2: ≤ 20 ppb

(1) Recommended indication levels only: 2013/165 on the presence of T-2 and HT-2 toxin in cereals and cereal products [69].

(2) The limit range is given here, individual limits depend on the type of food/feedstuff [70].

(3) Recommended indication levels only: 2006/576: on the presence of other mycotoxins in products intended for animal feed [71].

(4) Recommended indication levels only: 2012/154: on the presence of ergot alkaloids in feed and food [72].

(5) FDA Regulatory Guidance for Mycotoxins [73].

(6) CPG Sec.510.150 Apple juice, apple juice concentrates, and apple juice products - adulteration with patulin [74].

(7) CPG Sec. 683.100 Action levels for aflatoxins in animal feeds [75].

3. BEAUVERICIN AND ENNIATINS

Beauvericin (BEA) and enniatins (ENNs) are secondary metabolites mainly produced by *Fusarium* species [56]. Other fungal genera known to synthesise enniatins are *Alternaria*, *Halosarpheia* and *Verticillium* [76,77], while beauvericin was isolated from *Paecilomyces*, *Isaria* and *Beauveria* as well [78,79].

These lipophilic mycotoxins consist of three D- α -hydroxyisovaleric acid residues and three N-methylated amino acid units, alternatingly linked with peptide and ester bonds to form a cyclic hexadepsipeptide. In BEA, the amino acids are aromatic phenylalanines, whereas for the ENNs discussed in this thesis (ENNs A, A1, B, B1, C, D, E and F), it concerns aliphatic valines and/or (iso)leucines (Figure 3) [56].

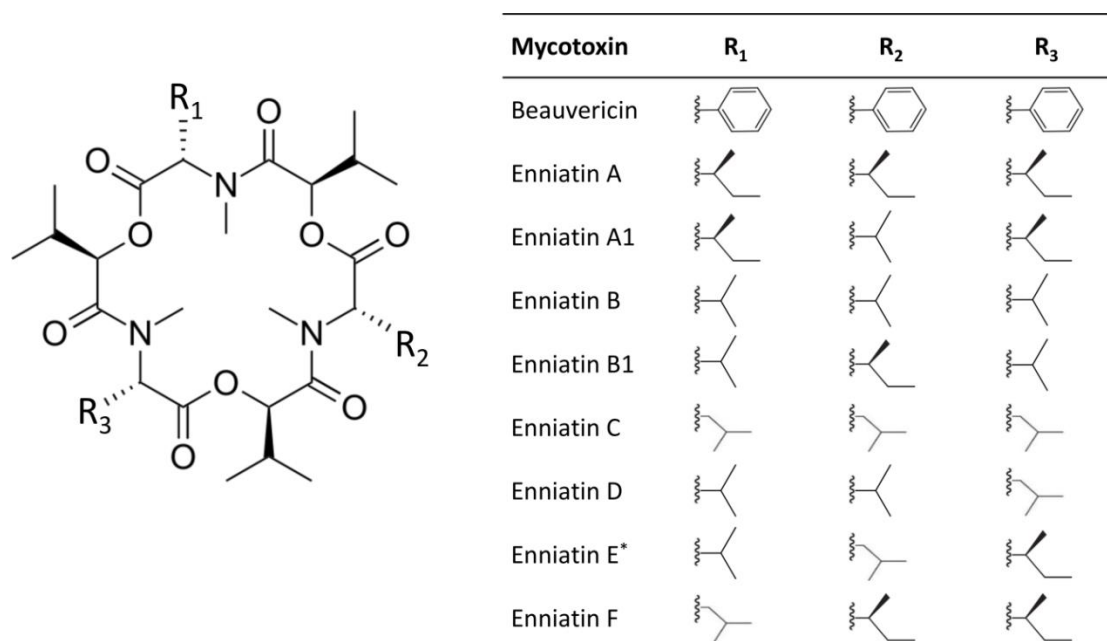


Figure 3: Chemical structures of BEA and ENNs A, A1, B, B1, C, D, E and F. * For ENN E two homologues were described, *i.e.* E1 and E2, for which R₂ and R₃ are switched (adapted from Sy-Cordero *et al.* [77]).

Many different useful biological activities have been ascribed to these cyclic hexadepsipeptides, *e.g.* antimicrobial, antiviral and insecticidal properties [56,77,80].

Tomoda *et al.* also suggested that, especially BEA and to a lesser extent ENNs are able to inhibit acyl-CoA:cholesterol acyltransferase (ACAT), by demonstrating their inhibitory activity *in vitro* in rodent enzyme and cell based assays [81]. ACAT is a membrane-bound enzyme that plays an important role in cellular cholesterol homeostasis [82] and is therefore a popular drug target in diseases like atherosclerosis [83] and hypercholesterolemia, but also in Alzheimer's disease [84-86] and even cancer [87]. In 1991, a patent was issued for a 5 mg BEA tablet to lower blood cholesterol levels [56,88].

Their cytotoxicity, with activities in the low micromolar range, was demonstrated *in vitro* in various cell lines, *e.g.* human colorectal (Caco-2, HCT-15 and HT-29), cervical (HeLa), breast (BC-1 and MCF-7), liver (Hep-G2), lung (A549, NCI-H460 and MRC-5), pancreatic (MIA Pa Ca-2), ovarian (SK-OV-3), glioma (SF-268) and skin (SK-MEL-2) cancer cells [56,76,89-97]. As a consequence, ENNs have been put forward as useful chemotherapeutics since they exert prominent cytostatic/cytotoxic effects against diverse malignant cells, whereas normal cells showed comparable insensitivity [91].

It was also demonstrated *in vitro* that BEA and ENNs are able to interact with different ABC (ATP binding cassette) transport proteins, which are a large family of ATP driven transmembrane proteins. Under normal physiological conditions, these act as efflux pumps of multiple xenobiotics at defined organ sites, such as the intestinal epithelial barrier and cerebral micro-vascular endothelial blood-brain barrier, whereas in certain cancer tissues, they are hyperactivated, leading to the efflux of chemotherapeutics and consequently therapy failure [98-102]. Overexpression of ABCG2 (breast cancer resistance protein) and ABCB1 (P-glycoprotein) showed a weak but significant reduction in BEA and/or ENN cytotoxicity, suggesting their interference with these cell membrane proteins, resulting in the prevention of these CDP mycotoxins to reach other cellular targets [98]. Moreover, these cyclic depsipeptides were also found to be potent inhibitors of ABCB1- and ABCG2-mediated efflux transport of substrates [98,103]. While these efflux inhibiting properties might be of interest in altering pharmacokinetics and bioavailability of certain drugs as it can improve their efficacy [104,105], they can have toxic consequences as well, *i.e.* since possible unwanted interactions with detoxification processes of *e.g.* drugs or other mycotoxins might occur. This is especially important as these inhibitory effects already occur at low concentrations, which are likely to be reached through continuous exposure via food intake and tissue accumulation [98,106,107].

On the other hand, ENNs and BEA have also evoked the interest of toxicologists, because of their potential harmful, undesirable properties. Recently, it was demonstrated *in vitro* in PK15 porcine kidney epithelial cells and human leukocytes and lymphocytes that BEA is potentially genotoxic [89,108,109], causing *i.a.* an increase in chromosomal aberrations, albeit the Ames test performed by Fotso and Smith was negative [110]. For ENN B, no significant mutagenic nor genotoxic potential could be demonstrated in the Ames, comet and micronucleus assay performed by Behm *et al.* [111]. Because of these conflicting results it cannot be excluded that prolonged exposure to these cyclic depsipeptide mycotoxins may contribute to carcinogenicity in humans.

In contrast to their earlier mentioned anticancer potential, Dornetshuber *et al.* also suggested that short-term exposure to low submicromolar concentrations of ENNs (which can be reached via food intake) might have tumour-promoting functions [91].

Moreover, an *in vitro* study on human dendritic cells and macrophages indicated immunological disorders could also occur after exposure to these mycotoxins [112].

Furthermore, Tonshin and colleagues demonstrated that both BEA and ENNs can cause mitochondrial dysfunction, an effect strongly connected with their potassium (K^+) ionophoric activity [113]. Presently, it is generally assumed that the primary toxic action of these cyclic depsipeptide mycotoxins is related to their ionophoric properties, allowing transport of cations across biological membranes, either by carrier sandwich complexes or pore forming channels [114-116]. Ionophores transport cations down their electrochemical gradient from one side of the membrane to the other side, diffusing across the bilayer, and thus act to collapse the gradients between cellular compartments, such as the plasma membrane, the sarcoplasmic/endoplasmic reticulum or mitochondria [117,118]. Exposure to enniatins thus caused an efflux of K^+ from the cytoplasm, decreasing the cytoplasmic $[K^+]$ [113]. It was also indicated that ENNs and BEA increase intracellular Ca^{2+} , which may play an important role in cell death signalling [113,116,119]. These disturbances of physiological ion balance and pH homeostasis lead to a combination of complex molecular responses, ultimately resulting in cell death. The induction of this cell death is believed to be both of apoptotic and necrotic nature [119]. Oxidative stress and DNA interactions play only a minor role [98], but with important involvement of mitochondrial dysfunction, which is suggested to be a more downstream event, following lysosomal membrane permeabilisation. However, for this lysosome-to-mitochondria flow, no direct evidence is available up till now [120]. Figure 4 gives a schematic overview of the different mechanisms that are currently believed to be involved in the toxic action of beauvericin and enniatins [113,114-120].

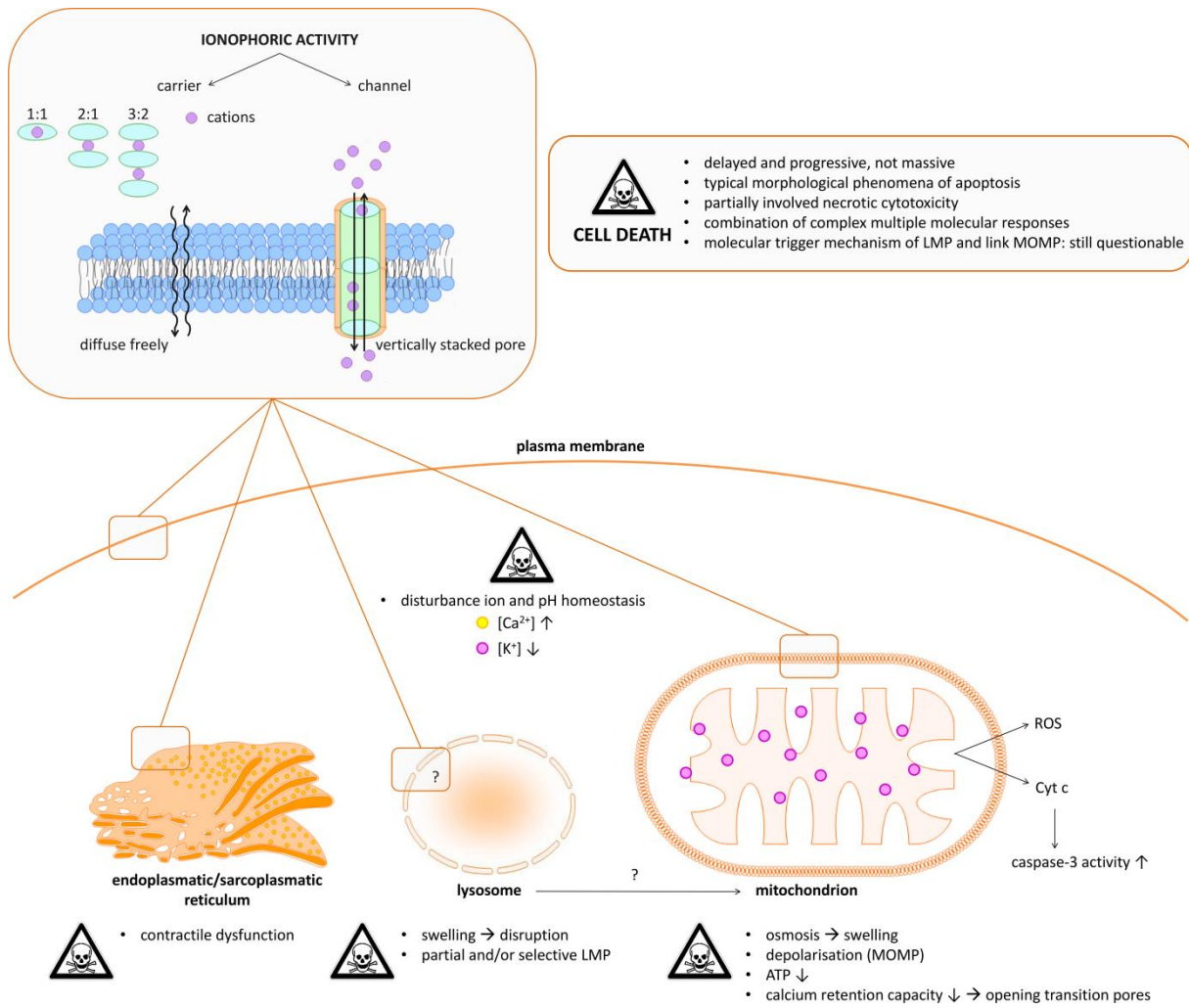


Figure 4: Schematic overview of the different mechanisms currently believed to be involved in BEA and ENNs toxicity. ATP = adenosine triphosphate; Cyt c = cytochrome c; LMP = lysosomal membrane permeabilisation; MOMP = mitochondrial outer membrane permeabilisation; ROS = reactive oxygen species.

Exposure to these emerging mycotoxins should thus not be considered trivial, seen their possible biological effects and as they were indeed found to be common contaminants in food and feed [56,121]. As an illustration, some of the most recent reported feed/food contamination data are given in Table 2.

Table 2: Examples of recent BEA and ENNs feed/food contamination data.

MT	Feed/food product	Positive samples (%)	Concentration range ($\mu\text{g}/\text{kg}$) ⁽¹⁾	Year	Origin	Reference	
BEA	Barley malt	10	48.2	2012	Germany	Habler and Rychlik [122]	
		10	7.08	2013			
		20	4.63 – 6.09	2014			
	Coffee	40	0.10 – 1.34	2013/2014	Spain	García-Moraleja <i>et al.</i> [123]	
		100	32.2	2009			Italy
	Durum wheat	100	0.6	2010			
	Farmed fish feed	95	0.1 – 6.6	n.m.	Spain	Tolosa <i>et al.</i> [125]	
	Pasta	18	0.10 – 20.96	2011	Spain	Serrano <i>et al.</i> [126]	
	Tiger-nuts	10	51600 – 228500	n.m.	Spain	Sebastià <i>et al.</i> [127]	
	Maize	96	12	2005/2006	Brazil	de Lourdes Mendes de Souza <i>et al.</i> [128]	
	Poultry feed	92	3.6				
	Factory residue	100	116				
	Barley	100	0.4	2011	Norway	Uhlig <i>et al.</i> [129]	
	Oats	100	3.5				
	Wheat	100	0.4				
	Oat	57	7.2 – 41	n.m.	Italy	Juan <i>et al.</i> [130]	
	Wheat	9	9.6 – 35				
	Barley	11	0.81				
	Rye	45	8.9 – 16.5				
	Hazelnuts shell	n.m.	30	n.m.	Spain	Tolosa <i>et al.</i> [131]	
	Dates	n.m.	6				
	General feed	98	6.7	2010/2012	Worldwide	Streit <i>et al.</i> [49]	
	ENN B	Barley malt	100	7.50 – 60200	2012	Germany	Habler and Rychlik [122]
80			3.19 – 1160	2013			
100			11.3 – 2070	2014			
Coffee		70	59.15 – 3569.92	2013/2014	Spain	García-Moraleja <i>et al.</i> [123]	
		100	290.22 – 659.27				
Durum wheat		60	2.74	2009	Italy	Covarelli <i>et al.</i> [124]	
		100	9.15	2010			
Soft wheat		100	9.08	2009			
		100	6.7	2010			
Fish (muscle)		65	1.3 – 44.6	n.m.	Spain	Tolosa <i>et al.</i> [125]	
Pasta		80	0.50 – 122.13	2011	Spain	Serrano <i>et al.</i> [126]	
Tiger-nuts		2	44800	n.m.	Spain	Sebastià <i>et al.</i> [127]	
Barley		100	440	2011	Norway	Uhlig <i>et al.</i> [129]	
Oats		100	69.6				
Wheat		100	347				
Oat		43	5.6 – 8.2	n.m.	Italy	Juan <i>et al.</i> [130]	
Wheat		28	5.5 – 97				
Rye		55	6.7 – 45				
Hazelnuts shell		n.m.	76	n.m.	Spain	Tolosa <i>et al.</i> [131]	
Dates		n.m.	490				
General feed		92	11	2010/2012	Worldwide	Streit <i>et al.</i> [49]	
ENN B1		Barley malt	90	21.6 – 1540	2012	Germany	Habler and Rychlik [122]
			60	6.49 – 203	2013		
	100		4.78 – 735	2014			
	Coffee	10	10.03 – 15.61	2013/2014	Spain	García-Moraleja <i>et al.</i> [123]	
		27	14.82 – 29.54				
	Soft wheat	93	7.98	2009	Italy	Covarelli <i>et al.</i> [124]	
	Fish (muscle)	50	1.4 – 31.5	n.m.	Spain	Tolosa <i>et al.</i> [125]	
	Pasta	71	0.50 – 979.56	2011	Spain	Serrano <i>et al.</i> [126]	
	Tiger-nuts	10	21600 – 346000	n.m.	Spain	Sebastià <i>et al.</i> [127]	
	Barley	100	529	2011	Norway	Uhlig <i>et al.</i> [129]	
	Oats	100	65.5				

(1) If a single value is given, it equals the median or mean (source dependent). Note that maximum levels can be even higher.
n.m. = not mentioned

Table 2: Examples of recent BEA and ENNs feed/food contamination data (continued).

	Wheat	100	296			
	Wheat	4	5.47 – 33.1	n.m.	Italy	Juan <i>et al.</i> [130]
	Barley	22	5.5 – 7.3			
	Hazelnuts shell	n.m.	417	n.m.	Spain	Tolosa <i>et al.</i> [131]
	General feed	92	14	2010/2012	Worldwide	Streit <i>et al.</i> [49]
ENN A1	Barley malt	70	28.2 – 1700	2012	Germany	Habler and Rychlik [122]
		30	41.3 – 74.9	2013		
		80	8.02 – 286	2014		
	Coffee	85	13.75 – 749.33	2013/2014	Spain	García-Moraleja <i>et al.</i> [123]
	Pre-portioned milk added coffee	91	57.54 – 224.39			
	Soft wheat	79	42.3	2009	Italy	Covarelli <i>et al.</i> [124]
	Fish (muscle)	40	1.7 – 7.5	n.m.	Spain	Tolosa <i>et al.</i> [125]
	Pasta	76	0.25 – 21.89	2011	Spain	Serrano <i>et al.</i> [126]
	Tiger nuts	20	32200 – 4440000	n.m.	Spain	Sebastià <i>et al.</i> [127]
	Grapes	n.m.	5930	2008	Slovakia	Mikušová <i>et al.</i> [132]
	Barley	100	145	2011	Norway	Uhlig <i>et al.</i> [129]
	Oats	100	21.4			
	Wheat	100	48.0			
	Oat	29	9 – 45.5	n.m.	Italy	Juan <i>et al.</i> [130]
	Wheat	19	5.3 - 55			
	Dates	n.m.	25	n.m.	Spain	Tolosa <i>et al.</i> [131]
	General feed	95	5.5	2010/2012	Worldwide	Streit <i>et al.</i> [49]
ENN A	Barley malt	40	37.3 – 362	2012	Germany	Habler and Rychlik [122]
		10	6.80	2013		
		50	1.43 – 25.1	2014		
	Coffee	39	1.20 – 935.53	2013/2014	Spain	García-Moraleja <i>et al.</i> [123]
	Soft wheat	93	180.6	2009	Italy	Covarelli <i>et al.</i> [124]
	Pasta	77	0.50 – 42.04	2011	Spain	Serrano <i>et al.</i> [126]
	Tiger-nuts	2	676500	n.m.	Spain	Sebastià <i>et al.</i> [127]
	Grapes	n.m.	7980	2008	Slovakia	Mikušová <i>et al.</i> [132]
	Barley	100	17.1	2011	Norway	Uhlig <i>et al.</i> [129]
	Oats	100	3.7			
	Wheat	100	4.1			
	Spelt	67	7.2 – 8.0	n.m.	Italy	Juan <i>et al.</i> [130]
	Wheat	11	8.4 – 29.8			
	Rye	36	7.8 – 9.8			
	Hazelnuts shell	n.m.	732	n.m.	Spain	Tolosa <i>et al.</i> [131]
	Dates	n.m.	666			
	General feed	87	0.8	2010/2012	Worldwide	Streit <i>et al.</i> [49]

(1) If a single value is given, it equals the median or mean (source dependent). Note that maximum levels can be even higher.
n.m. = not mentioned

At the start of the research described in this thesis, no formal regulatory opinion was yet adopted concerning these cyclic depsipeptides and no legal maximum levels were set for these compounds in food and feed [57,133,134]. As they became more of interest, in 2010 the European Commission asked the European Food Safety Authority (EFSA) for ‘a scientific opinion on the risk to human and animal health related to the presence of beauvericin and enniatins in food and feed’. This report was only recently (2014) released and stated that currently there is a lack of relevant toxicity data, making it impossible to perform a proper risk assessment. However, the EFSA CONTAM (Contaminants in the Food Chain) Panel concluded that acute exposure to these emerging

mycotoxins most probably does not indicate a concern for human health, but there might be a concern with respect to chronic exposure. So far, no adverse effects in humans or animals were reported due to contaminated food or feed. For beauvericin, the LD₅₀ for acute toxicity was 100 mg/kg body weight upon oral administration to mice, while for fusafungine (a mixture of enniatins) this was 350 mg/kg body weight [57]. Moreover, a recent subchronic feeding experiment on rats, where a dose of 21 mg ENN A/kg body weight was given during 28 days, showed no adverse effects [135].

The discrepancy between these *in vitro* and *in vivo* toxicity results might be ascribed to a low bioavailability. However, using different *in vitro* gastro-intestinal Caco-2 cell models, a relatively high bioavailability of approximately 52% was shown for BEA [94], while for ENNs (A, A1, B and B1) this ranged from 51% up to 77%, depending on the protocol [136,137]. A recent *in vivo* trial in pigs showed an even higher oral bioavailability of 91% for ENN B1, indicating a clear systemic exposure [138]. Other mechanisms such as rapid elimination from the systemic circulation could explain the low acute *in vivo* toxicity. The lipophilic character of these CDP mycotoxins, however, may allow for bioaccumulation in animal and human tissues, which could affect their chronic toxicity. In the 28 day study on rats, ENN A could not be detected in faeces and urine, while in serum an increasing concentration over time was noticed, suggesting indeed the distribution and accumulation in some organs, saturation of metabolism/detoxification enzymes and/or decrease in organ functionality [139]. An even more recent study in mice showed that the highest amounts of ENN B and BEA were found in liver and fat, demonstrating their tendency to bioaccumulate in lipophilic tissues. Moreover, in the tumour of the KB-3-1 xenograft mice, distinct levels of BEA and ENN B were measured, underlining their possible use as chemotherapeutics [140].

Remarkably, the European Medicines Agency (EMA) Pharmacovigilance Risk Assessment Committee (PRAC) recently recommended to withdraw nasal and mouth sprays containing fusafungine, originally patented in 1953 (FR1021824) and used topically to treat upper respiratory tract diseases [141-143], from the market in the European Union. The Committee concluded that the benefits of fusafungine do not outweigh its risks, especially the risk for serious allergic reactions and antibiotic resistance (EMA/H/A-31/1420, February 12th, 2016) [144]. This advice was followed by the CMDh (Coordination Group for Mutual Recognition and Decentralised Procedures – Human), which has authorised the revocation of marketing authorisations for fusafungine sprays in the EU. The different EU Member States are currently implementing this decision and start withdrawing the affected medicinal products in their territories, according to an agreed timetable (EMA/H/A-31/1420, April 1st, 2016) [145]. For example, in Belgium the Federal Agency for Medicines and Health Products (FAMHP) has issued the revocation of Locabiotol (May 4th, 2016) [146]. In several EU countries fusafungine was available under various trade names (Bioparox, Fusaloyos, Locabiotol and

Locabiosol) for over 50 years: Austria, Belgium, Bulgaria, Cyprus, Czech Republic, Estonia, Germany, Greece, Hungary, Ireland, Italy, Latvia, Lithuania, Luxembourg, Malta, Portugal, Romania, Slovakia and Spain. In some Member States, these medicines were even available without prescription [147]. It contains a mixture of the cyclic hexadepsipeptides enniatins mainly formulated in ethanol (EtOH) and isopropyl myristate (IPM), which are both chemical skin and mucosal penetration enhancers [148-157]. The summary of product characteristics (SmPC) explicitly indicated no systemic absorption of the active compound. However, no data substantiating this claim could be found in literature, questioning its validity.

4. BIOLOGICAL BARRIERS IN THE HUMAN BODY

The human body applies various defence mechanisms, designed by nature in order to protect and maintain its internal homeostasis. As a first frontier, the body is lined by the epithelial cells of skin and mucosa, which separate the internal milieu from the external environment. Additional internal barriers are also present, defining protected compartments within the human body. These barriers provide both a physical, as well as immunological/enzymatic defence, intended to strictly regulate the uptake and secretion of certain compounds, *i.e.* keep toxic/foreign material out and let necessary molecules pass [158]. An overview of the most important human biological barriers is presented in Figure 5. Other barriers exist as well, for example the peritoneal membrane lining the abdominal cavity and covering most of the intra-abdominal organs.

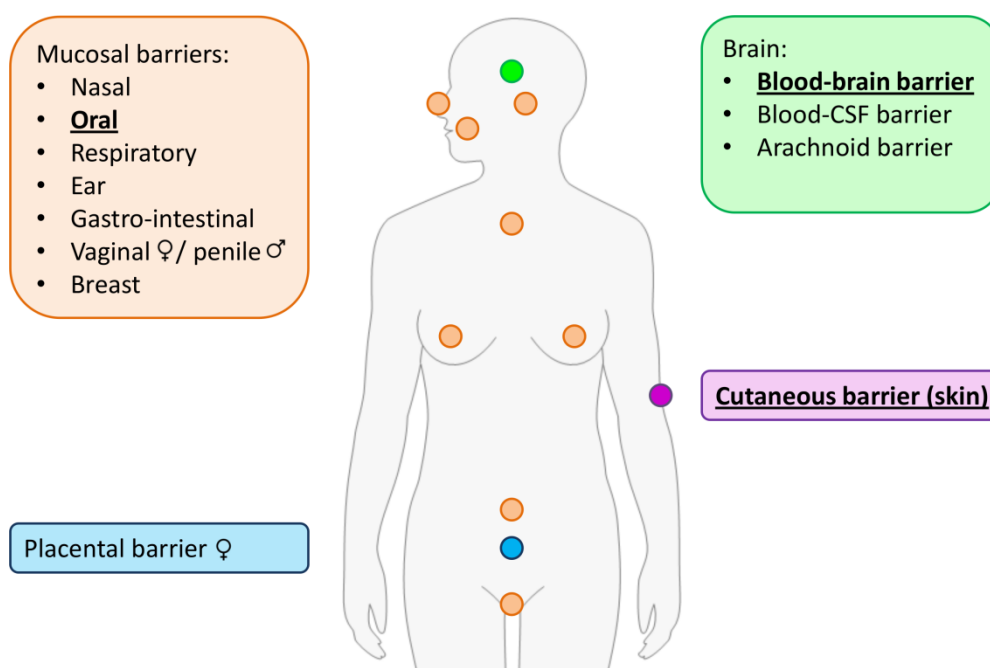


Figure 5: Overview of important human biological barriers.

Transport across these barriers can be achieved via either a transcellular or intercellular (paracellular) route and using passive and/or active transport mechanisms. The latter mechanism requires a carrier or receptor and is highly substrate specific, while the former is dependent on the diffusional concentration gradient [159,160]. The paracellular permeability is one of the most important routes in molecule transportation and differs greatly between various epithelial tissues and barriers. The lowest tightness is ascribed to the small intestine, which is considered a rather leaky epithelial tissue, whereas the colon and the stomach are of intermediate tightness. The brain capillaries and skin epithelial cells form the tightest barriers [161].

The largest human organ and apparent barrier is the **skin**, which protects against external, chemical, mechanical, microbial and physical influences. Because of its large surface area, the skin has a great drug delivery potential as well [162]. In Figure 6, the structure of the skin is schematically presented.

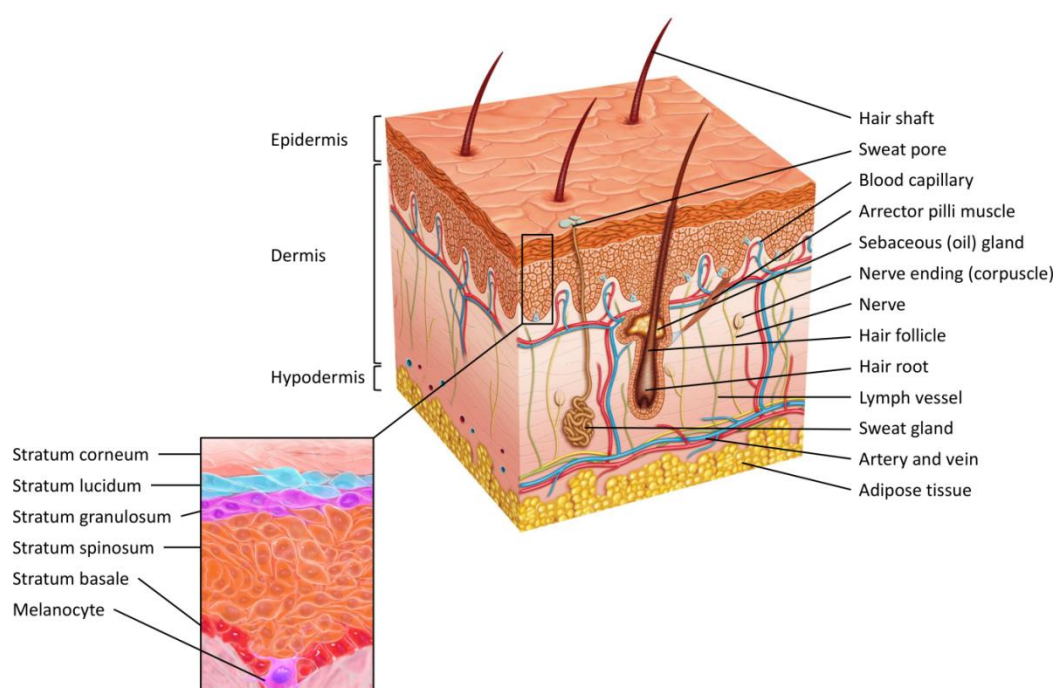


Figure 6: Structure of the skin (adapted from Blausen.com staff and Shutterstock Alexilusmedical).

In the basal cell layer, keratinocytes are formed, after which they differentiate and migrate in the direction of the skin surface. The most outer layer, *i.e.* the stratum corneum is composed of dead keratin filled cells (corneocytes) surrounded by covalently bound lipid envelope and embedded in long lipid lamellae filling the intercellular regions [163]. It is this outer ‘brick and mortar’ layer that mainly dominates skin permeation. In addition to the above mentioned transcellular or intercellular transport routes across the intact stratum corneum, skin permeation can also be achieved by the use of shunts like hair follicles and sweat glands, although these only account for approximately 0.1 % of the total skin area [159,160]. Moreover, it is generally accepted that skin permeation of small molecules occurs by diffusion and is not an active process [164]. Dermal and transdermal delivery of

larger molecules such as peptides, proteins and DNA and particles remains a significant challenge [165,166].

The **oral mucosa**, similar to the skin, is easily accessible and thus an attractive site for drug delivery. The rather limited surface area is compensated by the extensive vascularization. Due to the direct drainage of blood into the internal jugular vein, the gastrointestinal tract and first-pass metabolism in the liver are also by-passed [167,168]. Compared to skin permeability, that of the oral mucosa is significantly higher, *i.e.* in general, it is estimated there is a 5 to 100 fold difference [169-173]. Depending on the region in the oral cavity, there is a morphologic diversity between the different oral mucosae, with the sublingual mucosa being relatively thin and non-keratinised, the buccal mucosa also being non-keratinised but thicker and the palatal mucosa being intermediate in thickness but keratinised [174]. Based on this, the permeability of the oral mucosae increases in the following order: palatal < buccal < sublingual [175]. As for the skin, the major rate-limiting step and permeability barrier is also the outermost epithelial layer. Keratinisation itself is not expected to play a significant role; however, the components of the membrane coating granules (lamellar bodies) is [172-174,176,177]. Epidermis, palatal and gingival mucosa show similar lipid compositions, *i.e.* lamellar lipid stacks composed of non-polar lipids (mostly (O-acyl)(glucosyl)ceramides), whereas the non-keratinised sublingual and buccal mucosae contain less neutral, but more polar and amorphous lipids (*e.g.* cholesterol (esters) and glycosylceramides but only very small quantities of ceramides) [174,177-179]. The most superficial layer, *i.e.* the gel-structure mucus, is not expected to influence drug diffusion and thus seems to be of inferior importance as a physical barrier [180,181]. The main composition of the oral mucosa is shown in Figure 7.

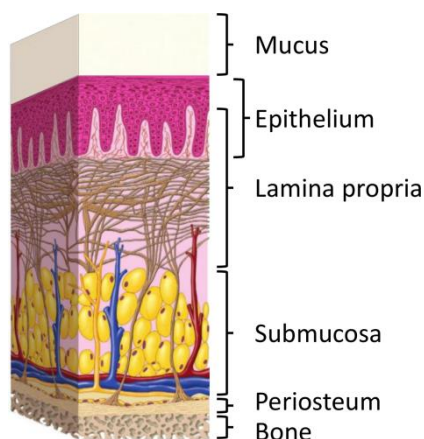


Figure 7: Structure of the oral mucosa (adapted from Nanci [182]).

It is suggested that hydrophilic molecules will permeate via the intercellular route, while lipophilic molecules are preferably absorbed via the transcellular route [168,183,184], although the validity of the latter has been questioned [167].

Once the systemic circulation is reached, molecules encounter another important biological barrier, namely the **blood-brain barrier (BBB)**, which is an anatomical defence barrier characterised by capillary endothelial cells with an extensive network of tight junctions (physical barrier), energy-dependent efflux transporters such as P-glycoproteins (transport barrier) and bordered by astrocytic foot, serving to protect the central nervous system (CNS) from toxic substances and maintaining brain homeostasis [185,186]. The tight junctions normally severely restrict the permeation of water-soluble compounds. However, lipid-soluble agents are able to use the large surface area of the lipid membranes of the endothelium, which offers an effective diffusive pathway. Another route of transportation across the BBB is specific receptor-mediated transcytosis (*e.g.* insulin and transferrin) [187,188]. Most CNS drugs are believed to be transported across the BBB using the direct transcellular diffusional pathway, due to the presence of tight junctions between the adjacent endothelial cells hampering the paracellular route [189]. It has also been demonstrated that peptides are able to cross the BBB, either by using the passive membrane diffusional permeation, or by a saturable, active or facilitated, transport mechanism, or both [190-194]. A schematic representation of the BBB is shown in Figure 8.

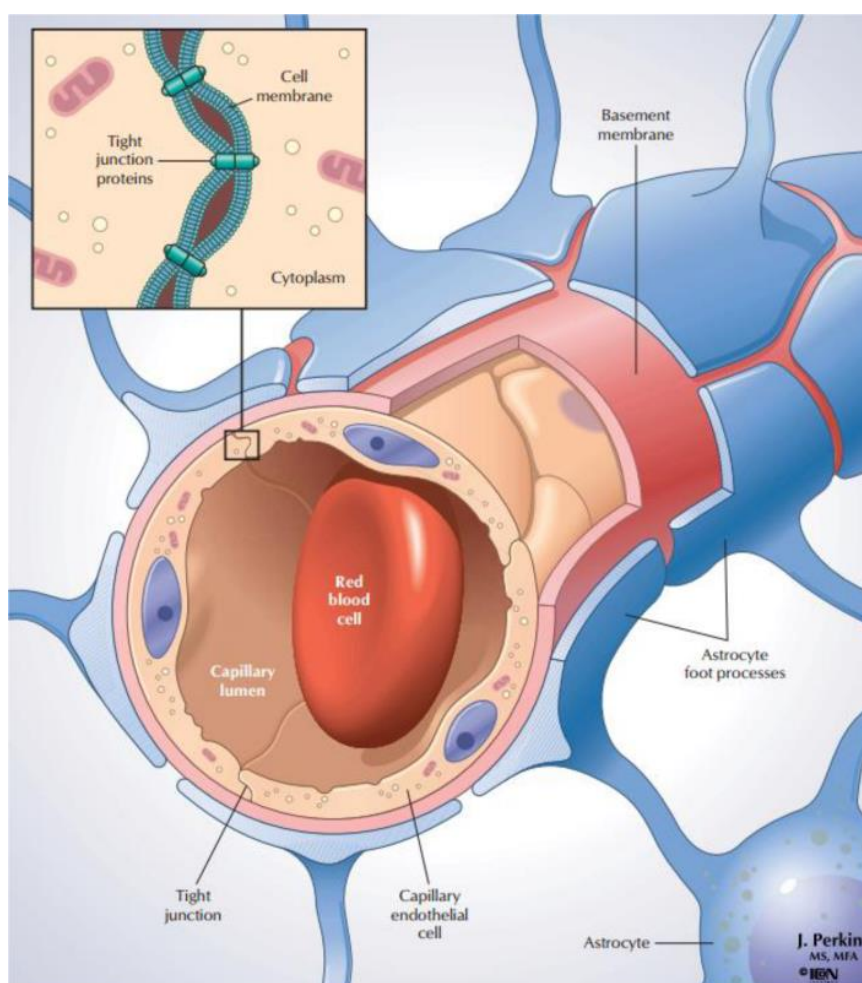


Figure 8: Schematic representation of the blood-brain barrier (adopted from Perkins *et al.* [195]).

5. STUDY OBJECTIVES

This research project will mainly focus on beauvericin (BEA) and the most abundant enniatins (ENNs A, A1, B, B1, C, D, E and F) as selected relevant bioactive cyclic hexadepsipeptides, currently investigated both as potential hazardous emerging mycotoxins, as well as useful therapeutics. To better understand and appreciate their biological role, their kinetic interaction with some of the most important and relevant biological barrier systems should be known. This knowledge is not only required for the urgently needed global risk assessment of these emerging mycotoxins due to skin-contact of contaminated food, feed, indoor surfaces and airborne particles, but also in the development of topically applied new drugs with CDP structure, treating dermatological diseases like eczema or skin cancers, or having systemic functions after transdermal penetration. **Therefore, the main goal of this research project is to quantitatively investigate the local skin, mucosa and BBB kinetics of the model cyclic depsipeptide mycotoxins BEA and ENNs.**

In order to answer the central question of this research project, following objectives were set:

(1) Explore the CDP chemical space to allow positioning of BEA and ENNs as model CDPs and propose a comprehensive classification system for CDPs.

Cyclic depsipeptides are a chemically diverse group of secondary metabolites produced by a variety of both marine and terrestrial organisms, which exert a wide range of biological activities, making them potentially interesting biomedical compounds. However, an enormous amount of CDP data are scattered in literature and a comprehensive classification for these compounds is currently lacking, although important for global scientific understanding in terms of differentiation, relation, standardization, organization and conservation of all efforts related to these CDPs.

(2) Introduce a clear, unambiguous and quantitatively expressed ‘mycotoxin’ definition and apply it on a set of fungal CDPs to determine whether these metabolites should also be classified as mycotoxins.

Currently, BEA and ENNs are (nearly) the only CDPs positioned as mycotoxins. However, as there are hundreds more fungal cyclic depsipeptides already identified, should these not be considered as mycotoxins as well? Today a huge amount of information about mycotoxins is already available, but in the scientific community, authors do not all share the same vision about what should be called a mycotoxin, revealing a lack of consistency and leading to confusion about what compounds should or should not be called mycotoxins. A re-evaluation of the traditional concept is thus most certainly required, since this is of pivotal importance in risk assessment prioritization and allowing more awareness of the now underestimated potential hazard of some of these fungal metabolites.

(3) Development and verification of a quantitative, selective and high throughput bioanalytical method for the determination of BEA and ENNs.

In order to calculate their barrier (skin – oral mucosa – BBB) kinetics, we need to quantitatively determine BEA and ENNs in different matrix samples. Therefore, a high throughput bioanalytical method must be developed and verified allowing the quantitative, selective and simultaneous determination of the cyclic depsipeptide mycotoxins BEA and ENNs (A, A1, B, B1, C, D, E and F). Special attention should also be paid to analytical stability and adsorption to glass, possibly leading to loss of the analyte and increased analytical variability.

(4) Quantitatively determine the transdermal kinetics of BEA and ENNs and evaluate the impact of dermal exposure.

Studying the local pharmacokinetics of molecules through human skin is not only important within the pharmaceutical industry, but also in the field of environmental toxicology. For the cyclic depsipeptide mycotoxins BEA and ENNs, however, the skin remains unexplored as exposure route, with skin permeability data being non-existing. However, in view of the accumulating evidence of their toxic potential, this information is essential for risk assessment.

(5) Characterise the blood-brain barrier transport of BEA and ENNs.

Once they have entered the blood stream, xenobiotics (such as CDPs) might be able to pass the BBB and enter the brain parenchyma, where they can exert local CNS effects. However to date, no information is available about the transport kinetics of CDPs, including the mycotoxins BEA and ENNs, across the BBB.

(6) Investigate if enniatins, marketed as oral sprays, are able to permeate the mucosa and reach the systemic circulation and determine what the influence of formulation variability is on their mucosal kinetics.

At the start of this research, fusafungine, a mixture of different ENNs, was marketed in several European countries under different trade names (Bioparox, Fusaloyos, Locabiosol and Locabiotol), recommended for topical use to treat upper respiratory tract diseases. As these CDP mycotoxins are formulated in ethanol and isopropyl myristate, both being chemical skin and mucosal penetration enhancers, variability in their excipient composition may thus result in a different bioavailability of the enniatins, due to a difference in mucosal permeation.

6. THESIS OUTLINE

The different aspects covered in this thesis are outlined in Figure 9. The first two chapters will focus on (1) the exploration of cyclic depsipeptides and (2) defining mycotoxins, while subsequent chapters will deal with the biological barrier interaction of the cyclic depsipeptide mycotoxins BEA and ENNs.

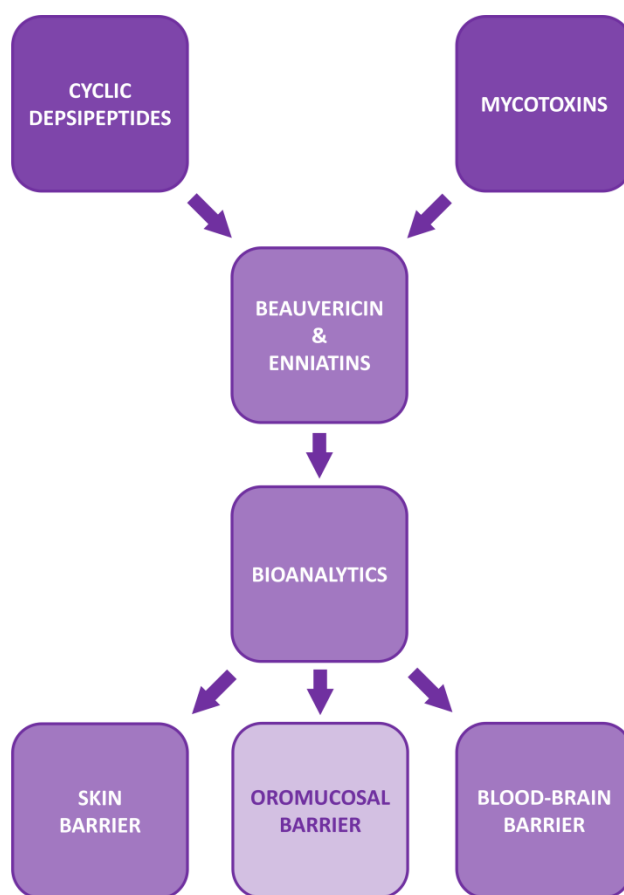


Figure 9: Thesis outline.

The last chapter is dedicated to the broader international context, relevance and future perspectives related to this research. Each chapter of this thesis is presented as a stand-alone text, with the introduction giving the specific context of that section.

In **Chapter II**, an extensive literature search is performed to gather an almost exhaustive amount of scattered CDP data, leading to a database composed of 1348 naturally occurring cyclic depsipeptides. A chemical classification system is proposed, based on the different structures of these CDPs, using their apparent chemical characteristics and the validity of this approach is confirmed with the current literature knowledge. Ultimately, for the first time a comprehensive chemical classification tool is presented, which allows researchers working in the field to get a better global understanding of the wide diversity in CDP structures, their chemical interrelationships and identification of existing and newly found CDPs. In this classification system, the cyclic hexadepsipeptides beauvericin and enniatins constitute an important group of CDPs.

Chapter III starts with revealing the current lack of consistency, confounding approaches and obvious disagreement in scientific literature concerning the mycotoxin definition. Using a philosophical explanation approach, a clear, unambiguous and quantitatively expressed mycotoxin definition is proposed, based upon hazard data of some already well-known and widely accepted “traditional”

mycotoxins. Finally, this concept is applied to a set of fungal cyclic depsipeptides to determine whether or not these metabolites should be classified as mycotoxins.

Starting from **Chapter IV**, focus lies on BEA and ENNs as model cyclic hexadepsipeptides and emerging mycotoxins. First, a high throughput selective and sensitive UHPLC-MS/MS is developed, using state of the art technology, which allows for quantitative and simultaneous determination of the cyclic depsipeptide mycotoxins BEA and ENNs (A, A1, B, B1, C, D, E and F). Additionally, in view of succeeding experiments, analytical stability and adsorption to glass of these peptides is also studied.

In **Chapter V**, the quantitative characterisation of the transdermal kinetics of BEA and ENNs is evaluated using intact and damaged human skin in an *ex vivo in vitro* Franz diffusion cell (FDC) set-up, by kinetic profiling of the FDC receptor fluid, yielding the experimentally obtained secondary flux parameters, as well as the derived calculated primary permeability coefficient. This latter is then used to determine the daily dermal exposure (DDE) in a worst-case scenario, as well as in a typical industrial occupational scenario.

Chapter VI comprises the *in vivo* BBB transport study of BEA and ENNs. In addition to the UHPLC-MS/MS method earlier described in Chapter IV, sample preparation methods for mouse serum and brains are developed and verified. Also, the metabolic stability of the mycotoxins is evaluated *in vitro* in mouse serum and brain homogenate. The BBB rate kinetics of BEA and ENNS are studied, using an *in vivo* mouse model, applying multiple time regression for studying the blood-to-brain influx, capillary depletion for determination of the fraction transported into the brain versus the fraction trapped by the endothelial cells lining the BBB, and finally an efflux study is performed to investigate brain-to-blood transport kinetics.

To determine whether fusafungine ENNs are able to permeate the mucosa and reach blood circulation, as the summary of product characteristics of marketed oral sprays (*e.g.* Locabiotol) indicates this is not the case, an *ex vivo in vitro* Franz diffusion cell experiment is performed using porcine buccal mucosa in **Chapter VII**. Moreover, the concentration of the two main excipients and known penetration enhancers, isopropyl myristate and ethanol, is determined in several marketed samples, using an in-house developed and verified GC-FID method. Finally, the influence of excipient concentration variability on mucosal permeation bioavailability is also investigated, by quantifying the transdermal kinetics of the ENNs.

To conclude the research presented in this thesis, the **broader international context, relevance and future perspectives** are discussed.

7. REFERENCES

- [1] Gevaert B, Stalmans S, Wynendaele E, Taevernier L, Bracke N, D’Hondt M, De Spiegeleer B. Exploration of the medicinal peptide space. *Protein & Peptide Letters* 2016; 23(4): 324-335.
- [2] Losse G, Bachmann G. Chemie der Depsipeptide Teil II. *Zeitschrift für Chemie* 1964; 4: 241-253.
- [3] Russell DW. Cyclodepsipeptides. *Q Rev Chem Soc* 1966; 20: 559-576.
- [4] Andavan GSB, Lemmens-Gruber R. Cyclodepsipeptides from marine sponges: natural agents for drug research. *Mar Drugs* 2010; 8(3): 810-834.
- [5] Moss GP, Smith PAS, Tavernier D. Glossary of class names of organic compounds and reactivity intermediates based on structure (IUPAC Recommendations 1995). *Pure & Appl Chem* 1995; 67: 1307-1375.
- [6] Gaumann E, Naef-Roth S, Ettlinger L, Plattner PA, Nager U. Ionophore antibiotics produced by the fungus *Fusarium orthoceras* var. *enniatum* and other. *Fusaria Experientia* 1947; 3: 202-203.
- [7] Lipmann F. Attempts to map a process evolution of peptide biosynthesis. *Science* 1971; 173: 875-84.
- [8] Zocher R, Keller U, Kleinkauf H. Enniatin synthetase, a novel type of multifunctional enzyme catalyzing depsipeptide synthesis in *Fusarium oxysporum*. *Biochemistry* 1982; 21(1): 43-48.
- [9] Al Toma RS, Brieke C, Cryle MJ, Süßmuth RD. Structural aspects of phenylglycines, their biosynthesis and occurrence in peptide natural products. *Nat Prod Rep* 2015; 32(8): 1207-1235.
- [10] Baltz RH. Combinatorial biosynthesis of cyclic lipopeptide antibiotics: a model for synthetic biology to accelerate the evolution of secondary metabolite biosynthetic pathways. *ACS Synth Biol* 2014; 3(10): 748-758.
- [11] Brito A, Gaifem J, Ramos V, Glukhov E, Dorrestein PC, Gerwick WH, Vasconcelos VM, Mendes M, V Tamagnini P. Bioprospecting Portuguese Atlantic coast cyanobacteria for bioactive secondary metabolites reveals untapped chemodiversity. *Algal Research* 2015; 9: 218-226.
- [12] Hotta K, Keegan RM, Ranganathan S, Fang M, Bibby J, Winn MD, Sato M, Lian M, Watanabe K, Rigden DJ, Kim CY. Conversion of a disulfide bond into a thioacetal group during echinomycin biosynthesis. *Angew Chem Int Ed Engl* 2014; 53(3): 824-828.
- [13] Ishidoh K, Kinoshita H, Nihira T. Identification of a gene cluster responsible for the biosynthesis of cyclic lipopeptide verlamelin. *Appl Microbiol Biotechnol* 2014; 98: 7501-7510.
- [14] Marxen S, Stark TD, Rüttschle A, Lücking G, Frenzel E, Scherer S, Ehling-Schul, M Hofmann T. Depsipeptide intermediates interrogate proposed biosynthesis of cereulide, the emetic toxin of *Bacillus cereus*. *Sci Rep* 2015; 5: 10637.
- [15] Micallef ML, D’Agostino PM, Sharma D, Viswanathan R, Moffitt MC. Genome mining for natural product biosynthetic gene clusters in the subsection V cyanobacteria. *BMC Genomics* 2015; 16: 669.

-
- [16] Marahiel MA, Stachelhaus T, Mootz HD. Modular peptide synthetases involved in nonribosomal peptide synthesis. *Chem Rev* 1997; 97: 2651-2674.
- [17] Grünewald J, Marahiel MA. Chemoenzymatic and template-directed synthesis of bioactive macrocyclic peptides. *Microbiol Mol Biol Rev* 2006; 70: 131-146.
- [18] Sieber SA, Marahiel MA. Molecular mechanisms underlying nonribosomal peptide synthesis: approaches to new antibiotics. *Chem Rev* 2005; 105: 715-738.
- [19] Desriac F, Jégou C, Balnois E, Brillet B, Le Chevalier P, Fleury Y. Antimicrobial peptides from marine proteobacteria. *Mar Drugs* 2013; 11: 3632-3660.
- [20] Du L, Sanchez C, Shen B. Hybrid peptide-polyketide natural products: Biosynthesis and prospects toward engineering novel molecules. *Metabolic Engineering* 2001; 3: 78-95.
- [21] Fisch KM. Biosynthesis of natural products by microbial iterative hybrid PKS-NRPS. *RSC Adv* 2013; 3: 18228-18247.
- [22] Uytterhoeven B, Appermans K, Song L, Masschelein J, Lathouwers T, Michiels CW, Lavigne R. Systematic analysis of the kalimantacin assembly line NRPS module using an adapted targeted mutagenesis approach. *MicrobiologyOpen* 2016; 5(2): 279-286.
- [23] Wang H, Fewer DP, Holm L, Rouhiainen L, Sivonen K. Atlas of nonribosomal peptide and polyketide biosynthetic pathways reveals common occurrence of nonmodular enzymes. *Proc Natl Acad Sci USA* 2014; 111(25): 9259-9264.
- [24] Sieber SA, Marahiel MA. Learning from nature's drug factories: Nonribosomal synthesis of macrocyclic peptides. *J Bacteriol* 2003; 185(24): 7036-7043.
- [25] Huang T, Wang Y, Yin J, Du Y, Tao M, Xu J, Chen W, Lin S, Deng Z. Identification and characterization of the pyridomycin biosynthetic gene cluster of *Streptomyces pyridomyceticus* NRRL B-2517. *J Biol Chem* 2011; 286(23): 20648-20657.
- [26] Walsh CT, Chen H, Keating TA, Hubbard BK, Losey HC, Luo L, Marshall CG, Miller DA, Patel HM. Tailoring enzymes that modify nonribosomal peptides during and after chain elongation on NRPS assembly lines. *Curr Opin Chem Biol* 2001; 5(5): 525-534.
- [27] Keating TA, Ehmann DE, Kohli RM, Marshall CG, Trauger JW, Walsh CT. Chain termination steps in nonribosomal peptide synthetase assembly lines: directed acyl-S-enzyme breakdown in antibiotic and siderophore biosynthesis. *Chembiochem* 2001; 2(2): 99-107.
- [28] Mootz HD, Schwarzer D, Marahiel MA. Ways of assembling complex natural products on modular nonribosomal peptide synthetases. *Chembiochem* 2002; 3(6): 490-504.
- [29] Sivanathan S, Scherkenbeck J. Cyclodepsipeptides: A rich source of biologically active compounds for drug research. *Molecules* 2014; 19: 12368-12420.
- [30] Caboche S, Pupin M, Leclère V, Fontaine A, Jacques P, Kucherov G. NORINE: a database of nonribosomal peptides. *Nucleic Acids Res* 2008; 36: D326-31.
- [31] Marahiel MA. Protein templates for the biosynthesis of peptide antibiotics. *Chem Biol* 1997; 4(8): 561-567.
- [32] Smith S. Modular NRPSs are monomeric. *Chem Biol* 2002; 9(9): 955-956.
-

- [33] von Döhren H, Keller U, Vater J, Zocher R. Multifunctional Peptide Synthetases. *Chem Rev* 1997; 97(7): 2675-2706.
- [34] Salomon CE, Magarvey NA, Sherman DH. Merging the potential of microbial genetics with biological and chemical diversity: an even brighter future for marine natural product drug discovery. *Nat Prod Rep* 2004; 21(1): 105-121.
- [35] Gao X, Haynes SW, Ames BD, Wang P, Vien LP, Walsh CT, Tang Y. Cyclization of fungal nonribosomal peptides by a terminal condensation-like domain. *Nat Chem Biol* 2012; 8(10): 823-830.
- [36] Peraica M, Radic A, Lucic A, Pavlovic A. Toxic effects of mycotoxins in humans. *Bulletin of the World Health Organization* 1999; 77 (9): 754-766.
- [37] van Dongen PW, de Groot AN. History of ergot alkaloids from ergotism to ergometrine. *Eur J Obstet Gynecol Reprod Biol* 1995; 60(2): 109-116.
- [38] Blount WP. Turkey 'X' disease. *Turkeys* 1961; 9: 55-58.
- [39] Forgacs J, Carll WT. Preliminary mycotoxic studies on hemorrhagic disease in poultry. *Veterinary Medicine* 1955; 50: 172-177.
- [40] Thomas NJ, Hunter DB, Atkinson CT. *Infectious diseases of wild birds*. Wiley-Blackwell, Hoboken, New Jersey, 2007, pp. 484.
- [41] Bennett JW, Klich M. Mycotoxins. *Clinical Microbiology Reviews* 2003; 16: 497-516.
- [42] D'Mello, JPF, Placinta, CM, Macdonald AMC. *Fusarium* mycotoxins: a review of global implications for animal health, welfare and productivity. *Animal Feed Science and Technology* 1999; 80(3-4): 183-205.
- [43] De Vries JW, Truckess MW, Jackson LS. *Mycotoxins and food safety*. Kluwer, New York, 2002, pp. 298.
- [44] Wyllie T, Morehouse L. *Mycotoxic fungi, mycotoxins, mycotoxicoses*, vol. 3. Marcel Dekker, New York, 1978, pp. 202.
- [45] Marroquín-Cardona AG, Johnson NM, Phillips TD, Hayes AW. Mycotoxins in a changing global environment--a review. *Food Chem Toxicol* 2014; 69: 220-230.
- [46] Paterson RRM, Lima N. Further mycotoxin effects from climate change. *Food Research International* 2011; 44: 2555-2566.
- [47] Streit E, Schatzmayr G, Tassis P, Tzika E, Marin D, Taranu I, Tabuc C, Nicolau A, Aprodu I, Puel O, Oswald IP. Current situation of mycotoxin contamination and co-occurrence in animal feed - focus on Europe. *Toxins (Basel)* 2012; 4(10): 788-809.
- [48] Adamse P, van Egmond HJ, Driessen JJM, de Rijk TC, de Jong J, de Nijs M. Trend analysis of mycotoxins in animal feed. *RIKILT (Institute of Food Safety)*, Wageningen, 2012, pp. 52.
- [49] Streit E, Naehrer K, Rodrigues I, Schatzmayr G. Mycotoxin occurrence in feed and feed raw materials worldwide: long-term analysis with special focus on Europe and Asia. *J Sci Food Agric* 2013; 93(12): 2892-2899.

- [50] Ahmad B, Ashiq S, Hussain A, Bashir S, Hussain M. Evaluation of mycotoxins, mycobiota, and toxigenic fungi in selected medicinal plants of Khyber Pakhtunkhwa, Pakistan. *Fungal Biol* 2014; 118(9-10): 776-784.
- [51] Bugno A, Buzzo Almodovar AA, Caldas Pereira T, de Jesus Andreoli Pinto T., Sabino M. Occurrence of toxigenic fungi in herbal drugs. *Braz J Microbiol* 2006; 37(1): 317-326.
- [52] Santos L, Marin S, Sanchis V, Ramos AJ. Mycotoxin in medicinal/aromatic herbs - a review. *Boletín Latinoamericano y del Caribe de Plantas Medicinales y Aromáticas* 2013; 12(2): 119-142.
- [53] Fang LX, Xiong AZ, Wang R, Ji S, Yang L, Wang ZT. A strategy for screening and identifying mycotoxins in herbal medicine using ultra-performance liquid chromatography with tandem quadrupole time-of-flight mass spectrometry. *J Sep Sci* 2013; 36(18): 3115-3122.
- [54] CAST (Council for Agricultural Science and Technology). *Mycotoxins, risks in plant, animal and human systems*. Ames, 2003, pp. 217.
- [55] Hussein HS, Brasel JM. Toxicity, metabolism, and impact of mycotoxins on humans and animals. *Toxicology* 2001; 167(2): 101-134.
- [56] Jestoi M. Emerging *Fusarium*-mycotoxins fusaproliferin, beauvericin, enniatins, and moniliformin: a review. *Crit Rev Food Sci Nutr* 2008; 48(1): 21-49.
- [57] CONTAM (Contaminants in the Food Chain) Panel, EFSA (European Food Safety Authority). Scientific Opinion on the risks to human and animal health related to the presence of beauvericin and enniatins in food and feed. *EFSA Journal* 2014; 12(8): 3802.
- [58] Berthiller F, Sulyok M, Krska R, Schuhmacher R. Chromatographic methods for the simultaneous determination of mycotoxins and their conjugates in cereals. *Int J Food Microbiol* 2007; 119(1-2): 33-37.
- [59] Cole RJ, Cox RH. *Handbook of toxic fungal metabolites*, Academic Press, Cambridge, 1981, pp. 936.
- [60] Nielsen KF, Smedsgaard J. Fungal metabolite screening: database of 474 mycotoxins and fungal metabolites for dereplication by standardised liquid chromatography-UV-mass spectrometry methodology. *J Chromatogr A* 2003; 1002(1-2): 111-36.
- [61] Devreese M, De Baere S, De Backer P, Croubels S. Quantitative determination of the *Fusarium* mycotoxins beauvericin, enniatin A, A1, B and B1 in pig plasma using high performance liquid chromatography–tandem mass spectrometry. *Talanta* 2013; 106: 212-219.
- [62] Sulyok M, Krska R, Schuhmacher R. Application of an LC-MS/MS based multi-mycotoxin method for the semi-quantitative determination of mycotoxins occurring in different types of food infected by moulds. *Food Chem* 2010; 119(1): 408-416.
- [63] Betina V. *Mycotoxins - Production, isolation, separation and purification*. Elsevier, Amsterdam, 1984, pp. 528.
- [64] De Ruyck K, De Boevre M, Huybrechts I, De Saeger S. Dietary mycotoxins, co-exposure, and carcinogenesis in humans: Short review. *Mutat Res Rev Mutat Res* 2015; 766: 32-41.

- [65] Kuzdralinski A, Solarska E, Mazurkiewicz J. Mycotoxin content of organic and conventional oats from southeastern Poland. *Food Control* 2013; 33: 68-72.
- [66] Jarvis BB. Analysis for mycotoxins: the chemist's perspective. *Arch Environ Health* 2003; 58(8): 479-483.
- [67] Laatsch H. *AntiBase 2005, A Natural products database for rapid structure determination*. Chemical Concepts, Weinheim, 2005.
- [68] Miller JD, McMullin DR. Fungal secondary metabolites as harmful indoor air contaminants: 10 years on. *Appl Microbiol Biotechnol* 2014; 98(24): 9953-9966.
- [69] Commission recommendation 2013/165/EU: On the presence of T-2 and HT-2 toxin in cereals and cereal products; <http://eur-lex.europa.eu/LexUriServ/LexUriServ.do?uri=OJ:L:2013:091:0012:0015:EN:PDF>.
- [70] Regulation 1881/2006/EU: Setting maximum levels for certain contaminants in foodstuffs; <http://eur-lex.europa.eu/LexUriServ/LexUriServ.do?uri=CONSLEG:2006R1881:20100701:EN:PDF>.
- [71] Commission recommendation 2006/576/EC: On the presence of deoxynivalenol, zearalenone, ochratoxin A, T-2 and HT-2 and fumonisins in products intended for animal feeding; <http://eur-lex.europa.eu/LexUriServ/LexUriServ.do?uri=OJ:L:2006:229:0007:0009:EN:PDF>.
- [72] Commission recommendation 2012/154/EU: On the monitoring of the presence of ergot alkaloids in feed and food; <http://eur-lex.europa.eu/legal-content/EN/TXT/PDF/?uri=CELEX:32012H0154&rid=1>.
- [73] FDA Regulatory Guidance for Mycotoxins (2011); <https://www.ngfa.org/wp-content/uploads/NGFAComplianceGuide-FDARegulatoryGuidanceforMycotoxins8-2011.pdf>.
- [74] CPG Sec.510.150 Apple juice, apple juice concentrates, and apple juice products - adulteration with patulin (2005); <http://www.fda.gov/ICECI/ComplianceManuals/CompliancePolicyGuidanceManual/ucm074427.htm>.
- [75] CPG Sec. 683.100 Action levels for aflatoxins in animal feeds (1994); <http://www.fda.gov/ICECI/ComplianceManuals/CompliancePolicyGuidanceManual/ucm074703.htm>.
- [76] Ivanova L, Skjerve E, Eriksen GS, Uhlig S. Cytotoxicity of enniatins A, A1, B, B1, B2 and B3 from *Fusarium avenaceum*. *Toxicon* 2006; 47: 868-876.
- [77] Sy-Cordero, AA, Pearce, CJ, Oberlies NH. Revisiting the enniatins: a review of their isolation, biosynthesis, structure determination, and biological activities. *J Antibiot (Tokyo)* 2012; 65(11): 541-549.
- [78] Luangsa-Ard JJ, Berkaew P, Ridkaew R, Hywel-Jones NL, Isaka M. A beauvericin hot spot in the genus *Isaria*. *Mycol Res* 2009; 113: 1389-1395.
- [79] Wang Q, Xu L. Beauvericin, a bioactive compound produced by fungi: a short review. *Molecules* 2012; 17(3): 2367-2377.

- [80] Tedjitsop Feudjio F, Dornetshuber R, Lemmens M, Hoffmann O, Lemmens-Gruber R, Berger W. Beauvericin and enniatin: emerging toxins and/or remedies? *World Mycotoxin Journal* 2010; 3(4): 415-430.
- [81] Tomoda H, Huang XH, Cao J, Nishida H, Nagao R, Okuda S, Tanaka H, Omura S, Arai H, Inoue K. Inhibition of acyl-CoA: cholesterol acyltransferase activity by cyclodepsipeptide antibiotics. *J Antibiot (Tokyo)* 1992; 45(10): 1626-1632.
- [82] Rogers MA, Liu J, Song BL, Li BL, Chang CC, Chang TY. Acyl-CoA:cholesterol acyltransferases (ACATs/SOATs): Enzymes with multiple sterols as substrates and as activators. *J Steroid Biochem Mol Biol* 2015; 151: 102-107.
- [83] Chang, T, Li B, Chang CCY, Urano Y. Acyl-coenzyme A:cholesterol acyltransferases. *Am J Physiol Endocrinol Metab* 2009; 297(1): E1-E9.
- [84] Bryleva EY, Rogers MA, Chang CC, Buen F, Harris BT, Rousselet E, Seidah NG, Oddo S, LaFerla FM, Spencer TA, Hickey WF, Chang TY. ACAT1 gene ablation increases 24(S)-hydroxycholesterol content in the brain and ameliorates amyloid pathology in mice with AD. *Proc Natl Acad Sci USA* 2010; 107(7): 3081-3086.
- [85] Murphy SR, Chang CC, Dogbevia G, Bryleva EY, Bowen Z, Hasan MT, Chang TY. Acat1 knockdown gene therapy decreases amyloid- β in a mouse model of Alzheimer's disease. *Mol Ther* 2013; 21(8): 1497-1506.
- [86] Hutter-Paier B, Huttunen HJ, Puglielli L, Eckman CB, Kim DY, Hofmeister A, Moir RD, Domnitz SB, Frosch MP, Windisch M, Kovacs DM. The ACAT inhibitor CP-113,818 markedly reduces amyloid pathology in a mouse model of Alzheimer's disease. *Neuron* 2004; 44(2): 227-238.
- [87] Yue S, Li J, Lee SY, Lee HJ, Shao T, Song B, Cheng L, Masterson TA, Liu X, Ratliff TL, Cheng JX. Cholesteryl ester accumulation induced by PTEN loss and PI3K/AKT activation underlies human prostate cancer aggressiveness. *Cell Metab* 2014; 19(3): 393-406.
- [88] Omura S, Koda H and Nishida H, 1991. Hypolipemics containing beauvericin as acylcoenzyme A cholesterol acyltransferase inhibitor. Patent JP 89-16115019890623.
- [89] Celik M, Aksoy H, Yilmaz S. Evaluation of beauvericin genotoxicity with the chromosomal aberrations, sister-chromatid exchanges and micronucleus assays. *Ecotox Environ Safety* 2010; 73: 1553-1557.
- [90] Lee HS, Song HH, Jeong JH, Shin CG, Choi SU, Lee C. Cytotoxicities of enniatins H, I, and MK1688 from *Fusarium oxysporum* KFCC11363P. *Toxicon* 2008; 51: 1178-1185.
- [91] Dornetshuber R, Heffeter P, Kamyar MR, Peterbauer T, Berger W, Lemmens-Gruber R. Enniatin exerts p53-dependent cytostatic and p53-independent cytotoxic activities against human cancer cells. *Chem Res Toxicol* 2007; 20: 465-473.
- [92] Nilanonta C, Isaka M, Kittakoop P, Trakulnaleamsai S, Tanticharoen M, Thebtaranonth Y. Precursor-directed biosynthesis of beauvericin analogs by the insect pathogenic fungus *Paecilomyces tenuipes* BCC 1614. *Tetrahedron* 2002; 58: 3355-3360.
- [93] Meca G, Font G, Ruiz MJ. Comparative cytotoxicity study of enniatins A, A(1), A(2), B, B-1, B-4 and J(3) on Caco-2 cells, Hep-G(2) and HT-29. *Food Chem Toxicol* 2011; 49: 2464-2469.

- [94] Prosperini A, Meca G, Font G, Ruiz MJ. Study of the cytotoxic activity of beauvericin and fusaproliferin and bioavailability in vitro on Caco-2 cells. *Food Chem Toxicol* 2012; 50: 2356-2361.
- [95] Watjen W, Debbab A, Hohfeld A, Chovolou Y, Kampkotter A, Edrada RA, Ebel R, Hakiki A, Mosaddak M, Totzke F, Kubbutat MH, Proksch P. Enniatins A1, B and B1 from an endophytic strain of *Fusarium tricinctum* induce apoptotic cell death in H4IIE hepatoma cells accompanied by inhibition of ERK phosphorylation. *Mol Nutr Food Res* 2009; 53: 431-440.
- [96] Zahn JX, Burns AM, Liu MPX, Faeth SH, Gunatilaka AAL. Search for cell motility and angiogenesis inhibitors with potential anticancer activity: beauvericin and other constituents of two endophytic strains of *Fusarium oxysporum*. *J Nat Prod* 2007; 70: 227-232.
- [97] Macchia L, Di Paola R, Fornelli F, Nenna S, Moretti A, Napoletano R, Logrieco A, Caiaffa MF, Tursi A, Bottalico A. Cytotoxicity of beauvericin to mammalian cells. In Abstracts of the international seminar on 'Fusariums: Mycotoxins, taxonomy and pathogenicity', May 9-13, Martina Franca, Italy, 1995; 72-73.
- [98] Dornetshuber R, Heffeter P, Sulyok M, Schumacher R, Chiba P, Kopp S, Koellensperger G, Micksche M, Lemmens-Gruber R, Berger W. Interactions between ABC-transport proteins and the secondary *Fusarium* metabolites enniatin and beauvericin. *Mol Nutr Food Res* 2009; 53(7): 904-920.
- [99] Shen S, Zhang W. ABC transporters and drug efflux at the blood-brain barrier. *Rev Neurosci* 2010; 21(1): 29-53.
- [100] Glavinas H, Krajcsi P, Cserepes J, Sarkadi B. The role of ABC transporters in drug resistance, metabolism and toxicity. *Curr Drug Deliv* 2004; 1(1): 27-42.
- [101] Gottesman MM, Fojo T, Bates SE. Multidrug resistance in cancer: role of ATP-dependent transporters. *Nat Rev Cancer* 2002; 2(1): 48-58.
- [102] Leslie EM, Deeley RG, Cole SP. Multidrug resistance proteins: role of P-glycoprotein, MRP1, MRP2, and BCRP (ABCG2) in tissue defense. *Toxicol Appl Pharmacol* 2005; 204(3): 216-237.
- [103] Sharom FJ, Lu P, Liu R, Yu X. Linear and cyclic peptides as substrates and modulators of P-glycoprotein: Peptide binding and effects on drug transport and accumulation. *Biochem J* 1998; 333: 621-630.
- [104] Zhang L, Yan K, Zhang Y, Huang R, Bian J, Zheng C, Sun H, Chen Z, Sun N, An R, Min F, Zhao W, Zhuo Y, You J, Song Y, Yu Z, Lio Z, Yang K, Gao H, Dai H, Zhang X, Wang J, Fu C, Pei G, Liu J, Zhang S, Goodfellow M, Jiang Y, Kuai J, Zhou G, Chen X. High-throughput synergy screening identifies microbial metabolites as combination agents for the treatment of fungal infections. *Proc Natl Acad Sci USA* 2007; 104: 4606-4611.
- [105] Szczepaniak J, Lukaszewicz M, Krasowska A. Detection of inhibitors of *Candida albicans* Cdr transporters using a diS-C3(3) fluorescence. *Front Microbiol* 2015; 6: 176.
- [106] Jestoi M, Rokka M, Peltonen M. Mol. An integrated sample preparation to determine coccidiostats and emerging *Fusarium*-mycotoxins in various poultry tissues with LC-MS/MS. *Nutr Food Res* 2007; 51: 625-637.

-
- [107] Sarkadi B, Özvegy-Laczka C, Német K, Váradi A. ABCG2 - A transporter for all seasons. *FEBS Lett* 2004; 567(1): 116-120.
- [108] Klaric MS, Pepeljnjak S, Rozgaj R. Genotoxicity of fumonisin B1, beauvericin and ochratoxin A in porcine kidney PK15 cells: Effects of individual and combined treatment. *Croatica Chemica Acta* 2008; 81(1): 139-146.
- [109] Klaric MS, Darabos D, Rozgaj R, Kasuba V, Pepeljnjak S. Beauvericin and ochratoxin A genotoxicity evaluated using the alkaline comet assay: single and combined genotoxic action. *Arch Toxicol* 2010; 84: 641-650.
- [110] Fotso J, Smith JS. Evaluation of beauvericin toxicity with the bacterial bioluminescence assay and the Ames mutagenicity bioassay. *J Food Sci* 2003; 68: 1938-1941.
- [111] Behm C, Degen GH, Follmann W. The *Fusarium* toxin enniatin B exerts no genotoxic activity, but pronounced cytotoxicity in vitro. *Mol Nutr Food Res* 2009; 53: 423-430.
- [112] Ficheux AS, Sibiril Y, Parent-Massin D. Effects of beauvericin, enniatin b and moniliformin on human dendritic cells and macrophages: an in vitro study. *Toxicon* 2013; 71: 1-10.
- [113] Tonshin AA, Teplova VV, Andersson MA, Salkinoja-Salonen MS. The *Fusarium* mycotoxins enniatins and beauvericin cause mitochondrial dysfunction by affecting the mitochondrial volume regulation, oxidative phosphorylation and ion homeostasis. *Toxicology* 2010; 276: 49-57.
- [114] Ivanov VT, Evstratov AV, Sumskeya LV, Melnik EI, Chumburidze TS, Portnova SL, Balashova TA, Ovchinnikov YA. Sandwich complexes as a functional form of the enniatin ionophores. *FEBS Lett* 1973; 36(1): 65-71.
- [115] Kamyar M, Rawnduzi P, Studenik CR, Kouri K, Lemmens-Gruber R. Investigation of the electrophysiological properties of enniatins. *Arch Biochem Biophys* 2004; 429(2): 215-223.
- [116] Kouri K, Kamyar MR, Lemmens-Gruber R. Actions of the antibiotic mycotoxins beauvericin and enniatin on mammalian tissue. *Forum Nutr* 2003; 56: 413-414.
- [117] Alberts B, Johnson A, Lewis J, Raff M, Roberts K, Walter P. *Molecular biology of the cell* 4th edition. Garland Science, New York, 2002, pp. 1616.
- [118] Kouri K, Duchon MR, Lemmens-Gruber R. Effects of beauvericin on the metabolic state and ionic homeostasis of ventricular myocytes of the guinea pig. *Chem Res Toxicol* 2005; 18(11): 1661-1668.
- [119] Jow GM, Chou CJ, Chen BF, Tsai JH. Beauvericin induces cytotoxic effects in human acute lymphoblastic leukemia cells through cytochrome c release, caspase 3 activation: the causative role of calcium. *Cancer Lett* 2004; 216(2): 165-173.
- [120] Ivanova L, Egge-Jacobsen WM, Solhaug A, Thoen E, Fæste CK. Lysosomes as a possible target of enniatin B-induced toxicity in Caco-2 cells. *Chem Res Toxicol* 2012; 25(8): 1662-1674.
- [121] Santini A, Meca G, Uhlig S, Ritieni A. Fusaproliferin, beauvericin and enniatins: Occurrence in food - A review. *World Mycotoxin J* 2012; 5: 71-81.
- [122] Habler K, Rychlik M. Multi-mycotoxin stable isotope dilution LC-MS/MS method for *Fusarium* toxins in cereals. *Anal Bioanal Chem* 2016; 408(1): 307-317.
-

- [123] García-Moraleja A, Font G, Mañes J, Ferrer E. Analysis of mycotoxins in coffee and risk assessment in Spanish adolescents and adults. *Food Chem Toxicol* 2015; 86: 225-233.
- [124] Covarelli L, Beccari G, Prodi A, Generotti S, Etruschi F, Meca G, Juan C, Mañes J. Biosynthesis of beauvericin and enniatins in vitro by wheat *Fusarium* species and natural grain contamination in an area of central Italy. *Food Microbiol* 2015; 46: 618-626.
- [125] Tolosa J, Font G, Mañes J, Ferrer E. Natural occurrence of emerging *Fusarium* mycotoxins in feed and fish from aquaculture. *J Agric Food Chem* 2014; 62(51): 12462-12470
- [126] Serrano AB, Font G, Mañes J, Ferrer E. Emerging *Fusarium* mycotoxins in organic and conventional pasta collected in Spain. *Food Chem Toxicol* 2013; 51: 259-266.
- [127] Sebastia N, Meca G, Soriano JM, Manes J. Presence of *Fusarium* emerging mycotoxins in tiger-nuts commercialized in Spain. *Food Control* 2012; 25(2); 631-635.
- [128] de Lourdes Mendes de Souza M, Sulyok M, Freitas-Silva O, Costa SS, Brabet C, Machinski Junior M, Sekiyama BL, Vargas EA, Krska R, Schuhmacher R. Cooccurrence of mycotoxins in maize and poultry feeds from Brazil by liquid chromatography/tandem mass spectrometry. *Scientific World Journal* 2013; 2013: 427369.
- [129] Uhlig S, Erkisen GS, Hofgaard IS, Krska R, Beltrán E, Sulyok M. Faces of a changing climate: Semi-quantitative multi-mycotoxin analysis of grain grown in exceptional climatic conditions in Norway. *Toxins (Basel)* 2013; 5(10): 1682-1697.
- [130] Juan C, Manes J, Raiola A, Ritieni A. Evaluation of beauvericin and enniatins in Italian cereal products and multicereal food by liquid chromatography coupled to triple quadrupole mass spectrometry. *Food Chem* 2013; 140(4): 755-762.
- [131] Tolosa J, Font G, Manes F, Ferrer E. Nuts and dried fruits: natural occurrence of emerging *Fusarium* mycotoxins, *Food Control* 2013; 33: 215-220.
- [132] Mikušová P, Šrobárová A, Sulyok M, Santini A. *Fusarium* fungi and associated metabolites presence on grapes from Slovakia. *Mycotoxin Res* 2013; 29(2): 97-102.
- [133] FAO (Food and Agriculture Organization of the United Nations). Worldwide regulations for mycotoxins in food and feed in 2003. FAO Food and Nutrition Paper No 81, Rome, 2004.
- [134] Leatherhead Food Research. Guide to contaminants in foodstuffs. An international overview of maximum limits. Volumes 1, 2 and 3. Leatherhead Food International Limited, Leatherhead, 2010.
- [135] Manyes L, Escrivá L, Serrano AB, Rodríguez-Carrasco Y, Tolosa J, Meca G, Font G. A preliminary study in Wistar rats with enniatin A contaminated feed. *Toxicol Mech Methods* 2014; 24(3): 179-90.
- [136] Meca G, Mañes J, Font G, Ruiz MJ. Study of the potential toxicity of enniatins A, A(1), B, B(1) by evaluation of duodenal and colonic bioavailability applying an in vitro method by Caco-2 cells. *Toxicon* 2012; 59(1): 1-11.
- [137] Meca G, Mañes J, Font G, Ruiz MJ. Study of the potential toxicity of commercial crispy breads by evaluation of bioaccessibility and bioavailability of minor *Fusarium* mycotoxins. *Food Chem Toxicol* 2012; 50(2): 288-294.

- [138] Devreese M, Broekaert N, De Mil T, Fraeyman S, De Backer P, Croubels S. Pilot toxicokinetic study and absolute oral bioavailability of the *Fusarium* mycotoxin enniatin B1 in pigs. *Food Chem Toxicol* 2014; 63: 161-165.
- [139] Juan C, Manyes L, Font G, Juan-García A. Evaluation of immunologic effect of Enniatin A and quantitative determination in feces, urine and serum on treated Wistar rats. *Toxicol* 2014; 87: 45-53.
- [140] Rodríguez-Carrasco Y, Heilos D, Richter L, Süßmuth RD, Heffeter P, Sulyok M, Kenner L, Berger W, Dornetshuber-Fleiss R. Mouse tissue distribution and persistence of the food-born fusariotoxins enniatin B and beauvericin. *Toxicol Lett* 2016; 247: 35-44.
- [141] Hamann KF. Therapy of isolated acute laryngitis with fusafungin. A phase IV study. *HNO*. 1994; 42(2): 113-118.
- [142] German-Fattal M. Fusafungine, an antimicrobial with anti-inflammatory properties in respiratory tract infections: Review, and recent advances in cellular and molecular activity. *Clinical Drug Investigation* 2001; 21(9): 653-670.
- [143] Lund VJ, Grouin JM, Eccles R, Bouter C, Chabolle F. Efficacy of fusafungine in acute rhinopharyngitis: a pooled analysis. *Rhinology* 2004; 42(4): 207-212.
- [144] EMEA/H/A-31/1420, February 12th, 2016; http://www.ema.europa.eu/docs/en_GB/document_library/Referrals_document/Fusafungine_31/Recommendation_provided_by_Pharmacovigilance_Risk_Assessment_Committee/WC500201885.pdf.
- [145] EMEA/H/A-31/1420, April 1st, 2016; http://www.ema.europa.eu/docs/en_GB/document_library/Referrals_document/Fusafungine_31/Position_provided_by_CMDh/WC500203975.pdf.
- [146] http://www.fagg-afmps.be/nl/news/intrekking_geneesmiddelen_met_fusafungine_locabiotal.
- [147] http://www.ema.europa.eu/ema/index.jsp?curl=pages/medicines/human/referrals/Fusafungine_for_ormucosal_and_nasal_use/human_referral_prac_000054.jsp&mid=WC0b01ac05805c516f.
- [148] Squier CA, Cox P, Hall BK. Enhanced penetration of nitrososornicotine across oral mucosa in the presence of ethanol. *Journal of Oral Pathology & Medicine* 1986; 15(5): 276-279.
- [149] Kai T, Mak VHW, Potts RO, Guy RH. Mechanism of percutaneous penetration enhancement: Effect of n-alkanols on the permeability barrier of hairless mouse skin. *Journal of Controlled Release* 1990; 12(2): 103-112.
- [150] Coutel-Egros A, Maitani Y, Veillard M, Machida Y, Nagai T. Combined effects of pH, cosolvent and penetration enhancers on the in vitro buccal absorption of propranolol through excised hamster cheek pouch. *International Journal of Pharmaceutics* 1992; 84: 117-128.
- [151] Obata Y, Takayama K, Maitani Y, Machida Y, Nagai T. Effect of ethanol on skin permeation of nonionized and ionized diclofenac. *International Journal of Pharmaceutics* 1993; 89(3): 191-198.

- [152] Turunen TM, Urtti A, Paronen P, Audus KL, Rytting JH. Effect of some penetration enhancers on epithelial membrane lipid domains: evidence from fluorescence spectroscopy studies. *Pharmaceutical Research* 1994; 11(2): 288-294.
- [153] Brinkmann I, Muller-Goymann CC. An attempt to clarify the influence of glycerol, propylene glycol, isopropyl myristate and a combination of propylene glycol and isopropyl myristate on human stratum corneum. *Pharmazie* 2003; 60(3): 215-220.
- [154] Williams AC, Barry BW. Penetration enhancers. *Advanced Drug Delivery Reviews* 2004; 56(5): 603-618.
- [155] Nicolazzo JA, Reed BL, Finnin BC. Modification of buccal drug delivery following pretreatment with skin penetration enhancers. *Journal of Pharmaceutical Sciences* 2004; 93(8): 2054-2063.
- [156] Engelbrecht TN, Demé B, Dobner B, Neubert RH. Study of the influence of the penetration enhancer isopropyl myristate on the nanostructure of stratum corneum lipid model membranes using neutron diffraction and deuterium labelling. *Skin Pharmacology and Physiology* 2012; 25(4): 200-207.
- [157] Santos P, Watkinson AC, Hadgraft J, Lane ME. Influence of penetration enhancer on drug permeation from volatile formulations. *International Journal of Pharmaceutics* 2012; 439: 260-268.
- [158] Doran KS, Banerjee A, Disson O, Lecuit M. Concepts and mechanisms: crossing host barriers. *Cold Spring Harb Perspect Med* 2013; 3(7).
- [159] Barry BW. Novel mechanisms and devices to enable successful transdermal drug delivery. *Eur J Pharm Sci* 2001; 14(2): 101-114.
- [160] Nasrollahi SA, Taghibiglou C, Azizi E, Farboud ES. Cell-penetrating peptides as a novel transdermal drug delivery system. *Chemical Biology & Drug Design* 2012; 80(5): 639-646.
- [161] Deli MA. Potential use of tight junction modulators to reversibly open membranous barriers and improve drug delivery. *Biochim Biophys Acta* 2009; 1788(4): 892-910.
- [162] Desai P, Patlolla RR, Singh M. Interaction of nanoparticles and cell-penetrating peptides with skin for transdermal drug delivery. *Mol Membr Biol* 2010; 27(7): 247-259.
- [163] Bouwstra JA, de Graaff A, Gooris GS, Nijse J, Wiechers JW, van Aelst AC. Water distribution and related morphology in human stratum corneum at different hydration levels. *J Invest Dermatol* 2003; 120(5): 750-758.
- [164] Frasch HF, Barbero AM. Application of numerical methods for diffusion-based modeling of skin permeation. *Adv Drug Deliv Rev* 2013; 65(2): 208-220.
- [165] Desmet E, Bracke S, Forier K, Taevernier L, Stuart MC, De Spiegeleer B, Raemdonck K, Van Gele M, Lambert J. An elastic liposomal formulation for RNAi-based topical treatment of skin disorders: Proof-of-concept in the treatment of psoriasis. *Int J Pharm* 2016; 500(1-2): 268-274.
- [166] Boonen J, Baert B, Lambert J, De Spiegeleer B. Skin penetration of silica microparticles. *Pharmazie*. 2011; 66(6): 463-464.

- [167] Nicolazzo JA, Reed BL, Finnin BC. Buccal penetration enhancers - How do they really work? *J Control Release* 2005; 105(1-2): 1-15.
- [168] Sattar M, Sayed OM, Lane ME. Oral transmucosal drug delivery - Current status and future prospects. *Int J Pharm* 2014; 471(1-2): 498-506.
- [169] Adams D. Penetration of water through human and rabbit oral mucosa in vitro. *Arch Oral Biol* 1974; 19(10): 865-872.
- [170] Adams D. The mucus barrier and absorption through the oral mucosa. *J Dent Res* 1975; 54 Spec No B: B19-26.
- [171] Galey WR, Lonsdale HK, Nacht S. The in vitro permeability of skin and buccal mucosa to selected drugs and tritiated water. *Journal of Investigative Dermatology* 1976; 67: 713-717.
- [172] Squier CA, Hall BK. In-vitro permeability of porcine oral mucosa after epithelial separation, stripping and hydration. *Arch Oral Biol* 1985; 30(6): 485-491.
- [173] Squier CA. The permeability of oral mucosa. *Crit Rev Oral Biol Med* 1991; 2(1): 13-32.
- [174] Madhav NV, Shakya AK, Shakya P, Singh K. Orotransmucosal drug delivery systems: a review. *J Control Release* 2009; 140(1): 2-11.
- [175] Petelin M, Šentjurc M, Stolič Z, Skalerič U. EPR study of mucoadhesive ointments for delivery of liposomes into the oral mucosa. *International Journal of Pharmaceutics* 1998; 173(1-2): 193-202.
- [176] Squier CA, Hopps RM. A study of the permeability barrier in epidermis and oral epithelium using horseradish peroxidase as a tracer in vitro. *British Journal of Dermatology* 1976; 95: 123-129.
- [177] Wertz PW, Cox PS, Squier CA, Downing DT. Lipids of epidermis and keratinized and non-keratinized oral epithelia. *Comp Biochem Physiol B* 1986; 83(3): 529-531.
- [178] Ganem-Quintanar A, Falson-Rieg F, Buri P. Contribution of lipid components to the permeability barrier of oral mucosa. *European Journal of Pharmaceutics and Biopharmaceutics* 1997; 44(2): 107-120.
- [179] Squier CA, Cox P, Wertz PW. Lipid content and water permeability of skin and oral mucosa. *J Invest Dermatol* 1991; 96(1): 123-126.
- [180] Saltzman WM, Radomsky ML, Whaley KJ, Cone RA. Antibody diffusion in human cervical mucus. *Biophys J* 1994; 66: 508-515.
- [181] Khanvilkar K, Donovan MD, Flanagan DR. Drug transfer through mucus. *Adv Drug Deliv Rev* 2001; 48(2-3): 173-193.
- [182] Nanci A. *Ten cate's oral histology: Development, structure and function*. 8th Edition. Elsevier, Amsterdam, 2013, pp. 389.
- [183] Rathbone MJ. *Oral mucosal drug delivery*. Marcel Dekker, New York, 1996, pp. 440.
- [184] Deneer VH, Drese GB, Roemelé PE, Verhoef JC, Lie-A-Huen L, Kingma JH, Brouwers JR, Junginger HE. Buccal transport of flecainide and sotalol: effect of a bile salt and ionization state. *Int J Pharm* 2002; 241(1): 127-134.

- [185] Abbott NJ, Patabendige AAK, Dolman DEM, Yusof SR, Begley DJ. Structure and function of the blood–brain barrier. *Neurobiology of Disease* 2010; 37: 13-25.
- [186] Ballabh P, Braun A, Nedergaard M. The blood-brain barrier: an overview: structure, regulation, and clinical implications. *Neurobiol Dis* 2004; 16(1): 1-13.
- [187] Fishman JB, Rubin JB, Handrahan JV, Connor JR, Fine RE. Receptor-mediated transcytosis of transferrin across the blood-brain barrier. *J Neurosci Res* 1987; 18(2): 299-304.
- [188] Duffy KR, Pardridge WM. Blood-brain barrier transcytosis of insulin in developing rabbits. *Brain Res* 1987; 420(1): 32-38.
- [189] Abbott NJ, Rönnbäck L, Hansson E. Astrocyte-endothelial interactions at the blood-brain barrier. *Nat Rev Neurosci* 2006; 7(1): 41-53.
- [190] Banks WA, Kastin AJ. Interactions between the blood–brain barrier and endogenous peptides: emerging clinical implications. *Am J Med Sci* 1988; 295: 459-465.
- [191] Stalmans S, Bracke N, Wynendaele E, Gevaert B, Peremans K, Burvenich C, Polis I, Spiegeleer B. Cell-Penetrating peptides selectively cross the blood-brain barrier in vivo. *PLOS ONE* 2015; 10: e0139652.
- [192] Stalmans S, Gevaert B, Wynendaele E, Nielandt J, De Tré G, Peremans K, Burvenich C, De Spiegeleer B. Classification of peptides according to their blood-brain barrier influx. *Protein Pept Lett* 2015; 22: 768-775.
- [193] Van Dorpe S, Bronselaer A, Nielandt J, Stalmans S, Wynendaele E, Audenaert K, Van De Wiele C, Burvenich C, Peremans K, Hsuchou H, De Tré G, De Spiegeleer B. Brainpeps: the blood-brain barrier peptide database. *Brain Struct Funct* 2012; 217(3): 687-718.
- [194] Verbeken M, Wynendaele E, Mauchauffée E, Bracke N, Stalmans S, Bojnik E, Benyhe S, Peremans K, Polis I, Burvenich C, Gjedde A, Hernandez JF, De Spiegeleer B. Blood-brain transfer and antinociception of linear and cyclic N-methyl-guanidine and thiourea-enkephalins. *Peptides* 2015; 63: 10-21.
- [195] Perkins J. *Atlas of neuroanatomy and neurophysiology*. Icon Custom Communications, Teterboro, New Jersey, 2004, pp. 98.

CHAPTER II

CHEMICAL CLASSIFICATION OF CYCLIC DEPSIPEPTIDES

“Although our intellect always longs for clarity and certainty,
our nature often finds uncertainty fascinating.”

Carl von Clausewitz
(°1780 - †1831, Prussian general and military theorist)

Parts of this chapter were submitted for publication:

Taevernier L, Wynendaele E, Gevaert B, De Spiegeleer B. Chemical classification of cyclic depsipeptides. *Current Protein and Peptide Science* (under revision).

ABSTRACT

Cyclic depsipeptides (CDPs) are a family of cyclic peptide-related compounds, of which the ring is mainly composed of amino- and hydroxy-acid residues joined by amide and ester bonds (at least one), leading to a wide diversity of fascinating chemical structures. They differ not only in their ring structure but also in their side chains, especially by the nature of the unusual and non-amino acid building blocks. To date, however, there is no overall uniform chemical classification system available for CDPs and naming of the diverse family members is done rather arbitrarily. Therefore, a broad evaluation of different CDP structures is done, *i.e.* 1348 naturally occurring CDPs were included, and a straightforward chemical classification system using apparent chemical characteristics is proposed, in order to organize the currently scattered CDP data. The overall validity of the classification approach is verified and the compounds categorized in the same groups are considered to be structurally related. This evaluation also revealed that traditionally formed CDP subfamilies, like the dolastatins, might be misleading from a chemical point of view seen the structural differences in this subfamily. This up-to-date CDP overview enables peptide and natural product scientists to study the wide diversity in CDP structures, their chemical interrelationships and identification of existing and newly found CDPs. Together with the available information on the species producing these CDPs and their reported biological activities, this paper provides a useful tool to gain new insights into this diverse group of peptides.

CHAPTER II

CHEMICAL CLASSIFICATION OF CYCLIC DEPSIPEPTIDES

Main focus in this chapter:

- Organize and structure the scattered cyclic depsipeptide data:
 - present an up-to-date overview containing 1348 naturally occurring CDPs;
 - propose and validate a uniform and straightforward chemical classification system.

1. CYCLIC DEPSIPEPTIDES: A DIVERSE FAMILY

The term ‘cyclic depsipeptides’ (CDPs), also known as ‘cyclodepsipeptides’ or ‘peptolides’, was first introduced in scientific literature in mid-1960s [1,2] and is used to describe cyclic peptide-related compounds of which the ring is mainly composed of amino- and hydroxy-acid residues joined by amide and ester bonds (at least one is required to refer to a depsipeptide), which are commonly, but not necessarily, regularly alternating [1,3,4].

Reports on the isolation of these compounds started as early as the 1940s, *i.e.* with the isolation of enniatin A from the fungus *Fusarium orthoceras* var. *enniatinum* [5]; however, it took decades before scientists began to unravel their biosynthesis [6,7], which is still an active research field today [8-14]. Inspection of the structures of diverse CDP members illustrates that many of these compounds are not only synthesized by non-ribosomal peptide synthases (NRPS) [15-17], but actually are hybrids formed by both NRPS and polyketide synthase (PKS) [10,18,19] or fatty acid (FA) synthase enzyme systems. The latter, however, is still under debate, as Ishidoh and colleagues [12] surprisingly demonstrated that for the cyclic lipodepsipeptide verlamelin, there are no genes coding for fatty acid synthase or even polyketide synthase, suggesting that the hydroxytetradecanoic acid moiety of the CDP is supplied via the primary fatty acid metabolism and then loaded onto the NRPS. It should also be noted that the genes responsible for this biosynthesis reside exclusively in prokaryotic genomes; therefore, it is generally proposed that invertebrate derived CDPs (*e.g.* from sponge origin) are actually synthesized by symbiotic microorganisms [20-22]. Complete understanding of these biosynthetic processes thus seems distant future, especially since only a few enzymes are currently

linked to their biosynthetic products and programming of these enzymes is still poorly understood [19].

These nonribosomal peptides are thus not only comprised of natural amino acids, but also of other unique building blocks, including unusual amino acids and non-amino acid moieties, such as D-amino acids, glycosylated amino acids, N-terminally attached fatty acid chains and N- and C-methylated residues [16,17]. A common feature is their constrained structure, which seems to be required for their bioactivity and is ensured by macrocyclization, whereby parts of the molecule distant in the linear peptide precursor are covalently linked to one another [16,23]. The members of the CDP family differ thus in the ring structure as well as side chains, *i.a.* number of amino- and hydroxy-acids, ring size, molecular mass, lipophilicity and nature of the unusual amino acids and non-amino acid moieties.

Beside their chemical diversity, these peptides also exert a wide range of biological activities, such as histone deacetylase (HDAC) and protease inhibiting activities (*e.g.* romidepsin and cyanopeptolin S, respectively) [24-26], antibacterial (*e.g.* blocking of transglycosylation in bacterial cell wall peptidoglycan synthesis by plusbacins) [27], antifungal (*e.g.* dentigerumycin) [28], immunosuppressive (*e.g.* FK506 (= tacrolimus) and rapamycin, also known as sirolimus) [29], antimalarial (*e.g.* lagunamides) [30], HIV-inhibitory (*e.g.* mirabamides) [31] and cytotoxic activities (*e.g.* kahalalide F is currently under investigation as anti-cancer drug in clinical trials) [32,33].

Overall, a significant number of original research papers has already been published, presenting the identification and structural elucidation of newfound CDPs, sometimes complemented with limited biological activity data. Upon their discovery, these compounds are named very arbitrarily: for some, this is (i) after the geographic location where they were first found (*e.g.* sansalvamide was isolated from a fungal strain obtained from the surface of a sea grass collected in the inner lagoon of Little San Salvador Island, Bahamas) [34], (ii) after the organism they were first isolated from (*e.g.* aureobasidins are synthesized by *Aureobasidium pullulans*) [35] or (iii) after their chemical structure (*e.g.* leualacin consists of the amino acids leucine, N-methylphenylalanine and β -alanine; stevastelin also known as 3,5-dihydroxy-2,4-dimethylstearylvalylthreonyl) [36-38], while for others the origin of the name remains unclear. To date, no clear overall chemical classification system for cyclic depsipeptides exists, despite that different research groups have published reviews with limited scopes: (i) oriented towards only a selected group of organism(s) producing them, (ii) highlighting a limited group of compounds, (iii) focusing on a specific potential biomedical interest, or (iv) placing emphasis on a selected structural or synthesis-related feature (Table 1). Thus, none of them took into account the entire CDP population.

Table 1: Typical examples of cyclic depsipeptide review articles with limited scopes.

Scope	Cyclic depsipeptides discussed	Ref.
<u>General</u>	angolide, amidomycin, enniatins, isariin, pithomycolide, serratamolide, sporidesmolides, valinomycin	[2]
<u>Origin</u>		
<ul style="list-style-type: none"> ▪ <i>Cyanobacteria</i> <ul style="list-style-type: none"> ○ General 	<p>antanapeptin A, cryptophycins, aeruginopeptin 917S-C, anabaenoheptilide 90-A, cyanoheptolin S, hofmannolin, microcystilide A, micropeptin 88-A, nostocyclin, scyptolin A, somamide A, symprostatin 2, tasipeptin, kulolides, lyngbyabellins, malevamide C, microviridins, pitipeptolides, yanucamides</p> <p>anabaenoheptolides, cryptophycins, cyanoheptolins, dolastatins, lyngbyabellins, majusculamide C, oscillapeptins</p>	[39]
<ul style="list-style-type: none"> ○ Lyngbya species 	alotamide A, apratoxins, carriebowamide, cryptophycins, dolastatins, dudawalamide, grassypeptolides, guineamides, hantupeptins, hoiamides, itralamides, kempopeptins, largamides, lyngbyastatins, majusculamide, palmyramide A, pompanopeptin A, somamides, scyptolins, tiglicamides, trungapeptins	[41]
<ul style="list-style-type: none"> ▪ <i>Marine organisms</i> <ul style="list-style-type: none"> ○ General 	arenastatin A, didemnins, discodermins, dolastatins, geodiamolides, halicylindramides, jaspamide, jasplakinolide, microspinosamide, onchidin B, papuamides, polydiscamides, tamandarins, theonellapeptolides	[42]
<ul style="list-style-type: none"> ○ Cyanobacteria 	antillatoxin, apratoxins, coibamide, hoiamides, largazole	[43]
	antanapeptins, antillatoxins, apratoxins, aurilides, guineamides, homodolastatin 16, kulokekahlides, largamides, lyngbyabellins, lyngbyastatin 3, malevamide D, obyanamide, palau'amide, pitipeptolides, somamides, tasipeptins, trungapeptins, ulongamides, wewakpeptins	[44]
<ul style="list-style-type: none"> ○ Indopacific vertebrates 	acremolides, hapalasin, stereocalpin A, taumycins, tausalarins	[45]
<ul style="list-style-type: none"> ○ Macroalgae 	kahalalide A, F	[46]
<ul style="list-style-type: none"> ○ Sponges 	aplidin, arenastatin A, callipeltin A, celebesides, geodiamolides, homophymines, jasplakinolide, microsponosamide, mirabamides, neamphamide A, papuamides, spongidepsin, theopapuamides callipeltins, cyclolithiside A, discodermins, halicylindramides, microspinosamide, papuamides, phoriospongins, polydiscamide A, theonellapeptolides	[3]
<ul style="list-style-type: none"> ○ Lithistid sponges 	callipeltins, discodermins, discokiolides, geodiamolides, jaspamides, neosiphoniamolide A, polydiscamides, theonellapeptolides	[47]
<ul style="list-style-type: none"> ▪ <i>Myxobacteria</i> 	chondramide, miuraenamamide	[48]
<u>Specific class of compounds</u>		
<ul style="list-style-type: none"> ▪ <i>Beauverolides</i> 	beauverolides	[49]
<ul style="list-style-type: none"> ▪ <i>Cyanoheptolins</i> 	aeruginopeptins, cryptophycins, cyanoheptolins, dolastatins, hapalasin, majusculamide C, microcystilide A, micropeptins	[50]
<ul style="list-style-type: none"> ▪ <i>Destruixins</i> 	destruxins, isaridins, roseotoxins	[51]
	destruxins	[52]
<ul style="list-style-type: none"> ▪ <i>Didemnins</i> 	didemnins, tamandarins	[53]
<ul style="list-style-type: none"> ▪ <i>Dolastatins</i> 	dolastatins	[54]
<ul style="list-style-type: none"> ▪ <i>Enniatins</i> 	beauvericin, destruxins, enniatins	[55]
	beauvericin, enniatins	[56]
<u>Biomedical interest</u>	aplidin, apratoxins, beauvericin, beauverolides, celebesides, destruxins, enniatins, eujavanicin, grassypeptolides, guangomides, hantupeptin, hirsutellide, homophymine A, ichtyopeptins, isaridins, isariins, kahalalide F, kempopeptins, largazole, lysobactin, malevamide, mirabamides, miuraenamides, neamphamide A, obyanamide, paecilodepsipeptides, papuamide B, PF1022A, romidepsin, salinamide A, sansalvamide A, serratamolide, spiruchostatin, scopularide, SW-163s, symplocamide A, tasipeptin, ulongapeptin, unnarmicins	[57]
	A83586C, aureobasidin A, azinothricin, beauvericins, callipeltins, citropeptin, cryptophycins, destruxin B, didemnins, dolastatins, emodepside, GE3, geodiamolides, globomycin, haliclamide, hapalasin, himastatin, jasplakinolides, kahalalide F, luzopeptins, lyngbyabellin A, papuamides, PF1022s, pholipeptin, polyoxypeptins, pseudomycins, quinoxapeptins, ramoplanins, romidepsin (FR901228, FK228), sansalvamide, somamide A, stevastellins, ulongamide F, verucopeptin	[58]

Table 1: Typical examples of cyclic depsipeptide review articles with limited scopes (continued).

<u>Structural, synthesis related features</u>		
▪ <i>Bisintercalator products</i>	echinomycins, luzopeptins, quinoxapeptins, sandramycin, SW-163s, triostin	[59]
▪ <i>Cyclisation of depsipeptides</i>	cryptophycins, destruxins, didemnins, dolastatins, dolicolide, enniatins, geodiamolides, hapalosin, jasplakinolides, kahalalides, luzopeptins, stevastelins, tamandarins, valinomycin	[60]
▪ <i>Head-to-side chain cyclic depsipeptides</i>	aeruginopeptins, callipeltins, corticiamide, didemnins, discodermins, halicylindramides, homophymines, kahalalides, largamides, lyngbyastatins, micropeptins, microspinosamide, mirabamides, neamphamides, nostopeptins, oscillapeptins, papuamides, pipecolidepsin, polydiscamides, somamide A, stellatolides, symplocamide A, tamandarins, theopapuamides	[61]
▪ <i>Lipodepsipeptides</i>	A5415s, daptomycins (A21978s), enduracidins, fusaricidins, katanosin, lysobactin, plusbacins, ramoplanins, SF1902s, synringopeptins	[62]
▪ <i>Synthesis challenges</i>	chondramide C, largazole, oxathiocoraline, romidepsin, spiruchostatins, symplocamide A	[63]
▪ <i>Solid-phase synthesis</i>	cotransin/HUN-7293	[64]

Therefore, it was our objective to structure these scattered CDP data and present a broad evaluation of different CDP structures, by proposing an overall classification system for cyclic depsipeptides based on their chemical properties. This should allow natural product researchers to more easily find similar structures. Moreover, this classification can be used for further exploring the taxonomic origin and bio-functionality. More than 1300 unique naturally occurring CDPs were gathered from literature and classified, providing insights into the cyclic depsipeptides as a whole.

2. METHODS

There were three stages in the literature retrieval and appraisal: (i) search of literature databases and searching the reference lists of relevant manuscripts (including reviews) to supplement the electronic searching, (ii) screening search hits for potential eligibility based on the presence of (a) cyclic depsipeptide structure(s) and (iii) data extraction.

2.1. Literature search strategy

An extensive literature search was performed using the search engine ‘Web of Science’, an online web interface providing access to a scientific citation indexing platform that allows a comprehensive cross-disciplinary search in multiple databases. All subscribed databases were used up to March 2016 and the following terms were independently searched for in the ‘topic’ field, including the use of an asterisk to obtain a more comprehensive overview: ‘cyclodepsipeptide*’ (693 hits), ‘peptolide*’ (62 hits), ‘cyclic depsipeptide*’ (1012 hits), ‘cyclic lipodepsipeptide*’ (93 hits), ‘*glyc* cycl* *depsipeptide*’ (140 hits). Additionally, relevant references cited in each of these studies were also included.

2.2. Inclusion assessment

All acquired hits were reviewed for inclusion if the study reported the chemical structure of the cyclic depsipeptide. If reported structures were not cyclic depsipeptides (*e.g.* dolastatins 10 and 15 were excluded, while dolastatins 11-14 and 16 and 17 were included; scytonemide B included, while scytonemide A was excluded) or no chemical structure was given, the hit was excluded. A compound was considered a cyclic depsipeptide if it contained at least an amide and ester bond in the ring structure. Synthetic analogues of CDPs were excluded. In case the absolute stereochemistry remained unassigned or doubtful, the compound was still included in order to obtain a more comprehensive overview. Moreover, only CDPs with allocated unique (trivial) names were included, as for some CDPs no names were yet assigned. For foreign-language papers, the same strategy was followed.

2.3. Data extraction

Data of each withheld CDP were extracted, gathering information concerning the chemical structure, originating organism and reported biological functionality. It should be noted that isolation of the same CDP from a variety of organisms, that have a dietary or a symbiotic relationship, can cloud the issue of the compound's true origin, as was already warned for by Williams *et al.* [65]. For example, bacteria may comprise up to 60% of the total biomass of sponges [66-68]. These microorganisms may be removed from the seawater and pass into the mesohyl of the sponge. Hence, CDPs isolated from sponges may actually be produced by these microorganisms [69-72]. However, the originating species as originally reported in the literature references were listed in the data set of Supporting Information S1. It should also be acknowledged that the reported biological activities suffer from bias, as natural products are often not broadly screened for diverse biological activities, *i.e.* similar structures are often screened for the activity of a known congener, and hence, the reported activities are by no means complete or exhaustive, but rather exemplary. In our list, we thus only have included the reported activities, acknowledging that the absence of a reported activity does not mean the absence of this activity. This has ultimately led to our set of compounds, composed of 1348 naturally occurring cyclic depsipeptides, which is given in Supplementary Information S1, ordered alphabetically on their trivial name and including references, which formed the basis of the list.

3. PROPOSED CLASSIFICATION

A uniform classification system for 1348 cyclic depsipeptides is proposed based on their apparent chemical structures. In this approach, distinctive structural and directly observable features, often

used by peptide and natural product scientists, are used to cluster the diverse members of the cyclic depsipeptide family into different classes.

Ester type

The ester-type in the macrocycle is the first variable, since this chemical characteristic is a required necessity for a compound to be referred to as a cyclic depsipeptide. Formation of the ester bond is achieved between a C-terminus carboxyl group and a hydroxyl acid group. This hydroxyl acid group can either be an α -hydroxy, β -hydroxy or longer chain hydroxyl acid, which are likely of distinct biosynthetic origin (Figure 1).

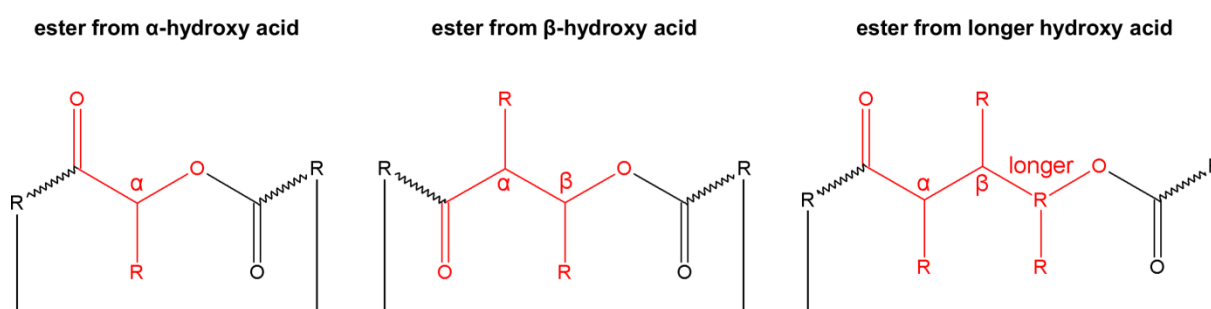


Figure 1: Generic structures for esters of α -hydroxy, β -hydroxy and longer chain hydroxyl acids. The different R-groups can vary depending on the cyclic depsipeptide.

Depsipeptides with a macrocyclic region closed by a β -hydroxy group have already been recognized as a separate CDP category by Pelay-Gimeno *et al.* and termed ‘head-to-side-chain’ CDPs [61].

Additionally, some compounds contain more than one ester bond, therefore combinations are also possible: α + β -hydroxy acid, longer chain + α -hydroxy acid and longer chain + β -hydroxy acid. Based on the hydroxy acid(s) involved in the ester in the ring, six major groups are thus distinguished (Figure 2). However, seen the great structural diversity, further sub-classification per group is required.

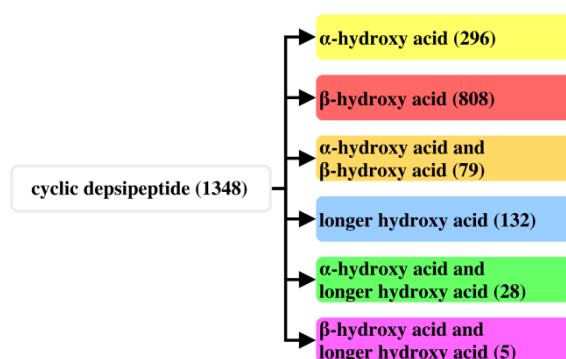


Figure 2: Based on the hydroxy acid(s) involved in the ring ester(s), six major groups are distinguished. Between brackets are the number of CDPs classified in each of the major groups (total $n = 1348$, see Supporting Information S1).

α -hydroxy acid CDPs

For the first group of α -hydroxy acid CDPs (Figure 3), a subdivision is made based on the number of ester bonds in the macrocycle, *i.e.* either one or >1 , which in the latter case can be regularly alternating or irregular, referring again to distinct biosynthetic assembly lines, *i.e.* iterative versus non-iterative [19]. A structural example of each group is shown in Figure 4. Further following down the hierarchical categorisation system for the CDPs with one ester bond, leads to CDPs built up of either solely α -amino acids or both α -amino acids as well as other amino acid building blocks. This split was also made for CDPs containing multiple ester bonds comprised in a single CDP-ring. Figure 4 shows the classification of the α -hydroxy acid CDPs into four major groups after two splits. Depending on the use of this classification system, these groups can be further structured into more well-defined classes, thereby however increasing the complexity of the classification.

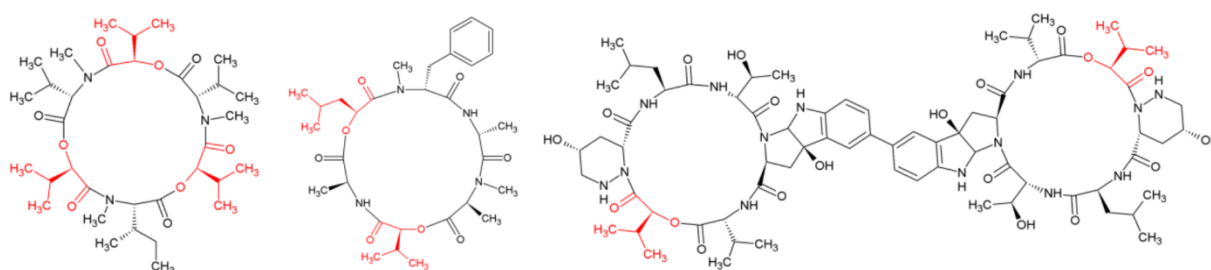


Figure 4: Some examples of CDPs containing multiple ester bonds closed through α -hydroxy acids; in the case of enniatin B1 these are regularly alternating (left), while irregular for guangomide B (mid) and himastatin (right), the former is composed of a single CDP ring, while the latter is built up of two joined CDP rings.

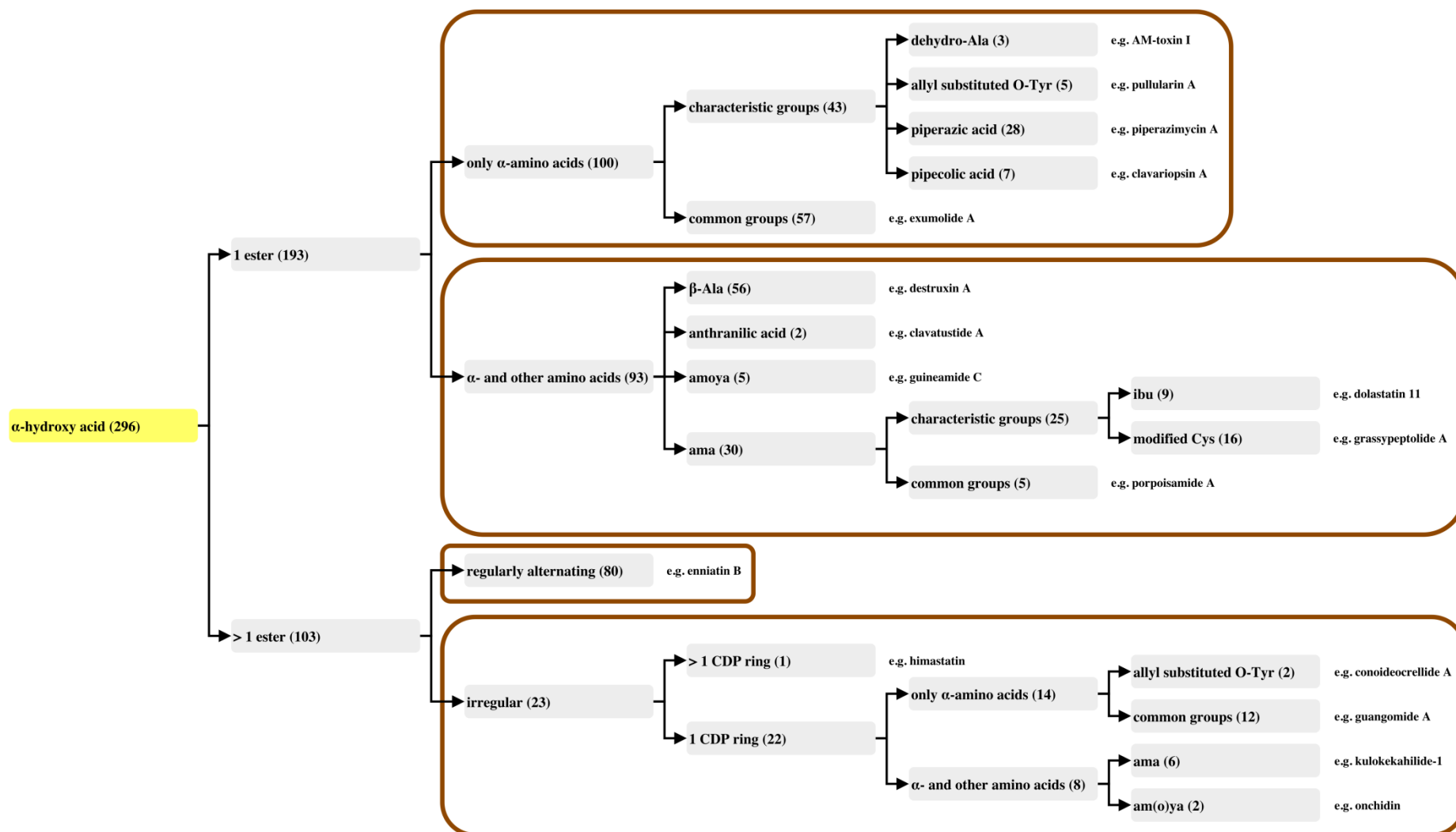


Figure 3: Classification for α-hydroxy acid CDPs, dividing them into four major groups after two splits. Between brackets are the number of CDPs classified in each of the groups.

β -hydroxy acid CDPs

The β -hydroxy acid CDPs or ‘head-to-side-chain’ CDPs (Figure 5) are also first classified based on the number of ester bonds, similar as for the α -hydroxy acid CDPs. Following this first split, the type of β -hydroxy acid is evaluated, originating from a (modified) amino acid or from a short or long chain acid. Illustrative examples are given in Figure 6.

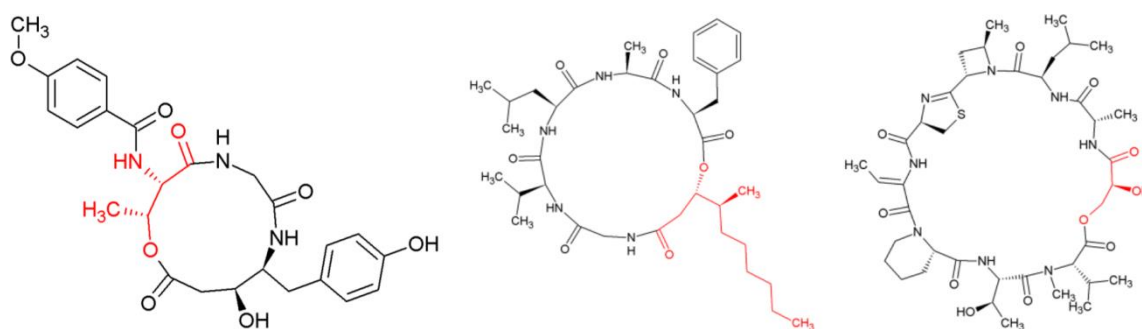


Figure 6: Different types of β -hydroxy acid CDPs containing one ester: melleumin A contains a β -hydroxy acid from threonine (left), whereas arenamide A (mid) and vioprolide A (right) contain a β -hydroxy acid originating from a long, respectively short (glyceric acid) fatty acid.

For the CDPs of which the sole β -hydroxy acid is formed through a (modified) amino acid, further partitioning is based on the identification of some typical building blocks (*e.g.* amino hydroxy/methoxy piperidone (ahp/amp) and piperazic acid, as shown in Figure 7).

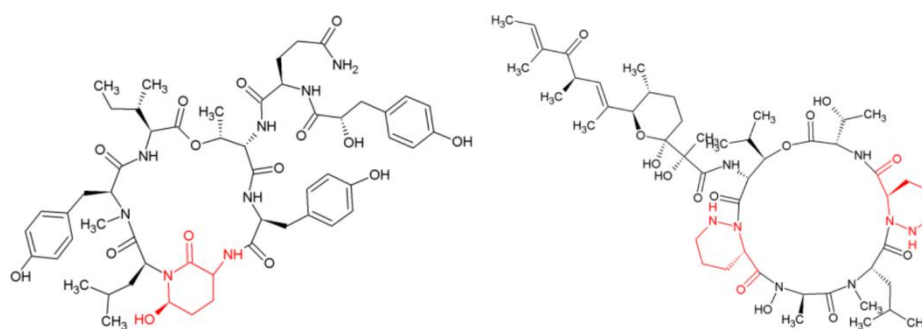


Figure 7: Ahp-containing aeruginopeptin 917S-A (left) and piperazic acid containing GE3 (right).

The CDPs containing more common groups are further classified based on their side chain and four main groups are identified: (i) containing solely amino acids (incl. modified and nonproteinogenic amino acid residues), (ii) both containing amino acids as well as α -hydroxy acids, (iii) a polyketide or FA side chain attached to a (modified) amino acid tail, and finally (iv) the last group does not contain additional amino acids in the side chain. An illustrative example is given for each group in Figure 8. The latter group can also be further distinguished according to the chart in Figure 5. In the case of CDPs from which the sole β -hydroxy acid originates from an acid chain, subdivision is based on saturated or unsaturated.

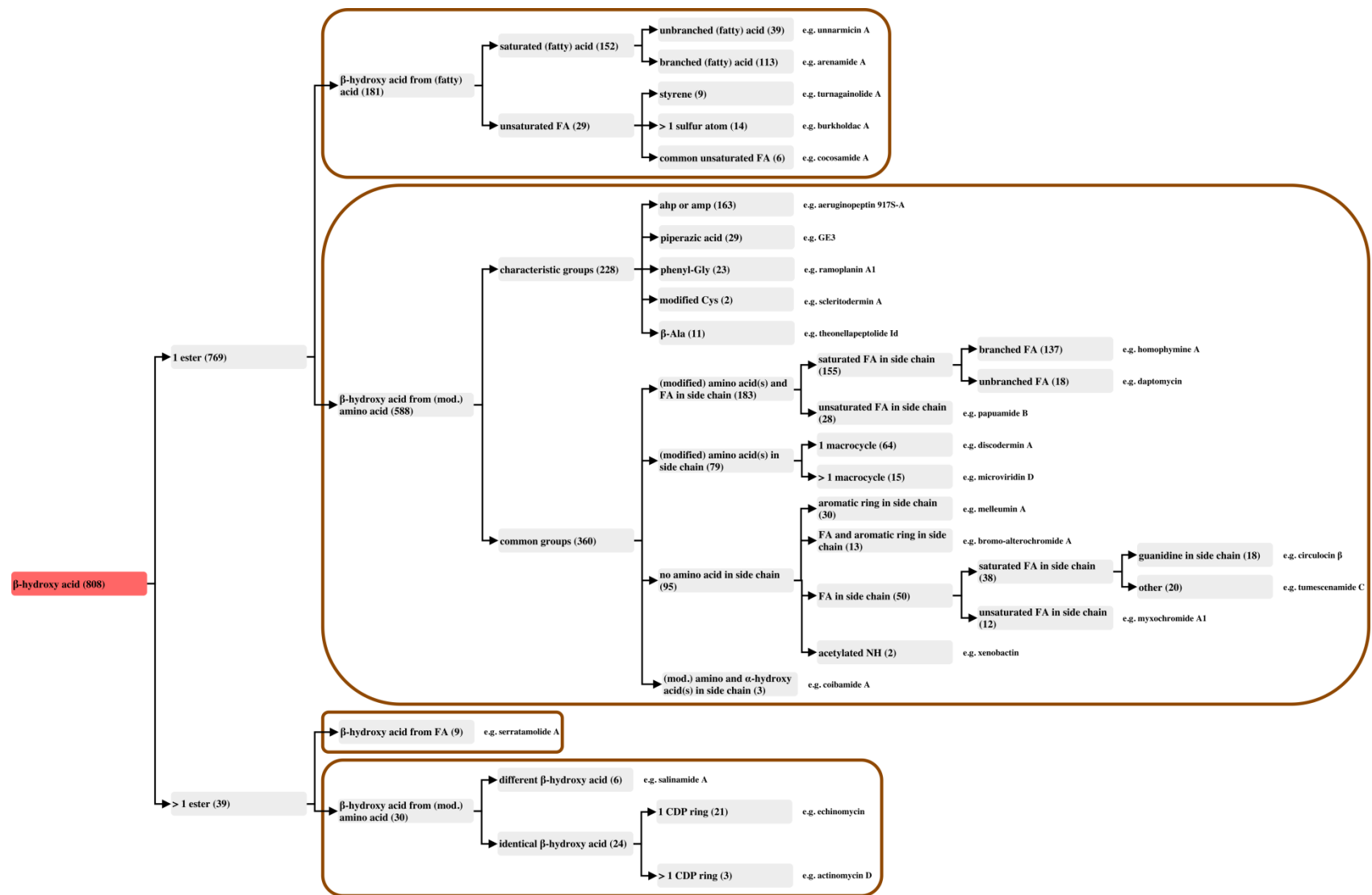
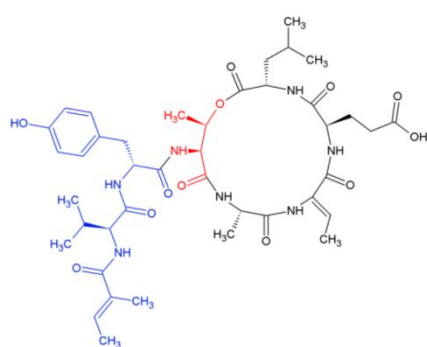


Figure 5: Classification for β -hydroxy acid CDPs, dividing them into four major groups after two splits. Between brackets are the number of CDPs classified in each of the groups.

For CDPs containing multiple β -hydroxy acid esters, distinction is also first made based on the type of β -hydroxy acid. Following the β -hydroxy acid CDPs originating from a (modified) amino acid, distinction is made between CDPs containing different (*e.g.* salinamide A contains 2 ester bonds, one obtained from a threonine residue and another originating from a serine residue) or similar β -hydroxy acid (*e.g.* echinomycin contains 2 ester bonds, both originating from a serine residue), the latter being further divided into one or multiple CDP ring systems.

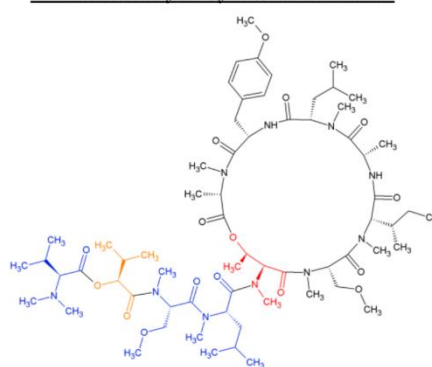
Figure 5 shows the classification of the β -hydroxy acid CDPs into four major groups, again after two splits. As mentioned for the α -hydroxy acids, depending on the use of this classification system, these 4 groups can again be further structured into the proposed, more well-defined classes.

• **Only amino acids in side chain**



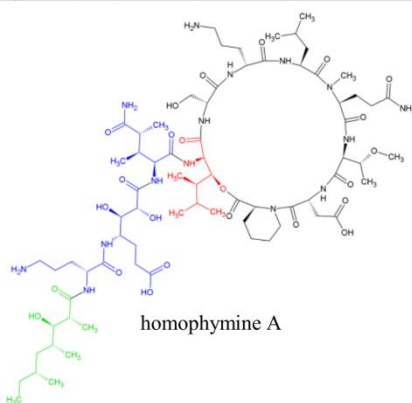
largamide A

• **Amino and α -hydroxy acids in side chain**



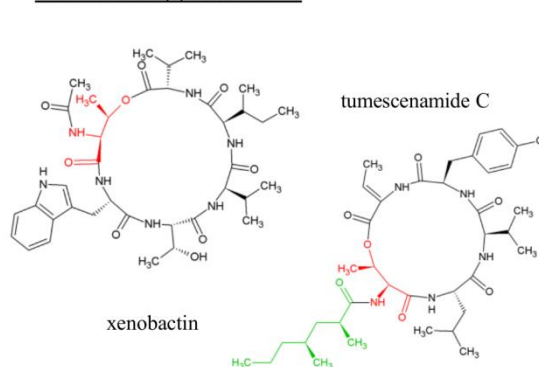
coibamide A

• **Polyketide/FA side chain attached to amino acid tail**



homophymine A

• **No amino acid(s) in side chain**



xenobactin

tumescenamide C

Figure 8: Different types of side chains attached to the β -hydroxy acid CDPs formed from a (modified) amino acid. Ring β -hydroxy acid (red); amino acid tail (blue); α -hydroxy residue (orange); polyketide or FA chain (green).

α - and β -hydroxy acid CDPs

A third group of CDPs contains both an α -hydroxy and β -hydroxy acid (Figure 9), of which the type of β -hydroxy acid is the next relevant feature for further classification, similar as for the β -hydroxy acids. Figure 9 shows their classification into two major groups, which can be further divided into other distinct classes, depending on the level of complexity allowed and needed.

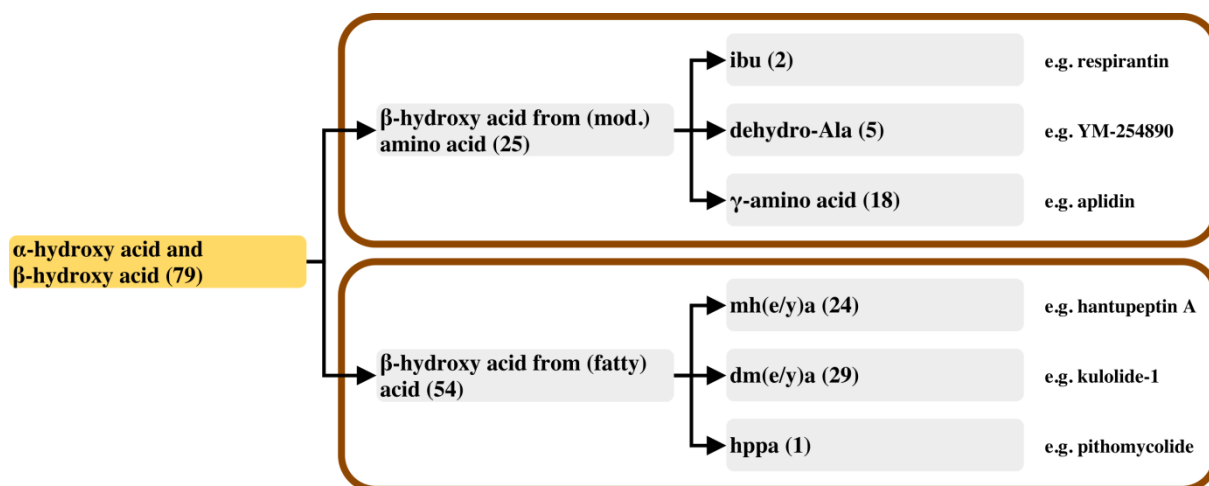


Figure 9: Classification for CDPs containing both an α -hydroxy and β -hydroxy acid, dividing them into two major groups. Between brackets are the number of CDPs classified in each of the groups.

Longer hydroxy acid CDPs

The longer chain hydroxy acid CDPs (Figure 10), whether or not in combination with an α -hydroxy or β -hydroxy acid, are first categorized based on the presence of a modified cysteine residue within the long hydroxyl acid chain, *i.e.* a thiazole or thiazoline unit, which strictly cannot be considered as amino acids anymore. The more common CDPs are categorized based on the type of amino acids in the ring, *i.e.* solely built up of α -amino acids or containing both α -amino acids as well as other amino acid building blocks. Figure 10 shows the classification of the longer hydroxy acid CDPs into four major groups, after two splits.



Figure 10: Classification for CDPs containing a longer hydroxy acid, dividing them into four major groups. Between brackets are the number of CDPs classified in each of the groups.

α/β -hydroxy acid and longer hydroxy acid CDPs

CDPs containing a combination of a longer hydroxy acid and either an α -hydroxy or β -hydroxy acid comprise only a small number of CDP members, as shown in Figure 11.

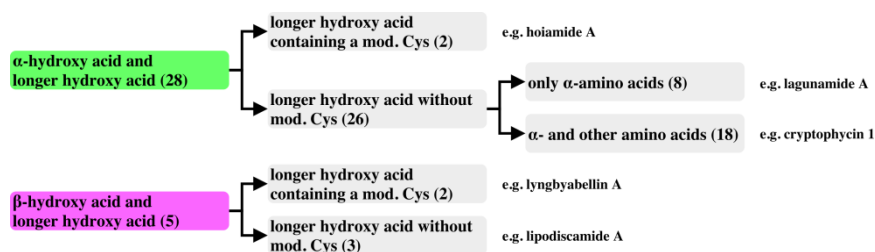


Figure 11: Chart for CDPs containing a longer hydroxy and α -hydroxy/ β -hydroxy acid (top/bottom).

Between brackets are the number of CDPs classified in each of the groups.

Numerical classification code

A numerical classification code is allocated to each of the different groups, creating a workable system, which also allows easy searching for similar CDPs in the list in Supporting Information S1. The first number of the code indicates the type of hydroxy acid(s) involved in the ring ester(s): 1. α -hydroxy acid, 2. β -hydroxy acid, 3. α -hydroxy acid and β -hydroxy acid, 4. longer hydroxy acid, 5. α -hydroxy acid and longer hydroxy acid, and 6. β -hydroxy acid and longer hydroxy acid (see also Figure 2). The second number in the code represents the next split, *e.g.* in the case of longer hydroxy acid CDPs (first number of the code is 4), the second number is 1. for CDPs with a longer hydroxy acid containing a modified cysteine, while for CDPs without a modified cysteine in the longer hydroxy acid this is 2. This way, a number is given to every split, always in descending order from top to bottom. An explanatory example is presented in Figure 12. Moreover, for each of the classes, a structural example is given in Supplementary Information S2.

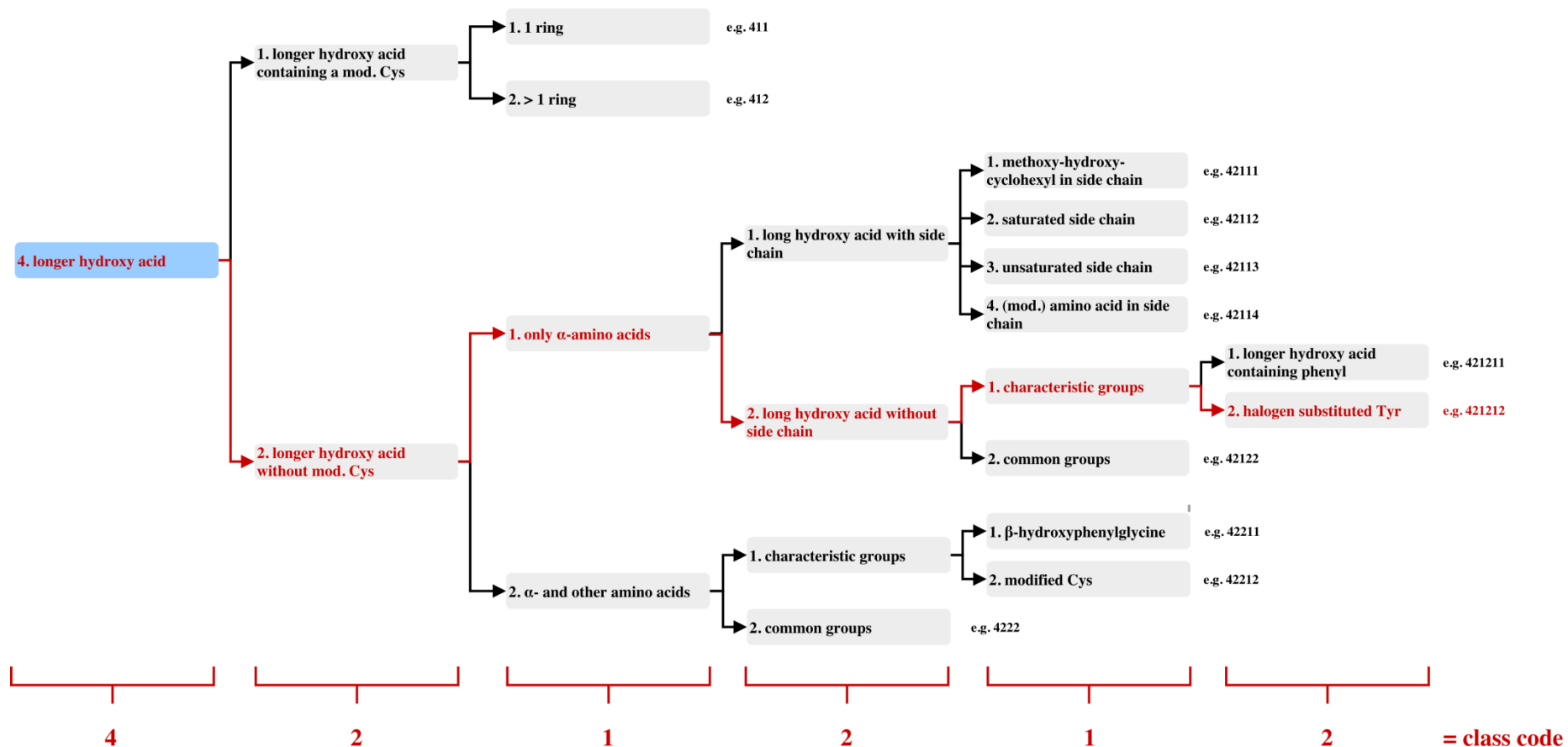
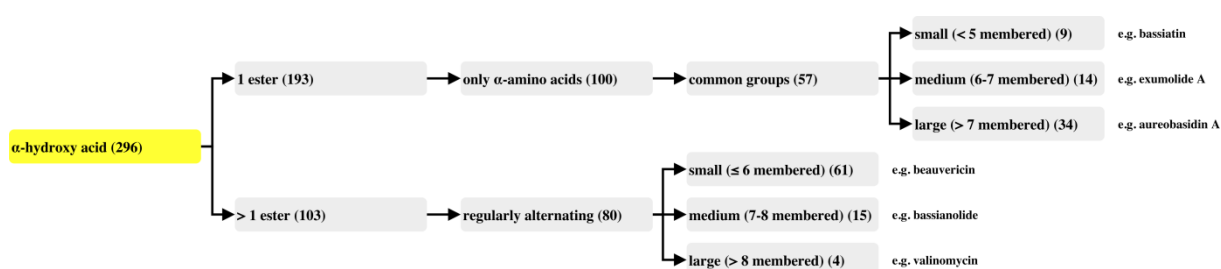


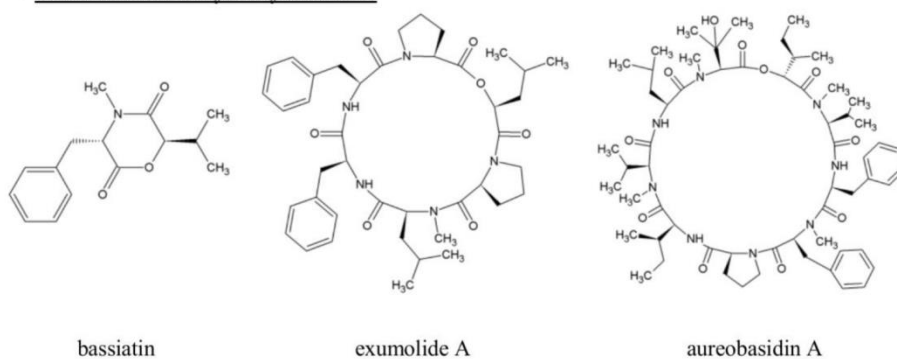
Figure 12: Explanation of the numbering classification code. A number is allocated to each split, forming in the end the classification code for a certain group of CDPs. The example in red is 421212.

Ring size

Moreover, for each of the groups formed after the desired split, ring size can be used as a final cut-off. This variable was not used as primary feature, as the different building blocks/units are considered as repeated chemical subunits and the number of repetitions does not alter its primary chemistry. However, this system allows the ring size to be included as a variable feature, which can be used at any level in addition to the chemical classification features. Some examples of ring size differences within certain groups are given in Figures 13 and 14. It should be noted that to obtain the CDP ring size, the number of building blocks within the main CDP ring is counted, neglecting other rings formed through side chain bridges, *e.g.* disulfide bridge in echinomycin (Figure 14).



• CDPs with one α -hydroxy acid ester



• CDPs with multiple regularly alternating α -hydroxy acid esters

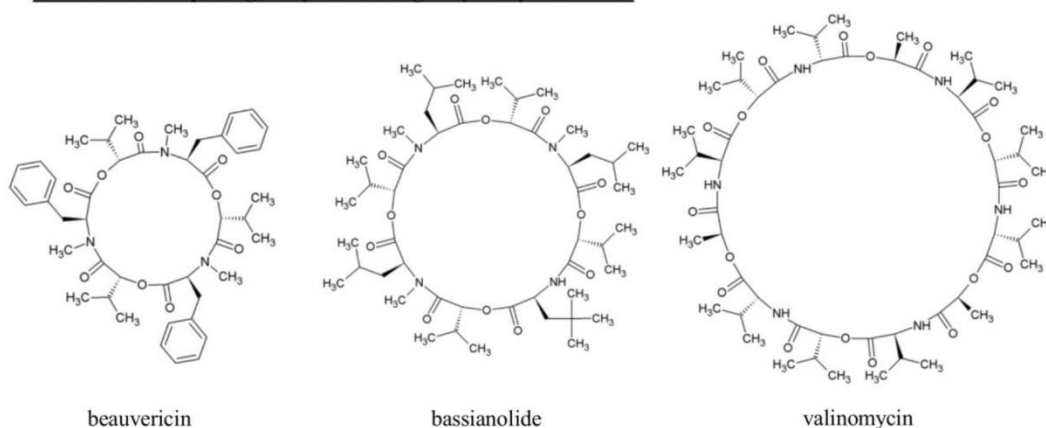
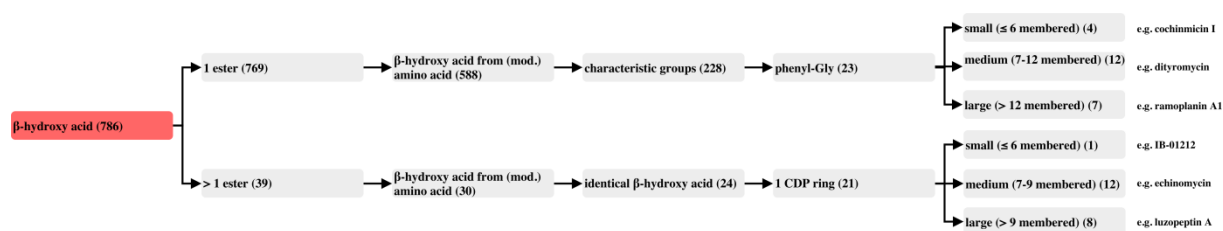
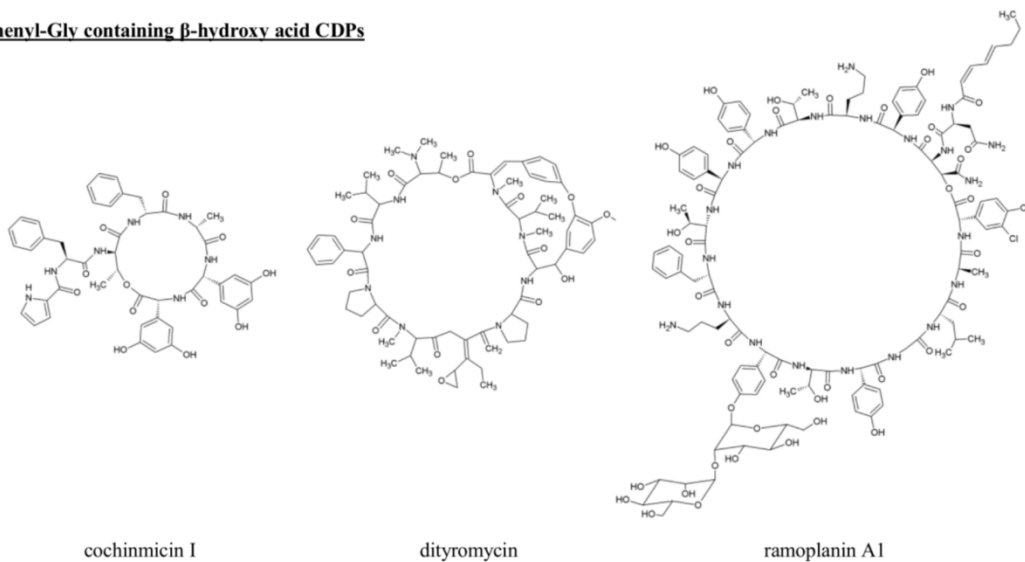


Figure 13: Examples of α -hydroxy acid CDPs with increasing ring sizes (from left to right). Between brackets are the number of CDPs classified in each of the groups.



• **Phenyl-Gly containing β -hydroxy acid CDPs**



• **CDPs with multiple identical β -hydroxy acid esters**

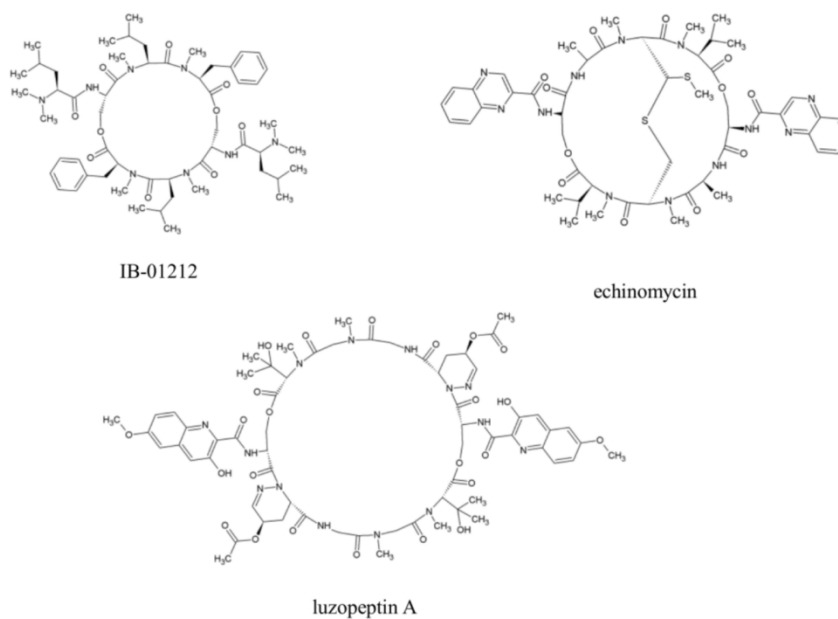


Figure 14: Examples of β -hydroxy acid CDPs with increasing ring sizes (from left to right). Between brackets are the number of CDPs classified in each of the groups.

4. DISCUSSION

The descriptors used in this classification approach are not based on mathematically calculated descriptors such as applied in different software (*e.g.* Dragon), intended for small molecules, but on apparent functional chemical characteristics which have the advantage that the classification system can be applied without the use of chemometric tools.

The 1348 CDPs were classified according to the proposed classification scheme (Supporting Information S1). In order to verify the presented classification system and possibly point to the need for revision of current CDP subfamilies, a comparison with the current literature knowledge of structurally similar CDPs and already existing cyclic depsipeptide families was performed.

α -hydroxy acid CDPs

For the group containing CDPs with a single α -hydroxy acid (Figure 4), consisting of only α -amino acids and lacking other typical building blocks, after 4 splits and an additional split with ring size cut-off, the small 2-membered CDPs (*e.g.* bassiatin, lateritin and ergosecalinine) are clustered together [73]. The classification validity is again confirmed by the literature reported similarity of exumolides, sansalvamides and zygosporamide [74], which are also classified together after 4 splits (class code: 1112).

According to Bai *et al.* dolastatin 11, dolastatin 12, ibu-epidolastatin 12, ibu-epilyngbyastatin 1 and lyngbyastatin 1 are structurally similar [75]. Additionally, majusculamide C and lyngbyastatin 3 have also been reported as congeners [65]. Following the proposed classification strategy, all these CDPs are clustered together in the same group after 6 splits (class code: 112411), *i.e.* single α -hydroxy acid, with both α - as well as other amino acids and the typical ibu (4-amino-2,2-dimethyl-3-oxopentanoic acid, see Figure 15) building block.

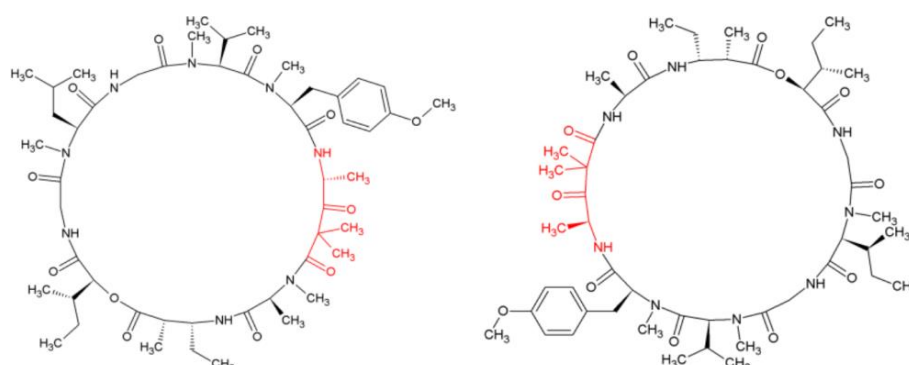


Figure 15: Lyngbyastatin 1 (left) and majusculamide C (right), with their structural ibu (4-amino-2,2-dimethyl-3-oxopentanoic acid) moiety in red.

It should be noted that other members of the ‘dolastatin family’ were found structurally very different, some illustrative examples are shown in Figure 16. Dolastatin 10 and dolastatin E are not

CDPs [76,77]. Dolastatin 13 is an ahp containing β -hydroxy acid CDP (class code: 21211), while dolastatin 14 is a longer hydroxy acid CDP (class code: 42122) and dolastatin 17 is a CDP containing multiple irregular α -hydroxy acids (class code: 12222). This highlights the currently used arbitrary nomenclature for newly discovered compounds (*e.g.* dolastatins were all originally isolated from the sea hare *Dolabella auricularia*,) and the lack of a uniform classification system.

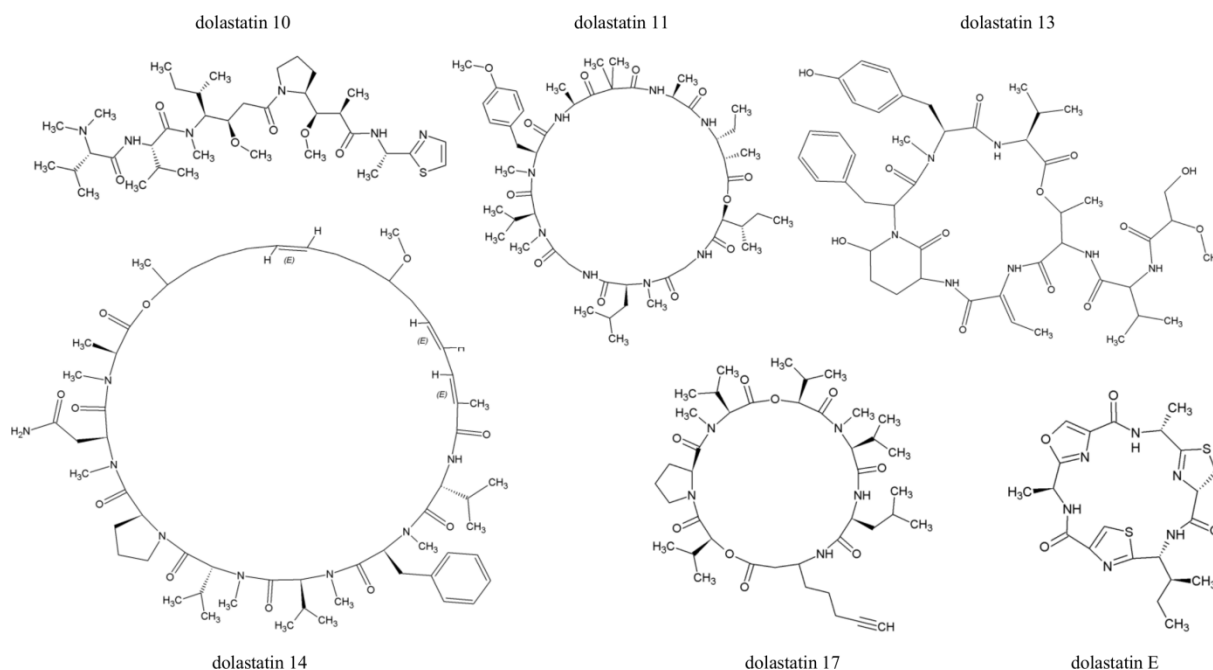


Figure 16: Different members of the ‘dolastatin family’.

Xu and co-workers reported that bassianolide, beauvericin, enniatins and PF1022A are related cyclooligomer nonribosomal depsipeptides derived from repeated structural units, consisting of amino acid and α -hydroxy acid building blocks, undergoing oligomerization via head-to-tail condensation or ligation through side chains and followed by macrocycle closure [78]. Following our proposed classification, all above mentioned CDPs were clustered in the same class after 3 splits (multiple regularly alternating α -hydroxy acids with class code: 121), together with other CDPs, *i.e.* allobauvericins, amidomycin, angolide, arthogalin, bacillistatins, beauvenniatins, cereulide, cordycecin A, montanastatin, sporidesmolides, valinomycin and verticilides. Structural resemblance of bacillistatins, cereulide and valinomycin has also been confirmed in literature [79].

Conoideocrellide A and paecilodepsipeptide A (synonym gliotide) are closely related cyclohexadepsipeptides [80], which are also classified into the same class after 6 splits, *i.e.* CDPs containing multiple α -hydroxy acids that are not regularly alternating (irregular), composed of 1 macrocycle and only α -amino acids and bearing an O-prenyl-L-tyrosine residue (class code: 122211). After 6 splits, other similar cyclohexadepsipeptides are grouped together (class code: 122212): guangomides, hirsutatins, hirsutellide A, pimaydolide, trichodepsipeptides, phomalide and BZR-

cotoxins I, II and III. Trichodepsipeptides and guangomides were also previously reported together [81].

β -hydroxy acid CDPs

Largazole, burkholdacs, thailandepsins, romidepsin and spiruchostatins are considered structurally related and they all exert a similar biological activity as HDAC inhibitors [82]. According to our classification, these CDPs are indeed clustered together after 5 splits, as β -hydroxy acids (Figure 5) with an unsaturated acid chain and containing multiple sulfur atoms (class code: 21122).

According to literature, an important subfamily of closely related compounds are the ahp/amp (amino hydroxy/methoxy piperidone) containing CDPs [50,83-93]. This structural moiety was also considered as relevant feature in the classification of the β -hydroxy acid CDPs (class code: 21211).

The cyclic lipodepsipeptides viscosin, massetolides A-L, viscosinamides A-D, WLIP (white line-inducing principle), pseudophomins A-B and pseudodesmins A-B were previously categorized under the 'viscosin group' by Geudens *et al.* [94] and following our proposed classification system, these are also grouped in the same class after 7 splits, *i.e.* CDPs with a single β -hydroxy acid ester from a (modified) amino acid, consisting of common building blocks and a FA coupled to an amino acid tail as their side chain (class code: 2122111).

Furthermore, Zolova and colleagues appointed the CDPs echinomycin, quinomycins, triostin A, sandramycin, luzopeptins, SW-163 C-G and quinoxapeptins to the same family of natural bisintercalator compounds [59], which also classify together after 5 splits into group 22221.

α - and β -hydroxy acid CDPs

Han and colleagues recognized structural similarity between kulolide-1 and wewakpeptins [95], while Sittachitta *et al.* mentioned that also yanucamides and kulokainalide-1 are related to kulolide-1 [96]. Following our classification system, these compounds were all classified in the same group after 2 splits, *i.e.* containing both an α - and β -hydroxy acid (Figure 9), with a long chain as β -hydroxy acid type. Other compounds belonging to the same class are: antanapeptins, dudawalamide, georgamide, guineamide E, hantupeptins, hapalysin, kulomo'opunalides, mantillamide, naopopeptin, onchidin B, palmyramide A, pitipeptolides, pitiprolamide, trungapeptins, veraguamides and viequeamides. Indeed, hantupeptins and trungapeptins were found structurally similar according to Gupta *et al.* [97] and veraguamides are related to viequamides as reported by Wang *et al.* [98]. Further categorization of this group of compounds can be done in a third split, based on the (fatty) acid chain.

Aplidin (synonyms dehydrodidemnin B, plitidepsin) and tamandarins are acknowledged to be structurally very similar CDPs [99,100], which are also classified together after 3 splits according to our proposed classification strategy (class 313). Both are CDPs consisting of a α -hydroxy acid, as well

as a β -hydroxy acid, with the latter formed through the hydroxyl group of threonine and also with the presence of a γ -amino acid. One additional compound was found in this group, namely pyridomycin, which can eventually be distinguished due to its smaller ring size, *i.e.* 3-membered instead of the 6- and 7-membered tamandarins and didemnins, respectively.

Longer hydroxy acid CDPs

Chondramides, dolicolide, geodiamolides, jaspamides, miuraenamides, neosiphoniamolide A, pipistelides and seragamides were previously found to be closely related [101-105] and according to our classification system, these indeed classify into the same group after 2 splits, *i.e.* longer chain hydroxy-acids (Figure 10) without the presence of a modified cysteine (thiazole/thiazoline) residue. However, as can be seen in Figure 17, these CDPs are clearly further divided into two distinct groups after 2 additional splits: consisting only of α -amino acids and having a halogen atom substitution on the tyrosine residue (dolicolide, geodiamolides (except for geodiamolides H and I), neosiphoniamolide A, miuraenamides and seragamides: class 421212), versus containing also other amino acids, namely β -hydroxy phenyl glycine (chondramides, geodiamolides H and I, jaspamides and pipistelides: class 42211).

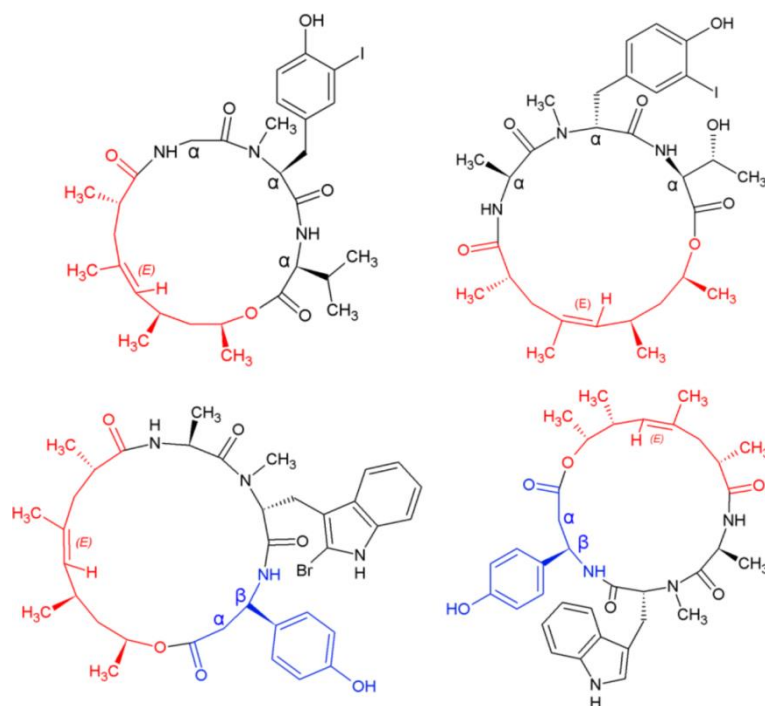


Figure 17: CDPs with longer hydroxy-acids without a modified cysteine residue. Top: consisting only of α -amino acids and having a halogen atom substitution on the tyrosine residue (left: neosiphoniamolide A; right: seragamide A); bottom: containing also other amino acids, namely β -hydroxy phenyl glycine (left: Jaspamide A; right: chondramide C).

The case of geodiamolides is another example indicating that current traditional categorization of compounds in families is rather arbitrarily done, *i.e.* geodiamolides H and I were also named after the sponge (*Geodia* sp.) they were isolated from. However, the presence of their β -hydroxy phenyl glycine moiety, which is absent in the other geodiamolides, but present in *e.g.* pipestelides and jaspamides, suggests a distinct biosynthetic process. As an illustrative example the structure of geodiamolides and are shown in Figure 18.

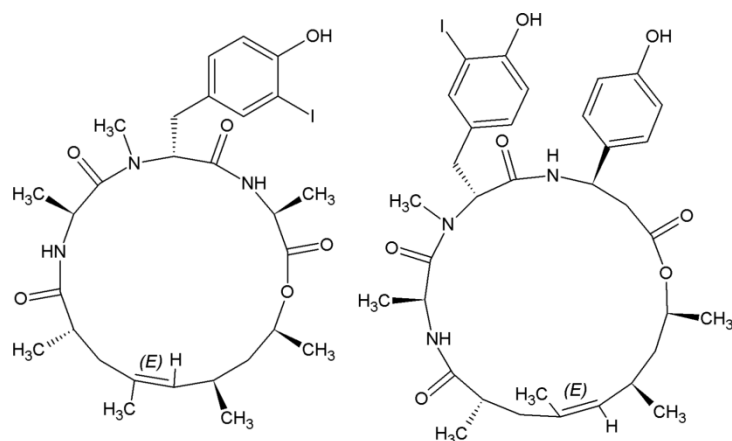


Figure 18: The structurally different geodiamolide A (left) and geodiamolide H (right).

α/β -hydroxy acid and longer hydroxy acid CDPs

According to Tripathi *et al.*, aurilides A, B and C, kulokekahilide-2 and lagunamides A, B and C and palau'amide, CDPs composed of both an α - and longer hydroxy acid, are all structurally related and belong to what is arbitrarily called the 'aurilide class' [30,106,107]. Following the above proposed classification system (Figure 11, top), all of these CDPs were also grouped together after 3 splits (class code: 521).

5. CONCLUSIONS

The presented chemical classification system is a first proposal for a straightforward classification of the diverse CDP compounds based on their apparent chemical characteristics. The overall validity of the classification approach has been verified and the compounds categorized in the same groups are considered to be structurally related, using apparent chemical characteristics. Moreover, it is confirmed that traditional CDP subfamilies (*e.g.* dolastatins and geodiamolides) are named arbitrarily, which might be misleading from a chemical point of view. This large overview enables peptide and natural product scientists to appreciate the wide diversity in CDP structures and their chemical interrelationships and also allows them to identify existing and newly found CDPs. It provides a useful tool to gain new insights into this diverse group of peptides.

6. REFERENCES

- [1] Losse G, Bachmann G. Chemie der Depsipeptide Teil II. Zeitschrift für Chemie 1964; 4: 241-253.
- [2] Russell DW. Cyclodepsipeptides. Q Rev Chem Soc 1966; 20: 559-576.
- [3] Andavan GSB, Lemmens-Gruber R. Cyclodepsipeptides from marine sponges: natural agents for drug research. Mar Drugs 2010; 8(3): 810-834.
- [4] Moss GP, Smith PAS, Tavernier D. Glossary of class names of organic compounds and reactivity intermediates based on structure (IUPAC Recommendations 1995). Pure & Appl Chem 1995; 67: 1307-1375.
- [5] Gaumann E, Roth S, Ettlinger L, Plattner PA, Nager U. Ionophore antibiotics produced by the fungus *Fusarium orthoceras* var. *enniatum* and other. Fusaria Experientia 1947; 3: 202-203.
- [6] Lipmann F. Attempts to map a process evolution of peptide biosynthesis. Science 1971; 173(4000): 875-84.
- [7] Zocher R, Keller U, Kleinkauf H. Enniatin synthetase, a novel type of multifunctional enzyme catalyzing depsipeptide synthesis in *Fusarium oxysporum*. Biochemistry 1982; 21(1): 43-48.
- [8] Al Toma RS, Brieke C, Cryle MJ, Süßmuth RD. Structural aspects of phenylglycines, their biosynthesis and occurrence in peptide natural products. Nat Prod Rep 2015; 32(8): 1207-1235.
- [9] Baltz RH. Combinatorial biosynthesis of cyclic lipopeptide antibiotics: a model for synthetic biology to accelerate the evolution of secondary metabolite biosynthetic pathways. ACS Synth Biol 2014; 3(10): 748-758.
- [10] Brito A, Gaifem J, Ramos V, Glukhov E, Dorrestein PC, Gerwick, WH, Vasconcelos VM, Mendes MV, Tamagnini P. Bioprospecting Portuguese Atlantic coast cyanobacteria for bioactive secondary metabolites reveals untapped chemodiversity. Algal Research 2015; 9: 218-226.
- [11] Hotta K, Keegan RM, Ranganathan S, Fang M, Bibby J, Winn MD, Sato M, Lian M, Watanabe K, Rigden DJ, Kim CY. Conversion of a disulfide bond into a thioacetal group during echinomycin biosynthesis. Angew Chem Int Ed Engl 2014; 53(3): 824-828.
- [12] Ishidoh K, Kinoshita H, Nihira T. Identification of a gene cluster responsible for the biosynthesis of cyclic lipopeptide verlamelin. Appl Microbiol Biotechnol 2014; 98: 7501-7510.
- [13] Marxen S, Stark TD, Rüttschle A, Lücking G, Frenzel E, Scherer S, Ehling-Schulz M, Hofmann T. Depsipeptide intermediates interrogate proposed biosynthesis of cereulide, the emetic toxin of *Bacillus cereus*. Sci Rep 2015; 5: 10637.
- [14] Micallef ML, D'Agostino PM, Sharma D, Viswanathan R, Moffitt MC. Genome mining for natural product biosynthetic gene clusters in the subsection V cyanobacteria. BMC Genomics 2015; 16: 669.
- [15] Marahiel MA, Stachelhaus T, Mootz HD. Modular peptide synthetases involved in nonribosomal peptide synthesis. Chem Rev 1997; 97: 2651-2674.

- [16] Grünewald J, Marahiel MA. Chemoenzymatic and template-directed synthesis of bioactive macrocyclic peptides. *Microbiol Mol Biol Rev* 2006; 70: 131-146.
- [17] Sieber SA, Marahiel MA. Molecular mechanisms underlying nonribosomal peptide synthesis: approaches to new antibiotics. *Chem Rev* 2005; 105: 715-738.
- [18] Desriac F, Jégou C, Balnois E, Brillet B, Le Chevalier P, Fleury Y. Antimicrobial peptides from marine proteobacteria. *Mar Drugs* 2013; 11: 3632-3660.
- [19] Fisch KM. Biosynthesis of natural products by microbial iterative hybrid PKS–NRPS. *RSC Adv* 2013; 3: 18228-18247.
- [20] Piel J. Metabolites from symbiotic bacteria. *Nat Prod Rep* 2004; 21(4): 519-538.
- [21] Faulkner DJ. Highlights of marine natural products chemistry (1972-1999). *Nat Prod Rep* 2000; 17: 1-6.
- [22] Xu Y, Kersten RD, Nam S, Lu L, Al-Suwailem AM, Zheng H, Fenical W, Dorrestein PC, Moore BS, Qian P. Bacterial biosynthesis and maturation of the didemnin anti-cancer agents. *J. Am. Chem Soc* 2012; 134: 8625-8632.
- [23] Kohli RM, Walsh CT. Enzymology of acyl chain macrocyclization in natural product biosynthesis. *Chem Commun* 2003; 7: 297-307.
- [24] Chen Y, Gambs C, Abe Y, Wentworth P, Janda KD. Total synthesis of the depsipeptide FR-901375. *J Org Chem* 2003; 68: 8902-8905.
- [25] Lifshits M, Carmeli S. Metabolites of *Microcystis aeruginosa* bloom material from Lake Kinneret, Israel. *J Nat Prod* 2012; 75: 209-219.
- [26] Mizutani H, Hiraku Y, Tada-Oikawa S, Murata M, Ikemura K, Iwamoto T, Kagawa Y, Okuda M, Kawanishi S. Romidepsin (FK228), a potent histone deacetylase inhibitor, induces apoptosis through the generation of hydrogen peroxide. *Cancer Sci* 2010; 101(10): 2214-2219.
- [27] Maki H, Miura K, Yamano Y. Katanosin B and plusbacin A(3), inhibitors of peptidoglycan synthesis in methicillin-resistant *Staphylococcus aureus*. *Antimicrob Agents Chemother* 2001; 45(6): 1823-1827.
- [28] Oh D, Poulsen M, Currie CR, Clardy J. Dentigerumycin: a bacterial mediator of an ant-fungus symbiosis. *Nat Chem Biol* 2009; 5(6): 391-393.
- [29] Odom A, Muir S, Lim E, Toffaletti DL, Perfect J, Heitman J. Calcineurin is required for virulence of *Cryptococcus neoformans*. *EMBO J* 1997; 16(10): 2576-2589.
- [30] Tripathi A, Puddick J, Prinsep MR, Rottmann M, Tan LT. Lagunamides A and B: cytotoxic and antimalarial cyclodepsipeptides from the marine cyanobacterium *Lyngbya majuscula*. *J Nat Prod* 2010; 73(11): 1810-1814.
- [31] Lu Z, Van Wagoner RM, Harper MK, Baker HL, Hooper JN, Bewley CA, Ireland CM. Mirabamides E-H, HIV-inhibitory depsipeptides from the sponge *Stelletta clavosa*. *J Nat Prod* 2011; 74(2): 185-193.
- [32] Cruz LJ, Luque-Ortega JR, Rivas L, Albericio F. Kahalalide F, an antitumor depsipeptide in clinical trials, and its analogues as effective antileishmanial agents. *Mol Pharm* 2009; 6(3): 813-824.

- [33] Miguel-Lillo B, Valenzuela B, Peris-Ribera JE, Soto-Matos A, Pérez-Ruixo JJ. Population pharmacokinetics of kahalalide F in advanced cancer patients. *Cancer Chemother Pharmacol* 2015; 76(2): 365-374.
- [34] Belofsky GN, Jensen IPR, Fenical W. Sansalvamide: A new cytotoxic cyclic depsipeptide produced by a marine fungus of the genus *Fusarium*. *Tetrahedron Lett* 1999; 40: 2913-2916.
- [35] Ikai K, Shiomi K, Takesako K, Mizutani S, Yamamoto J, Ogawa Y, Ueno M, Kato I. Structure of aureobasidin A. *J Antibiot* 1991; 44: 1187-1198.
- [36] Hamaguchi T, Masuda A, Merino T, Osada H. Stevastelins, a novel group of immunosuppressants, inhibit dual-specificity protein phosphatases. *Chem Biol* 1997; 4: 279-286.
- [37] Morino T, Masuda A, Yamada M, Nishimoto M, Nishikiori T, Saito S, Shimada N. Stevastelins, novel immunosuppressants produced by *Penicillium*. *J Antibiot* 1994; 47: 1341-1343.
- [38] Yoda K, Haruyama H, Kuwano H, Hamano K, Tanzawa K. Conformational analysis of a new cyclic depsipeptide calcium blocker, leualacin, by NMR spectroscopy. *Tetrahedron* 1994; 50: 6537-6548.
- [39] Welker M, von Dohren H. Cyanobacterial peptides - Nature's own combinatorial biosynthesis. *FEMS Microbiology reviews* 2006; 30(4): 530-563.
- [40] Dittmann E, Neilan BA, Borner T. Molecular biology of peptide and polyketide biosynthesis in cyanobacteria. *Appl Microbiol Biotechnol* 2001; 57(4): 467-473.
- [41] Liu L, Rein KS. New peptides isolated from *Lyngbya* species: A Review. *Mar Drugs* 2010; 8(6): 1817-1837.
- [42] Aneiros A, Garateix AA. Bioactive peptides from marine sources: pharmacological properties and isolation procedures. *Journal of Chromatography B* 2004; 803(1): 41-53.
- [43] Nunnery JK, Mevers E, Gerwick WH. Biologically active secondary metabolites from marine cyanobacteria. *Current Opinion in Biotechnology* 2010; 21(6): 787-793.
- [44] Tan LT. Bioactive natural products from marine cyanobacteria for drug discovery. *Phytochemistry* 2007; 68(7): 954-979.
- [45] Kashman Y, Bishara A, Akinin M. Recent N-Atom containing compounds from Indo-Pacific invertebrates. *Mar Drugs* 2010; 8(11): 2810-2836.
- [46] Harnedy PA, FitzGerald RJ. Bioactive proteins, peptides, and amino acids from macroalgae. *Journal of Phycology* 2011; 47(2): 218-232.
- [47] Bewley CA, Faulkner D.J. Lithistid sponges: Star performers or hosts to the stars. *Angewandte Chemie International Edition* 1998; 37(16): 2163-2178.
- [48] Weissman KJ, Mueller R. Myxobacterial secondary metabolites: bioactivities and modes-of-action. *Nat Prod Rep* 2010; 27(9): 1276-1295.
- [49] Tomoda H, Doi T. Discovery and combinatorial synthesis of fungal metabolites beauveriolides, novel antiatherosclerotic agents. *Accounts of Chemical Research* 2008; 41(1): 32-39.

- [50] Weckesser J, Martin C, Jakobi C. Cyanopeptolins, depsipeptides from cyanobacteria. *System Appl Microbiol* 1996; 19(2): 133-138.
- [51] Liu BL, Tzeng YM. Development and applications of destruxins: A review. *Biotechnology Advances* 2012; 30(6): 1242-1254.
- [52] Pedras MSC, Zaharia LI, Ward DE. The destruxins: synthesis, biosynthesis, biotransformation, and biological activity. *Phytochemistry* 2002; 59(6): 579-596.
- [53] Vera MD, Joullie MM. Natural products as probes of cell biology: 20 years of didemnin research. *Medicinal Research Reviews* 2002; 22(2): 102-145.
- [54] Poncet J. The dolastatins, a family of promising antineoplastic agents. *Current Pharmaceutical Design* 1999; 5(3): 139-162.
- [55] Sy-Cordero AA, Pearce CJ, Oberlies NH. Revisiting the enniatins: a review of their isolation, biosynthesis, structure determination and biological activities. *J Antibiot* 2012; 65(11): 541-549.
- [56] Firakova S, Proksa B, Sturdikova M. Biosynthesis and biological activity of enniatins. *Pharmazie* 2007; 62(8): 563-568.
- [57] Lemmens-Gruber R, Kamyar MR, Dornetshuber R. Cyclodepsipeptides - Potential drugs and lead compounds in the drug development process. *Curr Med Chem* 2009; 16(9): 1122-1137.
- [58] Sarabia F, Chammaa S, Ruiz AS, Ortiz LM, Herrera FJ. Chemistry and biology of cyclic depsipeptides of medicinal and biological interest. *Curr Med Chem* 2004; 11(10): 1309-1332.
- [59] Zolova OE, Mady ASA, Garneau-Tsodikova S. Recent developments in bisintercalator natural products. *Biopolymers* 2010; 93: 777-790.
- [60] Davies JS. The cyclization of peptides and depsipeptides. *Journal of Peptide Science* 2003; 9(8): 471-501.
- [61] Pelay-Gimeno M, Tulla-Puche J, Albericio, F. "Head-to-side-chain" cyclodepsipeptides of marine origin. *Mar Drugs* 2013; 11: 1693-1717.
- [62] Bionda N, Cudic P. Cyclic lipodepsipeptides in novel antimicrobial drug discovery. *Croatica Chemica Acta* 2011; 84(2): 315-329.
- [63] Stolze SC, Kaiser M. Challenges in the syntheses of peptidic natural products. *Synthesis-Stuttgart* 2012; 44(12): 1755-1777.
- [64] Coin I. The depsipeptide method for solid-phase synthesis of difficult peptides. *Journal of Peptide Science* 2010; 16(5): 223-230.
- [65] Williams PG, Moore RE, Paul VJ. Isolation and structure determination of lyngbyastatin 3, a lyngbyastatin 1 homologue from the marine cyanobacterium *Lyngbya majuscula*. Determination of the configuration of the 4-amino-2,2-dimethyl-3-oxopentanoic acid unit in majusculamide C, dolastatin 12, lyngbyastatin 1, and lyngbyastatin 3 from cyanobacteria. *J Nat Prod* 2003; 66: 1356-1363.
- [66] Reiswig HM. Particle feeding in natural populations of three marine demosponges. *Biol Bull* 1971; 141: 568-591.

- [67] Reiswig HM. Partial carbon and energy budgets of the bacteriosponge *Verongia fistularis* (Porifera: Demospongiae) in Barbados. *Mar Ecol Prog Ser* 1981; 2: 273-293.
- [68] Ribes M, Coma R, Gili JM. Natural diet and grazing rate of the temperate sponge *Dysidea avara* (Demospongiae, Dendroceratida) throughout an annual cycle. *Mar Ecol Prog Ser* 1999; 176: 179-190.
- [69] Vacelet J, Boury-Esnault N, Fiala-Medioni A, Fisher CR. A methanotrophic carnivorous sponge. *Nature* 1995; 377: 296.
- [70] Beer S, Ilan M. In situ measurements of photosynthetic irradiance responses of two Red Sea sponges growing under dim light conditions. *Mar Biol* 1998; 131: 613-617.
- [71] Schirmer A, Gadkari R, Reeves CD, Ibrahim F, DeLong EF, Hutchinson CR. Metagenomic analysis reveals diverse polyketide synthase gene clusters in microorganisms associated with the marine sponge *Discodermia dissoluta*. *Appl Env Microbiol* 2005; 71: 4840-4849.
- [72] Brück WM, Reed JK, McCarthy PJ. The bacterial community of the lithistid sponge *Discodermia* spp. as determined by cultivation and culture-independent methods. *Mar Biotech* 2012; 14: 762-773.
- [73] Smelcerovic A, Dzodic P, Pavlovic V, Cherneva E, Yancheva D. Cyclodipeptides with a promising scaffold in medicinal chemistry. *Amino Acids* 2014; 46: 825-840.
- [74] Oh D, Jensen PR, Fenical W. Zygosporamide, a cytotoxic cyclic depsipeptide from the marine-derived fungus *Zygosporium masonii*. *Tetrahedron Lett* 2006; 47(48): 8625-8628.
- [75] Bai R, Bates RB, Hamel E, Moore RE, Nakkiew P, Pettit GR, Sufi BA. Lyngbyastatin 1 and ibu-epilyngbyastatin 1: Synthesis, stereochemistry, and NMR line broadening. *J Nat Prod* 2002; 65: 1824-1829.
- [76] Luesch H, Moore RE, Paul VJ, Mooberry SL, Corbett TH. Isolation of dolastatin 10 from the marine cyanobacterium *Symploca* species VP642 and total stereochemistry and biological evaluation of its analogue symplostatins 1. *J Nat Prod* 2001; 64(7): 907-10.
- [77] Ojika M, Nemoto T, Nakamura M, Yamada K. Dolastatin E, a new cyclic hexapeptide isolated from the sea hare *Dolabella auricularia*. *Tetrahedron Lett* 1995; 36(28): 5057-5058.
- [78] Xu Y, Orozco R, Wijeratne EMK, Espinosa-Artiles P, Gunatilaka AAL, Stock SP, Molnár I. Biosynthesis of the cyclooligomer depsipeptide bassianolide, an insecticidal virulence factor of *Beauveria bassiana*. *Fungal Genet Biol* 2009; 46(5): 353-364.
- [79] Pettit GR, Arce PM, Chapuis J, Macdonald CB. Antineoplastic Agents. 600. From the South Pacific Ocean to the silstatins. *J Nat Prod* 2015; 78: 510-523.
- [80] Sivanathan S, Scherkenbeck J. Cyclodepsipeptides: A rich source of biologically active compounds for drug research. *Molecules* 2014; 19: 12368-12420.
- [81] Sy-Cordero AA, Graf TN, Adcock AF, Kroll DJ, Shen Q, Swanson SM, Wani MC, Pearce CJ, Oberlies NH. Cyclodepsipeptides, sesquiterpenoids, and other cytotoxic metabolites from the filamentous fungus *Trichothecium* sp. (MSX 51320). *J Nat Prod* 2011; 74: 2137-2142.

- [82] Benelkebir H, Hodgkinson C, Duriez PJ, Hayden AL, Bulleid RA, Crabb SJ, Packham G, Ganesan A. Enantioselective synthesis of tranlycypromine analogues as lysine demethylase (LSD1) inhibitors. *Bioorg Med Chem* 2011; 19(12): 3709-3716.
- [83] Bonjouklian R, Smitka TA, Hunt AH, Occolowitz JL, Perun TJJ, Doolin L, Stevenson S, Knauss L, Wijayarathne R, Szweczyk S, Patterson GML. A90720A, A serine protease inhibitor isolated from a terrestrial blue-green alga *Microchaete loftakensis*. *Tetrahedron* 1996; 52: 395-404.
- [84] Fujii K, Sivonen K, Naganawa E, Harada KI. Non-toxic peptides from toxic cyanobacteria, *Oscillatoria agardhii*. *Tetrahedron* 2000; 56: 725-733.
- [85] Gunasekera SP, Miller MW, Kwan JC, Luesch H, Paul VJ. Molassamide, a depsipeptide serine protease inhibitor from the marine cyanobacterium *Dichothrix utahensis*. *J Nat Prod* 2010; 73(3): 459-462.
- [86] Kang H-S, Kronic A, Orjala J. Stigonemapeptin, an ahp-containing depsipeptide with elastase inhibitory activity from the bloom-forming freshwater cyanobacterium *Stigonema* sp. *J Nat. Prod* 2012; 75: 807-811.
- [87] Linington RG, Edwards DJ, Shuman CF, McPhail KL, Matainaho T, Gerwick WH. Symplocamide A, a potent cytotoxin and chymotrypsin inhibitor from the marine Cyanobacterium *Symploca* sp. *J Nat Prod* 2008; 71: 22-27.
- [88] Matthew S, Ross C, Paul VJ, Luesch, H. Intramolecular modulation of serine protease inhibitor activity in a marine cyanobacterium with antifeedant properties. *Tetrahedron* 2008; 64: 4081-4089.
- [89] Nogle LM, Okino T, Gerwick WH. Somamides A and B, two new depsipeptide analogues of dolastatin 13 from a Fijian cyanobacterial assemblage of *Lyngbya majuscula* and *Schizothrix* species. *J Nat Prod* 2001; 64: 983-985.
- [90] Okino T, Qi S, Matsuda H, Murakami M, Yamaguchi K. Nostopeptins A and B, elastase inhibitors from the cyanobacterium *Nostoc minutum*. *J Nat Prod* 1997; 60: 158-161.
- [91] Rubio BK, Parrish SM, Yoshida W, Schupp PJ, Schils T, Williams PG. Depsipeptides from a Guamanian marine cyanobacterium, *Lyngbya bouillonii*, with selective inhibition of serine proteases. *Tetrahedron Lett* 2010; 51: 6718-6721.
- [92] Taori K, Matthew S, Rocca JR, Paul VK, Luesch H. Lyngbyastatins 5-7, potent elastase inhibitors from Floridian marine cyanobacteria, *Lyngbya* spp. *J Nat Prod* 2007; 70: 1593-1600.
- [93] Taori K, Paul VJ, Luesch H. Kempopeptins A and B, serine protease inhibitors with different selectivity profiles from a marine cyanobacterium, *Lyngbya* sp. *J Nat Prod* 2008; 71: 1625-1629.
- [94] Geudens N, De Vleeschouwer M, Feher K, Rokni-Zadeh H, Ghequire MGK, Madder A, De Mot R, Martins JC, Sinnaeve D. Impact of a stereocentre inversion in cyclic lipodepsipeptides from the viscosin group: a comparative study of the viscosinamide and pseudodesmin conformation and self-assembly. *Chembiochem* 2014; 15: 2736-2746.
- [95] Han B, Goeger D, Maier CS, Gerwick WH. The wewakpeptins, cyclic depsipeptides from a Papua New Guinea collection of the marine cyanobacterium *Lyngbya semiplena*. *J Org Chem* 2005; 70(8): 3133-3139.

- [96] Sitachitta N, Williamson RT, Gerwick WH. Yanucamides A and B, two new depsipeptides from an assemblage of the marine cyanobacteria *Lyngbya majuscula* and *Schizothrix* species. *J Nat Prod* 2000; 63(2): 197-200.
- [97] Gupta DK, Ding GC, Teo YC, Tan LT. Absolute stereochemistry of the β -hydroxy acid unit in hantupeptins and trungapeptins. *Nat Prod Commun* 2016; 11(1): 69-72.
- [98] Wang D, Song S, Tian Y, Xu Y, Miao Z, Zhang A. Total synthesis of the marine cyclic depsipeptide viequeamide A. *J Nat Prod* 2013; 76(5): 974-978.
- [99] Gutiérrez-Rodríguez M, Martín-Martínez M, García-López MT, Herranz R, Cuevas F, Polanco C, Rodríguez-Campos I, Manzanares I, Cárdenas F, Feliz M, Lloyd-Williams P, Giralt E. Synthesis, conformational analysis, and cytotoxicity of conformationally constrained aplidine and tamandarin A analogues incorporating a spirolactam beta-turn mimetic. *J Med Chem* 2004; 47(23): 5700-5712.
- [100] Lee J, Currano JN, Carroll PJ, Joullié MM. Didemnins, tamandarins and related natural products. *Nat Prod Rep* 2012; 29(3): 404-424.
- [101] Ghosh AK, Dawson ZL, Moon DK, Bai R, Hamel E. Synthesis and biological evaluation of new jasplakinolide (jaspamide) analogs. *Bioorg Med Chem Lett* 2010; 20(17): 5104-5107.
- [102] Jansen R, Kunze B, Reichenbach H, Höfle G. Antibiotics from gliding bacteria, LXX Chondramides A–D, new cytostatic and antifungal cyclodepsipeptides from *Chondromyces crocatus* (Myxobacteria): Isolation and structure elucidation. *Liebigs Ann* 1996; 2: 285-290.
- [103] Karmann L, Schultz K, Herrmann J, Miller R, Kazmaier U. Total syntheses and biological evaluation of miuraenamides. *Angew Chem Int Ed* 2015; 54: 4502-4507.
- [104] Sorres J, Martin M-T, Petek S, Levaique H, Cresteil T, Ramos S, Thoison O, Debitus C, Al-Mourabit A. Pipestelides A–C: Cyclodepsipeptides from the Pacific marine sponge *Pipestela candelabra*. *J Nat Prod* 2012; 75: 759-763.
- [105] Tanaka C, Tanaka J, Bolland RF, Marriott G, Higa, T. Seragamides A-F, new actin-targeting depsipeptides from the sponge *Suberites japonicus* Thiele. *Tetrahedron* 2006; 62: 3536-3542.
- [106] Tripathi A, Puddick J, Prinsep MR, Rottmann M, Chan KP. Lagunamide C, a cytotoxic cyclodepsipeptide from the marine cyanobacterium *Lyngbya majuscula*. *Phytochem* 2011; 72: 2369-2375.
- [107] Tripathi A, Fang W, Leong DT, Tan LT. Biochemical studies of the lagunamides, potent cytotoxic cyclic depsipeptides from the marine cyanobacterium *Lyngbya majuscula*. *Mar Drugs* 2012; 10: 1126-1137.

SUPPLEMENTARY INFORMATION

S1. List of 1348 naturally occurring cyclic depsipeptides.

S2. Structural examples of cyclic depsipeptides for each of the proposed classes.

Table S1-1: List of 1348 naturally occurring cyclic depsipeptides.

See CD-ROM attached at the end of this thesis.

Table S1-2: References.

See CD-ROM attached at the end of this thesis.

Table S2: Structural examples of cyclic depsipeptides for each of the proposed classes.

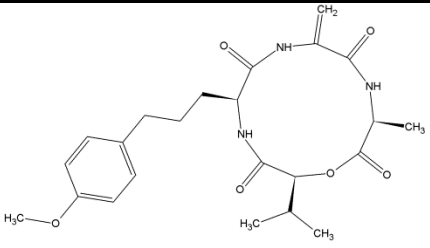
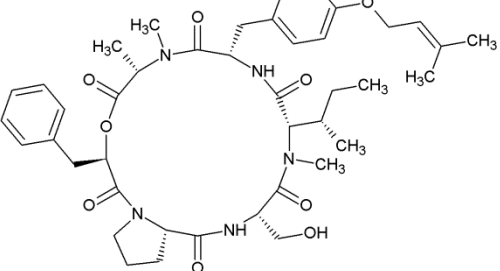
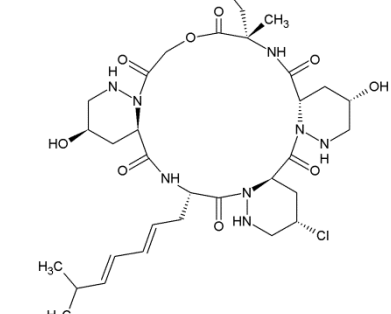
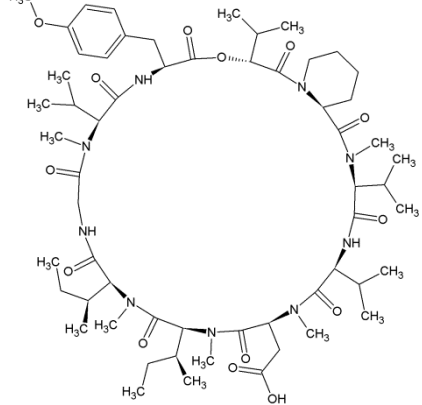
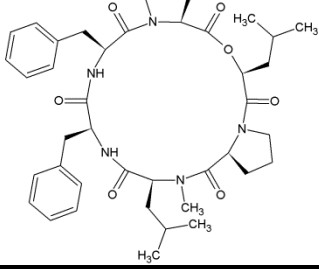
Class code	Cyclic depsipeptide	Structure
11111	AM-toxin I	
11112	Pullularin A	
11113	Piperazimycin A	
11114	Clavariopsin A	
1112	Exumolide A	

Table S2: Structural examples of cyclic depsipeptides for each of the proposed classes (continued).

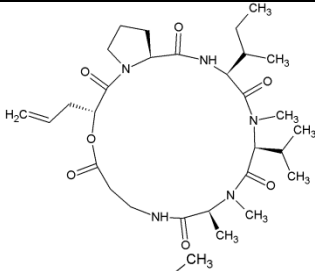
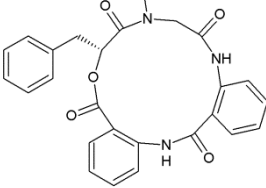
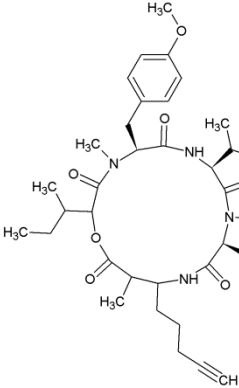
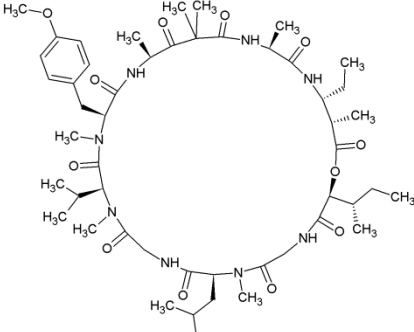
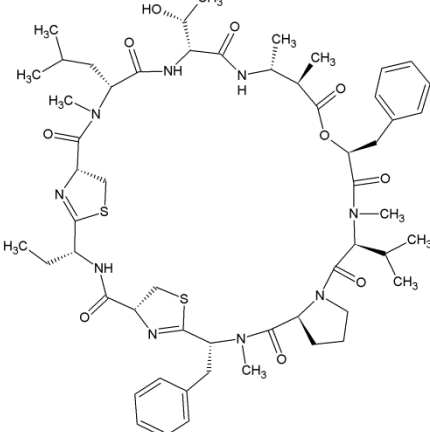
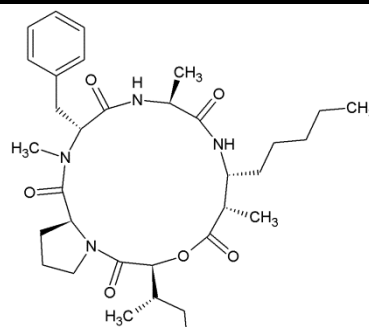
1121	Destruxin A	
1122	Clavatustide A	
1123	Guineamide C	
<i>The absolute stereochemistry of the Hmpa and Maoya substructures remain unassigned.</i>		
112411	Dolastatin 11	
112412	Grassypeptolide A	

Table S2: Structural examples of cyclic depsipeptides for each of the proposed classes (continued).

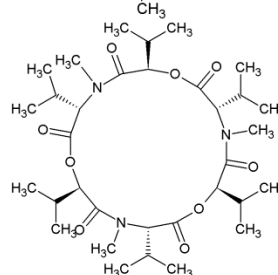
11242

Porpoisamide A



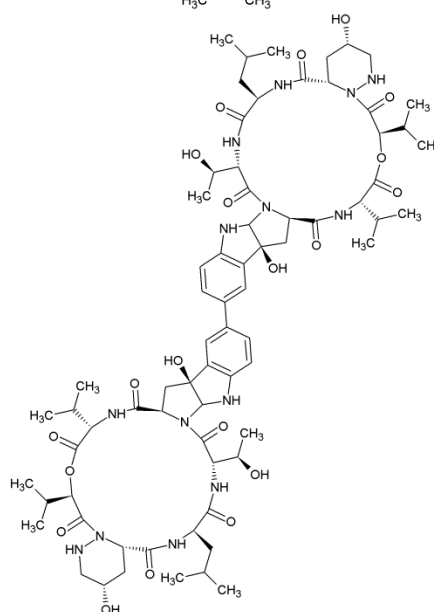
121

Enniatin B



1221

Himastatin



122211

Conoideocrellide A

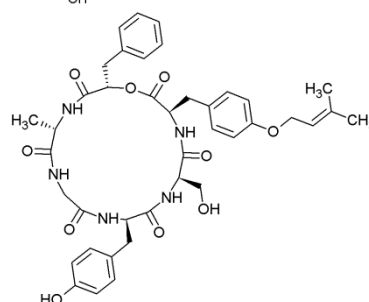
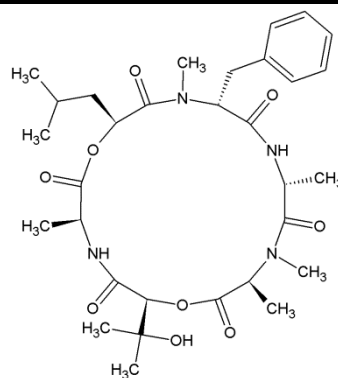
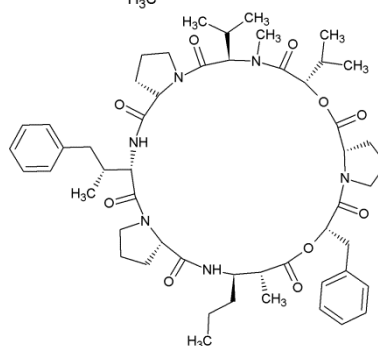


Table S2: Structural examples of cyclic depsipeptides for each of the proposed classes (continued).

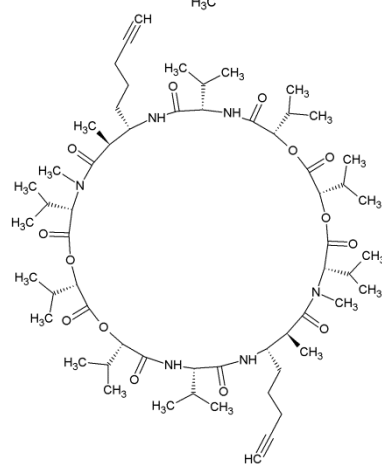
122212 Guangomide A



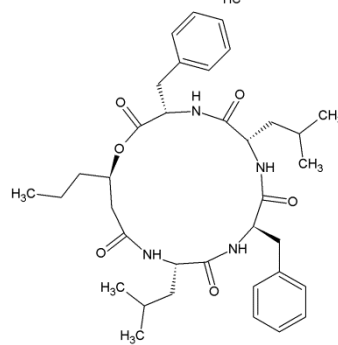
122221 Kulokekahilide-1



122222 Onchidin



21111 Unnarmicin A



21112 Arenamide A

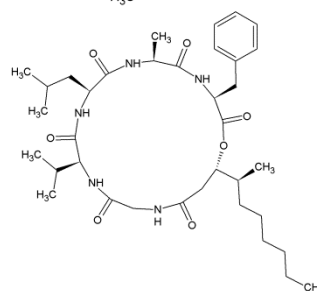
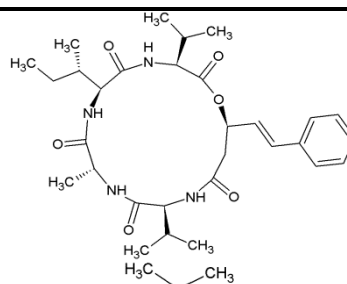
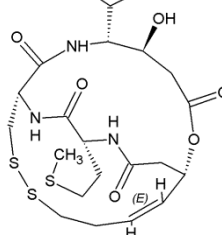


Table S2: Structural examples of cyclic depsipeptides for each of the proposed classes (continued).

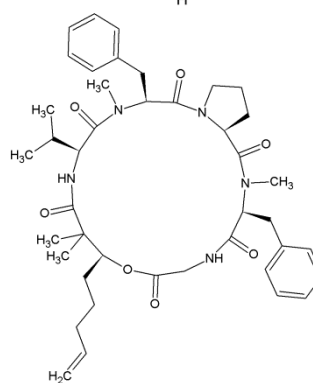
21121 Turnagainolide A



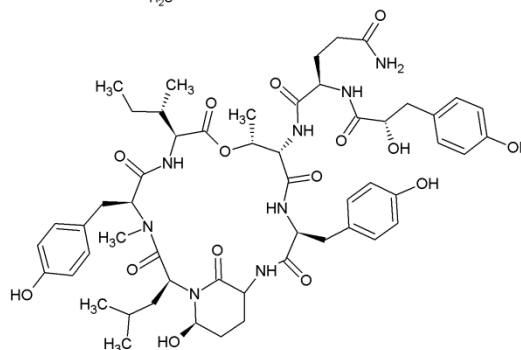
21122 Burkholdac A



21123 Cocosamide A



21211 Aeruginopeptin 917S-A



21212 GE3

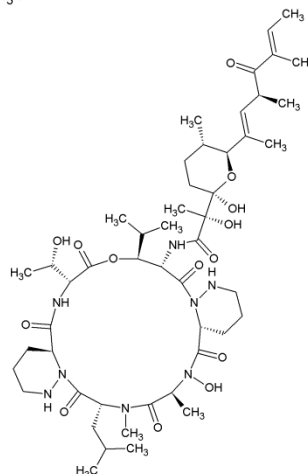
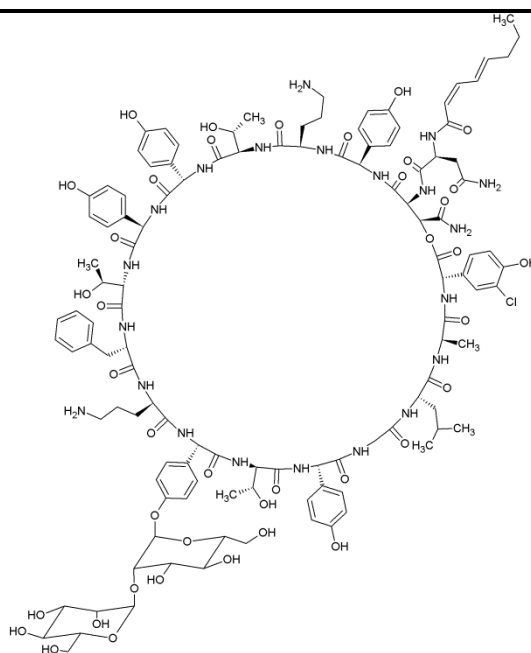


Table S2: Structural examples of cyclic depsipeptides for each of the proposed classes (continued).

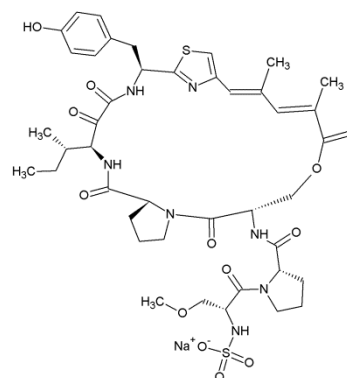
21213

Ramoplanin A1



21214

Scleritodermin A



21215

Theonellapeptolide Id

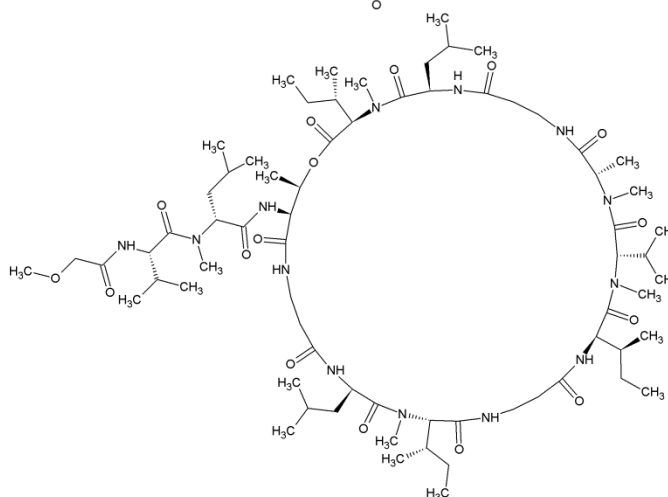
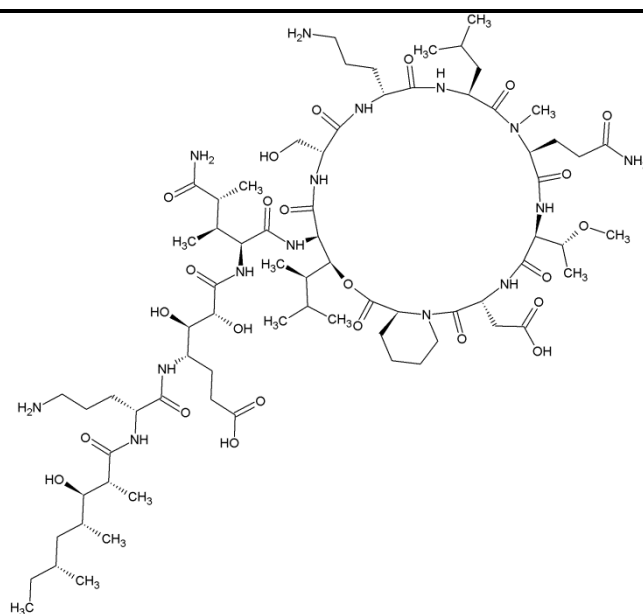
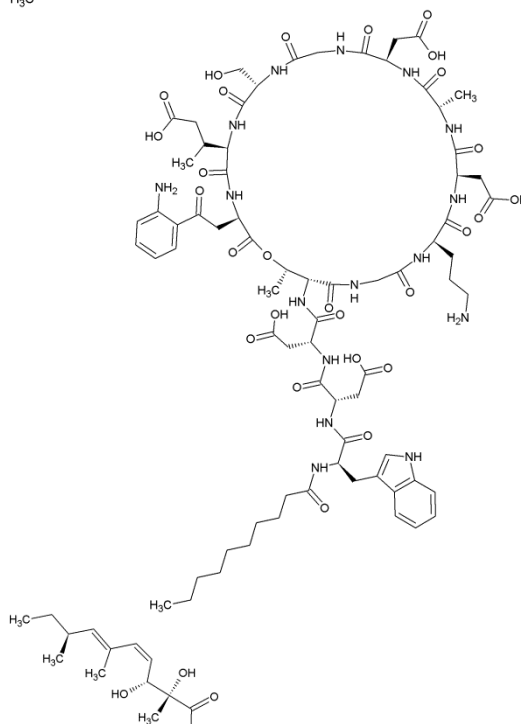


Table S2: Structural examples of cyclic depsipeptides for each of the proposed classes (continued).

2122111 Homophymine A



2122112 Daptomycin



212212 Papuamide B

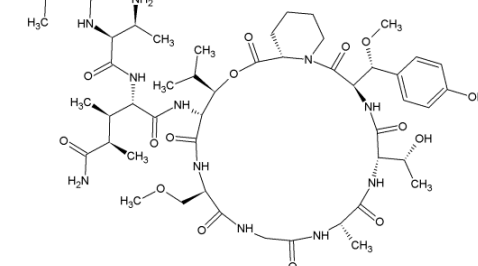
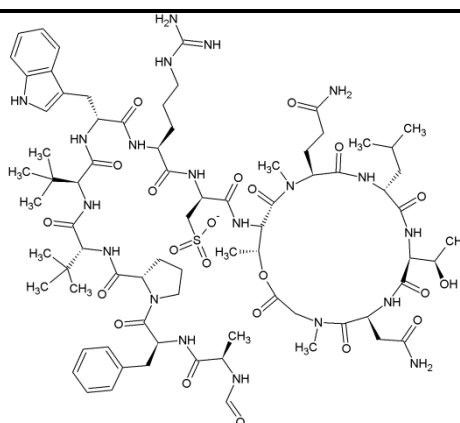


Table S2: Structural examples of cyclic depsipeptides for each of the proposed classes (continued).

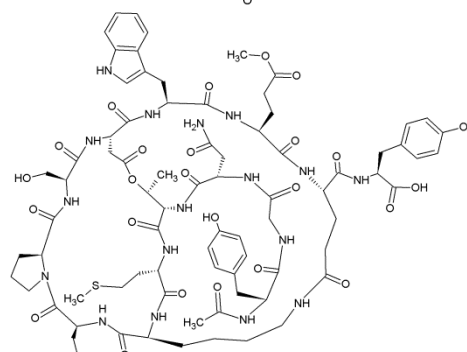
212221

Discodermin A



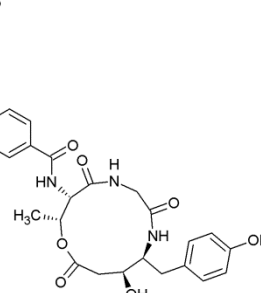
212222

Microviridin D



212231

Melleumin A



212232

Bromo-alterochromide A

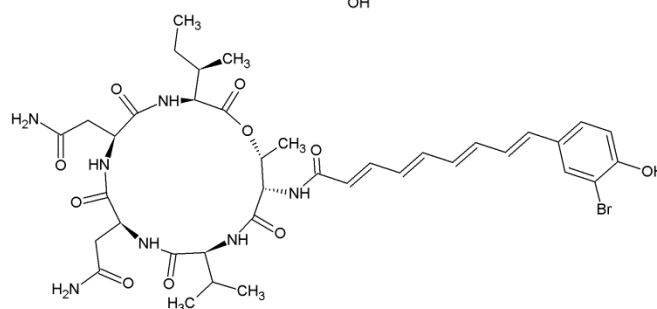
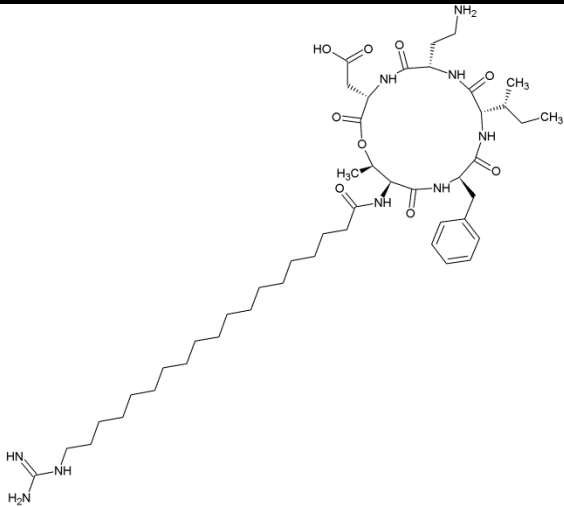
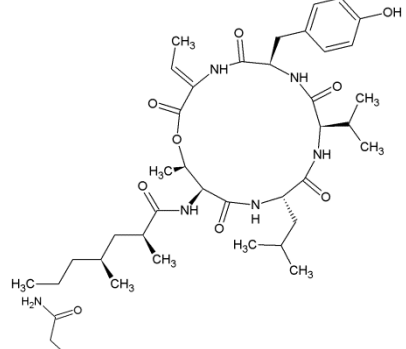
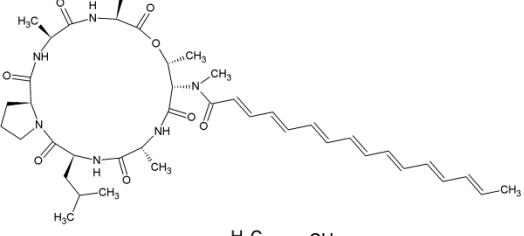
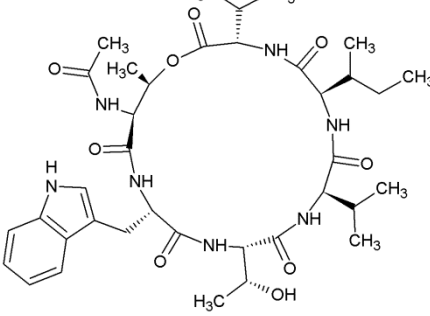


Table S2: Structural examples of cyclic depsipeptides for each of the proposed classes (continued).

21223311	Circulocin β	
21223312	Tumescenamide C	
2122332	Myxochromide A1	
212234	Xenobactin	

The stereochemistry of the Ile β -carbon was not indicated.

Table S2: Structural examples of cyclic depsipeptides for each of the proposed classes (continued).

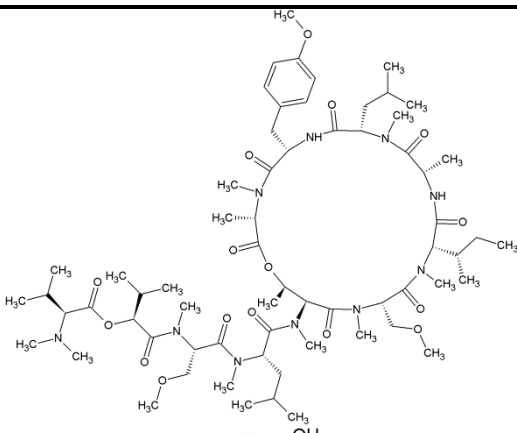
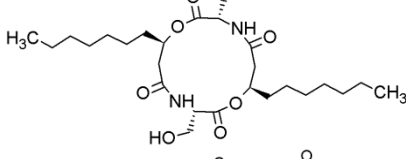
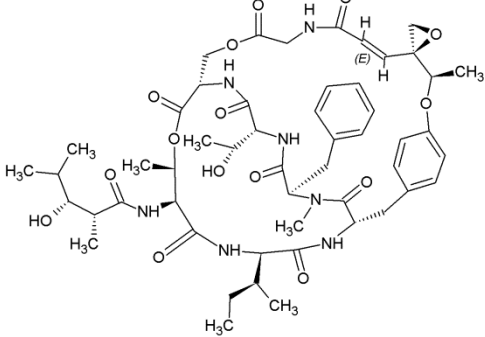
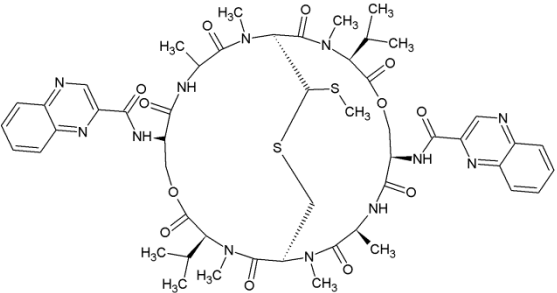
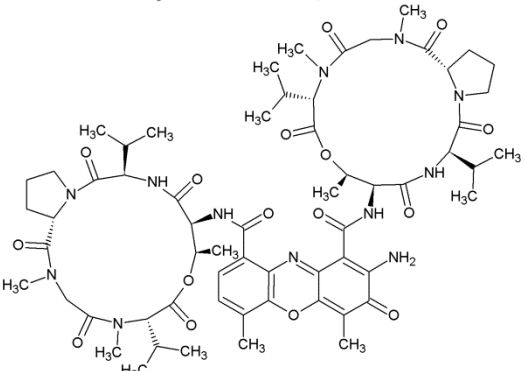
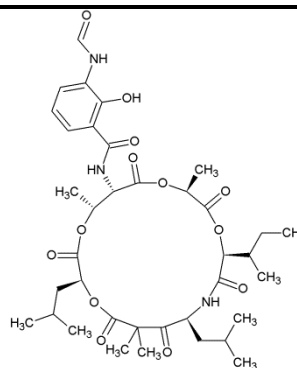
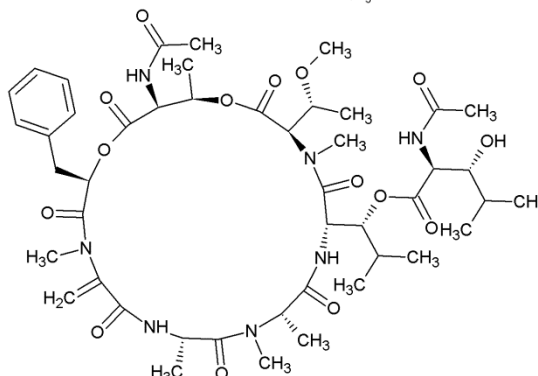
21224	Coibamide A	
221	Serratamolide A	
2221	Salinamide A	
22221	Echinomycin	
22222	Actinomycin D	

Table S2: Structural examples of cyclic depsipeptides for each of the proposed classes (continued).

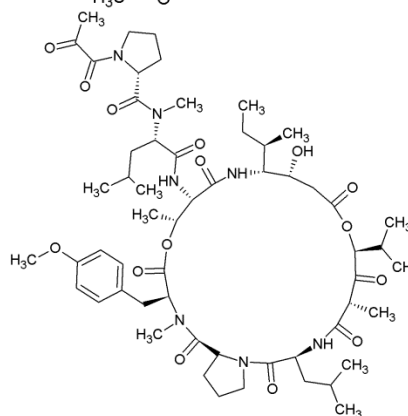
311 Respirantin



312 YM-254890



313 Aplidin



321 Hantupeptin A

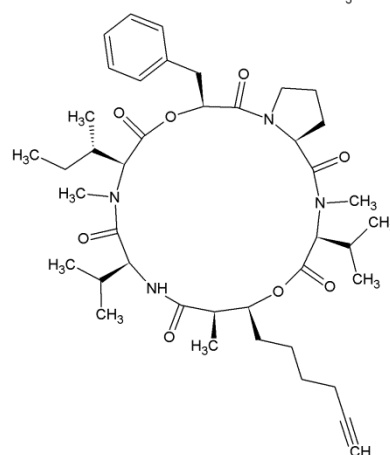
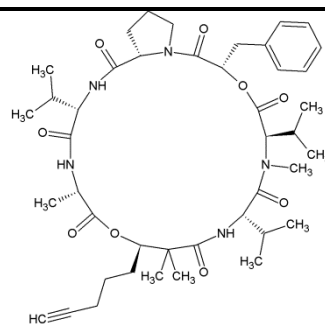


Table S2: Structural examples of cyclic depsipeptides for each of the proposed classes (continued).

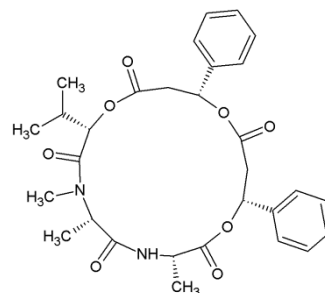
322

Kulolide-1



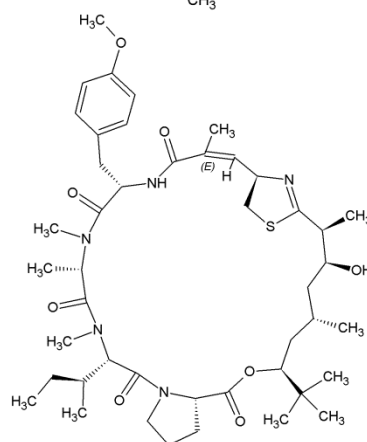
323

Pithomycolide



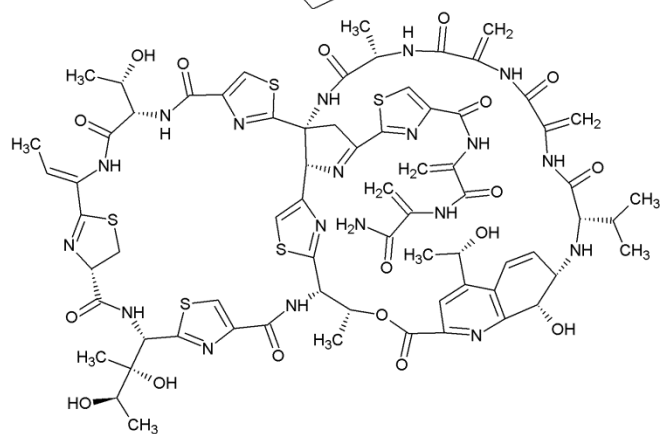
411

Apratoxin A



412

Siomycin A



42111

Rapamycin

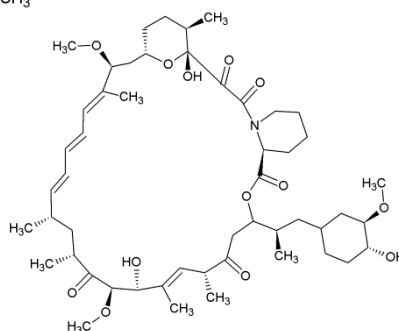
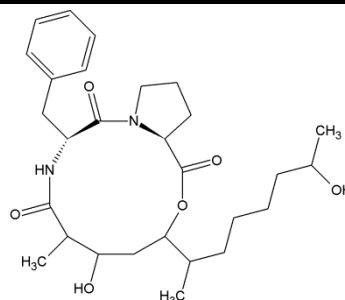


Table S2: Structural examples of cyclic depsipeptides for each of the proposed classes (continued).

42112

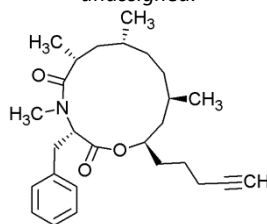
Acremolide A



The absolute stereochemistry of the fatty acid substructure remains unassigned.

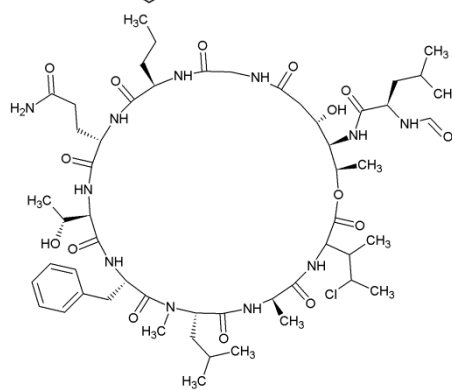
42113

Spongidepsin



42114

Cyclolithistide A



The absolute configuration of Cl-Ile remains unassigned.

421211

Aetheramide A

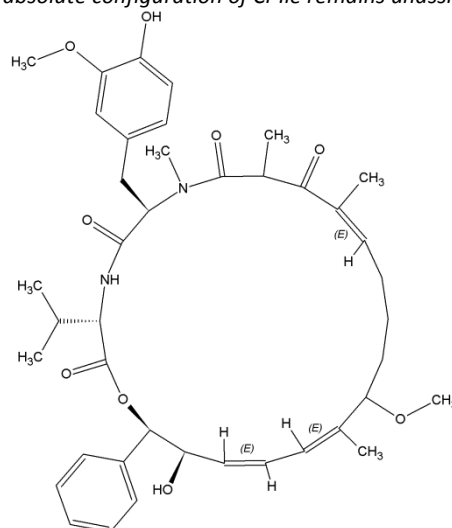
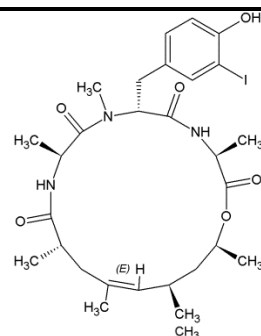
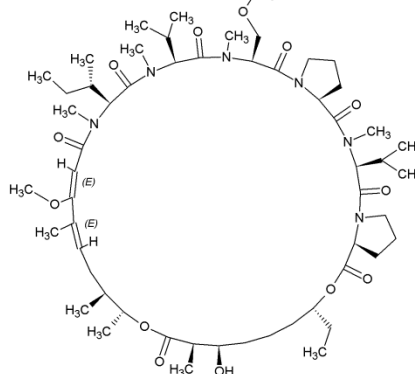


Table S2: Structural examples of cyclic depsipeptides for each of the proposed classes (continued).

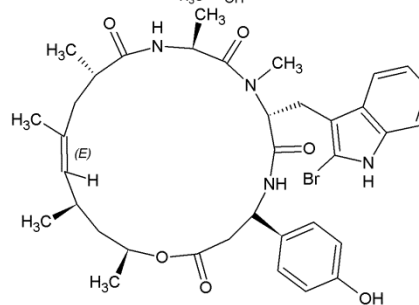
421212 Geodiamolide A



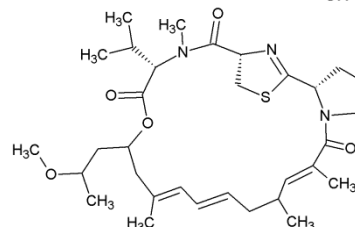
42122 Lyngbyastatin 2



42211 Jaspamide



42212 Alotamide A



The absolute stereochemistry of the polyketide substructure remains unassigned.

4222 Nagahamide A

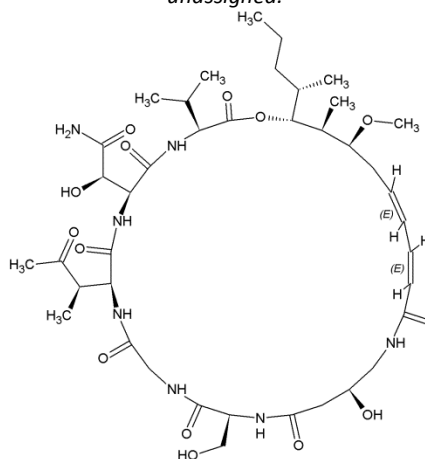
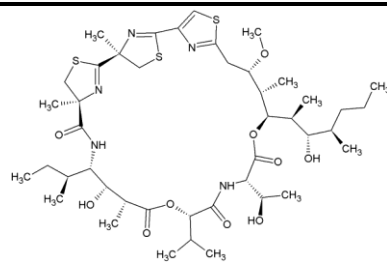
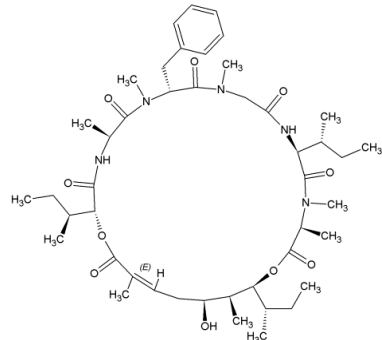


Table S2: Structural examples of cyclic depsipeptides for each of the proposed classes (continued).

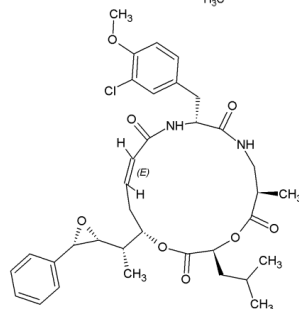
51 Hoiamide A



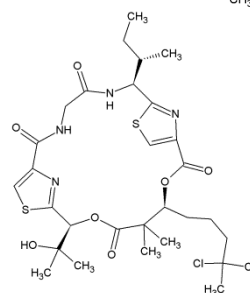
521 Lagunamide A



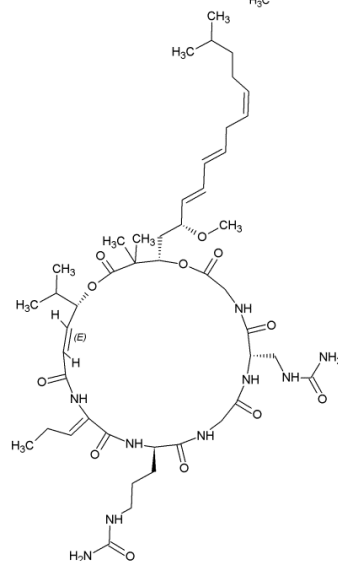
522 Cryptophycin 1



61 Lyngbyabellin A



62 Lipodiscamide A



CHAPTER III

THE MYCOTOXIN DEFINITION RECONSIDERED TOWARDS FUNGAL CYCLIC DEPSIPEPTIDES

“You can't do without philosophy, since everything has
its hidden meaning which we must know.”

Maxim Gorky

(°1868 - †1936, Russian and Soviet writer, dramatist and politician)

Parts of this chapter were published:

Taevernier L, Wynendaele E, De Vreese L, Burvenich C, De Spiegeleer B. The mycotoxin definition reconsidered towards fungal cyclic depsipeptides. *Journal of Environmental Science and Health, Part C*. 2016; **34**: 114-135, doi: 10.1080/10590501.2016.1164561.

ABSTRACT

Currently, next to the major classes, cyclic depsipeptides beauvericin and enniatins are also positioned as mycotoxins. However, as there are hundreds more fungal cyclic depsipeptides already identified, should these not be considered as mycotoxins as well? The current status of the mycotoxin definition revealed a lack of consistency, leading to confusion about what compounds should be called mycotoxins. Because this is of pivotal importance in risk assessment prioritization, a clear and quantitatively expressed mycotoxin definition is proposed, based upon data of widely accepted mycotoxins. Finally, this definition is applied to a set of fungal cyclic depsipeptides, revealing that some of these should indeed be considered as mycotoxins.

CHAPTER III

THE MYCOTOXIN DEFINITION

RECONSIDERED TOWARDS FUNGAL

CYCLIC DEPSIPEPTIDES

Main focus in this chapter:

- To introduce a clear, unambiguous and quantitatively expressed ‘mycotoxin’ definition.
- Apply this definition on a set of fungal cyclic depsipeptides to determine whether these should also be classified as mycotoxins.

1. THE MYCOTOXIN DEFINITION: CURRENT STATUS

The cyclic depsipeptides beauvericin (BEA) and enniatins (ENNs) have recently been positioned as mycotoxins, *i.e.* metabolites that are at least carcinogenic or toxic in experimental systems [1-3]. However, as there are hundreds more fungal cyclic depsipeptides already identified, an important question arises: should these not be considered as mycotoxins as well? An answer to this question is urgently required, due to its impact on the priority status in risk assessment. To determine whether or not these should be considered as mycotoxins, these compounds should meet the criteria posed by the mycotoxin definition. However, since the term was first introduced in the mid 1950s, when it was discovered that aflatoxins, which are secondary metabolites from the fungus *Aspergillus*, had caused the death of more than 100,000 turkeys in the England’s poultry industry [4-6], a lack of consistency in the definition and use of the word “mycotoxin” has arisen. Today a huge amount of information about mycotoxins is already available, but in scientific literature, the authors do not all share the same vision about what should be called a mycotoxin. A re-evaluation of the traditional concepts is thus most certainly required. In Table 1, an overview of the different mycotoxin definitions found in the literature is presented.

Table 1: Overview and current status of applied mycotoxin definitions.

Reference	Definition	Status discussion (level of detail)
FAO [7]	Mycotoxins are toxic secondary metabolites of fungi belonging, essentially, to the <i>Aspergillus</i> , <i>Penicillium</i> and <i>Fusarium</i> genera.	<ul style="list-style-type: none"> ▪ Secondary metabolites of specific fungi ▪ Definitely toxic
Berthiller <i>et al.</i> [8]	Mycotoxins are secondary metabolites of fungi toxic to animals and humans and have been reviewed.	<ul style="list-style-type: none"> ▪ Secondary metabolites of fungi ▪ Extensively investigated: definitely toxic
Pitt [9]	Mycotoxins are insidious poisons, produced when, and only when, common fungi grow in foods and feeds.	<ul style="list-style-type: none"> ▪ Metabolites of different fungi ▪ Agricultural/food and feed industry ▪ Definitely toxic (poison)
Frisvad [10]	Mycotoxins are fungal specific (secondary) metabolites that are toxic to vertebrates when introduced in small amounts via a natural route.	<ul style="list-style-type: none"> ▪ Secondary metabolites of fungi ▪ Exposure via a natural route ▪ Definitely toxic: in low amounts
Bhatnagar <i>et al.</i> [11]	Mycotoxins are secondary metabolites produced by filamentous fungi that cause a toxic response (mycotoxicosis) when ingested by higher animals.	<ul style="list-style-type: none"> ▪ Secondary metabolites of filamentous fungi ▪ Agricultural/food and feed industry ▪ Definitely toxic when ingested
Raghavender and Reddy [12]	Mycotoxins are toxic secondary metabolites produced by certain fungi or moulds in agricultural products that are susceptible to mould infestation.	<ul style="list-style-type: none"> ▪ Secondary metabolites of certain fungi/molds ▪ Agricultural/food and feed industry ▪ Definitely toxic
EFSA [13]	Mycotoxins are toxic compounds produced by different types of fungi, belonging mainly to the <i>Aspergillus</i> , <i>Penicillium</i> and <i>Fusarium</i> genera. They commonly enter the food chain through contaminated food and feed crops, mainly cereals.	<ul style="list-style-type: none"> ▪ Metabolites of different fungi ▪ Agricultural/food and feed industry ▪ Definitely toxic
Devreese <i>et al.</i> [14]	Mycotoxins are secondary metabolites produced by different fungal species contaminating several food and feed commodities. Over 100 mycotoxins have been identified, although only a few of them have been thoroughly investigated because of their distinct toxic effects.	<ul style="list-style-type: none"> ▪ Secondary metabolites of different fungi ▪ Agricultural/food and feed industry ▪ No thorough investigation: potentially toxic
FDA [15]	Mycotoxins are natural poisons produced by fungi as secondary metabolites. Foods may become contaminated with mycotoxins as a result of mold growth during harvest, or storage. Three genera are responsible for the majority of the mycotoxins with which FDA is concerned: the <i>Aspergillus</i> , <i>Penicillium</i> and <i>Fusarium sp.</i>	<ul style="list-style-type: none"> ▪ Secondary metabolites of fungi ▪ Agricultural/food and feed industry ▪ Definitely toxic (natural poison)
Yazar and Omurtag [16]	Mycotoxins are secondary metabolites produced by a wide variety of fungal species that cause nutritional losses and represent a significant hazard to the food chain. The exposure risk to human is either directly through foods of plant origin (cereal grains) or indirectly through foods of animal origin (kidney, liver, milk and eggs).	<ul style="list-style-type: none"> ▪ Secondary metabolites of different fungi ▪ Agricultural/food and feed industry ▪ Hazard/risk identification
Varga <i>et al.</i> [17]	Mycotoxins are secondary fungal metabolites, which are found in a broad range of food and feed, such as cereals, spices, coffee, nuts or dried fruits. They have the capability of causing acute toxic, carcinogenic, mutagenic, teratogenic, immunotoxic or oestrogenic effects in animals and humans and they show a huge structural diversity resulting in a variety of chemical and physicochemical properties.	<ul style="list-style-type: none"> ▪ Secondary metabolites of fungi ▪ Agricultural/food and feed industry ▪ Potentially toxic

Table 1: Overview and current status of applied mycotoxin definitions (continued).

Bennet and Klich [18]	All mycotoxins are low-molecular-weight natural products produced as secondary metabolites by filamentous fungi. These metabolites constitute a toxigenically and chemically heterogeneous assemblage that are grouped together only because the members can cause disease and death in human beings and other vertebrates. They are toxic to vertebrates and other animal groups in low concentrations... Skin contact with mold infested substrates and inhalation of spore-borne toxins are also important sources of exposure.	<ul style="list-style-type: none"> ▪ Secondary metabolites of filamentous fungi ▪ Other routes of exposure: dermal/respiratory ▪ Definitely toxic: in low concentrations
EMAN [19]	The term 'mycotoxin' is usually reserved for the toxic chemical products formed by a few fungal species that readily colonise crops in the field or after harvest and thus pose a potential threat to human and animal health through the ingestion of food products prepared from these commodities.	<ul style="list-style-type: none"> ▪ Metabolites of specific fungi ▪ Agricultural/food and feed industry ▪ Potentially toxic
Gravesen <i>et al.</i> [20]	Mycotoxins are secondary metabolites produced by filamentous fungi that in small concentrations can evoke an acute or chronic disease in vertebrate animals when introduced via a natural route.	<ul style="list-style-type: none"> ▪ Secondary metabolites of filamentous fungi ▪ Exposure via a natural route ▪ Potentially toxic in small concentrations ▪ Acute or chronic toxicity
Whitlow and Hagler, [21]	Molds also produce poisons called mycotoxins that affect animals when they consume mycotoxin contaminated feeds. Mycotoxins are produced by a wide range of different molds and are classified as secondary metabolites, meaning that their function is not essential to the mold's existence.	<ul style="list-style-type: none"> ▪ Secondary metabolites of molds ▪ Metabolites of different fungi ▪ Agricultural/food and feed industry ▪ Poisons which affect upon consumption
Jarvis and Miller [22]	Mycotoxins are low molecular weight (generally <1 kDa) natural products (secondary metabolites) produced by filamentous fungi or molds, restricted to those that pose a potential health risk to animals and humans exposed to these natural products, through contamination of our feed and food.	<ul style="list-style-type: none"> ▪ Secondary metabolites of filamentous fungi/molds ▪ Agricultural/food and feed industry ▪ Small/low molecular weight compounds ▪ Potentially toxic (risk identification)
Milićević <i>et al.</i> [23]	Mycotoxins are small molecular weight toxic compounds, produced by the secondary metabolism of toxigenic moulds in the <i>Aspergillus</i> , <i>Alternaria</i> , <i>Claviceps</i> , <i>Fusarium</i> , <i>Penicillium</i> and <i>Stachybotrys</i> genera occurring in food and feed commodities both pre- and post-harvest, causing serious risks for human and animal health.	<ul style="list-style-type: none"> ▪ Secondary metabolites of toxigenic molds ▪ Agricultural/food and feed industry ▪ Small/low molecular weight compounds ▪ Definitely toxic ▪ Risk identification
Richard [24]	Fungal secondary metabolites proven to be toxic when consumed by man and other animals... Its occurrence in house dust and other airborne particulates may be of significance in human disease... The determination of which of the many known mycotoxins are significant can be based upon their frequency of occurrence and/or the severity of the disease that they produce, especially if they are known to be carcinogenic.	<ul style="list-style-type: none"> ▪ Secondary metabolites of fungi ▪ Agricultural/food and feed industry ▪ Other routes of exposure: dermal/respiratory ▪ Significance based on occurrence and disease severity ▪ Definitely toxic
Barret [25]	Mycotoxins are secondary metabolites produced by certain molds that infect food crops in the field and during storage. Depending on the quantities produced and consumed, mycotoxins can cause acute or chronic toxicity in the animals and humans who eat contaminated crops or foods prepared for them. Health effects of mycotoxins may include immunological effects, organ-specific toxicity, cancer, and, in some cases, death. Agricultural workers are also at risk for dermal and respiratory exposures during crop harvest and storage.	<ul style="list-style-type: none"> ▪ Secondary metabolites of certain molds ▪ Agricultural/food and feed industry ▪ Other routes of exposure: dermal/respiratory ▪ Potentially toxic: depending on quantities ▪ Acute or chronic toxicity

Although it is clear that the used definitions differ greatly, by the term ‘mycotoxins’ they all mean compounds produced by fungi which are potentially toxic to a certain degree. So all definitions have similarities, however, some of them include more details concerning certain aspects, whereas others are more detailed about other aspects.

The vast majority of these definitions are situated within the agricultural and food industry, where it is indicated that mycotoxins are found in the food chain through contaminated food and feed, with the emphasis on harvest and storage. Whereas most sources focus on mycotoxin ingestion, Barret [25] also warns agricultural workers for the risk through dermal and respiratory exposure. Moreover, Bennet and Klich [18] and Richard [24] also recognize other routes of exposure besides food/feed contamination, *i.a.* contact with contaminated indoor surfaces and airborne particles which can be found *e.g.* in buildings which harbour high levels of molds. Moreover, some authors explicitly mention exposure via a natural route in their definition [10,20].

Additionally, Berthiller and co-workers defined a mycotoxin subgroup, termed ‘masked’ mycotoxins, as mycotoxin derivatives that are undetectable by conventional analytical techniques because their structure has been changed in the contaminated plant/crop [8]. Others have introduced another terminology, namely ‘emerging’ mycotoxins, as mycotoxins represent an emerging food safety risk [26,27]. According to the European Food and Safety Authority (EFSA) [28], an emerging risk can be defined as a risk to human, animal and/or plant health resulting from a newly identified hazard to which a significant exposure may occur, or from an unexpected new increased significant exposure and/or susceptibility to a known hazard.

According to Berthiller *et al.* [8], mycotoxins are “secondary metabolites of fungi toxic to animals and humans and have been reviewed”, meaning that they have been extensively investigated. On the contrary, Devreese *et al.* [14] state that over 100 mycotoxins have been identified, although only a few of them have been thoroughly investigated, with or without maximum acceptable levels regulated by law [29], suggesting a compound can already be identified as a mycotoxin without an extensive investigation of its toxic effects. The latter also leans more towards Yazar and Omurtag’s [16] idea of a mycotoxin, namely that it represents a significant hazard. Richard [24] on the other hand, determines ‘significant’ mycotoxins based upon their frequency of occurrence and/or the severity of the disease that they produce.

Moreover, it is suggested that (tens of) thousands of these potentially toxic fungal metabolites exist [30-34] leading to the European Mycotoxin Awareness Network’s (EMAN) question whether further important mycotoxins remain to be discovered [19].

However, according to Miller and McMullin, on many occasions it seems that nearly any fungal secondary metabolite is casually, but incorrectly referred to as a mycotoxin [35]. It has indeed been recognized that mycotoxins are hard to define and classify [18], and as a result there is a lack of

consistency and disagreement in scientific literature about what compounds should or should not be called mycotoxins. Overall, the confusion concerning the ‘mycotoxin claim’ is understandable and a few major shortcomings cannot be overlooked. It is obvious that there is definite disagreement about the mycotoxin definition, *e.g.* should mycotoxin identification and classification be viewed from a hazard or risk point of view? Furthermore, do we consider a precautionary approach or adapt a rather wait-and-see policy? What is considered to be toxic, *i.e.* how should this toxicity be tested and what quantitative specification thresholds should be applied? Should structurally related compounds automatically be considered as mycotoxins, although they are not produced by the commonly referred fungi, such as *Aspergillus*, *Penicillium* and *Fusarium*, or although their toxicity has not yet been (fully) evaluated/elucidated, *i.e.* to what extent do we allow false negatives and positives?

Therefore, by means of a literature review, we propose here a clear, unambiguous and quantitatively expressed definition, based upon data of some already well-known and widely accepted mycotoxins, allowing more awareness of the now underestimated potential hazard of some of these metabolites. Moreover, we apply our definition to a set of fungal cyclic depsipeptides to determine whether or not these metabolites should be classified as mycotoxins.

2. PHILOSOPHICAL APPROACH TO A ‘DEFINITION’

A definition is supposed “*to give the essence of a thing*”. This way a definition can be divided into (i) a definition which gives the ‘real essence’ (*e.g.* defining water in terms of H₂O) and (ii) a definition which gives the ‘nominal essence’ of something (*e.g.* defining water in terms of a transparent, odourless, potable liquid) [36,37].

As a starting point, the current mycotoxin concept and how it has been used thus far was evaluated. In that sense, the focus is on the nominal essence of a mycotoxin, *i.e.* all currently applied definitions are considered prototypical. This approach, however, automatically involves the rather undesirable and confusing result that different definitions will be given to the same word or concept [38], which is the case for mycotoxins. This indicates that currently mycotoxin definitions are likely made up by abstracting information from prototypical cases of mycotoxins of a certain, typical kind (*e.g.* aflatoxins).

Aiming to bring the mycotoxin definition closer to its real essence, an explicative approach was applied [39], as illustrated in Figure 1.

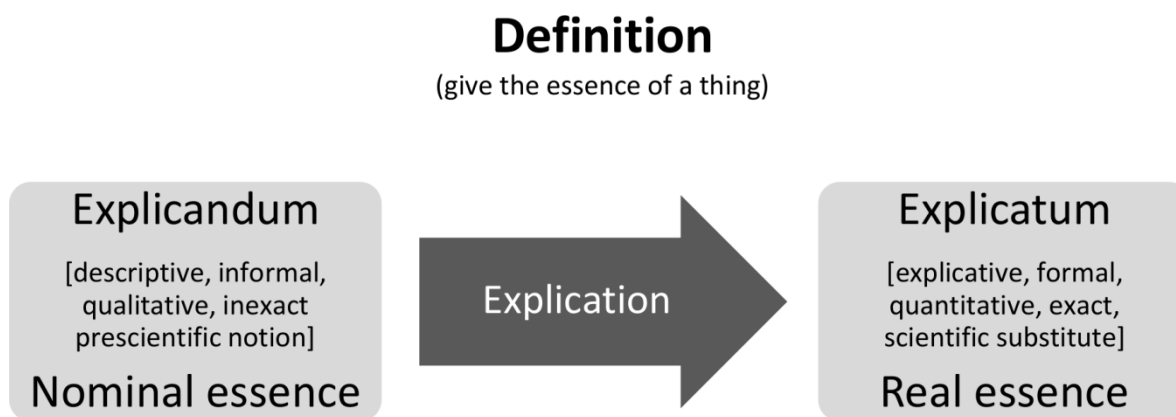


Figure 1: The concept of ‘explication’.

This is in accordance with the classical theory of concepts, which supposes that the meaning of a concept can be captured in a definitional structure. The definitional structure consists of simpler concepts, which express the necessary and sufficient conditions for the accurate use of the concept. For example, the necessary and sufficient conditions for something to be a “*rectangle*” are that (i) “*it concerns a geometrical form*”, (ii) “*it has two pairs of parallel lines*” and (iii) “*it has four right angles*”: something falls under the concept “*rectangle*” if and only if it is a “*geometrical form with four right angles and it has two pairs of parallel lines*”. Hence, “*geometrical form*”, “*two pairs of parallel lines*” and “*four right angles*” are the constituents of the concept “*rectangle*” [40]. In the case of the scientific concept of a mycotoxin, determining the necessary and sufficient conditions is required.

3. PROPOSED MYCOTOXIN DEFINITION

Something is a **mycotoxin** if and only if it is a **secondary metabolite** produced by **microfungi**, posing a **health hazard** to human and vertebrate animal species by exerting a **toxic activity** on human or vertebrate animal cells *in vitro* with **50% effectiveness levels < 1000 µM**.

3.1. Secondary microfungus metabolites

It is generally accepted that mycotoxins are indeed secondary fungal metabolites [7,8,11,12,14-18,21,23-25]. The term ‘mycotoxin’ refers only to metabolites produced by microfungi and by convention thus excluding mushroom and yeast toxins. However, opinions remain unclear and divided about the type of microfungi and its occurrence, responsible for the production of mycotoxins. International organizations, *i.e.* EFSA [28], FAO [7] and FDA [15], as well as scientific researchers [9,23], explicitly state that it especially involves common fungi such as *Aspergillus*, *Penicillium* and *Fusarium*. However, these definitions are all agricultural/food oriented, focusing only on fungi that contaminate feed and food, thereby completely neglecting other possible sources of

mycotoxin production. Therefore, this angle towards a proper and unambiguous mycotoxin definition seems insufficient, as traditional mycotoxins are also found in air particles or on walls of badly maintained, unventilated, humid houses [18,25]. Furthermore, marine derived fungi are not mentioned once, although these can also produce toxic secondary metabolites, some of which are structurally very similar to known mycotoxins such as beauvericin and enniatins, *e.g.* zygosporamide [36,37], causing thus a potential hazard not only to marine ecology, but also to humans through the fishing industry [38].

Thus, restricting the mycotoxin definition to common agricultural fungal origin is inadequate, because it underestimates the impact on the public health. Therefore, we suggest to only include the term ‘microfungal secondary metabolites’ as such into the definition, without further confining the fungal origin.

3.2. Hazard

The International Programme on Chemical Safety (IPCS) has harmonised the context of hazard and risk assessments. Some authors consider introduction via a natural route an important factor in the determination of mycotoxins [20] and therefore attach little importance to cytotoxicity tests or studies evaluating toxicity based on intraperitoneal injection [39]. However, based on the information available, the whole mycotoxin definition discussion should, in our opinion, be best placed within the context of hazard assessment, an important and first part of risk assessment, since the intrinsic toxicity of a compound cannot be altered, meaning that it will always remain a hazard, because it possesses the potential to cause an adverse/toxic effect. Risk, on the other hand, through the process of exposure assessment to the hazard concerned, can be reduced by preventive actions and is very hard to unambiguously determine. Moreover, especially early on, the routes of exposure are usually not clarified. Therefore, while awaiting more toxicity exposure data concerning hazardous compounds, which can take up to several years, a precautionary approach is preferred above a long during risk policy. In this respect, cytotoxicity studies performed on human or vertebrate animal cells are a cost-effective and animal-friendly way to determine potential toxicity already at an early stage in the hazard assessment. The mycotoxins identified by this approach could first carefully be called ‘pseudomycotoxins’, while awaiting formal mycotoxin nomination, which involves exposure and risk assessment.

Also to be included in this discussion is the ‘low molecular weight’ condition for defining a mycotoxin as proposed by Bennet and Klich [18], which is essentially directed towards exposure/risk and not a hazard, since high molecular weight compounds are considered not to be bioavailable due to unfavorable pharmacokinetic properties, *i.a.* not absorbed through cell membranes. In fact, it is generally accepted that small or low molecular weight molecules have a molecular weight (MW) cut-

off of 600 – 700 Da [40,41]. This limit, however, based upon the Lipinski's rule of five, is an artificial limit associated with the observation that the attrition rates of oral drug compounds in the clinical development are significantly reduced if the MW is kept below this 500 Da limit. Molecules with a MW below this cut-off are believed to rapidly diffuse across cell membranes so that they can reach intracellular sites of action, the molecular size thus reflects bioavailability, *i.e.* exposure and risk [42-44]. Recently, it has been shown by our group that also larger cyclic depsipeptide mycotoxins such as beauvericin and enniatins, with MW's up to 783.96 Da, are capable of crossing the human skin barrier and reaching the viable epidermis and dermis [45]. Furthermore, a recent *in vivo* study in pigs demonstrated a high oral bioavailability (91%) for enniatin B1 [3], confirming also an earlier *in vitro* study, which assessed the bioavailability of ENNs with Caco-2 cells to be 55-66% [46]. Moreover, the mycotoxin bassianolide, which has been shown to be cytotoxic to human cell lines in the low μ M range, has a MW of 909.36 Da and thus already exceeds this low molecular weight cut-off [47,48]. Also, toxic metabolites of high MW compounds, such as glycopeptides, may not be overlooked, as these can also pose an important health hazard. Therefore, a quantitative molecular weight restriction should not be included in the mycotoxin definition.

To further illustrate this, we would like to refer to the fumonisin paradox. Fumonisin B1 was confirmed to cause *i.a.* carcinoma, cirrhosis and nephrosis, but was shown to have a very poor oral bioavailability. These conflicting results are called the fumonisin paradox: "How can the toxin cause agriculturally significant diseases and possibly human cancer if it is not effectively absorbed after oral administration?" Shier explained that a higher bioavailability at lower doses, bioaccumulation and/or effective uptake of derivatives that are readily converted back in the body are plausible explanations. Also other important routes of exposure (*e.g.* dermal or respiratory) should be considered. As a consequence, the complete impact of a compound's threat will thus not be identified until all elements affecting oral bioavailability are understood [49].

3.3. Toxicity

Following the hazard approach, one could argue "*dosis sola facit venenum*", meaning everything can be considered toxic as long as the dose is high enough: the amount of a substance is what makes it harmful, not the substance itself (Paracelsus, 16th century). Therefore, a quantitative toxicity limit is required as a condition for defining compounds as mycotoxins.

In a first approach, the most objective/standardised, economic and ethically acceptable way for measuring a compound's toxicity is screening its *in vitro* cytotoxic capacity on various cell lines, preferably of human origin. *In vitro* tests in general have proven their value, *i.a.* in order to reduce animal/human toxicological studies and/or full-scale trials. Moreover, *in vitro-in vivo* correlation mathematical models, which describe the relationship between an *in vitro* property and an *in vivo*

response, are widely acknowledged. A direct cytotoxic effect is quantitatively expressed as IC_{50} , the concentration required for 50% inhibition of cell viability, a value generally agreed upon. The cell lines and concentration ranges used, together with the demonstrated IC_{50} of some already accepted mycotoxins are given in Supplementary Information S1. As we want to propose a quantitatively expressed definition, a toxicity IC_{50} threshold as a condition for claiming compounds as mycotoxins was set: $IC_{50} < 1000 \mu\text{M}$. This value can be justified by the data from Supplementary Information S1, which show that of all studies the maximum IC_{50} values quantitatively reported for well-established mycotoxins are within the 100-1000 μM class and by the fact that other low-molecular molecules toxic to humans, like ethanol, are not considered mycotoxins because these are only toxic in high concentrations [50]. Moreover, it is also important to note that multiple mycotoxins, such as ENNs, T-2, deoxynivalenol (DON), nivalenol (NIV), BEA and fusarenon X (FUS-X), can influence each other's toxicity, showing synergistic, additive and antagonistic effects [27,51-53], considering the well-documented co-occurrence of mycotoxins in real-life [54]. As the majority of the IC_{50} values are located between 1 and 100 μM , the chosen upper limit of 1000 μM can therefore also be considered as a 'worst case safety margin' for toxicity.

Moreover, it is recognised that toxic effects are not only concentration- but also time-dependent; therefore, both acute and chronic effects are of interest and are understood to be included in the mycotoxin definition. Furthermore, besides such direct cytotoxic effects, compounds can also exert indirect toxicity due to the formation of metabolites. It should thus be mentioned that a demonstrated *in vitro* toxicity does not per se implicate an *in vivo* effect and vice versa, e.g. *N*-acyl metabolites are more cytotoxic than the parent fumonisin B1 [55]. Therefore, we strongly encourage the inclusion of metabolites (from liver extracts, for example) and modified mycotoxins in these *in vitro* cell tests, to lower the probability of false negatives. And what about newly discovered compounds, of which the toxicity has not yet been thoroughly investigated? Since a lack of toxicity data does not mean that the compound itself is not toxic or has no toxic potential, within the context of risk assessment prioritization and precautionary approach, we suggest terming these compounds appropriately 'potential mycotoxins', defined as: secondary metabolites produced by microfungi, posing a health hazard to human and animal species, but for which the toxic activity is not yet investigated, i.e. no IC_{50} values are available. It goes without saying that these compounds should be further investigated with a prioritization according to their exposure level to humans.

Lastly, it should also be mentioned that endocrine disrupting properties, which could occur at lower non-cytotoxic doses, might also suggest an important potential hazard and such effects have already been reported for the mycotoxins DON, ENN B, T-2 and HT-2 toxins [56,57]. Screening potential mycotoxins for their endocrine disrupting properties in cell based assays (e.g. using U2OS and H295R cells) should therefore also be considered during hazard assessment.

4. APPLICATION OF DEFINITION ON FUNGAL CYCLIC DEPSIPEPTIDES

Lastly, we have applied our definition to a set of fungal cyclic depsipeptides, in order to determine whether or not these should also be considered as (potential) mycotoxins.

4.1. Data handling

Structural and functional information, as well as the origin of the producing species of nearly 800 naturally occurring cyclic depsipeptides were gathered, of which 194 individual compounds were found to be produced by fungi. Since these compounds have currently not yet been properly classified, although this information can be of great biological importance, *i.a.* understanding their structure-property relationships, these fungal cyclic depsipeptides were also subjected to a clustering analysis based upon their chemical properties. Considering that the majority of the compounds have already been categorised in small existing groups (*e.g.* enniatin A, B, A1, E, etc. all belong to the ‘enniatis group’), only a limited number of model compounds was selected, representative for the whole fungal CDP population. Therefore, sampling was done in a randomised way: first, all cyclic depsipeptides were stratified according to their already known existing groups, from which then randomly at least one representative cyclic depsipeptide compound per group was included. However, not every structure reported in literature has a completely clarified stereochemistry, which is of huge importance for many 3D descriptors, so wherever possible, another member of a group was taken. This strategy ultimately led to 32 CDPs retained for further analysis. Consequently, more than 3000 molecular descriptors were calculated, using Dragon 5.5 (Talete, Milan, Italy), HyperChem 8.0 (Hypercube, Gainesville, FL, USA) and MarvinSketch 5.10.3 (ChemAxon, Budapest, Hungary), for which the MM+ *in vacuo* structure was optimized, using HyperChem 8.0. The non-discriminating descriptors were eliminated, resulting in a 32x1363 data-matrix. All descriptors were transformed by z-scaling, ensuring an equal contribution of each descriptor to the resulting model [58]. Multivariate data-analysis was performed using both principal component analysis (PCA) and hierarchical cluster analysis (HCA) with SIMCA-P+12.0.1.0 (Umetrics AB, Umea, Sweden) and SPSS Statistics 22.0.0 (IBM Corp., Armonk, NY, USA) software programs, respectively. Average-linkage HCA clustering was performed using the Euclidean distance as the dissimilarity criterion. PCA resulted in an explained variance of PC1 = 0.51 and PC2 = 0.16 (cumulative R² of 0.67).

4.2. Chemical clustering classification

Based on the score plot of the first two principal components of the PCA, the 32 cyclic depsipeptides could be categorized into four main clusters with six subclusters, which is confirmed by the dendrogram of the HCA (Figure 2). The corresponding loading plot of the PCA allowed for further interpretation of these groups, by means of the most discriminating molecular descriptors displayed

on both principal components. From this, it was deduced that components situated towards the right side of the space are larger, have larger ring sizes, have higher molecular weights and are folded and less flexible, *i.e.* have less conformational variability, compared to the compounds on the left. Cyclic depsipeptides located in the lower part of the space are less symmetrical than compounds located in the upper part. Other discriminating descriptors at the second axis are the number of terminal primary and tertiary carbons, which may indicate that CDPs located at the upper right part of the space most likely contain more valine, leucine, isoleucine amino acids and/or long branched alkyl chain(s). Moreover, a number of molecular descriptors indicate a higher presence of aromatic/benzene-like rings in CDPs at the lower side of the y-axis. More detailed information can be found in Supplementary Information S2.

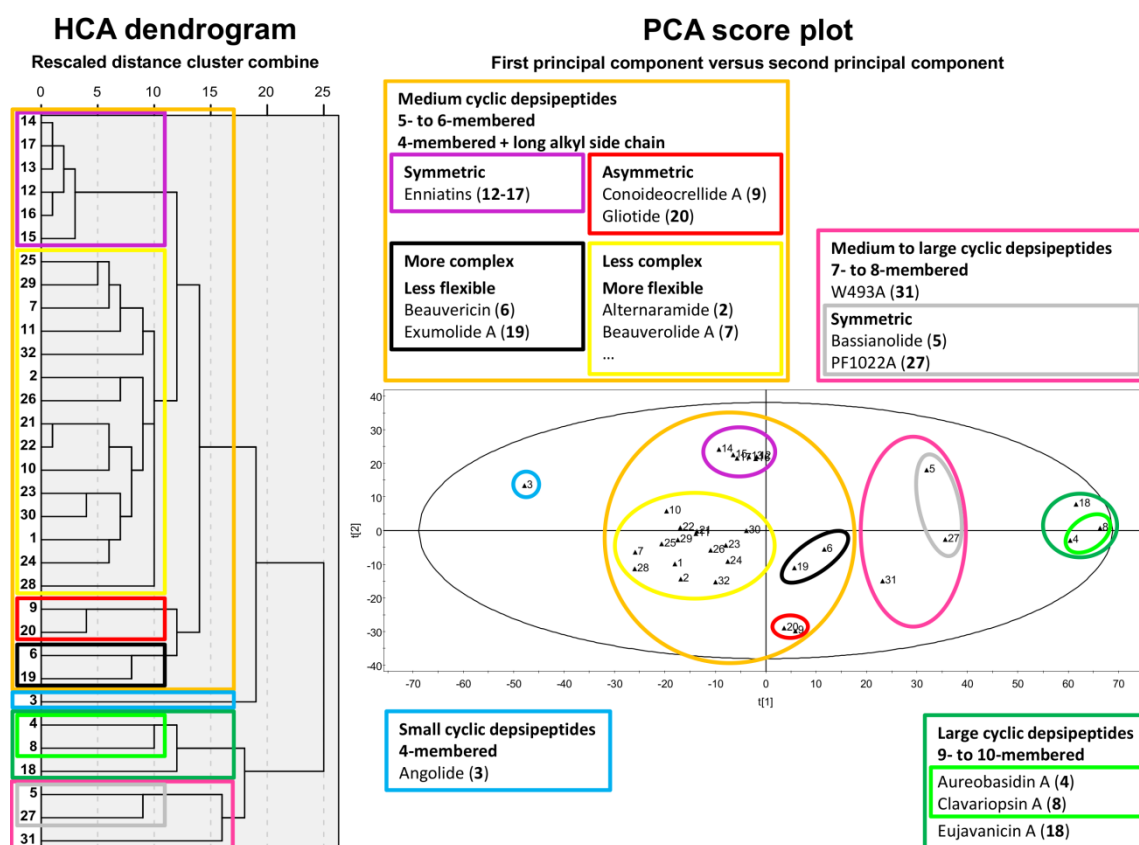


Figure 2: Clustering of 32 fungal cyclic depsipeptides. The four main clusters (blue, orange, pink and green clusters) and six subclusters (purple, yellow, black, red and grey clusters) are indicated by a bold coloured line.

Number identifications can be found in Table 2.

4.3. Mycotoxin claim

For these compounds, classified according to the clustering analysis, (i) available toxicity data, (ii) their fungal origin and (iii) mycotoxin claim from literature, as well as (iv) their mycotoxin claim resulting from our definition, are all gathered in Table 2.

Beside beauvericin and enniatins, only three of these (groups of) compounds have been previously called mycotoxins in scientific literature: bassianolide [48], beauverolides [59] and destruxins [60]. *In vitro* cytotoxicity of these compounds has indeed been studied and was found significant ($< 100 \mu\text{M}$). Therefore, based upon our proposed definition, these compounds should indeed be defined as mycotoxins. However, according to our definition, seven other fungal metabolites should also be considered as mycotoxins, namely 1962A, emericellamides, guangomides, PF1022A, sansalvamides, scopularamides and zygosporamide, of which sansalvamides and zygosporamide currently seem the most investigated and also the most toxic, based on the available data. So, for these identified hazards, further investigations, *i.a.* exposure and risk assessment, are strongly recommended. For the other cyclic depsipeptides mentioned in Table 2 no quantitative toxicity data are currently available and hence at this point, these peptides are considered as ‘potential mycotoxins’ for which further toxicity testing is required. In Figure 3, the identified mycotoxins are indicated in the clustering dendrogram (HCA) and score plot (PCA).

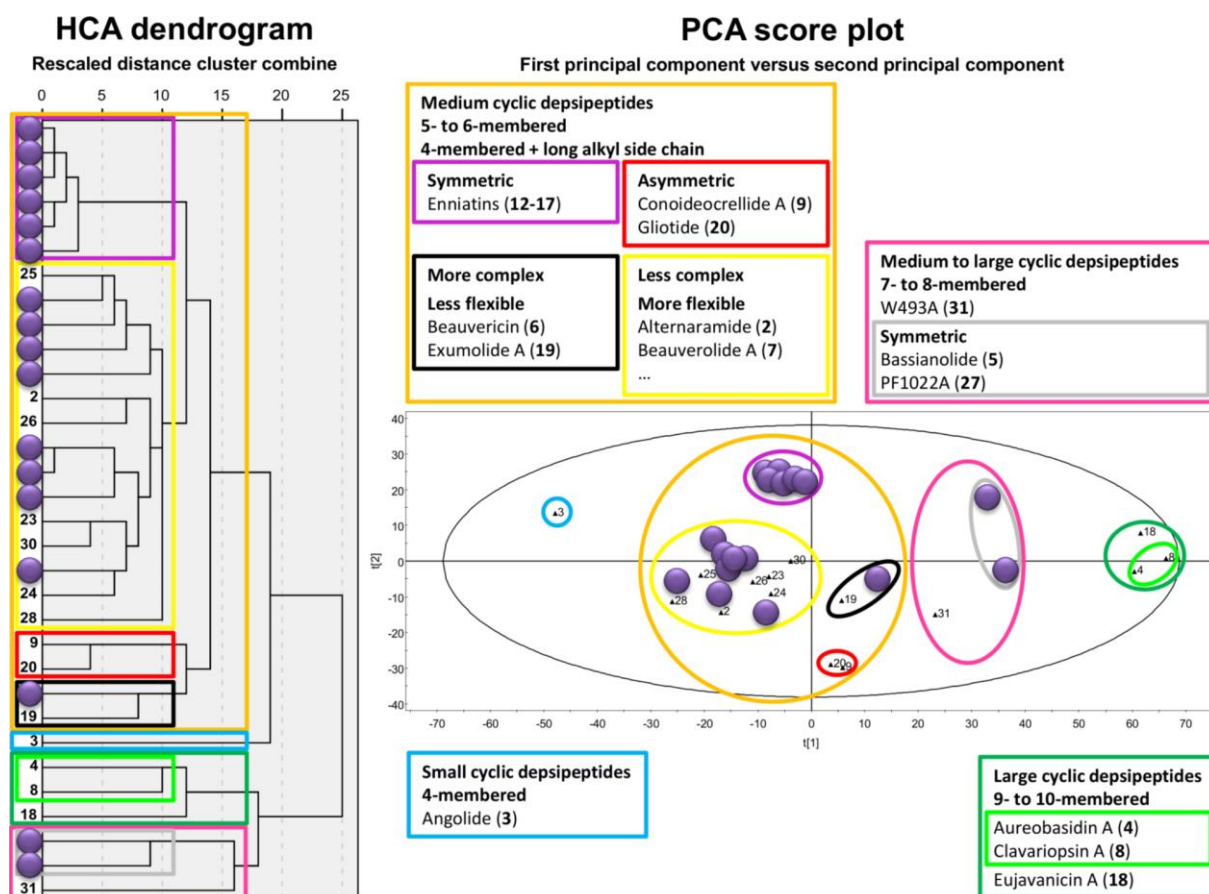


Figure 3: Clustering of 32 fungal cyclic depsipeptides. The identified mycotoxins are indicated by purple dots.

Table 2: Fungal cyclic depsipeptides as mycotoxin test group.

No°	Cyclic depsipeptide	Fungal origin	Available toxicity data	References	Lit. ⁽¹⁾	Mycotoxin claim Definition
Group 1: small cyclic depsipeptides						
3	Angolide	<i>Pithomyces</i> sp.	n.a.	Russell and Ward [61]	no	Potential mycotoxin
Group 2: medium cyclic depsipeptides						
12 → 17 ⁽³⁾	Enniatins ⁽²⁾	<i>Alternaria</i> sp. <i>Fusarium</i> sp. <i>Halosarpheia</i> sp. <i>Verticillium</i> sp.	IC ₅₀ = 1.6 – 6.8 µM (Caco-2 cells) IC ₅₀ = 13 – 14.8 µM (Caco-2 cells) IC ₅₀ = 11.7 µM (Caco-2 cells) IC ₅₀ = 2.8 – 11.3 µM (Caco-2 cells) IC ₅₀ = 15.80 µM (IPEC-1 cells)	Herrmann <i>et al.</i> [62] Ivanova <i>et al.</i> [63] Kolf-Clauw <i>et al.</i> [27] Prosperini <i>et al.</i> [53]	yes	Mycotoxins
9	Conoideocrellide A	Scale insect pathogenic fungus <i>Conoideocrella tenuis</i> (BCC 18627)	n.a.	Isaka <i>et al.</i> [64]	no	Potential mycotoxin
20	Gliotide	Marine alga-derived fungus <i>Gliocladium</i> sp.	n.a.	Lang <i>et al.</i> [65]	no	Potential mycotoxin
6	Beauvericin ⁽²⁾	<i>Beauveria</i> sp. <i>Paecilomyces fumosoroseus</i> <i>Fusarium</i> sp.	IC ₅₀ = 12.08 – 17.22 µM (CHO-K1 cells) IC ₅₀ = 6.25 – 11.08 µM (Vero cells) IC ₅₀ = 12.75 – 20.62 µM (Caco-2 cells) IC ₅₀ = 9.75 – 15.00 µM (HT-29 cells)	Ferrer <i>et al.</i> [66] Fukuda <i>et al.</i> [67] Prosperini <i>et al.</i> [68] Ruiz <i>et al.</i> [51] Sifou <i>et al.</i> [69] Song <i>et al.</i> [70] Wang <i>et al.</i> [71]	yes	Mycotoxin
19	Exumolides	Marine-derived <i>Scytalidium</i> sp.	Demonstrated antimicroalgal activity	Jenkins <i>et al.</i> [72]	no	Potential mycotoxins
1	1962A	Mangrove endophytic fungus (no. 1962)	IC ₅₀ = 165.64 µM (MCF-7 cells)	Huang <i>et al.</i> [73]	no	Mycotoxin
2	Alternaramide	Marine-derived <i>Alternaria</i> sp. (SF-5016)	n.a.	Kim <i>et al.</i> [74]	no	Potential mycotoxin

(1) Has literature ever referred (in any way) to this compound as being a mycotoxin?

(2) Already accepted mycotoxins, see also Supplementary Information S1.

(3) No° 12, 13, 14, 15, 16, 17 = enniatin A, A1, B, B1, C, D.

n.a. = not available

Table 2: Fungal cyclic depsipeptides as mycotoxin test group (continued).

7	Beauverolides	<i>Beauveria bassiana</i> <i>Paecilomyces fumosoroseus</i>	IC ₅₀ = 76.20 µM (CEM-DNR cells) IC ₅₀ = 32.16 µM (K562 cells) IC ₅₀ = 53.63 µM (K562-Tax cells) IC ₅₀ = 15.64 µM (B2.4 cells) IC ₅₀ = 22.77 µM (A549 cells) IC ₅₀ = 60.31 µM (HT-29 cells) IC ₅₀ = 52.41 µM (MCF-7 cells) IC ₅₀ = 82.63 µM (PC-3 cells) IC ₅₀ = 100.00 µM (U87MG cells) IC ₅₀ = 45.63 µM (lymphocytes)	Jegorov <i>et al.</i> [75] Kuzma <i>et al.</i> [76] Onstad <i>et al.</i> [59]	yes	Mycotoxins
10	Destruxins ⁽⁴⁾	Imperfect fungus (D1084) Marine-derived fungus <i>Beauveria f.</i> <i>Metarhizium anisopliae</i> <i>Nigrosabulum globosum</i> <i>Trichothecium roseum</i>	IC ₅₀ = 0.05 – >10 µM (KB-3-1 cells) IC ₅₀ = 0.05 – >10 µM (Caco-2 cells) IC ₅₀ = 0.04 – >10 µM (HCT116 cells) IC ₅₀ = 0.22 – >10 µM (A549 cells)	Boot <i>et al.</i> [77] Che <i>et al.</i> [78] Dornetshuber-Fleiss <i>et al.</i> [79] Dumas <i>et al.</i> [60] Engstrom <i>et al.</i> [80] Kawazu <i>et al.</i> [81] Lira <i>et al.</i> [82] Springer <i>et al.</i> [83] Sree <i>et al.</i> [84]	yes	Mycotoxins
11	Emericellamides	<i>Aspergillus nidulans</i> Marine-derived <i>Emericella</i> sp.	IC ₅₀ = 23 µM (HCT116 cells)	Chiang <i>et al.</i> [85] Ghosh and Pradhan [86] Oh <i>et al.</i> [87]	no	Mycotoxins
21 → 22	Guangomides ⁽⁵⁾	Terrestrial filamentous fungus, <i>Trichothecium</i> sp. Unidentified marine-derived fungus	IC ₅₀ = ± 15 µM (MCF-7 cells) IC ₅₀ = ± 15 µM (H460 cells) IC ₅₀ = ± 15 µM (SF268 cells)	Amagata <i>et al.</i> [88] Sy-Cordero <i>et al.</i> [89]	no	Mycotoxins
23	Hirsutatins	Insect pathogenic fungus <i>Hirsutella nivea</i> (BCC 2594)	Noncytotoxic at 73.9 µM (Vero cells)	Isaka <i>et al.</i> [90]	no	Potential mycotoxins
24	Hirsutellides	Entomopathogenic fungus <i>Hirsutella kobayashii</i> (BCC 1660)	Noncytotoxic at 75.2 µM (Vero cells)	Vongvanich <i>et al.</i> [91]	no	Potential mycotoxins
25	Leualacin	<i>Hapsidospora irregularis</i> (SANK17182)	Demonstrated calcium blocker	Hamano <i>et al.</i> [92]	no	Potential mycotoxin
26	Petrosifungins	Marine-derived <i>Penicillium brevicompactum</i>	n.a.	Bringmann <i>et al.</i> [93]	no	Potential mycotoxins
28	Pithomycolide	<i>Pithomyces chartarum</i>	n.a.	Moussa and Le Quesne [94]	no	Potential mycotoxin

(4) And its analogues (*i.a.* bursaphelocides, pseudodestruxins, roseotoxin, roseocardin).

(5) No° 21, 22 = guangomide A, B.

n.a. = not available

Table 2: Fungal cyclic depsipeptides as mycotoxin test group (continued).

29	Sansalvamides	Marine <i>Fusarium</i> sp.	IC ₅₀ = 5.96 µM (Colo 205 cells) IC ₅₀ = 10.06 µM (SK-MEL-2 cells) IC ₅₀ = 46.70 µM (mean of 60 cancer cell lines) Demonstrated inhibition of a poxvirus topoisomerase (IC ₅₀ for inhibition of DNA binding = ± 80 µM) IC ₅₀ = 3.6 – 8.3 µM (mean NCI human tumor cell line screen)	Belofsky <i>et al.</i> [95] Cueto <i>et al.</i> [96] Hwang <i>et al.</i> [97]	no	Mycotoxins
30	Trichodepsipetides	<i>Trichothecium</i> sp.	IC ₅₀ = >10 µM (noncytotoxic) (various cell lines)	Sy-Cordero <i>et al.</i> [89]	no	Potential mycotoxins
32	Zygosporamide	Marine-derived fungus <i>Zygosporium masonii</i>	IC ₅₀ = 0.0065 – 4.6 µM (SF268 cells) IC ₅₀ = 4.25 – 15 µM (SF295 cells) IC ₅₀ = 2.5– 7.4 µM (A549 cells) IC ₅₀ = 537 – 8.5 µM (MDA-MB-231) IC ₅₀ = < 5.0 nM (RXF 393 cells)	Oh <i>et al.</i> [36] Wang <i>et al.</i> [37]	no	Mycotoxin
Group 3: medium to large cyclic depsipeptides						
5	Bassianolide	<i>Beauveria bassiana</i> <i>Verticillium lecanii</i> Wood-decaying fungus <i>Xylaria</i> sp.	IC ₅₀ = 4.00 µM (KB cells) IC ₅₀ = 2.74 µM (BC-1 cells) IC ₅₀ = 1.21 µM (NCI-H187 cells) IC ₅₀ = 5.28 µM (Vero cells)	Jirakkakul <i>et al.</i> [47] Suzuki <i>et al.</i> [98] Yun <i>et al.</i> [99]	yes	Mycotoxin
27	PF1022A	Imperfect fungus <i>Mycelia sterilia</i> (<i>Rosellinia</i> sp.)	IC ₅₀ = 4.6 – 9.6 µM (HCT116 cells) IC ₅₀ = 4.3 – 7.5 µM (A549 cells)	Dornetshuber <i>et al.</i> [100] Sasaki <i>et al.</i> [101]	no	Mycotoxin
31	W493s	<i>Fusarium</i> sp.	Demonstrated antifungal activity	Nihei <i>et al.</i> [102]	no	Potential mycotoxins
Group 4: large cyclic depsipeptides						
4	Aureobasidins	Marine-derived <i>Aureobasidin</i> sp.	Demonstrated antibiotic effects	Abdel-Lateff <i>et al.</i> [103] Detwiller and Lubell [104] Sonda <i>et al.</i> [105] Tan and Tay [106] Tanaka <i>et al.</i> [107]	no	Potential mycotoxins
8	Clavariopsins	<i>Clavariopsis aquatica</i>	Demonstrated antifungal activity	Kaida <i>et al.</i> [108]	no	Potential mycotoxins
18	Eujavanicins	<i>Eupenicillium javanicum</i>	Demonstrated antifungal activity	Nakadate <i>et al.</i> [109]	no	Potential mycotoxins

Table 2: Fungal cyclic depsipeptides as mycotoxin test group (continued).

Cyclic depsipeptides with no assigned group ⁽⁶⁾						
-	Acremolides	Marine-derived <i>Acremonium</i> sp.	“Noncytotoxic”	Ratnayake <i>et al.</i> [110]	no	Potential mycotoxins
-	Brevigellin	<i>Penicillium brevicompactum</i>	n.a.	McCorkindale and Baxter [111]	no	Potential mycotoxin
-	Glomosporin	<i>Glomospora</i> sp. (BAUA 2825)	Demonstrated antifungal activity	Sato <i>et al.</i> [112]	no	Potential mycotoxin
-	Isarfelin	<i>Isaria felina</i>	Demonstrated antifungal and insecticidal activity	Guo <i>et al.</i> [113]	no	Potential mycotoxin
-	Isaridins	Entomopathogenic fungus <i>Beauveria felina</i> <i>Isaria</i> sp.	Demonstrated insecticidal activity	Langenfeld <i>et al.</i> [114] Ravindra <i>et al.</i> [115]	no	Potential mycotoxins
-	Isariins	Entomopathogenic fungus <i>Beauveria feline</i> <i>Isaria</i> sp.	Demonstrated insecticidal activity	Langenfeld <i>et al.</i> [114] Sabareesh <i>et al.</i> [116]	no	Potential mycotoxins
-	Scopularides	Marine-derived <i>Scopulariopsis brevicaulis</i>	IC ₅₀ = <15.51 μM (Colo357, Panc89, HT29 cells)	Yu <i>et al.</i> [117]	no	Mycotoxins
-	Sporidesmolides	Pasture fungus <i>Sporidesmium bakeri</i> <i>Pithomyces chartarum</i>	n.a.	Gillis <i>et al.</i> [118] Russell, 1960 [119] Russell, 1962 [120]	no	Potential mycotoxins
-	Stevastelins	<i>Penicillium</i> sp.	Demonstrated immunosuppressive effects	Morino <i>et al.</i> [121]	no	Potential mycotoxins

(6) These compounds' structures have not yet been fully elucidated. Therefore these were excluded from the clustering analysis.

n.a. = not available

5. CONCLUSIONS

Evaluation of the current status of the mycotoxin definition revealed a lack of consistency, confounding approaches and definite disagreement. We propose here a clear, unambiguous and quantitatively expressed mycotoxin definition, by means of explication and based upon hazard data of some already well-known and widely accepted “traditional” mycotoxins. This definition was then applied to a set of fungal cyclic depsipeptides, concluding that some of these compounds should also be considered as mycotoxins, for which exposure and risk assessment investigations are to be considered.

6. REFERENCES

- [1] Desjardins AE, Proctor RH. Molecular biology of *Fusarium* mycotoxins. *International Journal of Food Microbiology* 2007; 119: 47-50.
- [2] Jestoi M, Rokka M, Yli-Mattila T, Parikka P, Rizzo A, Peltonen K. Presence and concentrations of the *Fusarium*-related mycotoxins beauvericin, enniatins and moniliformin in Finnish grain samples. *Food Additives and Contaminants Part A – Chemistry Analysis Control Exposure and Risk Assessment* 2004; 21: 794-802.
- [3] Devreese M, Broekaert N, De Mil T, Fraeyman S, De Backer P, Croubels S. Pilot toxicokinetic study and absolute oral bioavailability of the *Fusarium* mycotoxin enniatin B1 in pigs. *Food and Chemical Toxicology* 2014; 63: 161-165.
- [4] Blount WP. Turkey “X” disease. *Turkeys* 1961; 9: 52-61.
- [5] Forgacs J, Carll WT. Preliminary mycotoxic studies on hemorrhagic disease in poultry. *Veterinary Medicine* 1955, 50: 172-177.
- [6] Thomas NJ, Hunter DB, Atkinson CT. *Infectious diseases of wild birds*. Wiley-Blackwell, Hoboken, New Jersey, 2007, pp. 484.
- [7] FAO (Food and Agriculture Organization of the United Nations), 2015, Food safety and quality: mycotoxins; <http://www.fao.org/food/food-safety-quality/a-z-index/mycotoxins/en/>.
- [8] Berthiller F, Crews C, Dall’Asta C, Saeger SD, Haesaert G, Karlovsky P, Oswald IP, Seefelder W, Speijers G, Stroka J. Masked mycotoxins: a review. *Molecular Nutrition and Food Research* 2013; 57: 165-186.
- [9] Njapau H, Trujillo S, van Egmond HP, Park DL. *Mycotoxins and phycotoxins – advances in determination, toxicology and exposure management*. Wageningen Academic Publishers, Wageningen, 2006 pp. 356.
- [10] De Saeger S. *Determining mycotoxins and mycotoxigenic fungi in food and feed*. Woodhead Publishing, Sawston, 2011; pp. 456.
- [11] Barug D, van Egmond H, López-García R, van Osenbruggen R, Visconti A. *Meeting the mycotoxin menace*. Wageningen Academic Publishers, Wageningen, 2004, pp. 320.
- [12] Raghavender CR, Reddy BN. Human and animal disease outbreaks in India due to mycotoxins other than aflatoxins. *World Mycotoxin Journal* 2009; 2: 23-30.
- [13] EFSA (European Food Safety Authority), 2015, Mycotoxins; <http://www.efsa.europa.eu/en/topics/topic/mycotoxins.htm>.
- [14] Devreese M, De Baere S, De Backer P, Croubels S. Quantitative determination of the *Fusarium* mycotoxins beauvericin, enniatin A, A1, B and B1 in pig plasma using high performance liquid chromatography–tandem mass spectrometry. *Talanta* 2013; 106: 212-219.
- [15] FDA (US Food and Drug Administration) Office of Regulatory Affairs, Office of Regulatory Science, 2015, ORA Laboratory Manual, Section 7: Mycotoxin analysis;

- <http://www.fda.gov/downloads/scienceresearch/fieldscience/laboratorymanual/ucm092245.pdf>.
- [16] Yazar S, Omurtag GZ. Fumonisin, trichothecenes and zearalenone in cereals. *International Journal of Molecular Sciences* 2008; 9: 2062-2090.
- [17] Varga E, Glauner T, Berthiller F, Krska R, Schuhmacher R, Sulyok M. Development and validation of a (semi-) quantitative UHPLC-MS/MS method for the determination of 191 mycotoxins and other fungal metabolites in almonds, hazelnuts, peanuts and pistachios. *Analytical and Bioanalytical Chemistry* 2013; 405: 5087-5104.
- [18] Bennett JW, Klich M. Mycotoxins. *Clinical Microbiology Reviews* 2003; 16: 497-516.
- [19] EMAN (European Mycotoxins Awareness Network), 2015; <http://www.mycotoxins.org/node/36>.
- [20] Gravesen S, Frisvad JC, Samson RA. *Microfungi*. Munksgaard, Copenhagen, 1994, pp. 192.
- [21] Whitlow LW, Hagler WM, 2015, Mycotoxins in dairy cattle: occurrence, toxicity, prevention and treatment; <https://www.msu.edu/~mdr/mycotoxins.pdf>.
- [22] Jarvis BB, Miller JD. Mycotoxins as harmful indoor air contaminants. *Applied Microbiology and Biotechnology* 2005; 66: 367-372.
- [23] Milicevic DR, Skrinjar M, Baltic T. Real and perceived risks for mycotoxin contamination in foods and feeds: Challenges for food safety control. *Toxins* 2010; 2: 572-592.
- [24] Richard JL. Some major mycotoxins and their mycotoxicoses - An overview. *International Journal of Food Microbiology* 2007; 119: 3-10.
- [25] Barrett JR. Mycotoxins: of molds and maladies. *Environmental Health Perspectives* 2000, 108: A20-A23.
- [26] Jestoi M. Emerging Fusarium mycotoxins fusaproliferin, beauvericin, enniatins, and moniliformin – a review. *Critical Reviews in Food Science and Nutrition* 2008; 48: 21-49.
- [27] Kolf-Clauw M, Sassahara M, Lucioli J, Rubira-Gerez J, Alassane-Kpembé I, Lyazhri F, Borin C, Oswald IP. The emerging mycotoxin, enniatin B1, down-modulates the gastrointestinal toxicity of T-2 toxin *in vitro* on intestinal epithelial cells and *ex vivo* on intestinal explants. *Archives of Toxicology* 2013; 87: 2233-2241.
- [28] EFSA (European Food Safety Authority), 2007, Definition and description of “emerging risks” within the EFSA’s mandate, EFSA/SC/415 Final, Parma; <http://www.efsa.europa.eu/en/scdocs/doc/escoemriskdefinition.pdf>.
- [29] Capriotti AL, Caruso G, Cavaliere C, Foglia P, Samperi R, Lagana A. Multiclass mycotoxin analysis in food, environmental and biological matrices, with chromatography/mass spectrometry. *Mass Spectrometry Reviews* 2012; 31: 466-503.
- [30] Laatsch H. *AntiBase 2005, A Natural products database for rapid structure determination*. Chemical Concepts, Weinheim, 2005.
- [31] Berthiller F, Sulyok M, Krska R, Schuhmacher R. Chromatographic methods for the simultaneous determination of mycotoxins and their conjugates in cereals. *Int J Food Microbiol* 2007; 119(1-2): 33-37.

- [32] CAST (Council for Agricultural Science and Technology). Mycotoxins, risks in plant, animal and human systems. Ames, 2003, pp. 217.
- [33] Kuzdralinski A, Solarska E, Mazurkiewicz J. Mycotoxin content of organic and conventional oats from southeastern Poland. *Food Control* 2013; 33: 68-72.
- [34] Jarvis BB. Analysis for mycotoxins: the chemist's perspective. *Arch Environ Health* 2003; 58(8): 479-483.
- [35] Miller JD, McMullin DR. Fungal secondary metabolites as harmful indoor air contaminants: 10 years on. *Appl Microbiol Biotechnol* 2014; 98(24): 9953-9966.
- [36] Oh DC, Jensen PR, Fenical W. Zygosporamide, a cytotoxic cyclic depsipeptide from the marine-derived fungus *Zygosporium masonii*. *Tetrahedron Letters* 2006; 47: 8625-8628.
- [37] Wang Y, Zhang F, Zhang Y, Liu JO, Ma D. Synthesis and antitumor activity of cyclodepsipeptide zygosporamide and its analogues. *Bioorganic and Medicinal Chemistry Letters* 2008; 18: 4385-4387.
- [38] Geiger M, Guitton Y, Vansteelandt M, Kerzaon I, Blanchet E, du Pont TR, Frisvad JC, Hess P, Pouchus YF, Grovel O. Cytotoxicity and mycotoxin production of shellfish-derived *Penicillium* spp., a risk for shellfish consumers. *Letters in Applied Microbiology* 2013; 57: 385-392.
- [39] Sidell FR, Takafuji ET, Franz DR. Medical aspects of chemical and biological warfare. TMM Publications, Phoenix, Arizona, 1997, pp 721.
- [40] Kim EE, Baker CT, Dwyer MD, Murcko MA, Rao BG, Tung RD, Navia MA. Crystal-structure of HIV-1 protease in complex with VW-478, a potent and orally bioavailable inhibitor of the enzyme. *Journal of the American Chemical Society* 1995; 117: 1881-1882.
- [41] Thompson LA, Elman JA. Synthesis and applications of small molecule libraries. *Chemical reviews* 1996; 96: 555-600.
- [42] Leeson PD, Springthorpe B. The influence of drug-like concepts on decision-making in medicinal chemistry. *Nature Reviews Drug Discovery* 2007; 6: 881-890.
- [43] Lipinski CA, Lombardo F, Dominy BW, Feeney PJ. Experimental and computational approaches to estimate solubility and permeability in drug discovery and development settings. *Advanced Drug Delivery Reviews* 1997; 23: 3-25.
- [44] Veber DF, Johnson SR, Cheng H-Y, Smith BR, Ward KW, Kopple KD. Molecular properties that influence the oral bioavailability of drug candidates. *Journal of Medicinal Chemistry* 2002; 45: 2615-2623.
- [45] Taevernier L, Veryser L, Roche N, Peremans K, Burvenich C, Delesalle C, De Spiegeleer B. Human skin permeation of emerging mycotoxins (beauvericin and enniatins). *Journal of Exposure Science and Environmental Epidemiology* 2015; doi:10.1038/jes.2015.10.
- [46] Meca G, Mañes J, Font G, Ruiz M-J. Study of the potential toxicity of commercial crispy breads by evaluation of bioaccessibility and bioavailability of minor *Fusarium* mycotoxins. *Food and Chemical Toxicology* 2012; 50: 288-294.
- [47] Jirakkakul J, Punya J, Pongpattanakitsote S, Paungmoung P, Vorapreeda N, Tachaleat A, Klomnara C, Tanticharoen M, Cheedvadhanarak S. Identification of the nonribosomal peptide

- synthetase gene responsible for bassianolide synthesis in wood-decaying fungus *Xylaria* sp. BCC1067. *Microbiology* 2008; 154: 995-1006.
- [48] Yu D, Xu F, Zi J, Wang S, Gage D, Zeng J, Zhan J. Engineered production of fungal anticancer cyclooligomer depsipeptides in *Saccharomyces cerevisiae*. *Metabolic Engineering* 2013; 18: 60-68.
- [49] Shier WT. The fumonisin paradox: A review of research on oral bioavailability of fumonisin B1, a mycotoxin produced by *Fusarium moniliforme*. *Journal of Toxicology: Toxin Reviews* 2000; 19: 161-187.
- [50] Jover R, Ponsoda X, Castell JV, Gomez-Lechon MJ. Evaluation of the cytotoxicity of ten chemicals on human cultured hepatocytes: Predictability of human toxicity and comparison with rodent cell culture systems. *Toxicology in vitro* 1992; 6: 47-52.
- [51] Ruiz MJ, Macakova P, Juan-Garcia A, Font G. Cytotoxic effects of mycotoxin combinations in mammalian kidney cells. *Food and Chemical Toxicology* 2011; 49: 2718-2724.
- [52] Alassane-Kpembé I, Kolf-Clauw M, Gauthier T, Abrami R, Abiola FA, Oswald IP, Puel OP. New insights into mycotoxin mixtures: The toxicity of low doses of type B trichothecenes on intestinal epithelial cells is synergistic. *Toxicology and Applied Pharmacology* 2013; 272: 191-198.
- [53] Prosperini A, Font G, Ruiz MJ. Interaction effects of *Fusarium* enniatins (A, A1, B and B1) combinations on *in vitro* cytotoxicity of Caco-2 cells. *Toxicology in vitro* 2014; 28: 88-94.
- [54] Grenier B, Oswald IP. Mycotoxin co-contamination of food and feed: meta-analysis of publications describing toxicological interactions. *World Mycotoxin Journal* 2011; 4: 285-313.
- [55] Harrer H, Laviad EL, Humpf HU, Futerman AH. Identification of N-acyl-fumonisin B1 as new cytotoxic metabolites of fumonisin mycotoxins. *Molecular Nutrition and Food Research* 2013; 57: 516-522.
- [56] Kayalou S, Ndossi D, Frizzell C, Groseth PK, Connolly L, Sorlie M, Verhaegen S, Ropstad E. An investigation of the endocrine disrupting potential of enniatin B using *in vitro* bioassays. *Toxicology Letters* 2015; 233: 84-94.
- [57] Ndossi DG, Frizzell C, Tremoen NH, Faeste CK, Verhaegen S, Dahl E, Eriksen GS, Sorlie M, Connolly L, Ropstad E. An *in vitro* investigation of endocrine disrupting effects of trichothecenes deoxynivalenol (DON), T-2 and HT-2 toxins. *Toxicology Letters* 2012; 214: 268-278.
- [58] Eriksson L, Johansson E, Kettaneh-Wold N, Trygg J, Wikström C, Wold S. Multi- and megavariable data analysis: part I – Basic principles and applications. Umetrics AB, Umea, 2006, pp. 355.
- [59] Onstad DW, Fuxa JR, Humber RA, Oestergaard J, Shapirollan DI, Gouli VV, Anderson RS, Andreadus TG, Lacey LA, 2006, An Abridged Glossary of Terms Used in Invertebrate Pathology, 3rd Ed. Society for Invertebrate Pathology; <http://www.sipweb.org/resources/glossary.html>.
- [60] Dumas C, Matha V, Quiot JM, Vey A. Effects of destruxins, cyclic depsipeptide mycotoxins, on calcium balance and phosphorylation of intracellular proteins in lepidopteran cell lines.

- Comparative Biochemistry and Physiology Part C Pharmacology, Toxicology and Endocrinology 1996; 114: 213-219.
- [61] Russell DW, Ward V. Abstract 1st Meeting Fed. European Biochem. Soc. London, Communication 1964; A97.
- [62] Herrmann M, Zocher R, Haese A. Enniatin production by *Fusarium* strains and its effect on potato tuber tissue. Applied and Environmental Microbiology 1996; 62: 393-398.
- [63] Ivanova L, Skjerve E, Eriksen GS, Uhlig S. Cytotoxicity of enniatins A, A1, B, B1, B2 and B3 from *Fusarium avenaceum*. *Toxicon* 2006; 47: 868-876.
- [64] Isaka M, Palasarn S, Supothina S, Komwijit S, Luangsa-ard JJ. Bioactive compounds from the scale insect pathogenic fungus *Conoideocrella tenuis* BCC 18627. *Journal of Natural Products* 2011; 74: 782-789.
- [65] Lang G, Mitova MU, Ellis G, van der Sar S, Phipps RK, Blunt JW, Cummings NJ, Cole ALJ, Munro MHG. Bioactivity profiling using HPLC/microtiter-plate analysis: application to a New Zealand marine alga-derived fungus, *Gliocladium* sp. *Journal of Natural Products* 2006; 69: 621-624.
- [66] Ferrer E, Juan-García A, Font G, Ruiz MJ. Reactive oxygen species induced by beauvericin, patulin and zearalenone in CHO-K1 cells. *Toxicology in vitro* 2009; 23: 1504-1509.
- [67] Fukuda T, Arai M, Yamaguchi Y, Masuma R, Tomoda H, Omura S. New beauvericins, potentiators of antifungal miconazole activity, produced by *Beauveria* sp. FKI-1366 – I. Taxonomy, fermentation, isolation and biological properties. *The Journal of Antibiotics* 2004; 57: 110-116.
- [68] Prosperini A, Meca G, Font G, Ruiz MJ. Study of the cytotoxic activity of beauvericin and fusaproliferin and bioavailability in vitro on Caco-2 cells. *Food and Chemical Toxicology* 2012; 50: 2356-2361.
- [69] Sifou A, Meca G, Serrano AB, Mahnine N, Abidi AE, Mañes J, Azzouzi ME, Zinedine A. First report on the presence of emerging *Fusarium* mycotoxins enniatins (A, A1, B, B1), beauvericin and fusaproliferin in rice on the Moroccan retail markets. *Food Control* 2011; 22: 1826-1830.
- [70] Song HH, Lee HS, Lee GP, Ha SD, Lee C. Structural analysis of enniatin H, I, and MK1688 and beauvericin by liquid chromatography-tandem mass spectrometry (LC-MS/MS) and their production by *Fusarium oxysporum* KFCC 11363P. *Food Additives and Contaminants: Part A* 2009; 26: 518-526.
- [71] Wang Q, Xu L. Beauvericin, a Bioactive Compound Produced by Fungi: A Short Review. *Molecules* 2012; 17: 2367-2377.
- [72] Jenkins KM, Renner MK, Jensen PR, Fenical W. Exumolides A and B: antimicrobial cyclic depsipeptides produced by a marine fungus of the genus *Scytalidium*. *Tetrahedron Letters* 1998; 39: 2463-2466.
- [73] Huang H, She Z, Lin Y, Vrijmoed LLP, Lin W. Cyclic peptides from an endophytic fungus obtained from a mangrove leaf (*Kandelia candel*). *Journal of Natural Products* 2007; 70: 1696-1699.

- [74] Kim MY, Sohn JH, Ahn JS, Oh H. Alternaramide, a cyclic depsipeptide from the marine-derived fungus *Alternaria* sp. SF-5016. *Journal of Natural Products* 2009; 72: 2065-2068.
- [75] Jegorov A, Hajduch M, Sulc M, Havlicek V. Nonribosomal cyclic peptides: specific markers of fungal infections. *Journal of Mass Spectrometry* 2006; 41: 563-576.
- [76] Kuzma M, Jegorov A, Kacer P, Havlicek V. Sequencing of new beauverolides by high performance liquid chromatography and mass spectrometry. *Journal of Mass Spectrometry* 2001; 36: 1108-1115.
- [77] Boot CM, Amagata T, Tenneya K, Comptona JE, Pietraskiewicz H, Valeriote FA, Crews P. Four classes of structurally unusual peptides from two marine-derived fungi: structures and bioactivities. *Tetrahedron* 2007; 63: 9903-9914.
- [78] Che Y, Swenson DC, Gloer JB, Koster B, Malloch D. Pseudodestruixins A and B: new cyclic depsipeptides from the Coprophilous fungus *Nigrosabulum globosum*. *Journal of Natural Products* 2001; 64: 555-558.
- [79] Dornetshuber-Fleiss R, Heffeter P, Mohr T, Hazemi P, Kryeziu K, Seger C, Berger W, Lemmens-Gruber R. Destruixins: fungal-derived cyclohexadepsipeptides with multifaceted anticancer and antiangiogenic activities. *Biochemical Pharmacology* 2013; 86: 361–377.
- [80] Engstrom GW, DeLance JV, Richard JL, Baetz AL. Purification and characterization of roseotoxin B, a toxic cyclodepsipeptide from *Trichothecium roseum*. *Journal of Agricultural and Food Chemistry* 1975; 23: 244-253.
- [81] Kawazu K, Murakami T, Ono Y, Kanzaki H, Kobayashi A, Mikawa T, Yoshikawa N. Isolation and characterization of two novel nematocidal depsipeptides from an imperfect fungus, strain D1084. *Bioscience, Biotechnology and Biochemistry* 1993; 57: 98-101.
- [82] Lira SP, Vita-Marques AM, Selegnum MHR, Bugni TS, LaBarbera DV, Sette LD, Sponchiado SRP, Ireland CM, Berlinck RGS. New destruxins from the marine-derived fungus *Beauveria felina*. *The Journal of Antibiotics* 2006; 59: 553-563.
- [83] Springer JP, Cole RJ, Dorner JW, Cox RH, Richard JL, Barnes CL, van der Helm D. Structure and conformation of roseotoxin B. *Journal of the American Chemical Society* 1984; 106: 2388-2392.
- [84] Sree KS Padmaja V, Murthy YL. Insecticidal activity of destruxin, a mycotoxin from *Metarhizium anisopliae* (Hypocreales), against *Spodoptera litura* (Lepidoptera: Noctuidae) larval stages. *Pest Management Science* 2008; 64: 119-125.
- [85] Chiang YM, Szewczyk E, Nayak T, Davidson AD, Sanchez JF, Lo HC, Ho WY, Simityan H, Kuo E, Praseuth A, Watanabe K, Oakley BR, Wang CCC. Molecular genetic mining of the *Aspergillus* secondary metabolome: discovery of the emericellamide biosynthetic pathway. *Chemistry and Biology* 2008; 15: 527-532.
- [86] Ghosh S, Pradhan TK. The first total synthesis of emericellamide A. *Tetrahedron Letters* 2008; 49: 3697-3700.
- [87] Oh DC, Kauffman CA, Jensen PR, Fenical W. Induced production of emericellamides A and B from the marine-derived fungus *Emericella* sp. in competing co-culture. *Journal of Natural Products* 2007; 70: 515-520.

- [88] Amagata T, Morinaka BI, Amagata A, Tenney K, Valeriote FA, Lobkovsky E, Clardy J, Crews PJ. A chemical study of cyclic depsipeptides produced by a sponge-derived fungus. *Journal of Natural Products* 2006; 69: 1560-1565.
- [89] Sy-Cordero AA, Graf TN, Adcock AF, Kroll DJ, Shen Q, Swanson SM, Wani MC, Pearce CJ, Oberlies NH. Cyclodepsipeptides, sesquiterpenoids, and other cytotoxic metabolites from the filamentous fungus *Trichothecium* sp. (MSX 51320). *Journal of Natural Products* 2011; 74: 2137-2142.
- [90] Isaka M, Palasarn S, Sriklung K, Kocharin K. Cyclohexadepsipeptides from the insect pathogenic fungus *Hirsutella nivea* BCC 2594. *Journal of Natural Products* 2005; 68: 1680-1682.
- [91] Vongvanich N, Kittakoop P, Isaka M, Trakulnaleamsai S, Vimuttipong S, Tanticharoen M, Thebtaranonth Y. Hirsutellide A, a new antimycobacterial cyclohexadepsipeptide from the entomopathogenic fungus *Hirsutella kobayashii*. *Journal of Natural Products* 2002; 65: 1346-1348.
- [92] Hamano K, Kinoshita M, Furuya K, Miyamoto M, Takamatsu Y, Hemmi A, Tanzawa K. Leualacin, a novel calcium blocker from *Hapsidospora irregularis*. 1. Taxonomy, fermentation, isolation, physicochemical and biological properties. *The Journal of Antibiotics* 1992; 45: 899-905.
- [93] Bringmann G, Lang G, Steffens S, Schaumann K. Petrosifungins A and B, novel cyclodepsipeptides from a sponge-derived strain of *Penicillium brevicompactum*. *Journal of Natural Products* 2004; 67: 311-315.
- [94] Moussa MM, Le Quesne PW. Total synthesis of the cyclodepsipeptide ionophore pithomycolide. *Tetrahedron Letters* 1996; 37: 6479-6482.
- [95] Belofsky GN, Jensen PR, Fenical W. Sansalvamide: a new cytotoxic cyclic depsipeptide produced by a marine fungus of the genus *Fusarium*. *Tetrahedron Letters* 1999; 40: 2913-2916.
- [96] Cueto M, Jensen PR, Fenical W. N-Methylsansalvamide, a cytotoxic cyclic depsipeptide from a marine fungus of the genus *Fusarium*. *Phytochemistry* 2000; 55: 223-226.
- [97] Hwang Y, Rowley D, Rhodes D, Gertsch J, Fenical W, Bushman F. Mechanism of inhibition of a poxvirus topoisomerase by the marine natural product sansalvamide A. *Molecular Pharmacology* 1999; 55: 1049-1053.
- [98] Suzuki A, Kanaoka M, Isogai A, Murakoshi S, Ichinoe M, Tamura, S. Bassianolide, a new insecticidal cyclodepsipeptide from *Beauveria bassiana* and *Verticillium lecanii*. *Tetrahedron Letters* 1977; 25: 2167-2170.
- [99] Yu D, Xu F, Zi J, Wang S, Gage D, Zeng J, Zahn J. Engineered production of fungal anticancer cyclooligomer depsipeptides in *Saccharomyces cerevisiae*. *Metabolic Engineering* 2013; 18: 60-68.
- [100] Dornetshuber R, Kamyar MR, Rawnduzi P, Baburin I, Kouri K, Pilz E, Hornbogen T, Zocher R, Berder W, Lemmens-Gruber R. Effects of the anthelmintic drug PF1022A on mammalian tissue and cells. *Biochemical Pharmacology* 2009; 77: 1437-1444.

- [101] Sasaki T, Takagi M, Yaguchi T, Miyadoh S, Okada T, Koyama M. A new anthelmintic cyclodepsipeptide, PF1022A. *The Journal of Antibiotics* 1992; 45: 692-697.
- [102] Nihei K, Itoh H, Hashimoto K, Miyairi K, Okuno T. Antifungal cyclodepsipeptides, W493 A and B, from *Fusarium* sp.: isolation and structural determination. *Bioscience, Biotechnology and Biochemistry* 1998; 62: 858-863.
- [103] Abdel-Lateff A, Elkhayat ES, Fouad MA, Okino T. Aureobasidin, new antifouling metabolite from marine-derived fungus *Aureobasidium* sp. *Natural Product Communications* 2009; 4: 389-394.
- [104] Detwiler JE, Lubell WD. Progress in a structure activity study of the aureobasidin peptide antibiotics. Abstract (P185) 18th American Peptide Symposium, *Biopolymers* 2003; 71: 344-345.
- [105] Sonda S, Sala G, Ghidoni R, Hemphill A, Pieters J. Inhibitory effect of aureobasidin A on *Toxoplasma gondii*. *Antimicrobial Agents and Chemotherapy* 2005; 49: 1794-1801.
- [106] Tan HW, Tay ST. The inhibitory effects of aureobasidin A on *Candida planktonic* and biofilm cells: Inhibitory effects of aureobasidin A on *Candida*. *Mycoses* 2013; 56: 150-156.
- [107] Tanaka AK, Valero VB, Takahashi HK, Straus AH. Inhibition of *Leishmania* (*Leishmania*) *amazonensis* growth and infectivity by aureobasidin A. *Journal of Antimicrobial Chemotherapy* 2007; 59: 487-492.
- [108] Kaida K, Fudou R, Kameyama T, Tubaki K, Suzuki Y, Ojika M, Sakagame Y. New cyclic depsipeptide antibiotics, clavariopsins A and B, produced by an aquatic hyphomycetes, *Clavariopsis aquatica*. *The Journal of Antibiotics* 2001; 54: 17-21.
- [109] Nakadate S, Nozawa K, Sato H, Horie H, Fujii Y, Nagai M, Hosoe T, Kawai K, Yaguchi T. Antifungal cyclic depsipeptide, eujavanicin A, isolated from *Eupenicillium javanicum*. *Journal of Natural Products* 2008; 71: 1640-1642.
- [110] Ratnayake R, Fremlin LJ, Lacey E, Gill JH, Capon RJ. Acremolides A-D, lipodepsipeptides from an Australian marine-derived fungus, *Acremonium* sp. *Journal of Natural Products* 2008; 71: 403-408.
- [111] McCorkindale NJ, Baxter RL. Brevigellin, a benzoylated cyclodepsipeptide from *Penicillium brevicompactum*. *Tetrahedron* 1981; 37: 1795-1801.
- [112] Sato T, Ishiyama D, Honda R, Senda H, Konno H, Tokumasu S, Kanazawa S. Glomosporin, a novel antifungal cyclic depsipeptide from *Glomospora* sp. I. Production, isolation, physico-chemical properties and biological activities. *The Journal of Antibiotics* 2000; 53: 597-602.
- [113] Guo YX, Liu QH, Ng TB, Wang HX. Isarfelin, a peptide with antifungal and insecticidal activities from *Isaria felina*. *Peptides* 2005; 26: 2384-2391.
- [114] Langenfeld A, Blond A, Gueye S, Herson P, Nay B, Dupont J, Prado S. Insecticidal cyclodepsipeptides from *Beauveria felina*. *Journal of Natural Products* 2011; 74: 825-830.
- [115] Ravindra G, Ranganayaki RS, Raghothama S, Srinivasan MC, Gilardi RD, Karle IL, Balaram P. Two novel hexadepsipeptides with several modified amino acid residues isolated from the fungus *Isaria*. *Chemistry and Biodiversity* 2004; 1: 489-504.

- [116] Sabareesh V, Ranganayaki RS, Raghothama S, Bopanna MP, Balaram H, Srinivasan MC, Balaram P. Identification and characterization of a library of microheterogeneous cyclohexadepsipeptides from the fungus *Isaria*. *Journal of Natural Products* 2007; 70: 715-729.
- [117] Yu Z, Lang G, Kajahn I, Schmaljohann R, Imhoff JF. Scopularides A and B, cyclodepsipeptides from a marine sponge-derived fungus, *Scopulariopsis brevicaulis*. *Journal of Natural Products* 2008; 71: 1052-1054.
- [118] Gillis HA, Russell DW, Taylor A, Walter JA. Isolation and structure of sporidesmolide V from cultures of *Pithomyces chartarum*. *Canadian Journal of Chemistry* 1990; 68: 19-21.
- [119] Russell DW. Sporidesmolide-I, a metabolic product of *Sporidesmium bakeri* SYD. *Biochimica et Biophysica Acta* 1960; 45: 411-412.
- [120] Russell DW. Depsipeptides of *Pithomyces chartarum* – Structure of sporidesmolide I. *Journal of the Chemical Society* 1962; 753-761.
- [121] Morino T, Masuda A, Yamada M, Nishimoto M, Nishikiori T, Saito S. Stevastelins, novel immunosuppressants produced by *Penicillium*. *The Journal of Antibiotics* 1994; 47: 1341-1343.

SUPPLEMENTARY INFORMATION

S1. Quantitative *in vitro* cytotoxicity of some accepted mycotoxins.

S2. Principal component analysis.

Table S1: Quantitative *in vitro* cytotoxicity of some accepted mycotoxins.

Mycotoxin		Cell line	Tested range	IC ₅₀ ⁽¹⁾	Reference
Aflatoxin B1	AFB1	A2780	0 – 96 µM	14.7 nM	Braicu <i>et al.</i> [1]
		HUVEC	0 – 96 µM	2.168 µM	Braicu <i>et al.</i> [1]
		HFL	0 – 96 µM	19.81 nM	Braicu <i>et al.</i> [1]
		SK-6	0.32 – 32.02 µM	5.89 µM	Stec <i>et al.</i> [2]
		PO	0.32 – 32.02 µM	14.54 µM	Stec <i>et al.</i> [2]
		FLK	0.32 – 32.02 µM	10.60 µM	Stec <i>et al.</i> [2]
		HepG2	0.01 – 100 µM	1 µM	McKean <i>et al.</i> [3]
		BEAS-2B	0.01 – 100 µM	n.d.	McKean <i>et al.</i> [3]
Aflatoxin B2	AFB2	A2780	0 – 96 µM	0.4804 µM	Braicu <i>et al.</i> [1]
		HUVEC	0 – 96 µM	15.34 µM	
		HFL	0 – 96 µM	0.2135 µM	
Aflatoxin G1	AFG1	A2780	0 – 96 µM	0.4707 µM	Braicu <i>et al.</i> [1]
		HUVEC	0 – 96 µM	2.607 µM	
		HFL	0 – 96 µM	0.2212 µM	
Aflatoxin G2	AFG2	A2780	0 – 96 µM	0.5264 µM	Braicu <i>et al.</i> [1]
		HUVEC	0 – 96 µM	5.824 µM	
		HFL	0 – 96 µM	0.2212 µM	
Alternariol	AOH	HCT116	10 – 200 µM	65 µM	Bensassi <i>et al.</i> [4]
Beauvericin	BEA	CHO-K1	1 – 100 µM	12.08 – 17.22 µM	Ferrer <i>et al.</i> [5]
		Vero	0.78 – 25 µM	6.25 – 11.08 µM	Ruiz <i>et al.</i> [6]
		Caco-2	0.6 – 30 µM	12.75 – 20.62 µM	Prosperini, <i>et al.</i> [7]
		HT-29	0.6 – 30 µM	9.75 – 15.00 µM	Prosperini, <i>et al.</i> [7]
Citrinin	CIT	SK-6	0.40 – 39.96 µM	12.99 µM	Stec <i>et al.</i> [2]
		PO	0.40 – 39.96 µM	18.54 µM	
		FLK	0.40 – 39.96 µM	15.38 µM	
Cytochalasin B	CB	HeLa	n.m. ⁽²⁾	7.9 µM	Hwang <i>et al.</i> [8]

(1) If a range is given, this is the result of either multiple assays (*e.g.* NR versus MTT assay) or multiple time spans (*e.g.* 24h, 48h or 72h).

(2) Only the abstract was available.

n.d. = not determined

n.m. = not mentioned

Table S1: Quantitative *in vitro* cytotoxicity of some accepted mycotoxins (continued).

Deoxynivalenol	DON	Caco-2	7.5 nM – 6.67 µM	1.19 – 1.39 µM	Alassane-Kpembi <i>et al.</i> [9]
		Caco-2	0.13 – 67.50 µM	3.40 µM	Cetin and Bullerman [10]
		Caco-2 (differentiated)	0 – 10 µM	>10 µM	Bony <i>et al.</i> [11]
		Caco-2 (dividing)	0 – 10 µM	3.7 – 10.0 µM	Bony <i>et al.</i> [11]
		Vero	0.25 – 8 µM	3.30 – 10 µM	Ruiz <i>et al.</i> [6]
		HCT116	10 – 200 µM	125 µM	Bensassi <i>et al.</i> [12]
		HepG2	0.1 – 100 µM	41.4 µM	Königs <i>et al.</i> [13]
		HepG2	0.13 – 67.50 µM	28.2 µM	Cetin and Bullerman [10]
		Human primary hepatocytes	0.1 – 100 µM	6.0 µM	Königs <i>et al.</i> [13]
		K562	0.13 – 135 µM	1.31 µM	Wu <i>et al.</i> [14]
		CHO-K1	0.13 – 67.50 µM	0.91 µM	Cetin and Bullerman [10]
		V79	0.13 – 67.50 µM	1.55 µM	Cetin and Bullerman [10]
		C5-O	0.13 – 67.50 µM	1.82 µM	Cetin and Bullerman [10]
		PAM	0 – 8 µM	1.0 – 1.7 µM	Döll <i>et al.</i> [15]
3-Acetyldeoxynivalenol	3-ADON	Caco-2	7.5 nM – 6.67 µM	1.99 – 2.94 µM	Alassane-Kpembi <i>et al.</i> [9]
15-Acetyldeoxynivalenol	15-ADON	Caco-2	7.5 nM – 6.67 µM	1.1 – 1.47 µM	Alassane-Kpembi <i>et al.</i> [9]
Enniatin A	ENN A	Caco-2	0.94 – 7.5 µM	1.6 – 6.8 µM	Prosperini <i>et al.</i> [16]
Enniatin A1	ENN A1	Caco-2	0.94 – 15 µM	1.3 – 14.8 µM	Prosperini <i>et al.</i> [16]
Enniatin B	ENN B	Caco-2	0.94 – 15 µM	11.7 µM	Prosperini <i>et al.</i> [16]
Enniatin B1	ENN B1	Caco-2	0.94 – 15 µM	2.8 – 11.3 µM	Prosperini <i>et al.</i> [16]
Fumonisin B1	FB1	IPEC-1	0.3 – 100 µM	15.80 µM	Kolf-Clauw <i>et al.</i> [17]
		Caco-2	0.28 – 138.54 µM	131 – >138 µM	Cetin and Bullerman [10]
		HepG2	0.28 – 138.54 µM	> 138 µM	
		CHO-K1	0.28 – 138.54 µM	118 – >138 µM	
		V79	0.28 – 138.54 µM	136 – >138 µM	
Fusaproliferin	FUS	C5-O	0.28 – 138.54 µM	> 138 µM	
		HT-29	0.6 – 30 µM	n.d.	Prosperini, <i>et al.</i> [7]
		Caco-2	0.6 – 30 µM	n.d.	
Fusarenon-X	FUS-X	Caco-2	7.5 nM – 6.67 µM	0.02 – 0.04 µM	Alassane-Kpembi <i>et al.</i> [9]
Gliotoxin	GLI	<i>Tetrahymena pyriformis</i> GL	0.06 – 2.02 µM	0.38 µM	Gräbsch <i>et al.</i> [18]
Moniliformin	MON	Caco-2	1.67 – 833.06 µM	315 – >1020 µM	Cetin and Bullerman [10]
		HepG2	1.67 – 833.06 µM	273 – 403 µM	
		CHO-K1	1.67 – 833.06 µM	>1020 µM	
		V79	1.67 – 833.06 µM	>1020 µM	
		C5-O	1.67 – 833.06 µM	349 – >1020 µM	
Nivalenol	NIV	Caco-2	7.5 nM – 6.67 µM	0.69 – 0.90 µM	Alassane-Kpembi <i>et al.</i> [9]

n.d. = not determined

Table S1: Quantitative *in vitro* cytotoxicity of some accepted mycotoxins (continued).

Ochratoxin A	OTA	SK-6	0.25 – 24.76 µM	2.58 µM	Stec <i>et al.</i> [2]	
		PO	0.25 – 24.76 µM	3.71 µM	Stec <i>et al.</i> [2]	
		FLK	0.25 – 24.76 µM	1.86 µM	Stec <i>et al.</i> [2]	
		SH-SY5Y neuroblastoma	0.1 – 2.5 µM	n.d.	Zhang <i>et al.</i> [19]	
		Primary neurons	0.1 – 2.5 µM	n.d.	Zhang <i>et al.</i> [19]	
Patulin	PAT	CHO-K1	0.2 – 25 µM	0.69 – 4.4 µM	Ferrer <i>et al.</i> [5]	
		SK-6	0.65 – 64.88 µM	2.01 µM	Stec <i>et al.</i> [2]	
		PO	0.65 – 64.88 µM	3.05 µM	Stec <i>et al.</i> [2]	
		FLK	0.65 – 64.88 µM	1.49 µM	Stec <i>et al.</i> [2]	
Penicillic acid	T-2	<i>Tetrahymena pyriformis</i> GL	73.5 – 588 µM	343.19 µM	Gräbsch <i>et al.</i> [18]	
T-2 toxin		Vero	0 – 100 nM	60 nM	Bouaziz <i>et al.</i> [20]	
		Vero	1.6 – 50 nM	4– 12 nM	Ruiz <i>et al.</i> [6]	
		IPEC-1	0.3 – 100 nM	9.35 nM	Kolf-Clauw <i>et al.</i> [17]	
		RPTEC	1 nM - 10 µM	0.2 µM	Königs <i>et al.</i> [21]	
		NHLF	1 nM - 10 µM	0.5 µM	Königs <i>et al.</i> [21]	
		HepG2	0.01 – 100 µM	980 nM	McKean <i>et al.</i> [3]	
		BEAS-2B	0.01 – 100 µM	32.1 nM	McKean <i>et al.</i> [3]	
		Ovarian rat granulosa	0 – 100 nM	± 100 nM	Wu <i>et al.</i> [22]	
Zearalenone		ZEA	Vero	0 – 100 nM	> 100 nM	Bouaziz <i>et al.</i> [20]
			CHO-K1	1.5 – 150 µM	79.40 – 108.76 µM	Ferrer <i>et al.</i> [5]
			CHO-K1	12.5 – 100 µM	60.3 – >100 µM	Tatay <i>et al.</i> [23]
			CHO-K1	0.63 – 314.11 µM	>313 µM	Cetin and Bullerman [10]
			Caco-2	0 – 100 µM	20 µM	Abid-Essefi <i>et al.</i> [24]
			Caco-2	0.63 – 314.11 µM	137 – >313 µM	Cetin and Bullerman [10]
	HeLa		0 – 140 µM	60 µM	Ayed <i>et al.</i> [25]	
	SK-6		0.31 – 31.41 µM	31.35 µM	Stec <i>et al.</i> [2]	
	PO		0.31 – 31.41 µM	>31.41 µM	Stec <i>et al.</i> [2]	
	FLK		0.31 – 31.41 µM	>31.41 µM	Stec <i>et al.</i> [2]	
	HepG2		1 – 200 µM	95 µM	Hassen <i>et al.</i> [26]	
	HepG2		0.63 – 314.11 µM	>313 µM	Cetin and Bullerman [10]	
	V79		0.63 – 314.11 µM	>313 µM	Cetin and Bullerman [10]	
C5-O	0.63 – 314.11 µM	75.5 – >313 µM	Cetin and Bullerman [10]			

n.d. = not determined

S1. References.

- [1] Braicu C, Berindan-Neagoe I, Chedea VS, Balacescu L, Brie I, Soritau O, Socaciu C, Irimie A. Individual and combined cytotoxic effects of the major four aflatoxines in different in vitro stabilized systems. *Journal of Food Biochemistry* 2010; 34: 1079-1090.
- [2] Stec J, Szczotka M, Kuzmak J. Cytotoxicity of feed-borne mycotoxins to animal cell lines in vitro using the MTT assay. *Bulletin of the Veterinary Institute in Pulawy* 2007; 51: 679-684.
- [3] McKean C, Tang L, Billam M, Tang M, Theodorakis CW, Kendall RJ, Wang JS. Comparative acute and combinative toxicity of aflatoxin B1 and T-2 toxin in animals and immortalized human cell lines. *Journal of Applied Toxicology* 2006; 26: 139-147.
- [4] Bensassi F, Gallerne C, El Dein OS, Hajlaoui MR, Bacha H, Lemaire C. Cell death induced by the *Alternaria* mycotoxin Alternariol. *Toxicology in vitro* 2012; 26: 915-923.
- [5] Ferrer E, Juan-García A, Font G, Ruiz MJ. Reactive oxygen species induced by beauvericin, patulin and zearalenone in CHO-K1 cells. *Toxicology in vitro* 2009; 23: 1504-1509.
- [6] Ruiz MJ, Macakova P, Juan-Garcia A, Font G. Cytotoxic effects of mycotoxin combinations in mammalian kidney cells. *Food and Chemical Toxicology* 2011; 49: 2718-2724.
- [7] Prosperini A, Meca G, Font G, Ruiz MJ. Study of the cytotoxic activity of beauvericin and fusaproliferin and bioavailability in vitro on Caco-2 cells. *Food and Chemical Toxicology* 2012; 50: 2356-2361.
- [8] Hwang J, Yi M, Zhang X, Xu Y, Jung JH, Kim DK. Cytochalasin B induces apoptosis through the mitochondrial apoptotic pathway in HeLa human cervical carcinoma cells. *Oncology Reports* 2013; 30: 1929-1935.
- [9] Alassane-Kpembé I, Kolf-Clauw M, Gauthier T, Abrami R, Abiola FA, Oswald IP, Puel OP. New insights into mycotoxin mixtures: The toxicity of low doses of type B trichothecenes on intestinal epithelial cells is synergistic. *Toxicology and Applied Pharmacology* 2013; 272: 191-198.
- [10] Cetin Y, Bullerman LB. Cytotoxicity of *Fusarium* mycotoxins to mammalian cell cultures as determined by the MTT bioassay. *Food and Chemical Toxicology* 2005; 43: 755-764.
- [11] Bony S, Carcelen M, Olivier L, Devaux A. Genotoxicity assessment of deoxynivalenol in the Caco-2 cell line model using the Comet assay. *Toxicology Letters* 2006; 166: 67-76.
- [12] Bensassi F, Gallerne C, El Dein OS, Lemaire C, Hajlaoui MR, Bacha H. Involvement of mitochondria-mediated apoptosis in deoxynivalenol cytotoxicity. *Food and Chemical Toxicology* 2012; 50: 1680-1689.
- [13] Königs M, Schwerdt G, Gekle M, Humpf HU. Effects of the mycotoxin deoxynivalenol on human primary hepatocytes. *Molecular Nutrition and Food Research* 2008; 52: 830-839.
- [14] Wu X, Murphy P, Cunnick J, Hendrich S. Synthesis and characterization of deoxynivalenol glucuronide: its comparative immunotoxicity with deoxynivalenol. *Food and Chemical Toxicology* 2007; 45: 1846-1855.

- [15] Döll S, Schrickx JA, Dänicke S, Fink-Gremmels J. Deoxynivalenol-induced cytotoxicity, cytokines and related genes in unstimulated or lipopolysaccharide stimulated primary porcine macrophages. *Toxicology Letters* 2009; 184: 97-106.
- [16] Prosperini A, Font G, Ruiz MJ. Interaction effects of *Fusarium* enniatins (A, A1, B and B1) combinations on in vitro cytotoxicity of Caco-2 cells. *Toxicology in vitro* 2014; 28: 88-94.
- [17] Kolf-Clauw M, Sassahara M, Lucioli J, Rubira-Gerez J, Alassane-Kpembé I, Lyazhri F, Borin C, Oswald IP. The emerging mycotoxin, enniatin B1, down modulates the gastrointestinal toxicity of T 2 toxin in vitro on intestinal epithelial cells and ex vivo on intestinal explants. *Archives of Toxicology* 2013; 87: 2233-2241.
- [18] Gräbsch C, Wichmann G, Loffhagen N, Herbarth O, Müller A. Cytotoxicity assessment of gliotoxin and penicillic acid in *Tetrahymena pyriformis*. *Environmental Toxicology* 2006; 21: 111-117.
- [19] Zhang X, Boesch-Saadatmandi C, Lou Y, Wolfram S, Huebbe P, Rimbach G. Ochratoxin A induces apoptosis in neuronal cells. *Genes and Nutrition* 2009; 4: 41-48.
- [20] Bouaziz C, Bouslimi A, Kadri R, Zaied C, Bacha H, Abid-Essefi S. The in vitro effects of zearalenone and T-2 toxins on vero cells. *Experimental and Toxicologic Pathology* 2013; 65: 497-501.
- [21] Königs M, Mulac D, Schwerdt G, Gekle M, Humpf HU. Metabolism and cytotoxic effects of T-2 toxin and its metabolites on human cells in primary culture. *Toxicology* 2009; 258: 106-115.
- [22] Wu J, Tu D, Yuan LY, Yuan H, Wen LX. T-2 toxin exposure induces apoptosis in rat ovarian granulosa cells through oxidative stress. *Environmental Toxicology and Pharmacology* 2013; 36: 493-500.
- [23] Tatay E, Meca G, Font G, Ruiz MJ. Interactive effects of zearalenone and its metabolites on cytotoxicity and metabolization in ovarian CHO-K1 cells. *Toxicology in vitro* 2014; 28: 95-103.
- [24] Abid-Essefi S, Bouaziz C, El Golli-Bennour E, Ouanes Z, Bacha H. Comparative study of toxic effects of zearalenone and its two major metabolites α -zearalenol and β -zearalenol on cultured human caco-2 cells, *Journal of Biochemical and Molecular Toxicology* 2009; 23: 233-243.
- [25] Ayed Y, Ayed-Boussema I, Ouanes Z, Bacha H. In vitro and in vivo induction of chromosome aberrations by alpha- and beta-zearalenols: comparison with zearalenone, *Mutation Research* 2011; 726: 42-46.
- [26] Hassen W, El Golli E, Baudrimont I, Mobio T, Ladjimi MM, Creppy EE, Bacha H. Cytotoxicity and Hsp 70 induction in Hep G2 cells in response to zearalenone and cytoprotection by sub-lethal heat shock. *Toxicology* 2005; 207: 293-301.

S2. Principal component analysis.

Based on the dendrogram of the HCA and the score plot of the first two principal components of the PCA, the 32 cyclic depsipeptides could be categorized into four main clusters with six subclusters, as denoted earlier in Figure 2. From the corresponding loading plot, the most discriminative molecular descriptors for principal components 1 and 2 could be deduced (see Tables S2-1 to S2-4 below). This indicated that principal component 1 on the horizontal axis, is mainly influenced by descriptors describing molecular size, volume and shape (*e.g.* MW, Sv, G1, nBTn nSK, etc.), connectivity (*e.g.* connectivity index X0, X1, X2, etc.) and flexibility (*e.g.* folding degree index FDI) of the peptides. So, cyclic depsipeptides situated towards the right side of the space are larger, have larger ring sizes, have higher molecular weights and are more folded and less flexible, *i.e.* have less conformational variability, compared to the compounds on the left. Compounds are further discriminated by principal component 2 on the vertical axis of the chemical space, which is highly influenced by a set of descriptors called complementary information content (CIC), which quantify the degree of heterogeneity and redundancy of topological neighbourhoods of atoms in molecules and is related to the symmetry of the molecule. Indeed, peptides located in the lower part of space are less symmetrical than compounds located at the upper part. Other discriminative descriptors at the second axis are nCp or C-001, the number of terminal primary carbons (CH3R), and nCt or C-003, the number of total tertiary carbons (CHR3), which may indicate that CDPs located at the upper right part of the space most likely contain more valine, leucine, isoleucine amino acids and/or long branched alkyl chain(s). Moreover, a number of molecular descriptors, such as ARR, nAB, nCar, nBnz, Ui, AROM, nCbH, nR06 and nBM, indicate a higher presence of aromatic/benzene-like rings in CDPs at the lower side of the y-axis.

Table S2-1: Discriminative descriptors on right side of principal component 1 (x-axis).

Descriptor	Meaning
MW	molecular weight
Mass	molecular mass
VED1	eigenvector coefficient sum from distance matrix
Sv	sum of atomic van der Waals volumes (scaled on Carbon atom)
X0	connectivity index chi-0
X0sol	solvation connectivity index chi-0
AMR	Ghose-Crippen molar refractivity
VEp1	eigenvector coefficient sum from polarizability weighted distance matrix
VEv1	eigenvector coefficient sum from van der Waals weighted distance matrix
Refractivity	polarizability
BID	Balaban ID number
nSK	number of non-H atoms
SRW01	self-returning walk count of order 01 (number of non-H atoms, nSK)
VEm1	eigenvector coefficient sum from mass weighted distance matrix
VEZ1	eigenvector coefficient sum from Z weighted distance matrix (Barysz matrix)
VEe1	eigenvector coefficient sum from electronegativity weighted distance matrix
X1v	valence connectivity index chi-1
Dz	Pogliani index
X2	connectivity index chi-2

Table S2-1: Discriminative descriptors on right side of principal component 1 (x-axis) (continued).

X2sol	solvation connectivity index chi-2
Sp	sum of atomic polarizabilities (scaled on Carbon atom)
RHyDp	reciprocal hyper-distance-path index
Har	Harary H index
LPRS	log of product of row sums (PRS)
Har2	square reciprocal distance sum index
TWC	total walk count
HTp	H total index / weighted by atomic polarizabilities
XMOD	modified Randic connectivity index
G1	gravitational index G1
IAC	total information index of atomic composition
TICO	total information content index (neighborhood symmetry of 0-order)
X1	connectivity index chi-1 (Randic connectivity index)
X1sol	solvation connectivity index chi-1
Xu	Xu index
X0v	valence connectivity index chi-0
SRW04	self-returning walk count of order 04
IDDM	mean information content on the distance degree magnitude
RDSQ	reciprocal distance squared Randic-type index
MPC02	molecular path count of order 02 (Gordon-Scantlebury index)
CID	Randic ID number
ZM1	first Zagreb index M1
IDM	mean information content on the distance magnitude
nBT	number of bonds
HTv	H total index / weighted by atomic van der Waals volumes
SEig	absolute eigenvalue sum on geometry matrix
G2	gravitational index G2 (bond-restricted)
Eig1p	Leading eigenvalue from polarizability weighted distance matrix
AEigp	Absolute eigenvalue sum from polarizability weighted distance matrix
Eig1v	Leading eigenvalue from van der Waals weighted distance matrix
AEigv	Absolute eigenvalue sum from van der Waals weighted distance matrix
VRZ1	Randic-type eigenvector-based index from Z weighted distance matrix (Barysz matrix)
VRm1	Randic-type eigenvector-based index from mass weighted distance matrix
VRe1	Randic-type eigenvector-based index from mass weighted distance matrix
VRD1	Randic-type eigenvector-based index from distance matrix
Mor01m	3D-MoRSE - signal 01 / weighted by atomic masses
VRv1	Randic-type eigenvector-based index from van der Waals weighted distance matrix
VRp1	Randic-type eigenvector-based index from polarizability weighted distance matrix
nBO	number of non-H bonds
MWC01	molecular walk count of order 01 (number of non-H bonds, nBO)
SRW02	Spectral moment 03 from edge adj. matrix weighted by resonance integrals
MPC01	molecular path count of order 01 (number of non-H bonds, nBO)
VRA1	Randic-type eigenvector-based index from adjacency matrix
Mor01v	3D-MoRSE - signal 01 / weighted by atomic van der Waals volumes
Se	sum of atomic Sanderson electronegativities (scaled on Carbon atom)
RDF025p	Radial Distribution Function - 2.5 / weighted by atomic polarizabilities
ZM2	second Zagreb index M2
HTe	H total index / weighted by atomic Sanderson electronegativities
ESpm03r	Spectral moment 03 from edge adj. matrix weighted by resonance integrals

Table S2-2: Discriminative descriptors on left side of principal component 1 (x-axis).

Descriptor	Meaning
VEp2	average eigenvector coefficient sum from polarizability weighted distance matrix
VEZ2	average eigenvector coefficient sum from Z weighted distance matrix (Barysz matrix)
VEm2	average eigenvector coefficient sum from mass weighted distance matrix
VEe2	average eigenvector coefficient sum from electronegativity weighted distance matrix
VEv2	average eigenvector coefficient sum from van der Waals weighted distance matrix
VED2	average eigenvector coefficient sum from distance matrix
Mor05p	3D-MoRSE - signal 05 / weighted by atomic polarizabilities
VEA2	average eigenvector coefficient sum from adjacency matrix
Mor05v	3D-MoRSE - signal 05 / weighted by atomic van der Waals volumes
HATS2u	leverage-weighted autocorrelation of lag 2 / unweighted
HATS0u	leverage-weighted autocorrelation of lag 0 / unweighted
HATS2e	leverage-weighted autocorrelation of lag 2 / weighted by atomic Sanderson electronegativities
HGM	geometric mean on the leverage magnitude
HATS4u	leverage-weighted autocorrelation of lag 4 / unweighted
Gs	G total symmetry index / weighted by atomic electrotopological states
SEigp	Eigenvalue sum from polarizability weighted distance matrix
SEigv	Eigenvalue sum from van der Waals weighted distance matrix
HATS0e	leverage-weighted autocorrelation of lag 0 / weighted by atomic Sanderson electronegativities
HATS4e	leverage-weighted autocorrelation of lag 4 / weighted by atomic Sanderson electronegativities
Mor05e	3D-MoRSE - signal 05 / weighted by atomic Sanderson electronegativities
Mor05u	3D-MoRSE - signal 05 / unweighted
Xt	Total structure connectivity index
HATS1u	leverage-weighted autocorrelation of lag 1 / unweighted
REIG	first eigenvalue of the R matrix
SHP2	average shape profile index of order 2
HATS1e	leverage-weighted autocorrelation of lag 1 / weighted by atomic Sanderson electronegativities
Mor05m	3D-MoRSE - signal 05 / weighted by atomic masses
HATS3u	leverage-weighted autocorrelation of lag 3 / unweighted
R4e+	R maximal autocorrelation of lag 4 / weighted by atomic Sanderson electronegativities
G2s	2st component symmetry directional WHIM index / weighted by atomic electrotopological states
Mor18e	3D-MoRSE - signal 18 / weighted by atomic Sanderson electronegativities
HATS3e	leverage-weighted autocorrelation of lag 3 / weighted by atomic Sanderson electronegativities
G1s	1st component symmetry directional WHIM index / weighted by atomic electrotopological states
Mor18u	3D-MoRSE - signal 18 / unweighted
R2u+	R maximal autocorrelation of lag 2 / unweighted
RARS	R matrix average row sum
R2e+	R maximal autocorrelation of lag 2 / weighted by atomic Sanderson electronegativities
FDI	folding degree index
R4u+	R maximal autocorrelation of lag 4 / unweighted
MSD	mean square distance index (Balaban)
HATS0p	leverage-weighted autocorrelation of lag 0 / weighted by atomic polarizabilities
Mor17p	3D-MoRSE - signal 17 / weighted by atomic polarizabilities
Mor08m	3D-MoRSE - signal 08 / weighted by atomic masses
G3s	3st component symmetry directional WHIM index / weighted by atomic electrotopological states
HATS3p	leverage-weighted autocorrelation of lag 3 / weighted by atomic polarizabilities
ISH	standardized information content on the leverage equality
Mor17u	3D-MoRSE - signal 17 / unweighted
Mor21u	3D-MoRSE - signal 21 / unweighted
HATS4p	leverage-weighted autocorrelation of lag 4 / weighted by atomic polarizabilities
Mor17v	3D-MoRSE - signal 17 / weighted by atomic van der Waals volumes
Mor18p	3D-MoRSE - signal 18 / weighted by atomic polarizabilities
BICO	bond information content (neighborhood symmetry of 0-order)
R2v+	R maximal autocorrelation of lag 2 / weighted by atomic van der Waals volumes
R2p+	R maximal autocorrelation of lag 2 / weighted by atomic polarizabilities
HATS0v	leverage-weighted autocorrelation of lag 0 / weighted by atomic van der Waals volumes
HATS1p	leverage-weighted autocorrelation of lag 1 / weighted by atomic polarizabilities
Mor17e	3D-MoRSE - signal 17 / weighted by atomic Sanderson electronegativities
R5m+	R maximal autocorrelation of lag 5 / weighted by atomic masses
Mor23p	3D-MoRSE - signal 23 / weighted by atomic polarizabilities
R8e+	R maximal autocorrelation of lag 8 / weighted by atomic Sanderson electronegativities

Table S2-2: Discriminative descriptors on left side of principal component 1 (x-axis) (continued).

Mor21e	3D-MoRSE - signal 21 / weighted by atomic Sanderson electronegativities
SIC0	structural information content (neighborhood symmetry of 0-order)
Mor12u	3D-MoRSE - signal 12 / unweighted
HATS3v	leverage-weighted autocorrelation of lag 3 / weighted by atomic van der Waals volumes
R3u+	R maximal autocorrelation of lag 3 / unweighted
HATS2p	leverage-weighted autocorrelation of lag 2 / weighted by atomic polarizabilities
HATS1v	leverage-weighted autocorrelation of lag 1 / weighted by atomic van der Waals volumes
G2p	2st component symmetry directional WHIM index / weighted by atomic polarizabilities

Table S2-3: Discriminative descriptors on upper side of principal component 2 (y-axis).

Descriptor	Meaning
XOAv	average valence connectivity index chi-0
JGI3	mean topological charge index of order3
MATS6v	Moran autocorrelation - lag 6 / weighted by atomic van der Waals volumes
MATS6m	Moran autocorrelation - lag 6 / weighted by atomic masses
MATS6p	Moran autocorrelation - lag 6 / weighted by atomic polarizabilities
MATS6e	Moran autocorrelation - lag 6 / weighted by atomic Sanderson electronegativities
Jhetm	Balaban-type index from mass weighted distance matrix
JhetZ	Balaban-type index from Z weighted distance matrix (Barysz matrix)
Jhete	Balaban-type index from electronegativity weighted distance matrix
J	Balaban distance connectivity index
Yindex	Balaban Y index
Vindex	Balaban V index
Xindex	Balaban X index
J3D	3D-Balaban index
XOA	average connectivity index chi-0
JGI6	mean topological charge index of order6
Jhetv	Balaban-type index from van der Waals weighted distance matrix
Jhetp	Balaban-type index from polarizability weighted distance matrix
GATS1v	Geary autocorrelation - lag 1 / weighted by atomic van der Waals volumes
JGI2	mean topological charge index of order2
GATS1p	Geary autocorrelation - lag 1 / weighted by atomic polarizabilities
GATS1m	Geary autocorrelation - lag 1 / weighted by atomic masses
GATS1e	Geary autocorrelation - lag 1 / weighted by atomic Sanderson electronegativities
C-003	CHR3 number of tertiary carbons
nCt	number of total tertiary C(sp3)
JGT	global topological charge index
R8u	R autocorrelation of lag 8 / unweighted
BLI	Kier benzene-likeness index
PW2	path/walk 2 - Randic shape index
X1Av	average valence connectivity index chi-1
R8e	R autocorrelation of lag 8 / weighted by atomic Sanderson electronegativities
C-001	CH3R / CH4 number of primary carbons
CIC2	complementary information content (neighborhood symmetry of 2-order)
CIC3	complementary information content (neighborhood symmetry of 3-order)
nCp	number of terminal primary C(sp3)
R2u	R autocorrelation of lag 2 / unweighted
CIC1	complementary information content (neighborhood symmetry of 1-order)
R4u	R autocorrelation of lag 4 / unweighted
R4e	R autocorrelation of lag 4 / weighted by atomic Sanderson electronegativities
R7u	R autocorrelation of lag 7 / unweighted
H-046	H attached to C0(sp3) no X attached to next C
CIC4	complementary information content (neighborhood symmetry of 4-order)
X2Av	average valence connectivity index chi-2
CIC5	complementary information content (neighborhood symmetry of 5-order)
R7e	R autocorrelation of lag 7 / weighted by atomic Sanderson electronegativities
Mor06u	3D-MoRSE - signal 06 / unweighted
Mor26v	3D-MoRSE - signal 26 / weighted by atomic van der Waals volumes
Mor18m	3D-MoRSE - signal 18 / weighted by atomic masses
Mor06e	3D-MoRSE - signal 06 / weighted by atomic Sanderson electronegativities
Mor26p	3D-MoRSE - signal 26 / weighted by atomic polarizabilities
F06[O-O]	frequency of O - O at topological distance 06
Mor26m	3D-MoRSE - signal 26 / weighted by atomic masses
EEig03r	Eigenvalue 03 from edge adj. matrix weighted by resonance integrals
R8p	R autocorrelation of lag 8 / weighted by atomic polarizabilities
Mor26u	3D-MoRSE - signal 26 / unweighted
Mor26e	3D-MoRSE - signal 26 / weighted by atomic Sanderson electronegativities
F02[O-O]	frequency of O - O at topological distance 02
EEig01d	Eigenvalue 01 from edge adj. matrix weighted by dipole moments
EEig03d	Eigenvalue 03 from edge adj. matrix weighted by dipole moments
GATS3p	Geary autocorrelation - lag 3 / weighted by atomic polarizabilities

Table S2-3: Discriminative descriptors on upper side of principal component 2 (y-axis) (continued).

R7p	R autocorrelation of lag 7 / weighted by atomic polarizabilities
PW3	path/walk 3 - Randic shape index
Mor14m	3D-MoRSE - signal 14 / weighted by atomic masses
Mor09v	3D-MoRSE - signal 09 / weighted by atomic van der Waals volumes
nRCOOR	number of esters (aliphatic)
EEig02d	Eigenvalue 02 from edge adj. matrix weighted by dipole moments
GATS3v	Geary autocorrelation - lag 3 / weighted by atomic van der Waals volumes
Mor21m	3D-MoRSE - signal 21 / weighted by atomic masses

Table S2-4: Discriminative descriptors on lower side of principal component 2 (y-axis).

Descriptor	Meaning
IC1	information content index (neighborhood symmetry of 1-order)
PCR	ratio of multiple path count over path count
HATSm	leverage-weighted total index / weighted by atomic masses
SIC1	structural information content (neighborhood symmetry of 1-order)
R1m	R autocorrelation of lag 1 / weighted by atomic masses
BIC1	bond information content (neighborhood symmetry of 1-order)
H0m	H autocorrelation of lag 0 / weighted by atomic masses
HATSV	leverage-weighted total index / weighted by atomic van der Waals volumes
HNar	Narumi harmonic topological index
PCD	difference between multiple path count and path count
ARR	aromatic ratio
H1m	H autocorrelation of lag 1 / weighted by atomic masses
nCb-	number of substituted benzene C(sp ²)
H0v	H autocorrelation of lag 0 / weighted by atomic van der Waals volumes
MATS1e	Moran autocorrelation - lag 1 / weighted by atomic Sanderson electronegativities
Mv	mean atomic van der Waals volume (scaled on Carbon atom)
MATS1m	Moran autocorrelation - lag 1 / weighted by atomic masses
GNar	Narumi geometric topological index
nAB	number of aromatic bonds
nBnz	number of benzene-like rings
nCar	number of aromatic C(sp ²)
C-025	R--CR--R
HOMT	HOMA total
HATSp	leverage-weighted total index / weighted by atomic polarizabilities
R1v	R autocorrelation of lag 1 / weighted by atomic van der Waals volumes
Mp	mean atomic polarizability (scaled on Carbon atom)
BEHp1	highest eigenvalue n. 1 of Burden matrix / weighted by atomic polarizabilities
BELe1	lowest eigenvalue n. 1 of Burden matrix / weighted by atomic Sanderson electronegativities
BELm1	lowest eigenvalue n. 1 of Burden matrix / weighted by atomic masses
Ui	unsaturation index
SIC2	structural information content (neighborhood symmetry of 2-order)
BEHv1	highest eigenvalue n. 1 of Burden matrix / weighted by atomic van der Waals volumes
HOMA	Harmonic Oscillator Model of Aromaticity index
H0p	H autocorrelation of lag 0 / weighted by atomic polarizabilities
ICR	radial centric information index
AMW	average molecular weight
MATS1v	Moran autocorrelation - lag 1 / weighted by atomic van der Waals volumes
IC2	information content index (neighborhood symmetry of 2-order)
piPC09	molecular multiple path count of order 09
AROM	aromaticity index
RCI	Jug RC index
nCbH	number of unsubstituted benzene C(sp ²)
C-024	R--CH--R
BIC2	bond information content (neighborhood symmetry of 2-order)
H1v	H autocorrelation of lag 1 / weighted by atomic van der Waals volumes
nR06	number of 6-membered rings
nBM	number of multiple bonds
MATS1p	Moran autocorrelation - lag 1 / weighted by atomic polarizabilities
GATS6e	Geary autocorrelation - lag 6 / weighted by atomic Sanderson electronegativities
HATS2m	leverage-weighted autocorrelation of lag 2 / weighted by atomic masses
GATS6m	Geary autocorrelation - lag 6 / weighted by atomic masses
R2m	R autocorrelation of lag 2 / weighted by atomic masses
HATS1m	leverage-weighted autocorrelation of lag 1 / weighted by atomic masses
GATS6v	Geary autocorrelation - lag 6 / weighted by atomic van der Waals volumes
SIC3	structural information content (neighborhood symmetry of 3-order)
R2v	R autocorrelation of lag 2 / weighted by atomic van der Waals volumes
R1p	R autocorrelation of lag 1 / weighted by atomic polarizabilities
GATS6p	Geary autocorrelation - lag 6 / weighted by atomic polarizabilities
piPC10	molecular multiple path count of order 10
Mor11p	3D-MORSE - signal 11 / weighted by atomic polarizabilities

Table S2-4: Discriminative descriptors on lower side of principal component 2 (y-axis) (continued).

BEHe2	highest eigenvalue n. 2 of Burden matrix / weighted by atomic Sanderson electronegativities
Mor15v	3D-MoRSE - signal 15 / weighted by atomic van der Waals volumes
Mor07u	3D-MoRSE - signal 07 / unweighted
BEHv2	highest eigenvalue n. 2 of Burden matrix / weighted by atomic van der Waals volumes
BEHp2	highest eigenvalue n. 2 of Burden matrix / weighted by atomic polarizabilities
PJl2	2D Petitjean shape index
H1p	H autocorrelation of lag 1 / weighted by atomic polarizabilities
Mor15p	3D-MoRSE - signal 15 / weighted by atomic polarizabilities

CHAPTER IV

UHPLC-MS/MS METHOD FOR THE DETERMINATION OF BEAUVERICIN AND ENNIATINS

“What gets measured, gets managed.”

Peter Ferdinand Drucker

(°1909 - †2005, Austrian-born American management consultant, educator and author)

Parts of this chapter were published:

Taevernier L, Veryser L, Vandercruyssen K, D’Hondt M, Vansteelandt S, De Saeger S, De Spiegeleer B. UHPLC-MS/MS method for the determination of the cyclic depsipeptide mycotoxins beauvericin and enniatins in *in vitro* transdermal experiments. *Journal of Pharmaceutical and Biomedical Analysis*. 2014; **100**: 50-57, doi: 10.1016/j.jpba.2014.07.021.

ABSTRACT

Currently, dermal exposure data of cyclic depsipeptide mycotoxins beauvericin and enniatins are completely absent with a lack of local skin and systemic kinetics, despite their widespread skin contact and intrinsic hazard. Therefore a sensitive and specific bioanalytical high-throughput UHPLC-MS/MS method was developed for the quantitative and simultaneous determination of cyclic depsipeptide mycotoxins beauvericin and enniatins (A, A1, B, B1, D, E, C/F) in human skin Franz diffusion cell samples. The limits of detection ranged between 10 and 17 pg/mL, while the total run time was only 4.5 minutes. There was no significant effect of endogenous skin compounds on the mycotoxin MS signal observed, and the accuracy and precision were considered acceptable for our purposes. Moreover, it was demonstrated that these cyclic depsipeptides are stable for at least 7 days when formulated in different organic or aqueous mixtures. Finally, adsorption to glass did occur: at least 50% organic solvent is required to prevent significant adsorption effects, which could be as high as 45%.

CHAPTER IV

UHPLC-MS/MS METHOD FOR THE DETERMINATION OF BEAUVERICIN AND ENNIATINS

Main focus in this chapter:

- To develop a high-throughput bioanalytical UHPLC-MS/MS method for BEA and ENNs.
- To evaluate their analytical stability and adsorption to Franz diffusion cell glass.

1. THE NEED FOR A QUANTITATIVE, SENSITIVE AND SELECTIVE HIGH-THROUGHPUT BIOANALYTICAL METHOD

Studying the local pharmacokinetics of molecules through human skin is not only important within the pharmaceutical industry but also in the field of environmental toxicology. The skin, being the largest organ, is considered as a route of administration for topically applied medicines [1,2], but is also important in the dermal risk assessment of hazardous compounds, such as mycotoxins [3]. Both *in vivo* and *in vitro* methods can be used to measure the skin absorption. Laboratory animals (such as guinea pigs, rats, mice and pigs), readily available, provide indeed a reproducible, physiologically and metabolically intact test system to investigate the skin absorption of all kinds of compounds (*e.g.* pharmaceuticals, cosmetics, hazardous chemicals). However, these also have their limitations, *i.a.* inter-species variability, with often a higher permeability than for human skin. Therefore, human skin studies remain the “gold standard” by which all methods for measuring percutaneous absorption should be judged. However, given the extreme toxicity of some chemicals, such as mycotoxins, it is ethically unacceptable to use living human beings in the transdermal studies [3,4]. *In vitro* Franz diffusion cell (FDC) methods are currently the ideal alternative, since (i) it is possible to maintain the barrier properties of the stratum corneum in excised skin, (ii) there is good evidence that the obtained *in vitro* data are predictive for *in vivo* percutaneous absorption (*in vitro in vivo* correlation)

and (iii) there are standardisation recommendations, guidelines and protocols on how to execute these diffusion cell studies available, proposed by both regulatory entities and committees of interested parties [4,5].

Cyclic depsipeptides are a large group of naturally occurring bioactive peptides. Some of these are secondary fungal metabolites, which are toxic to humans and animals, such as the emerging mycotoxins beauvericin (BEA) and enniatins (ENNs) [6-18]. Currently, dermal exposure data of these compounds are completely absent with a lack of local skin and systemic kinetics, despite their potential skin contact and intrinsic hazard. BEA and ENNs are well-known *Fusarium* cyclic hexadepsipeptides, but they are also produced by other fungi such as *Beauveria* and *Paecilomyces* and *Alternaria*, *Halosarpheia* and *Verticillium* species, respectively [19-25]. These compounds, possessing cation-complexing ionophoric and lipophilic properties, which act as inhibitors of acyl-CoA: cholesterol acyltransferase, exert cytotoxic effects in various cell lines [6-9,11-15,17,18] and have different effects on the immune system [26-30]. Moreover, it was also reported that BEA is genotoxic [6,10].

UHPLC-MS/MS analysis of these cyclic depsipeptides has only been reported in a few studies, all aiming for a multi-mycotoxin determination in food. Considering the abundance (up to 191 compounds) and diversity of the investigated mycotoxins, these methods have relatively long run times, *e.g.* up to 21 min [31-33]. Quantitative transdermal kinetics are characterised by multiple skin donors with sufficient replicates and time points, which result in a large amount of different samples, *i.e.* dose solutions, skin extraction samples and receptor fluid samples. Hence, there is a need for a sensitive, selective and rapid high-throughput method for analysis of these frequently low concentrated samples, obtained in each FDC experiment. During these FDC experiments, the analytes are also exposed to elevated temperatures for significant amounts of time, *i.e.* $\pm 32^{\circ}\text{C}$ (mimicking the human skin temperature) during 24 hours, indicating the importance of a stability study under these conditions. During analytical processes, adsorption of peptides, which is believed to be mostly due to non-covalent interactions and depending upon the experimental conditions, cannot only lead to significant loss of the analyte, but also to increased analytical variability [34,35]. The adsorption of these lipophilic cyclic depsipeptide analytes to the FDC glass wall, of which the quality differs from analytical volumetric glassware, was not yet investigated.

The goal of this study was to develop a sensitive, selective and rapid high-throughput bioanalytical method to quantitatively determine the cyclic depsipeptide mycotoxins beauvericin and enniatins (A, A1, B, B1, D, E, F or C) in different FDC samples, using Ultra High Performance Liquid Chromatography combined with electrospray ionisation (ESI) tandem Mass Spectrometry (UHPLC-MS/MS). In addition, stability and adsorption to glass under our *in vitro* test conditions were investigated as well.

In this chapter, the general UHPLC-MS/MS method is presented, together with the human skin sample preparation as an application. The sample preparation used for the mice serum and brain samples is described in the methods part of **Chapter VI**.

2. MATERIALS AND METHODS

2.1. Chemicals and reagents

Mycotoxins beauvericin (BEA) and enniatin B (ENN B) were supplied by BioAustralis (Smithfield NSW, Australia), while the enniatin mixture (ENNs) was obtained from Cfm Oscar Tropitzsch (Marktredwitz, Germany). No formal ENN composition was supplied by the manufacturer (only e-mail correspondence), therefore the composition was experimentally determined by our group, assuming a relative response factor (RRF) = 1 for the individual constituents: 43.8% ENN B, 34.4% ENN B1, 14.0% ENN A1, 3.6% ENN D, 1.8% ENN A, 1.8% ENN E and 0.4% ENN C or F. These data were obtained by UHPLC-MS and UHPLC-UV (205 nm) normalised areas. ULC-MS grade acetonitrile (ACN), formic acid (FA) and 2-propanol, used for preparation of the mobile phase, were purchased from Biosolve (Valkenswaard, The Netherlands). Ultrapure water (H₂O) was produced by an Arium pro VF TOC water purification system (Sartorius, Göttingen, Germany), resulting in ultrapure water of 18.2 MΩ × cm quality. Sigma-Aldrich (St. Louis, MO, USA) supplied 0.01 M phosphate buffered saline (PBS) and dimethyl sulfoxide (DMSO). Ethanol (EtOH), used for the dose solutions, was purchased from Merck (Darmstadt, Germany) and UHPLC grade ACN was bought from Fisher Scientific (Waltham, MA, USA). Pharma grade hydroxypropyl-β-cyclodextrin (HPBCD) was supplied by Cerestar (Mechelen, Belgium). This was used as a solubilising modifier to the receptor fluid (PBS), in order to guarantee sink conditions of the hydrophobic cyclic depsipeptide mycotoxins throughout the experiment [36].

2.2. Analytical method

Preparation of standard solutions

A separate stock solution of 100 µg/mL in ACN was prepared for BEA and the ENN mixture. ENN B (pure) was used as an internal standard (IS) for the determination of BEA, while BEA was used for the different enniatins present in the enniatin mixture. For each internal standard, a stock solution of 10 µg/mL in ACN was prepared and stored at -80°C. For all experiments, except for the stability and adsorption tests, an internal standard was added to each sample, with a final IS concentration of 20 ng/mL. From these four stock solutions (BEA 100 µg/mL in ACN, ENNs 100 µg/mL in ACN, ENN B 10 µg/mL in ACN and BEA 10 µg/mL in ACN), the standard solutions were prepared by dilution in 70/30 (V/V) ACN/H₂O.

***In vitro* FDC protocol**

The specific FDC protocols applied in this research are given in detail in **Chapter V** and **Chapter VII**. Briefly, the set-up consists of static Franz diffusion cells with a receptor compartment of 5 mL and an available diffusion area of 0.64 cm² (Logan Instruments Corp., New Jersey, USA). The topical layer of interest, *e.g.* human skin or buccal porcine mucosa, is cleaned with 0.01 M PBS pH 7.4 and the subcutaneous fat is removed [5]. These samples are wrapped in aluminium foil and stored in the freezer until their further use. Just before the start of the experiments, the samples are thawed, mounted on a template and dermatomed using an electrical powered dermatome (Integra Life Sciences, New Jersey, USA). Next, the dermatomed samples are visually inspected for damage and are then sandwiched between the donor and acceptor chambers, with the epidermis or epithelial layer facing upwards, making sure all air under the sample is removed. The whole assembly is fixed on a magnetic stirrer and the receptor fluid was continuously stirred using a Teflon coated magnetic stirring bar (600 rpm) to ensure sink conditions. Before starting the experiments, skin integrity is checked by measuring the skin impedance using an automatic micro-processor controlled LCR impedance bridge (Tinsley, Croydon, UK). Pieces with an impedance value < 10 k Ω , a validated system-suitability cut-off, are discarded and replaced by a new piece [37]. The dose solutions are topically applied and the donor chamber is covered with parafilm. The temperature of the receptor compartment is kept constant, depending on the topical layer used: 32 \pm 1 $^{\circ}$ C for human skin and 37 \pm 1 $^{\circ}$ C for buccal porcine mucosa. Samples (200 μ L) are drawn at regular time intervals from the sampling port and are immediately replaced by 200 μ L fresh receptor solution (the analytically determined assay values in the FDC samples are correspondingly corrected for these replenishments). At the end of the experiment, the topical surfaces are swabbed with cotton wool to remove the remaining donor solution and the exposed surfaces were carefully cut out using a scalpel and extracted. These samples are analysed as well and are used to construct a mass balance.

Ultra high performance liquid chromatography

The chromatography platform consisted of an Acquity UHPLC equipped with a temperature controlled autosampler tray and column oven, thermostated at 25 $^{\circ}$ C (\pm 5 $^{\circ}$ C) and 45 $^{\circ}$ C (\pm 5 $^{\circ}$ C), respectively (Waters, Milford, MA, USA). Chromatographic separation was achieved on an Acquity UHPLC charged surface hybrid (CSH) C18 column (1.7 μ m, 100 \times 2.1 mm, 130 \AA), attached to an Acquity UHPLC VanGuard pre-column (1.7 μ m, 5 \times 2.1 mm, 130 \AA), both obtained from Waters. The injection volume was 10 μ L and the needle wash consisted of 10/10/80 (V/V/V) DMSO/2-propanol/ACN. The isocratic flow rate was set to 0.6 mL/min, using 70/30 (V/V) ACN/H₂O containing 0.1% FA and 0.1% 2-propanol as mobile phase. The run time was 4.5 min, of which the first 1.5 min were diverted to the waste. A typical combined MRM overlay chromatogram is shown in Figure 1.

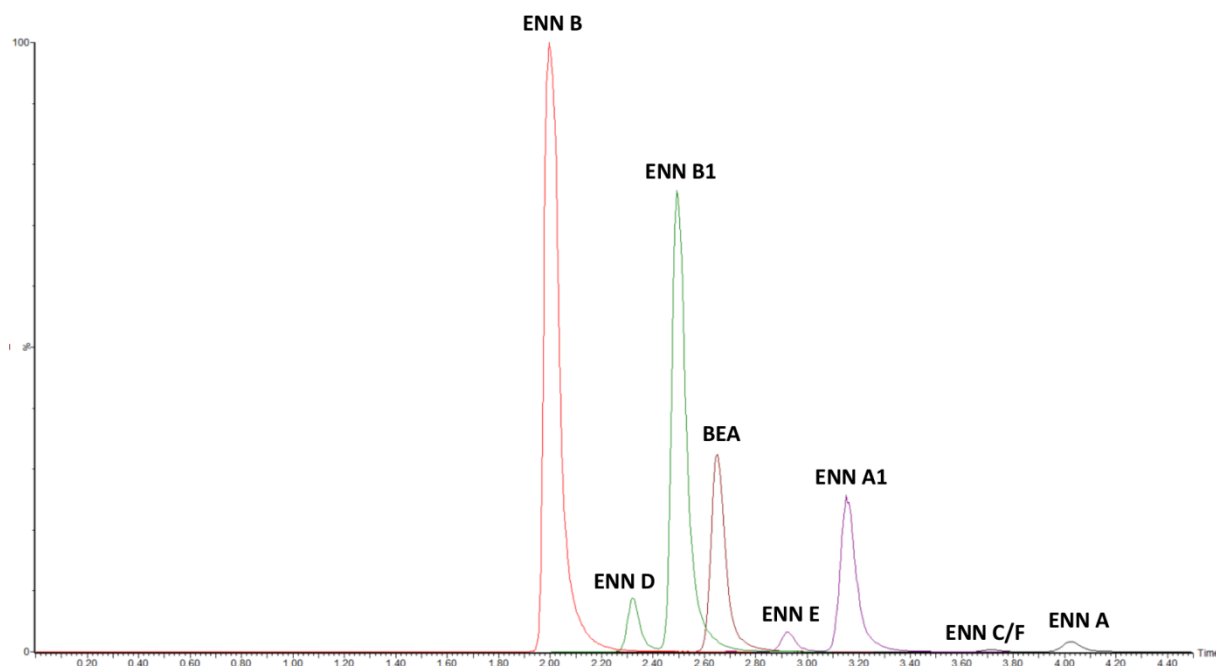


Figure 1: Combined UHPLC-MS/MS overlay chromatogram, normalised to the largest peak (ENN B). Beauvericin at a concentration of 20 ng/mL, whereas the enniatin mixture was 100 ng/mL.

Mass spectrometry

For the quantitative mycotoxin analysis, a multi-UHPLC-MS/MS method was developed, with the mass spectrometer being a Xevo TQ-S detector (Waters, Milford, MA, USA). The mass spectrometer was operated in the positive electrospray ionization mode (ESI+), with an optimised capillary voltage of 3.50 kV, cone voltage of 50 V and source offset of 60 V. Source and desolvation temperatures were set at 150°C and 600°C, respectively, while cone and desolvation gas flows were 150 and 1000 L/h, respectively. Acquisition was performed in the multiple reaction monitoring (MRM) mode. The selected precursor and product ions, together with the applied collision energies are given in Table 1. Data were acquired using Masslynx software (V4.1 SCN 843, Waters, Milford, MA, USA).

Table 1: MRM transitions and MS/MS parameters.

Compound	Precursor ion (m/z)	Product ions (m/z)	Collision energy (eV)
ENN B	639.91	[M+H] ⁺	196.08
			527.26
ENN D	653.99	[M+H] ⁺	196.09
			541.05
ENN B1	653.99	[M+H] ⁺	196.09
			541.05
BEA	783.94	[M+H] ⁺	244.01
			623.23
ENN E	668.07	[M+H] ⁺	209.99
			555.29
ENN A1	668.07	[M+H] ⁺	209.99
			555.29
ENN C/F	682.47	[M+H] ⁺	209.93
			555.01
ENN A	682.47	[M+H] ⁺	209.93
			555.01

For structure isomers (ENN D-B1, ENN E-A1 and ENN C/F-A) identical transitions were acquired.

2.3. Method verification

Adsorption to FDC glass

A critical aspect in terms of bioanalytical method development is the adsorption of analytes, which is often overlooked. Therefore the adsorption of BEA and ENNs to FDC glass was determined as part of the analytical robustness. Therefore, BEA and ENNs mixture were solubilised at a concentration of approximately 1000 ng/mL in six different solvent mixtures (formulations), with different percentages of organic solvents: aqueous solutions, *i.e.* 90/10 (V/V) H₂O/EtOH (1) and 90/10 (V/V) H₂O/ACN (4), as well as intermediate organic solutions, *i.e.* 50/50 (V/V) H₂O/EtOH (2) and 50/50 (V/V) H₂O/ACN (5) and high organic solutions, *i.e.* 5/95 (V/V) H₂O/EtOH (3) and 5/95 (V/V) H₂O/ACN (6). These were exposed to FDC glass in duplicate and left to equilibrate for 24h at 25°C while continuously stirred (600 rpm), after which three independent aliquots were taken and diluted 1:10 (V/V) with mobile phase, resulting in a final concentration of 100 ng/mL and assayed (hence, n = 2 × 3). Responses were analysed for each compound separately, using In-lin models which were fitted using generalised estimating equations with unstructured covariance to account for correlation within duplicates [38]. QQ-plots confirmed the normality of the raw residuals in these models. In general, the model can be described as: $\ln(\text{mean response}) = \alpha + \beta_1 \times F_2 + \beta_2 \times F_3 + \beta_3 \times F_4 + \beta_4 \times F_5 + \beta_5 \times F_6$, with $F_k = 1$ or 0, when the formulation is equal to or different from k, respectively. The complete models, including coefficients α and β_1 -5, can be found in Table 2.

Table 2: Adsorption models.

Compound	Model
BEA	$\ln(\text{mean response}) = 13.88 + 0.29 \times F_2 + 0.30 \times F_3 - 0.33 \times F_4 + 0.22 \times F_5 + 0.23 \times F_6$
ENN B	$\ln(\text{mean response}) = 14.46 + 0.0044 \times F_2 + 0.018 \times F_3 - 0.096 \times F_4 - 0.063 \times F_5 - 0.042 \times F_6$
ENN D	$\ln(\text{mean response}) = 11.82 + 0.036 \times F_2 + 0.029 \times F_3 - 0.077 \times F_4 - 0.006 \times F_5 - 0.009 \times F_6$
ENN B1	$\ln(\text{mean response}) = 14.09 + 0.023 \times F_2 + 0.033 \times F_3 - 0.20 \times F_4 - 0.14 \times F_5 - 0.071 \times F_6$
ENN E	$\ln(\text{mean response}) = 11.42 + 0.045 \times F_2 + 0.050 \times F_3 - 0.093 \times F_4 - 0.031 \times F_5 - 0.013 \times F_6$
ENN A1	$\ln(\text{mean response}) = 13.38 + 0.039 \times F_2 + 0.040 \times F_3 - 0.10 \times F_4 - 0.024 \times F_5 - 0.018 \times F_6$
ENN A	$\ln(\text{mean response}) = 11.64 + 0.095 \times F_2 + 0.11 \times F_3 - 0.086 \times F_4 + 0.045 \times F_5 + 0.054 \times F_6$
ENN C/F	$\ln(\text{mean response}) = 10.28 + 0.061 \times F_2 + 0.076 \times F_3 - 0.096 \times F_4 - 0.011 \times F_5 - 0.022 \times F_6$

For each compound separately, the mean response ratios (in %) were evaluated: (i) ACN and EtOH were compared per concentration level (10, 50 or 95% organic solvent) and (ii) the concentration levels (10 and 50%) were compared to the reference (95% = no adsorption assumed) per organic solvent (ACN or EtOH). Reported 95% confidence intervals were Bonferroni-adjusted to account for multiplicity in the analysis of each compound separately. An overview of these results is given in Tables 3 and 4, respectively.

Table 3: Comparison of EtOH (formulations 1, 2 and 3) and ACN (formulations 4, 5 and 6) adsorption per concentration level.

Formulation	Parameter	ENN B	ENN D	BEA	ENN E	ENN C/F	ENN A	ENN A1	ENN B1
1 vs. 4 10%	Ratio ⁽¹⁾	1.1009344571	1.0801792131	1.3931263473	1.0973838185	1.1008747212	1.0898055452	1.1076017992	1.2232474904
	Lower ⁽²⁾	1.0589059057	0.9701861861	1.3270702847	1.0497497746	1.0513850674	1.053952915	1.0664868921	0.9903668109
	Upper ⁽²⁾	1.1446311446	1.2026424919	1.4624704071	1.1471793319	1.1526938981	1.126877785	1.1503017568	1.5108891031
	p-value	4.385×10^{-7}	0.37932084	0	2.50182×10^{-5}	2.6206×10^{-5}	1.343×10^{-7}	2.69×10^{-8}	0.1269154224
2 vs. 5 50%	Ratio ⁽¹⁾	1.0697675314	1.0431657129	1.0709440924	1.0786857173	1.0513564029	1.0515199956	1.0649033717	1.1777382738
	Lower ⁽²⁾	1.0108595164	0.9690574018	1.0199887677	1.0441267413	1.0214767574	1.0243252176	1.0293588141	0.9633987272
	Upper ⁽²⁾	1.1321084212	1.12294143	1.1244449796	1.1143885418	1.0821100704	1.0794367669	1.1016753104	1.4397646608
	p-value	0.0338450626	0.666967444	0.0083143839	2.2261×10^{-6}	0.0006559261	0.0001351252	0.0002424968	0.2492662167
3 vs. 6 95%	Ratio ⁽¹⁾	1.0618465063	1.038585196	1.0708509518	1.0653750067	1.0549858861	1.0543339697	1.059351679	1.1095367724
	Lower ⁽²⁾	0.9978672433	0.9930840777	0.9991440757	1.012528248	1.0197746547	1.0138116989	0.9999545723	0.9756308191
	Upper ⁽²⁾	1.1299278642	1.0861710841	1.1477041088	1.1209799895	1.0914129065	1.0964759244	1.1222769621	1.2618214033
	p-value	0.1196561148	0.2163476343	0.106724426	0.0242321573	0.0023756713	0.0122032701	0.1004174304	0.2563858474

(1) Relative mean response ratio.

(2) Lower and upper limit of 95% confidence interval.

Table 4: Comparison of the adsorption results per organic solvent (ACN or EtOH).

Formulation	Parameter	ENN B	ENN D	BEA	ENN E	ENN C/F	ENN A	ENN A1	ENN B1
EtOH formulations									
10% vs. 95%	Ratio ⁽¹⁾	0.982344	0.971436	0.744290	0.951171	0.926925	0.898625	0.960837	0.967167
	Lower ⁽²⁾	0.931126	0.902527	0.702473	0.909795	0.889234	0.865178	0.915730	0.894629
	Upper ⁽²⁾	1.036380	1.045606	0.788595	0.994430	0.966213	0.933366	1.008165	1.045586
	p-value	1.000000	1.000000	9.651884×10^{-30}	0.046555	1.672715×10^{-4}	1.071749×10^{-9}	0.250225	1.000000
50% vs. 95%	Ratio ⁽¹⁾	0.986634	1.007389	0.990195	0.994518	0.985286	0.988508	0.998786	0.989831
	Lower ⁽²⁾	0.933328	0.947850	0.934108	0.957302	0.954840	0.950561	0.951130	0.916305
	Upper ⁽²⁾	1.042984	1.070667	1.049649	1.033181	1.016703	1.027970	1.048831	1.069257
	p-value	1.000000	1.000000	1.000000	1.000000	1.000000	1.000000	1.000000	1.000000
ACN formulations									
10% vs. 95%	Ratio ⁽¹⁾	0.947467	0.934029	0.572111	0.923427	0.888287	0.869376	0.9189801	0.877261
	Lower ⁽²⁾	0.896174	0.846819	0.534581	0.873590	0.850378	0.836277	0.870244	0.684238
	Upper ⁽²⁾	1.001695	1.030220	0.612276	0.976108	0.927886	0.903785	0.970445	1.124735
	p-value	0.119067	0.474466	2.189531×10^{-75}	0.005158	4.575133×10^{-9}	2.526985×10^{-15}	0.002040	0.950172
50% vs. 95%	Ratio ⁽¹⁾	0.979328	1.002965	0.990109	0.982246	0.988687	0.991153	0.993579	0.932511
	Lower ⁽²⁾	0.914051	0.937616	0.925418	0.933479	0.954814	0.961330	0.944353	0.734244
	Upper ⁽²⁾	1.044927	1.072869	1.059322	1.033560	1.023762	1.021902	1.045371	1.184368
	p-value	1.000000	1.000000	1.000000	1.000000	1.000000	1.000000	1.000000	1.000000

(1) Relative mean response ratio.

(2) Lower and upper limit of 95% confidence interval.

Analytical stability

From one duplicate of each of the six formulations from the adsorption experiment, multiple aliquots were taken and stored in HPLC glass vials protected from light at different conditions (-35°C, 5°C, 25°C and 40°C). These were analysed at T_0 , $T_{2\text{days}}$ and $T_{7\text{days}}$, after 1:10 (v/v) dilution with mobile phase and each compared with corresponding freshly prepared standard solutions (100 ng/mL). The percentage label claim (l.c.) was calculated for each compound separately, using the mean response factor of the standards, which were analysed on each experimental day, according to the following formulas: (1) response factor (RF) = area standard / theoretical concentration standard and (2) label claim percentage (%) = (area sample T_x / (theoretical concentration sample \times RF)) \times 100%. Next, for the worst case stability scenario of 40°C, these percentages were plotted against time (days) for each compound and formulation. Stability was evaluated based on the 95% confidence interval around the slope in a linear regression analysis of the recovery (%) against time (days) for the worst case scenario (40°C). If this interval contains zero, no significant degradation is observed.

Calibration curve

Linearity was evaluated by constructing a calibration curve using different standard solutions (1, 5, 10, 50, 100, 500 and 1000 ng/mL BEA or ENN mixture), containing the respective IS (20 ng/mL ENN B or BEA). For each compound the linear range was evaluated and the coefficient of determination (R^2) was determined.

Limit of detection

The limit of detection (LoD) was determined using the signal-to-noise approach, where LoD corresponds to a signal-to-noise ratio of 3:1. For BEA and ENNs B, B1, D, E, A and A1 a standard solution of 1 ng/mL beauvericin or enniatins mixture was used, while this was 5 ng/mL enniatins mixture for ENNs C/F and A. For each ENN, the concentration of the mixture was converted to the individual ENN concentration, according to the previously determined chemical composition.

Injection repeatability

The method injection repeatability was characterised by sextuplicate injections of standard solutions at 100 ng/mL beauvericin or enniatin mixture, containing their respective IS. The calculated percentage RSD should be \leq 10%, based on the EDQM guideline for qualification of mass spectrometers [39].

Accuracy and precision of receptor fluid samples

To evaluate the precision and accuracy, the receptor fluid (0.01 M PBS + 1% HPBCD) was spiked with beauvericin or enniatin mixture at two concentration levels (10 and 100 ng/mL), each in triplicate (n

= 2 × 3), and left to equilibrate for 24 ± 0.25 hours in pre-heated (32°C ± 1°C) FDCs. A 200 µL aliquot was taken at the end of the experiment, diluted with the respective IS in ACN and analysed. The percentage residual standard deviation (% RSD) and percentage bias were calculated. For the latter the following formula was used: bias (%) = (concentration sample – concentration standard) / concentration standard × 100%, where the concentration of the sample is calculated using the calibration curve.

Effect of skin components on the mycotoxin MS signal

Receptor fluid (0.01 M PBS + 1% HPBCD) and extraction solvent (95/5 (V/V) ACN/H₂O), both as such and previously exposed to a large piece of full-thickness skin for 3.5h ± 0.5h in an incubation shaker set at 32°C/150 rpm, were spiked with BEA or ENNs mixture (100 ng/mL) and their respective internal standard and analysed. For the receptor fluid, this was done in triplicate (n = 3). This was also done in triplicate for the extraction solvent and combined with two dilution procedures, *i.e.* 1:2 (V/V), resulting in a final concentration of 50 ng/mL, and 1:4 (V/V), resulting in a final concentration of 25 ng/mL (hence n = 2 × 3). The matrix effect is expressed as percentage recovery ($\text{response}_{\text{skin soaked}} / \text{response}_{\text{as such}} \times 100\%$).

3. RESULTS AND DISCUSSION

3.1. Method development

The method development was based upon the multi-mycotoxin method described by Van Pamel *et al.* [33], using an Acquity UPLC BEH (Ethylene Bridged Hybrid) C18 (1.7 µm, 100 × 2.1 mm, L1) column, thermostated at 45°C. A gradient mobile phase consisting of H₂O/ACN with 1mM ammonium acetate, 0.1% FA and 0.1% 2-propanol was used at a flow of 0.8 mL/min and an injection volume of 10 µL was applied. Considering the objective to determine only BEA and ENNs, an isocratic method was developed, using the same Acquity UPLC BEH C18 column, by first performing a scouting gradient, from which the optimal mobile phase composition was found to be approximately 70/30 (V/V) ACN/H₂O. However, this method resulted in significant and unacceptable tailing (Figure 2). Beside this BEH UPLC C18 column, other research groups have mentioned the use of other column chemistry types, *i.e.* Gemini LC C18 (5 µm, 150 × 4.6 mm, L1), ZORBAX UPLC Eclipse Plus C18 (1.8 µm, 150 × 2.1 mm, L1), Luna LC C18 (5 µm, 150 × 3 mm, L1), Shiseido Capcell LC C18 (5 µm, 250 × 4.6 mm, L1) and Gemini LC C6 phenyl (3 µm, 50 × 2 mm, L11) columns [40-44]. Therefore, we switched to a different stationary phase, *i.e.* Acquity UPLC BEH phenyl (1.7 µm, 100 × 2.1 mm, L11), which unfortunately still led to bad peak shapes with unacceptable tailing (Figure 3).

UHPLC-PDA conditions

Sample	BEA 0.005 mg/mL + ENNs 0.125 mg/mL in mobile phase
Injection volume	5 μ L
Isocratic mobile phase composition ⁽¹⁾	35/65 (V/V) A/B
UPLC-PDA	190 – 300 nm (quantification at 205 nm)
Flow	0.8 mL/min
Column temperature	45°C
Column	Acquity UPLC BEH C ₁₈ (1.7 μ m, 100 \times 2.1 mm, L1)

(1) Mobile phase composition: A: H₂O + 1 mM ammonium acetate + 0.1% formic acid + 0.1% 2-propanol; B: ACN + 0.1% formic acid + 0.1% 2-propanol.

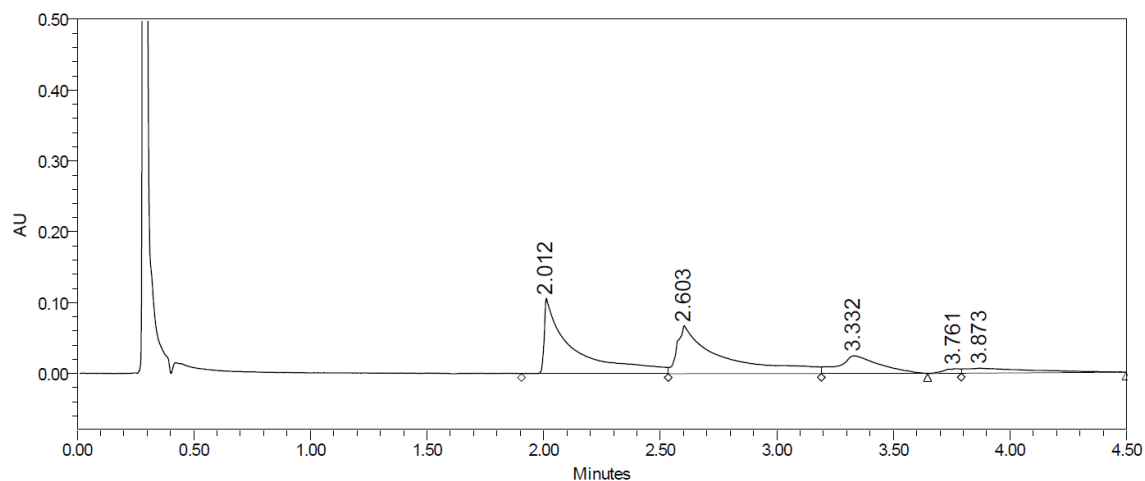


Figure 2: Acquity UPLC BEH C₁₈ (1.7 μ m, 100 \times 2.1 mm, L1) conditions and results.

UHPLC-PDA conditions

Sample	BEA 0.005 mg/mL + ENNs 0.125 mg/mL in mobile phase
Injection volume	10 μ L
Isocratic mobile phase composition ⁽¹⁾	40/60 (V/V) A/B
UPLC-PDA	190 – 300 nm (quantification at 205 nm)
Flow	0.3 mL/min
Column temperature	45°C
Column	Acquity UPLC BEH phenyl (1.7 μ m, 100 \times 2.1 mm, L11)

(1) Mobile phase composition: A: H₂O + 1 mM ammonium acetate + 0.1% formic acid + 0.1% 2-propanol; B: ACN + 0.1% formic acid + 0.1% 2-propanol.

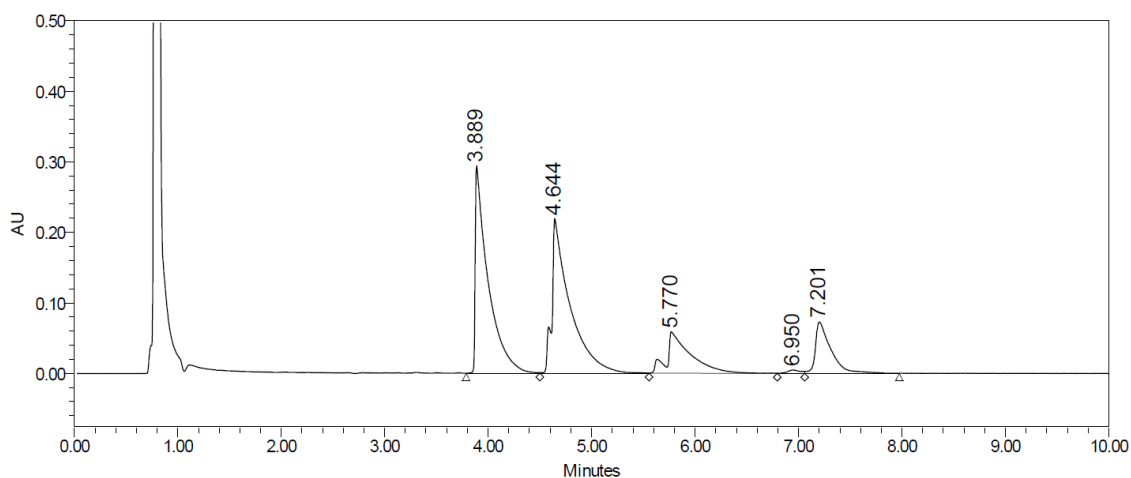


Figure 3: Acquity UPLC BEH phenyl (1.7 μ m, 100 \times 2.1 mm, L11) conditions and results.

Next, an Acquity UPLC BEH RP18 Shield column (1.7 μ m, 100 \times 2.1 mm, L1) was used, which incorporates a hydrophilic group within the C18 chain. This change in stationary phase resulted in

significantly improved peak shapes. However, not all enniatin stereoisomers in the mixture were baseline separated, an issue which remained unresolved even after lowering the organic amount in the mobile phase composition (Figure 4).

UHPLC-PDA conditions	
Sample	BEA 0.005 mg/mL + ENNs 0.125 mg/mL in mobile phase
Injection volume	10 μ L
Isocratic mobile phase composition ⁽¹⁾	40/60 (V/V) A/B
UPLC-PDA	190 – 300 nm (quantification at 205 nm)
Flow	0.8 mL/min
Column temperature	45°C
Column	Acquity UPLC BEH RP ₁₈ shield (1.7 μ m, 100 \times 2.1 mm, L1)

(1) Mobile phase composition: A: H₂O + 1 mM ammonium acetate + 0.1% formic acid + 0.1% 2-propanol; B: ACN + 0.1% formic acid + 0.1% 2-propanol.

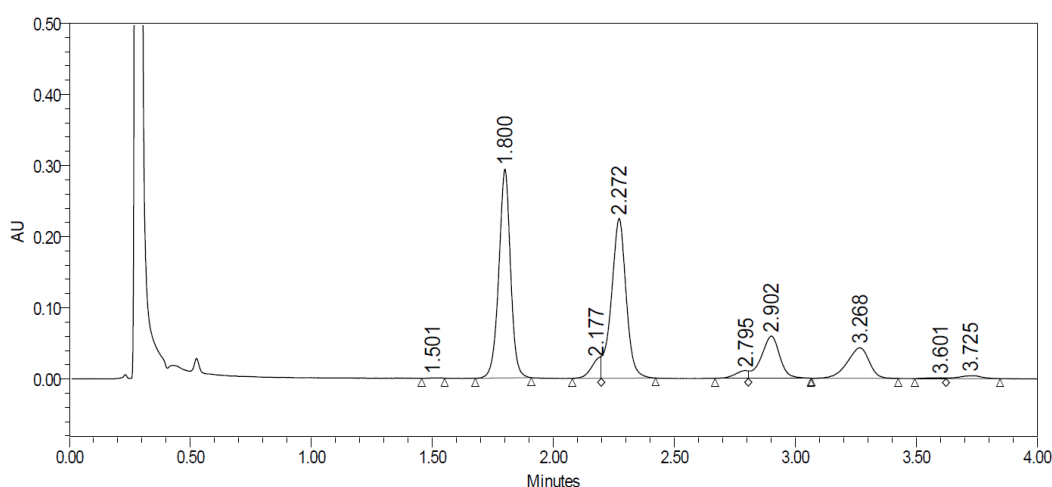


Figure 4: Acquity UPLC BEH RP₁₈ Shield (1.7 μ m, 100 \times 2.1 mm, L1) conditions and results.

Therefore, a switch was made to the Acquity UPLC CSH C18 column (1.7 μ m, 100 \times 2.1 mm), with a low level surface charge, designed to improve sample loadability and peak asymmetry in low-ionic-strength mobile phases. Indeed, higher resolution and overall better performance characteristics were achieved in comparison to the UPLC BEH RP18 Shield stationary phase (Table 5). It is also worth mentioning that the retention order changed upon switching between these stationary phases, from BEA eluting between ENN A1 and ENN C/F (BEH RP18 Shield) to BEA eluting between ENN B1 and ENN E (CSH C18). The MS instrument was operated in the positive ion electrospray mode, previously confirmed to be the most sensitive mode [33,40-42,44,45]. In our experiments, $[M+H]^+$ ions gave the most intense signal and were monitored, as did Van Pamel *et al.* [33] and Sorensen *et al.* [40]. By infusing mixture solutions of both BEA and ENNs at concentrations of 100 and 500 ng/mL, the MS parameters capillary voltage, cone voltage, source offset and probe position were optimised towards maximal signal intensity, as well as the selection of product ions and optimisation of collision energies.

Table 5: Comparison column performance BEH shield C₁₈ and CSH C₁₈.

Acquity UPLC BEH C ₁₈ shield								
Parameter	ENN B	ENN D	ENN B ₁	ENN E	ENN A ₁	BEA	ENN C/F	ENN A
N ⁽¹⁾	2549	6804	4123	6236	4341	1523	6630	4207
k' ⁽²⁾	9.97	12.66	13.17	16.43	17.17	19.46	21.46	22.26
AsF ⁽³⁾	1.30	0.75	1.17	0.63	1.06	1.07	0.68	0.92
α ⁽⁴⁾	1.27	1.04	1.25	1.05	1.14	1.10	1.04	
R ⁽⁵⁾	3.37	0.63	3.58	0.71	1.39	1.37	0.68	

Acquity UPLC C ₁₈ CSH								
Parameter	ENN B	ENN D	ENN B ₁	BEA	ENN E	ENN A ₁	ENN C/F	ENN A
N ⁽¹⁾	8921	21065	14352	6709	13512	11810	16395	14751
k' ⁽²⁾	8.78	10.38	11.41	12.59	13.47	14.78	17.59	19.41
AsF ⁽³⁾	1.50	1.10	1.25	0.94	1.00	1.08	1.07	1.14
α ⁽⁴⁾	1.18	1.10	1.10	1.07	1.10	1.19	1.10	
R ⁽⁵⁾	3.44	2.11	1.80	1.28	2.15	4.11	2.12	

(1) Number of theoretical plates: $N = 5.54 \times (T_r / w)^2$; with T_r = retention time and w = width of the peak at half-height.

(2) Capacity factor: $k' = (T_r - T_0) / T_0$; with T_0 = hold-up time.

(3) Asymmetry factor: $AsF = (a+b) / 2a$; with a the distance between the perpendicular dropped from the peak maximum and the leading edge of the peak at 10% of the peak height and $a+b$ the width of the peak at 10% of the peak height.

(4) Selectivity factor: $\alpha = k'_B / k'_A$.

(5) Resolution: $R = ((2 \times (T_{rB} - T_{rA})) / (w_A + w_B))$.

3.2. Method verification

Adsorption to FDC glass

The mean response ratios (in %) were evaluated for each compound separately: (i) ACN and EtOH were compared per concentration level (10, 50 or 95% organic solvent) (Figure 5) and (ii) the concentration levels (10 and 50%) were compared to the reference (95% = no adsorption assumed) per organic solvent (ACN or EtOH) (Figure 6). The target response ratio of 100% is indicated by a green line, while the pre-set specification limits are denoted by the red lines.

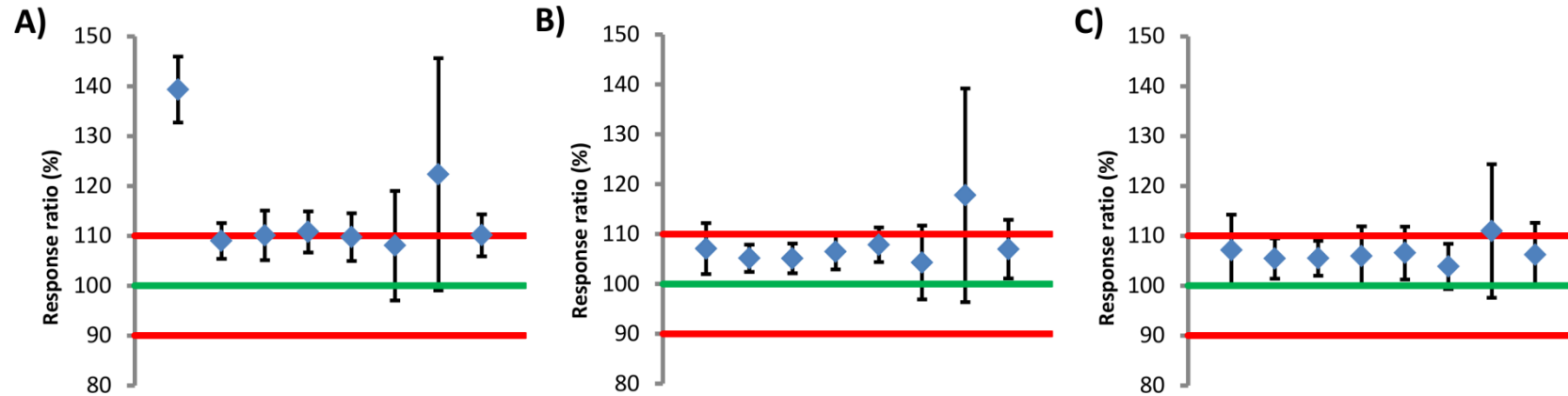


Figure 5: Adsorption to FDC glass: response ratios (in %) with 95% confidence intervals of EtOH versus ACN at 10% (A), 50% (B) and 95% (C) organic solvent. The target recovery (100%) is indicated by the green line, while the pre-set specification limits (90-110%) are denoted by the red lines. From left to right: BEA, ENN A, ENN C/F, ENN A1, ENN E, ENN D, ENN B1 and ENN B.

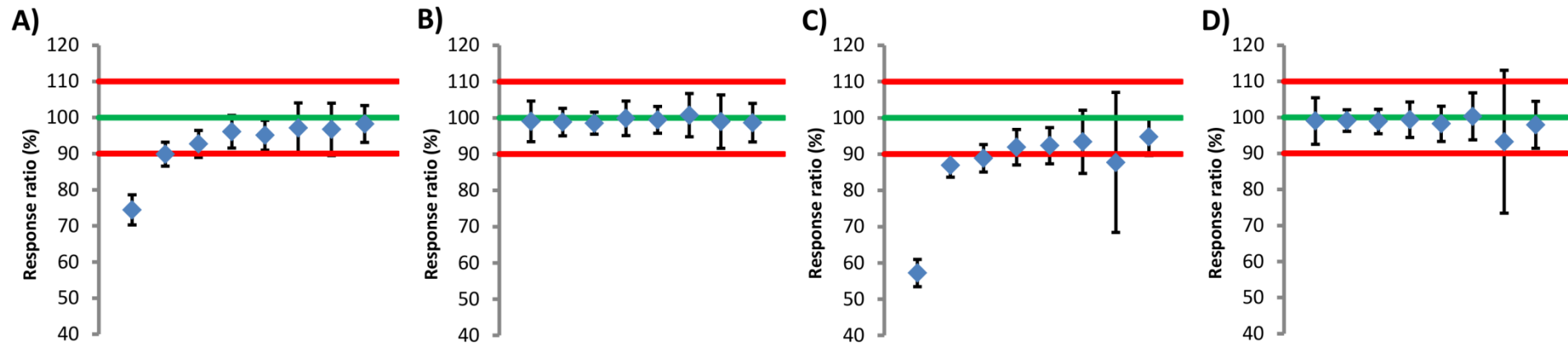


Figure 6: Adsorption to FDC glass: response ratios (in %) with 95% confidence intervals of EtOH_{10%}/EtOH_{95%} (A), EtOH_{50%}/EtOH_{95%} (B), ACN_{10%}/ACN_{95%} % (C) and ACN_{50%}/ACN_{95%}. The target recovery (100%) is indicated by the green line, while the pre-set specification limits (90-110%) are denoted by the red lines. From left to right: BEA, ENN A, ENN C/F, ENN A1, ENN E, ENN D, ENN B1 and ENN B.

For the majority of compounds, a statistically significant difference between EtOH and ACN was observed (p values < 0.05) for 10% and 50% organic solvent levels, and EtOH formulations tended to give lower adsorption. If not, this might be related to a larger variability (*e.g.* ENN B1). However, considering a 10% deviation from the target response ratio of 100% as biopharmaceutically negligible (*i.e.* the pre-set specification limits), a biopharmaceutically significant difference was only observed for BEA at 10% organic solvent (based on the 95% confidence interval excluding the specification limits). BEA, the most lipophilic compound (highest log P), showed significantly more adsorption to FDC glass when formulated in ACN. Moreover, there was no biopharmaceutically significant adsorption effect at a concentration of $\geq 50\%$ EtOH for all investigated cyclic depsipeptide mycotoxins. The latter also applied to the ACN formulations, except for ENN B1, where a possible significant adsorption effect could not be excluded. For BEA, significant adsorption was observed at low levels of organic solvent (10% EtOH or ACN), where adsorption losses as high as 45% were observed (Figure 6C). Most likely, the hydrophobicity of the compounds plays a role in the observed adsorption effects: compounds with higher log P values tend to give more adsorption to FDC glass. Log P values for all investigated cyclic depsipeptide mycotoxins are given in Table 6.

Table 6: Log P values of the investigated cyclic depsipeptide mycotoxins BEA and ENNs.

Compound	BEA	ENN A	ENN C/F	ENN A1	ENN E	ENN B1	ENN D	ENN B
Log $P^{(1)}$	7.13	5.87	5.66	5.48	5.40	5.08	5.01	4.68

(1) Calculated using Hyperchem, version 8.0.

These results were taken into account during the further method development: at least 50% organic solvent, either ACN or EtOH, was used when preparing solutions or samples containing BEA and/or ENNs. Only the receptor fluid (RF) itself did not contain any organic solvent, as the use of organic solvents is considered not well-suited as a biocompatible receptor medium [46]. Therefore, 1% HPBCD was added as a modifier. To investigate if this modifier can sufficiently inhibit adsorption of the cyclic depsipeptides to FDC glass and to further verify this method, precision and accuracy of the obtained RF samples were investigated as well.

Analytical stability

Linear regression analysis of the recovery (%) against time (days) was performed for each compound and formulation for the worst case scenario (40°C), after which the 95% confidence interval around the slope was investigated. If this interval contains zero, no significant degradation is observed. Figure 7 presents the plots, whereas regression analyses data can be found in Table 7. These data confirm that there was no significant degradation of BEA and ENNs in these sample solutions stored for a period of 7 days at 40°C. Considering this is the worst-case scenario, we conclude that there is likewise no evidence of degradation for the other storage conditions (-35°C, 5°C and 25°C).

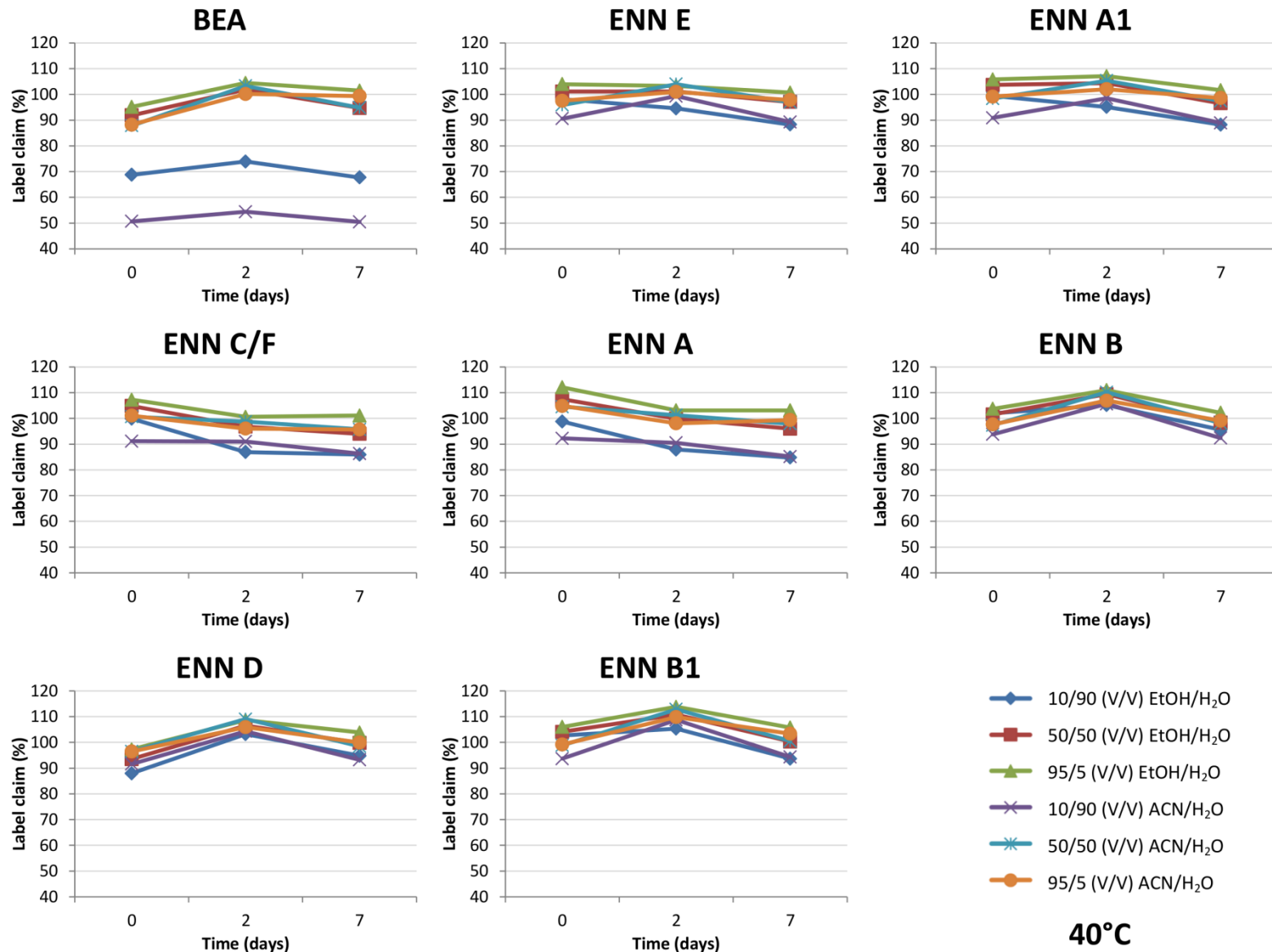


Figure 7: Stability profile for each cyclic depsipeptide mycotoxin stored at 40°C for 7 days in six different formulations.

Table 7: Analytical stability regression results (40°C).

Compound	Formulation	Slope		Intercept	
ENN B	10/90 (V/V) EtOH/H ₂ O	-1.11	[-10.94; 8.72]	104.24	[62.91; 145.56]
	50/50 (V/V) EtOH/H ₂ O	-0.79	[-18.07; -16.48]	105.46	[32.85; 178.07]
	95/5 (V/V) EtOH/H ₂ O	-0.51	[-15.67; 14.65]	107.16	[43.43; 170.88]
	10/90 (V/V) ACN/H ₂ O	-0.67	[-24.83; 23.48]	99.29	[-2.23; 200.81]
	50/50 (V/V) ACN/H ₂ O	-0.37	[-25.18; 24.44]	102.98	[-1.30; 207.26]
	95/5 (V/V) ACN/H ₂ O	-0.13	[-17.61; 17.34]	101.60	[28.15; 175.05]
ENN D	10/90 (V/V) EtOH/H ₂ O	0.46	[-25.75; 26.68]	93.93	[-16.25; 204.12]
	50/50 (V/V) EtOH/H ₂ O	0.47	[-21.57; 22.51]	98.51	[5.88; 191.14]
	95/5 (V/V) EtOH/H ₂ O	0.57	[-18.15; 19.30]	101.53	[22.82; 180.23]
	10/90 (V/V) ACN/H ₂ O	-0.24	[-24.42; 23.94]	97.07	[-4.56; 198.70]
	50/50 (V/V) ACN/H ₂ O	-0.18	[-23.86; 23.49]	101.89	[2.38; 201.39]
	95/5 (V/V) ACN/H ₂ O	0.18	[-16.52; 16.88]	100.25	[30.05; 170.45]
ENN B1	10/90 (V/V) EtOH/H ₂ O	-1.48	[-11.78; 8.82]	104.99	[61.70; 148.29]
	50/50 (V/V) EtOH/H ₂ O	-0.84	[-16.06; 14.39]	107.56	[43.55; 171.56]
	95/5 (V/V) EtOH/H ₂ O	-0.34	[-15.87; 15.19]	109.55	[44.29; 174.82]
	10/90 (V/V) ACN/H ₂ O	-0.48	[-29.86; 28.90]	100.35	[-23.13; 223.82]
	50/50 (V/V) ACN/H ₂ O	-0.28	[-26.95; 26.38]	104.92	[-7.17; 217.01]
	95/5 (V/V) ACN/H ₂ O	0.24	[-18.49; 18.96]	103.43	[24.72; 182.13]
BEA	10/90 (V/V) EtOH/H ₂ O	-0.36	[-11.13; 10.42]	71.18	[25.89; 116.47]
	50/50 (V/V) EtOH/H ₂ O	0.06	[-18.07; 18.18]	95.98	[19.79; 172.18]
	95/5 (V/V) EtOH/H ₂ O	0.61	[-14.20; 15.42]	98.51	[36.25; 160.76]
	10/90 (V/V) ACN/H ₂ O	-0.18	[-7.68; 7.33]	52.36	[20.82; 83.91]
	50/50 (V/V) ACN/H ₂ O	0.48	[-26.12; 27.09]	93.87	[-17.95; 205.70]
	95/5 (V/V) ACN/H ₂ O	1.25	[-16.03; 18.54]	92.14	[19.48; 164.80]
ENN E	10/90 (V/V) EtOH/H ₂ O	-1.38	[-2.92; 0.15]	97.81	[91.37; 104.25]
	50/50 (V/V) EtOH/H ₂ O	-0.62	[-2.89; 1.64]	101.64	[92.12; 111.16]
	95/5 (V/V) EtOH/H ₂ O	-0.48	[-0.97; 0.01]	104.09	[102.02; 106.15]
	10/90 (V/V) ACN/H ₂ O	-0.54	[-18.48; 17.40]	94.67	[19.27; 170.07]
	50/50 (V/V) ACN/H ₂ O	-0.14	[-15.45; 15.17]	99.36	[35.01; 163.71]
	95/5 (V/V) ACN/H ₂ O	-0.09	[-6.73; 6.56]	99.02	[71.07; 126.96]
ENN A1	10/90 (V/V) EtOH/H ₂ O	-1.56	[-3.80; 0.69]	98.94	[89.49; 108.38]
	50/50 (V/V) EtOH/H ₂ O	-1.12	[-6.52; 4.29]	104.88	[82.17; 127.60]
	95/5 (V/V) EtOH/H ₂ O	-0.69	[-5.61; 4.23]	106.91	[86.23; 127.58]
	10/90 (V/V) ACN/H ₂ O	-0.60	[-16.80; 15.60]	94.55	[26.45; 162.65]
	50/50 (V/V) ACN/H ₂ O	-0.41	[-14.71; 13.89]	101.61	[41.49; 161.72]
	95/5 (V/V) ACN/H ₂ O	-0.20	[-6.10; 5.71]	100.50	[75.67; 125.32]
ENN C/F	10/90 (V/V) EtOH/H ₂ O	-1.65	[-19.34; 16.05]	95.83	[21.45; 170.21]
	50/50 (V/V) EtOH/H ₂ O	-1.36	[-11.08; 8.37]	102.61	[61.74; 143.49]
	95/5 (V/V) EtOH/H ₂ O	-0.68	[-10.40; 9.03]	105.04	[64.22; 145.85]
	10/90 (V/V) ACN/H ₂ O	-0.74	[-3.22; 1.75]	91.68	[81.25; 102.11]
	50/50 (V/V) ACN/H ₂ O	-0.68	[-1.68; 0.33]	100.41	[96.19; 104.62]
	95/5 (V/V) ACN/H ₂ O	-0.64	[-7.53; 6.25]	99.52	[70.56; 128.47]
ENN A	10/90 (V/V) EtOH/H ₂ O	-1.74	[-15.32; 11.85]	95.69	[38.57; 152.80]
	50/50 (V/V) EtOH/H ₂ O	-1.47	[-9.96; 7.02]	105.49	[69.81; 141.17]
	95/5 (V/V) EtOH/H ₂ O	-1.03	[-13.63; 11.56]	109.18	[56.24; 162.13]
	10/90 (V/V) ACN/H ₂ O	-1.02	[-1.54; -0.49]	92.34	[90.13; 94.55]
	50/50 (V/V) ACN/H ₂ O	-0.89	[-3.62; 1.84]	103.90	[92.43; 115.37]
	95/5 (V/V) ACN/H ₂ O	-0.59	[-10.86; 9.68]	102.54	[59.37; 145.71]

In one case, namely for ENN A solubilised in 10/90 (V/V) ACN/H₂O, the 95% confidence interval around the slope did not contain zero (-1.54; -0.49). However, following justifications allow us to assume that there is also no biopharmaceutically significant degradation for this compound in this formulation: (i) no significant difference between the different storage conditions at 7 days was observed, (ii) for the other tested formulations there was no significant degradation observed, (iii)

given the many tests, this may well be a false positive finding (*e.g.* the 99% confidence level interval does contain zero (-3.65; 1.62)), (iv) ENN A is a stereoisomer of ENN C/F and its chemical structure is also very similar to the other enniatins (A1, B, B1, C, D and E), which were demonstrated to be stable under these experimental conditions, and (v) the difference between T_0 and $T_{7\text{days}}$ results were still <10% relative (7%). Overall, it was concluded that there is no biopharmaceutically, nor statistically significant degradation of enniatins or beauvericin after 7 days, when formulated in an organic or aqueous mixture, indicating no evidence of an unacceptable analytical stability of these compounds. Also no trend could be demonstrated, *i.e.* harsher conditions (ranging between -35°C and 40°C) do not translate into higher degradation.

Calibration curve

The linear calibration curve was forced through zero, which is justified by the fact that the difference in slope between the normal calibration curve and the one forced through zero is not significant, *i.e.* the 95% confidence interval around the intercept (without zero inclusion) also contains zero. For BEA a linear range was obtained from 1 to 100 ng/mL with an acceptable coefficient of determination of 0.998. For ENNs B and B1 the same linear range was used, whereas for ENN A1 this was 1 – 500 ng/mL and for ENN A this was 5 – 1000 ng/mL. For all other ENNs a linear range was obtained from 1 to 1000 ng/mL. For all enniatins the determination coefficients were equal to 1.000.

Limit of detection

All compounds have similar experimentally determined detection limits, which was expected due to their structural similarity: 17 pg/mL for BEA and ENN B, 14 pg/mL for ENN D and ENN B1, 15 pg/mL for ENN E, ENN A1 and ENN A and 10 pg/mL for ENN C/F.

Injection repeatability

The RSDs ranged between 0.15% and 1.84% for all cyclic depsipeptide mycotoxins investigated, which means that the injection repeatability of the method is below the pre-set limit of 10% and thus acceptable for our purposes.

Accuracy and precision of receptor fluid samples

At the 100 ng/mL concentration level, the precision ranged between 0.57% to 9.25%, which is within the normal expected variability range of 10%. At the lower concentration level (*i.e.* 10 ng/mL), these values were slightly higher (3.62% to 10.70%), but still acceptable for our purposes. The only exception was for ENN C/F at the lowest level with a precision of 24.37%: this can be ascribed to the concentration being below the limit of quantification (ENN C/F accounts for only 0.4% of the total amount enniatins in the mixture). The bias at the highest concentration level (*i.e.* 100 ng/mL) ranged

between 0.91% and 24.47%. For the 10 ng/mL concentration level, this was 0.68% and 24.86%. These values are slightly higher than the specification limits given by the FDA in their guidelines for formal bioanalytical method validation ($\leq 15.0\%$ and 20.0% at LoQ, $n = 5$), but are considered sufficient for our purposes [47]. From these acceptable accuracies, it is concluded that there are no significant adsorption losses upon using 1% HPBCD in PBS as a modifier in the receptor fluid.

Effect of skin components on the mycotoxin MS signal

All obtained recoveries were between 103.1% and 107.7% for the extraction solvent and between 95.0% and 113.4% for the receptor fluid. These results indicate no significant effect of skin compounds on the MS signal. Moreover, in an experimental FDC set-up the skin is only exposed at a 0.64 cm² dermal surface area and not fully soaked in the receptor fluid, as in this method verification, representing a worst-case situation.

4. CONCLUSIONS

This chapter described the development of a sensitive, specific and high-throughput UHPLC-MS/MS method for the quantitative and simultaneous determination of cyclic depsipeptide mycotoxins beauvericin and enniatins (B, B1, A, A1, D, E, C/F) in human skin Franz diffusion cell samples from *in vitro* transdermal experiments. Special attention was paid to analytical stability and adsorption to glass.

5. REFERENCES

- [1] Benson HAE, Watkinson AC. Topical and transdermal drug delivery – Principles and practice. John Wiley and Sons, New Jersey, 2012, pp. 446.
- [2] Williams AC. Transdermal and topical drug delivery – From theory to clinical practice. Pharmaceutical Press, London, 2003, pp. 242.
- [3] Boonen J, Malysheva SV, Taevernier L, Di Mavungu JD, De Saeger S, De Spiegeleer B. Human skin penetration of selected model mycotoxins. *Toxicology* 2012; 301: 21-32.
- [4] Howes D, Guy R, Hadgraft J, Heylings J, Hoeck U, Kemper F, Maibach H, Marty JP, Merk H, Parra J, Rekkas D, Rondelli I, Schaefer H, Täuber U, Verbieste N. Methods for assessing percutaneous absorption – The report and recommendations of ECVAM workshop. *ATLA* 1996; 24: 81-106.
- [5] Organisation for Economic Co-operation and Development (OECD). Guidance document for the conduct of skin absorption studies. OECD series on testing and assessment, Paris, 2004, pp. 31.
- [6] Celik M, Aksoy H, Yilmaz S. Evaluation of beauvericin genotoxicity with the chromosomal aberrations, sister-chromatid exchanges and micronucleus assays. *Ecotox Environ Safety* 2010; 73: 1553-1557.
- [7] Dornetshuber R, Heffeter P, Kamyar MR, Peterbauer T, Berger W, Lemmens-Gruber R. Enniatin exerts p53-dependent cytostatic and p53-independent cytotoxic activities against human cancer cells. *Chem Res Toxicol* 2007; 20: 465-473.
- [8] Ivanova L, Skjerve E, Eriksen GS, Uhlig S. Cytotoxicity of enniatins A, A1, B, B1, B2 and B3 from *Fusarium avenaceum*. *Toxicon* 2006; 47: 868-876.
- [9] Jestoi M. Emerging *Fusarium*-mycotoxins fusaproliferin, beauvericin, enniatins, and moniliformin - A review. *Crit Rev Food Sci Nutr* 2008; 48: 21-49.
- [10] Klaric MS, Darabos D, Rozgaj R, Kasuba V, Pepeljnjak S. Beauvericin and ochratoxin A genotoxicity evaluated using the alkaline comet assay: single and combined genotoxic action. *Arch Toxicol* 2010; 84: 641-650.
- [11] Lee HS, Song HH, Jeong JH, Shin CG, Choi SU, Lee C. Cytotoxicities of enniatins H, I, and MK1688 from *Fusarium oxysporum* KFCC11363P. *Toxicon* 2008; 51: 1178-1185.
- [12] Macchia L, Di Paola R, Fornelli F, Nenna S, Moretti A, Napoletano R, Logrieco A, Caiaffa MF, Tursil MF, Bottalico A. Cytotoxicity of beauvericin to mammalian cells. Abstracts of the International Seminar on *Fusarium*, Martina Franca, Italy, 1995, pp. 72-73.
- [13] Meca G, Font G, Ruiz MJ. Comparative cytotoxicity study of enniatins A, A(1), A(2), B, B-1, B-4 and J(3) on Caco-2 cells, Hep-G(2) and HT-29. *Food Chem Toxicol* 2011; 49: 2464-2469.
- [14] Nilanonta C, Isaka M, Kittakoop P, Trakulnaleamsai S, Tanticharoen M, Thebtaranonth Y. Precursor-directed biosynthesis of beauvericin analogs by the insect pathogenic fungus *Paecilomyces tenuipes* BCC 1614. *Tetrahedron* 2002; 58: 3355-3360.

- [15] Prosperini A, Meca G, Font G, Ruiz MJ. Study of the cytotoxic activity of beauvericin and fusaproliferin and bioavailability in vitro on Caco-2 cells. *Food Chem Toxicol* 2012; 50: 2356-2361.
- [16] Tonshin AA, Teplova VV, Andersson MA, Salkinoja-Salonen MS. The *Fusarium* mycotoxins enniatins and beauvericin cause mitochondrial dysfunction by affecting the mitochondrial volume regulation, oxidative phosphorylation and ion homeostasis. *Toxicol* 2010; 276: 49-57.
- [17] Watjen W, Debbab A, Hohfeld A, Chovolou Y, Kampkotter A, Edrada RA, Ebel R, Hakiki A, Mosaddak M, Totzke F, Kubbutat MHG, Proksch P. Enniatins A1, B and B1 from an endophytic strain of *Fusarium tricinctum* induce apoptotic cell death in H4IIE hepatoma cells accompanied by inhibition of ERK phosphorylation. *Mol Nutr Food Res* 2009; 53: 431440.
- [18] Zahn JX, Burns AM, Liu MPX, Faeth SH, Gunatilaka AAL. Search for cell motility and angiogenesis inhibitors with potential anticancer activity: beauvericin and other constituents of two endophytic strains of *Fusarium oxysporum*. *J Nat Prod* 2007; 70: 227-232.
- [19] Gäumann E, Naef-Roth S, Etlinger L, Plattner PA, Nager U. Enniatin, ein neues gegen mykobakterien wirksames antibiotikum. *Experimentia* 1947; 3: 202-203.
- [20] Hamill RL, Higgins CE, Boaz HE, Gorman M. The structure of beauvericin, a new depsipeptide antibiotic toxic to *Artemia salina*. *Tetrahedron Lett* 1969; 49: 4255-4258.
- [21] Lin YC, Wang J, Wu XY, Zhou SN, Vrijmoed LLP, Jones EBG. A novel compound enniatin G from the mangrove fungus *Halosarpheia* sp. (strain 732) from the south China sea. *Aust J Chem* 2002; 55: 225-227.
- [22] McKee TC, Bokesch HR, McCormick JL, Rashid MA, Spielvogel D, Gustafson KR, Alavanja MM, Cardellina JH, Boyd MR. Isolation and characterization of new anti-HIV and cytotoxic leads from plants, marine and microbial origins. *J Nat Prod* 1997; 60: 431-438.
- [23] Nilanonta C, Isaka M, Chanphen R, Thong-Orn N, Tanticharoen M, Thebtaranonth Y. Unusual enniatins produced by the insect pathogenic fungus *Verticillium hemipterigenum*: isolation and studies on precursor-directed biosynthesis. *Tetrahedron* 2003; 59: 1015-1020.
- [24] Supothina S, Isaka M, Kirtikara K, Tanticharoen M, Thebtaranonth Y. Enniatin production by the entomopathogenic fungus *Verticillium hemipterigenum* BCC 1449. *J Antibiot* 2004; 57: 732-738.
- [25] Wang Q, Xu L. Beauvericin, a bioactive compound produced by fungi: a short review. *Molecules* 2012; 17: 2367-2377.
- [26] Ficheux AS, Sibiril Y, Parent-Massin D. Effects of beauvericin, enniatin b and moniliformin on human dendritic cells and macrophages: an in vitro study. *Toxicon* 2013; 71: 1-10.
- [27] Gammelsrud A, Solhaug A, Dendele B, Sandberg WJ, Ivanova L, Bolling AK, Lagadic-Gossmann D, Refsnes M, Becher R, Eriksen G, Holme JA. Enniatin B-induced cell death and inflammatory responses in RAW 267.4 murine macrophages. *Toxicol Appl Pharmacol* 2012; 261: 74-87.
- [28] Schaeuble K, Hauser MA, Rippl AV, Bruderer R, Otero C, Groettrup M, Legler DF. Ubiquitylation of the chemokine receptor CCR7 enables efficient receptor recycling and cell migration. *J Cell Sci* 2012; 125: 4463-4474.

- [29] Tomoda H, Nishida H, Huang XH, Masuma R, Kim YK, Omura S. New cyclodepsipeptides, enniatin-D, enniatin-E and enniatin-F produced by *Fusarium* sp FO-1305. *J Antibiot* 1992; 45: 1207-1215.
- [30] Wu XF, Xu R, Ouyang ZJ, Qian C, Shen Y, Wu WD, Gu YH, Xu Q, Sun Y. Beauvericin ameliorates experimental colitis by inhibiting activated T cells via downregulation of the PI3K/Akt signaling pathway. *PLoS ONE* 2013; 8: e83013.
- [31] Frenich AG, Romero-Gonzalez R, Gomez-Perez ML, Vidal JLM. Multi-mycotoxin analysis in eggs using a QuEChERS-based extraction procedure and ultra-high-pressure liquid chromatography coupled to triple quadrupole mass spectrometry. *J Chrom A* 2011; 1218: 4349-4356.
- [32] Varga E, Glauner T, Berthiller F, Krska R, Schuhmacher R, Sulyok M. Development and validation of a (semi-)quantitative HPLC-MS/MS method for the determination of 191 mycotoxins and other fungal metabolites in almonds, hazelnuts, peanuts and pistachios. *Anal Bioanal Chem* 2013; 405: 5087-5104.
- [33] Van Pamel E, Verbeken A, Vlaemynek G, De Boever J, Daeseleire E. Ultrahigh-performance liquid chromatographic-tandem mass spectrometric multimycotoxin method for quantitating 26 mycotoxins in maize silage. *J Agric Food Chem* 2011; 59: 9747-9755.
- [34] Herath HMDR, Kim RR, Cabot PJ, Shaw PN, Hewavitharana AK. Inaccuracies in the quantification of peptides – A case study using β -endorphin assay. *LCGC North America* 2013; 31: 58-61.
- [35] Pezeshki A, Vergote V, Van Dorpe S, Baert B, Burvenich C, Popkov A, De Spiegeleer B. Adsorption of peptides at the sample drying step: influence of solvent evaporation technique, vial material and solution additive. *J Pharm Biomed Anal* 2009; 49: 607-612.
- [36] Baert B, Boonen J, Burvenich C, Roche N, Stillaert F, Blondeel P, Van Bocxlaer J, De Spiegeleer B. A new discriminative criterion for the development of Franz diffusion tests for transdermal pharmaceuticals. *J Pharm Pharmaceut Sci* 2010; 13: 218-230.
- [37] De Spiegeleer B, Baert B, Vergote V, Van Dorpe S. Development of system suitability tests for in vitro skin integrity control: impedance and capacitance. *The Eleventh International Perspectives in Percutaneous Penetration Conference*. La Grande Motte, France, 2008, 43-43.
- [38] Liang KY, Zeger SL. Longitudinal data analysis using generalized linear models. *Biometrics* 1986; 78: 13-22.
- [39] European Directorate for the Quality of Medicines and HealthCare (EDQM). Qualification of equipment – Annex 7: qualification of mass spectrometers. 2011, pp. 11.
- [40] Sorensen JL, Nielsen KF, Rasmussen PH. Development of a LC-MS/MS method for the analysis of enniatins and beauvericin in whole fresh and ensiled maize. *J Agric Food Chem* 2008; 56: 10439-10443.
- [41] Jestoi M, Rokka M, Rizzo A, Peltonen K. Determination of *Fusarium*-mycotoxins beauvericin and enniatins with liquid chromatography-tandem mass spectrometry (LC-MS/MS). *J Liq Chromatogr Relat Technol* 2005; 28: 369-381.

- [42] Sulyok M, Krska R, Schuhmacher R. A liquid chromatography/tandem mass spectrometric multi-mycotoxin method for the quantification of 87 analytes and its application to semi-quantitative screening of moldy food samples. *Anal Bioanal Chem* 2007; 389: 1505-1523.
- [43] Monti SM, Fogliano V, Logrieco A, Ferracane R, Ritieni A. liquid chromatography/tandem mass spectrometric multi-mycotoxin method for the quantification of 87 analytes and its application. *J Agric Food Chem* 2000; 48: 3317-3320.
- [44] Sulyok M, Berthiller F, Krska R, Schuhmacher R. Development and validation of a liquid chromatography/tandem mass spectrometric method for the determination of 39 mycotoxins in wheat and maize. *Rapid Commun Mass Spec* 2006; 20: 2649-2659.
- [45] Devreese M, De Baere S, De Backer P, Croubels S. Quantitative determination of the *Fusarium* mycotoxins beauvericin, enniatin A, A1, B and B1 in pig plasma using high performance liquid chromatography-tandem mass spectrometry. *Talanta* 2013; 106: 212-219.
- [46] Dressman J, Kramer J. *Pharmaceutical Dissolution Testing*. Taylor & Francis Group, UK, 2005, pp. 429
- [47] Food and Drug Administration (FDA). *Guidance for industry – Bioanalytical method validation*. 2013, pp. 34.

CHAPTER V

HUMAN SKIN PERMEATION OF BEAUVERICIN AND ENNIATINS

*“You have to grow thick skin
and that only comes with time and learning.”*

*Karlie Kloss
(°1992, American fashion model)*

Parts of this chapter were published:

Taevernier L, Veryser L, Roche N, Peremans K, Burvenich C, Delesalle C, De Spiegeleer B. Human skin permeation of emerging mycotoxins (beauvericin and enniatins). *Journal of Exposure Science and Environmental Epidemiology*. 2016; **26**: 277-287, doi: 10.1038/jes.2015.10.

ABSTRACT

Currently, dermal exposure data of cyclic depsipeptide mycotoxins are completely absent. There is a lack of understanding about the local skin and systemic kinetics and effects, despite their widespread skin contact and intrinsic hazard. Therefore, we provide a quantitative characterisation of their dermal kinetics. The emerging mycotoxins enniatins and beauvericin were used as model compounds and their transdermal kinetics were quantitatively evaluated, using intact and damaged human skin in an *in vitro* Franz diffusion cell set-up and UHPLC-MS/MS analytics. We demonstrated that all investigated mycotoxins are able to penetrate through the skin. ENN B showed the highest permeation ($k_{p,v} = 9.44 \times 10^{-6}$ cm/h), whereas BEA showed the lowest ($k_{p,v} = 2.35 \times 10^{-6}$ cm/h) and the other ENNs ranging in between. Combining these values with experimentally determined solubility data, J_{max} values ranging from 0.02 to 0.35 $\mu\text{g}/(\text{cm}^2 \times \text{h})$ for intact skin and from 0.07 to 1.11 $\mu\text{g}/(\text{cm}^2 \times \text{h})$ for damaged skin were obtained. These were used to determine the daily dermal exposure (DDE) in a worst-case scenario. On the other hand, DDE's for a typical occupational scenario were calculated based on real-life mycotoxin concentrations for the industrial exposure of food-related workers. In the latter case, for contact with intact human skin, DDE's up to 0.0870 ng/(kg BW \times day) for ENN A were calculated, whereas for impaired skin barrier this can even rise up to 0.3209 ng/(kg BW \times day) for ENN B1. This knowledge is needed for the risk assessment after skin exposure of contaminated food, feed, indoor surfaces and airborne particles with mycotoxins.

CHAPTER V

HUMAN SKIN PERMEATION OF BEAUVERICIN AND ENNIATINS

Main focus in this chapter:

- To quantitatively determine the human skin kinetics of CDPs beauvericin and enniatins.
- Evaluate the impact on risk assessment after dermal exposure of these CDP mycotoxins.

1. INTRODUCTION

Cyclic depsipeptides are a group of naturally occurring bioactive peptides, some of which are already developed as pharmaceutical drugs, *e.g.* valinomycin. They are not only produced by fungi, *e.g.* the mycotoxins enniatins (ENNs) are produced by strains of some species of fungal genera *Alternaria*, *Fusarium*, *Halosarpheia* and *Verticillium* [1-5] and beauvericin (BEA) by *Paecilomyces fumosoroseus* and *Fusarium* and *Beauveria* species [6,7], but also by bacteria (*e.g.* the anti-lymphoma romidepsin) and many marine organisms (*e.g.* the anti-HIV papuamides) [8-10]. The emerging mycotoxins beauvericin and enniatins are non-ionised, cyclic hexadepsipeptides with cation-complexing ionophoric and lipophilic properties. Besides their well-known antibiotic and insecticidal activity, BEA and ENNs are also inhibitors of acyl-CoA:cholesterol acyl transferase [11-13]. Furthermore, their cytotoxicity has already been demonstrated in various cell lines, such as human colorectal (Caco-2, HCT-15 and HT-29), cervical (HeLa), breast (BC-1 and MCF-7), liver (Hep-G2), lung (A549, NCI-H460 and MRC-5), pancreatic (MIA Pa Ca-2), ovarian (SK-OV-3), glioma (SF-268) and skin (SK-MEL-2) cancer cells, exerting cytotoxic activities in the low micromolar range [11,12,14-22]. Recently, it has also been demonstrated that beauvericin is potentially genotoxic to human lymphocytes *in vitro*, causing a significant increase in chromosomal aberrations, sister-chromatid exchanges and micronuclei formation on one hand and significantly decreasing the mitotic index on the other hand [14]. At the same time, Klaric *et al.* have concluded, using the Comet assay to PK15 cells, that exposure to BEA could induce DNA damage [23]. Despite these positive results for BEA, Fotso and Smith showed a negative mutagenicity in the Ames test [24]. For enniatin B also negative genotoxic potential was found in a Comet, Ames and micronucleus assay [25]. Although these conflicting results exist, it

cannot be excluded that prolonged exposure to these cyclic depsipeptide mycotoxins may contribute to carcinogenicity in humans. Tonshin and co-workers have also indicated that both ENNs and BEA cause significant mitochondrial dysfunction by affecting the mitochondrial volume regulation, oxidative phosphorylation and ion homeostasis [26]. The inherent cation-complexing properties of these cyclic depsipeptide mycotoxins, which might also cause changes in intracellular calcium concentrations, may partly explain their toxicity.

It can thus be stated that the cyclic depsipeptides enniatins and beauvericin pose a potential health hazard and are considered as emerging mycotoxins. A number of studies have already been performed to evaluate the amount of BEA and ENNs present in food, as absorption of mycotoxins often occurs by ingestion of contaminated food [27-32]. However, inhalation and dermal exposure to air, dust and food (such as natural fruit waxes for example), containing these toxins may not be overlooked as well [33]. To date, only two studies, both in school buildings, have investigated the amount of BEA and ENNs in airborne samples [34,35] and up till now, no studies have been performed to investigate the transdermal behaviour of these cyclic depsipeptide mycotoxins. Our group has already recommended to limit dermal exposure to the traditional mycotoxins [33], however, the skin remains unexplored as exposure route for enniatins and beauvericin and to date, skin permeability data of these emerging mycotoxins are non-existing. However, in view of the accumulating evidence of their toxic potential, this information is essential for proper risk management [33,36].

On the other hand, there is also an increasing appreciation for these cyclic depsipeptides as topically applied medicines, for the treatment of dermatological diseases like eczema, psoriasis and skin cancers or having systematic functions after transdermal permeation. For example, kahalalide F is currently under phase II clinical trials for several types of cancer and psoriasis [37]. Romidepsin or FR901228, a potent class 1 selective histone deacetylase (HDAC) inhibitor, has been shown to be effective *in vitro* to the cutaneous melanomas cancer cell lines SK-MEL2 and SK-MEL28, with IC_{50} values ranging in the low nanomolar range [38]. Other cyclic depsipeptides like emodepside and PF1022, with structures closely resembling that of beauvericin and enniatins, have been patented in certain topical formulations for controlling endoparasites [39].

At this moment, there is a significant lack of knowledge about both the local skin and systemic effects that can occur due to dermal exposure to cyclic depsipeptides in general. Moreover, mechanical pathways and models are completely absent. Therefore, the transdermal kinetics of the cyclic depsipeptide mycotoxins beauvericin and enniatins were quantitatively evaluated in this study, using excised human skin in an *ex vivo in vitro* Franz diffusion cell (FDC) set-up.

2. MATERIALS AND METHODS

2.1. Chemicals and reagents

Mycotoxins beauvericin (BEA) and enniatin B (ENN B) were supplied by BioAustralis (Smithfield NSW, Australia), while the enniatin mixture (ENNs) was obtained from Cfm Oscar Tropitzsch (Marktredwitz, Germany). No formal ENN composition was supplied by the manufacturer (only e-mail correspondence), therefore the composition was experimentally determined by our group, assuming a relative response factor (RRF) = 1 for the individual constituents: 43.8% ENN B, 34.4% ENN B1, 14.0% ENN A1, 3.6% ENN D, 1.8% ENN A, 1.8% ENN E and 0.4% ENN C or F. These data were obtained by UHPLC-MS and UHPLC-UV (205 nm) normalised areas. ULC-MS grade acetonitrile (ACN), formic acid (FA) and 2-propanol, used for preparation of the mobile phase, were purchased from Biosolve (Valkenswaard, The Netherlands). Ultrapure water (H₂O) was produced by an Arium pro VF TOC water purification system (Sartorius, Göttingen, Germany), resulting in ultrapure water of 18.2 MΩ × cm quality. Sigma-Aldrich (St. Louis, MO, USA) supplied 0.01 M phosphate buffered saline (PBS) and dimethyl sulfoxide (DMSO). Ethanol (EtOH), used for preparation of the dose solutions, was purchased from Merck (Darmstadt, Germany) and UHPLC grade ACN and EtOH, used in the solubility experiments, was bought from Fisher Scientific (Waltham, MA, USA). Pharma grade hydroxypropyl-β-cyclodextrin (HPBCD) was supplied by Cerestar (Mechelen, Belgium). This was used as a solubilising modifier to the receptor fluid (PBS), in order to guarantee sink conditions of the hydrophobic cyclic depsipeptide mycotoxins throughout the experiment [40].

2.2. Analytical method

We previously developed a sensitive, specific and high-throughput bioanalytical ultra high performance liquid chromatography tandem mass spectrometry (UHPLC-MS/MS) method for the quantitative and simultaneous determination of cyclic depsipeptide mycotoxins beauvericin and enniatins (A, A1, B, B1, D, E, C/F) in human skin Franz diffusion cell samples. Briefly, the UHPLC-MS/MS platform consisted of an Acquity UHPLC equipped with a Xevo TQ-S MS detector (Waters, Milford, MA, USA). An Acquity UHPLC CSH C18 column (1.7 μm, 100 × 2.1 mm, 130Å), attached to an Acquity UHPLC VanGuard pre-column (1.7 μm, 5 × 2.1 mm, 130Å), was used for the chromatographic separation, thermostated at 45°C (Waters, Milford, MA, USA). The injection volume was 10 μL and the needle wash consisted of 10/10/80 (V/V/V) DMSO/2-propanol/ACN. The isocratic flow rate was set to 0.6 mL/min, using 70/30 (V/V) ACN/H₂O with 0.1% FA and 0.1% 2-propanol as mobile phase. The run time was 4.5 min. The mass spectrometer was operated in the positive electrospray ionization mode (ESI+), with a capillary voltage of 3.50 kV and cone voltage of 50 V. Source and desolvation temperatures were set at 150°C and 600°C, respectively, while cone and desolvation gas

flows were 150 and 1000 L/h, respectively. Data were acquired using Masslynx software (V4.1 SCN 843, Waters, Milford, MA, USA). ENN B was used as an internal standard (IS) for the determination of BEA, while BEA was used for the enniatin mixture. The selected precursor and product ions, with the applied collision energies between brackets, are given. The selected precursor ion for ENN B was m/z 639.91 with two selected product ions at m/z 196.08 (25 V) and m/z 527.26 (22 V), for ENN D and B1 the precursor ion was m/z 653.99 and m/z 196.09 (23 V) and m/z 541.05 (21 V) were the product ions. For ENN E and A1, m/z 668.07 was the precursor ion and m/z 209.99 (24 V) and m/z 555.29 (21 V) were its product ions. ENNs A and C or F have a precursor ion of m/z 682.47 with product ions m/z 209.93 (26 V) and m/z 555.01 (23 V). Lastly BEA has a precursor ion at m/z 783.94, with m/z 244.01 (24 V) and m/z 623.23 (23 V) as its product ions.


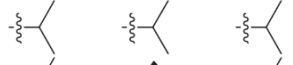
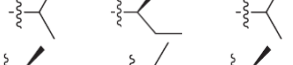
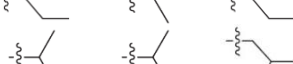
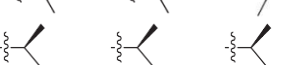
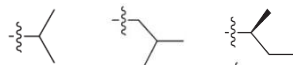
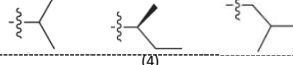
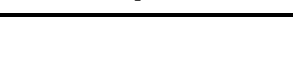
This method has also been successfully verified. It was demonstrated that beauvericin and enniatins are stable for at least 7 days when formulated in different organic or aqueous mixtures. Additional attention was paid to the investigation of analyte losses due to adsorption issues. It was shown that at least 50% organic solvent is required to prevent significant adsorption to glass. The limits of detection were 17 pg/mL for BEA and ENN B, 14 pg/mL for ENN D and ENN B1, 15 pg/mL for ENN E, ENN A1 and ENN A and 10 pg/mL for ENN C/F. There was no significant effect of skin compounds on the mycotoxin MS signal observed and the accuracy and precision of the obtained receptor fluid samples were considered acceptable for our purposes. More details about the development and verification of the applied bioanalytical method are given in **Chapter IV**.

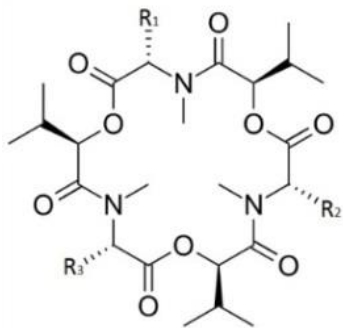
2.3. In vitro FDC study using human skin

Seen the potential toxicity of the cyclic depsipeptide mycotoxins beauvericin and enniatins, it is ethically unacceptable to use living human beings in the transdermal study. Therefore, the permeation of these mycotoxins through human skin was determined using a static Franz diffusion cell set-up with a receptor compartment of 5 mL and an available diffusion area of 0.64 cm² (Logan Instruments Corp., New Jersey, USA). Beside intact skin samples, this study also included damaged skin (tape-stripped 20 times with Scotch magic tape, 3M, Minnesota, USA) to evaluate the effect of an impaired skin barrier. The experiments were replicated four times for each compound (beauvericin and enniatin mixture) with three different skin donors, for both intact ($n = 12$) as well as damaged skin ($n = 12$). Human skin from the abdominal region was collected from healthy female patients (32 ± 4 years old (BEA) and 35 ± 2 years old (ENNs), mean \pm SEM) who had undergone aesthetic reduction surgery, with informed consent and confidentiality procedures in place (University Hospital, Ghent, Belgium). Skin preparation was done according to the internationally accepted guidelines [41]. Immediately after surgical removal, the skin was cleaned with 0.01 M PBS pH 7.4 and the subcutaneous fat was removed. The skin samples were wrapped in aluminium foil and

stored at $-20\text{ }^{\circ}\text{C}$ for no longer than 6 months. Just before the start of the experiments, the full-thickness skin was thawed, tape-stripped or left intact, mounted on a template and dermatomed to split-thickness skin using an electrical powered dermatome (Integra Life Sciences, New Jersey, USA). The experimentally obtained thickness of the skin, determined with a micrometer (Mitutoyo, Tokyo, Japan), was $270 \pm 13\text{ }\mu\text{m}$ and $384 \pm 14\text{ }\mu\text{m}$ (BEA) and $331 \pm 13\text{ }\mu\text{m}$ and $287 \pm 12\text{ }\mu\text{m}$ (ENNs), for the intact and stripped skin, respectively (mean \pm SEM, $n = 29\text{-}46$). After visual inspection to avoid pinholes, the skin samples were sandwiched between the donor and acceptor chambers, with the epidermis facing upwards, making sure all air under the skin was removed. The whole assembly was fixed on a magnetic stirrer and the receptor fluid (1% HPBCD in 0.01 M PBS pH 7.4) was continuously stirred using a Teflon coated magnetic stirring bar (600 rpm) to ensure sink conditions. Before starting the experiments, skin integrity was checked by measuring the skin impedance using an automatic microprocessor-controlled LCR impedance bridge (Tinsley, Croydon, UK). Skin pieces with an impedance value $< 10\text{ k}\Omega$, a previously validated system-suitability cut-off, were discarded and replaced by a new piece [42]. Overall impedance values of $52 \pm 7\text{ k}\Omega$ and $20 \pm 3\text{ k}\Omega$ (BEA) and $50 \pm 7\text{ k}\Omega$ and $21 \pm 2\text{ k}\Omega$ (ENNs) (mean \pm SEM, $n = 12$) were obtained for respectively intact and stripped skin pieces, indicating significant skin damaging by tape-stripping ($p < 0.05$). The dose solutions at a concentration of 1 mg/mL BEA or ENNs mixture (total concentration enniatins = 1 mg/mL) in 60/40 (V/V) EtOH/H₂O, were topically applied to the epidermal surface of the skin (400 μL). The experimentally determined applied concentration of each mycotoxin is given in Table 1. The donor chamber was covered with parafilm and the temperature of the receptor compartment was kept at $32 \pm 1\text{ }^{\circ}\text{C}$. Samples (200 μL) were drawn at regular time intervals (3, 6, 8, 10, 15, 17, 20, 22 and 24h) from the sampling port and were immediately replaced by 200 μL fresh receptor solution. The analytically determined mycotoxin assay values in the FDC samples were correspondingly corrected for the replenishments. At the end of the experiment (*i.e.* after 24h), the skin surfaces were swabbed with cotton wool to remove the remaining donor solution, then epidermis and dermis were separated and mycotoxins were extracted. These were all used to construct a mass balance: the recovery of each mycotoxin was between $100.4 \pm 0.35\%$ and $105.3 \pm 0.39\%$ (mean \pm SEM, $n = 23\text{-}24$). Moreover, the recoveries of the individual replicates were all within 90 – 100%, confirming the quantitative validity of our data. Notwithstanding the confirmed stability of the mycotoxins for as long as 7 days under diverse storage conditions, all samples (*i.a.* skin extracts and receptor fluid samples) were analysed as soon as possible (within 72h).

Table 1: Cyclic depsipeptide mycotoxins used in the transdermal investigation: structure, some molecular descriptors and the experimentally determined solubility in different solvent mixtures.

Mycotoxin	Structure ⁽¹⁾	Log P ⁽²⁾	Molecular weight (Da)	Conc. applied DS (mg/mL) ⁽³⁾	Solubility (mg/mL) ⁽⁵⁾		
					100% H ₂ O	30% EtOH in H ₂ O	60% EtOH in H ₂ O
Beauvericin	BEA 	7.13	783.96	1.13	0.082	0.069	7.151
Enniatin B	ENN B 	4.68	639.82	0.44	_(6)	_(6)	_(6)
Enniatin B1	ENN B1 	5.08	653.85	0.38	_(6)	_(6)	_(6)
Enniatin A1	ENN A1 	5.48	667.88	0.15	_(6)	_(6)	_(6)
Enniatin D	ENN D 	5.01	653.85	3.50 x 10 ⁻²	_(6)	_(6)	_(6)
Enniatin A	ENN A 	5.87	681.90	1.80 x 10 ⁻²	_(6)	_(6)	_(6)
Enniatin E	ENN E1 	5.40	667.88	1.71 x 10 ⁻²	_(6)	_(6)	_(6)
	ENN E2 						
Enniatins total	ENNs _(4)	_(4)	_(4)	1.03	0.294	0.847	36.918



(1)

(2) Hyperchem, version 8.0.

(3) Experimentally determined; DS = dose solution.

(4) Not applicable.

(5) Experimentally determined; solvent mixtures are expressed as V/V.

(6) Enniatin solubility is expressed as the solubility of the total enniatin complex.

2.4. Sample preparation

Prior to analysis, the 200 µL receptor fluid samples, drawn from the FDC sampling port at regular time intervals, were 1:2 diluted with ACN, containing the respective IS. At the end of the experiment, the skin samples (*i.e.* separated in dermis and epidermis) were extracted overnight at 25°C, while shaking (750 rpm) in a mixture of 95/5 (V/V) ACN/H₂O. Following this incubation, the skin samples were centrifuged at 20000 rpm at room temperature, after which an aliquot was appropriately diluted with a mixture of 70/30 ACN/H₂O to prevent MS overload. The IS was added during the final dilution step. The samples containing the remaining dose solution swabs were also extracted overnight at 40°C (150 rpm) in a mixture of 70/30 ACN/H₂O. Prior to analysis, an aliquot was appropriately diluted, whereby the IS was added in the final dilution step.

2.5. Kinetic data analysis

The skin permeation parameters were calculated from the individual curves of the cumulative amount of each mycotoxin permeated as a function of time. Steady-state flux (J_{ss}) was obtained from the slope of the linear portion of the curve divided by 0.64 to correct for the exposed skin area. The lag time (t_{lag}) was estimated by extrapolating the linear portion of the curve to the time-axis. The cumulative quantity, expressed as percentage of the effective dose applied, obtained after one day is Q_{1d} . From these experimentally determined secondary kinetic parameters, the apparent primary parameters could be calculated according to the European Centre for Ecotoxicology and Toxicology of Chemicals [43]. The permeability coefficient $k_{p,v}$ was obtained using the following equation: $k_{p,v} = J_{ss}/C_v$, where C_v is the concentration of each mycotoxin in the vehicle (dose formulation). From the skin extractions, the mycotoxin concentrations within the skin (*i.e.* separated in dermis and epidermis) were also determined, taking the respective skin volumes into account: skin volume (cm³) = skin thickness (cm) × skin surface (0.64 cm²). An epidermis thickness of 50 µm was taken for intact skin, while this was 46 µm for tape-stripped skin. The dermis thickness was then calculated as follows: dermis thickness (cm) = experimentally determined skin thickness (cm) – epidermis thickness (cm). Considering the actual amount applied is different for each mycotoxin, skin concentrations as such cannot be directly compared. Therefore these were normalised to estimate a skin concentration after application of 1 mg/mL, assuming a linear relationship and using the following calculation: normalised skin concentration (µg/mL) = experimentally determined skin concentration (µg/mL) × [1 (mg/mL)/ concentration dose solution applied (mg/mL)].

2.6. Solubility experiments

Since there was no data available about the solubility of these compounds in EtOH/H₂O mixtures, these were experimentally determined using the shake flask technique. For each compound, *i.e.* beauvericin and enniatin mixture, three different solvents were tested (H₂O, 30/70 (V/V) EtOH/H₂O and 60/40 (V/V) EtOH/H₂O), each in duplicate. In an 0.5 mL LoBind Eppendorf tube approximately 1.0 mg compound was weighed, to which solvent increments of 10 µL were added to maximally 100 µL to assure saturation. These were then stirred at 300 rpm for 48h at room temperature (22.5 ± 2.5°C) in an Eppendorf thermomixer (Eppendorf, Hamburg, Germany). Next, the tubes were centrifuged at 20,000 g for 30 minutes in an Eppendorf centrifuge 5417R (Eppendorf, Hamburg, Germany) to sediment the remaining undissolved compound material. An aliquot of the supernatant solution was appropriately diluted and analysed according to the previously mentioned UHPLC-MS/MS method [44]. It is also acknowledged that the unavailability of isolated ENN compounds hinders a detailed physicochemical solubility study, as currently only a mixture of ENN compounds was available.

2.7. Risk assessment after dermal exposure

In risk assessment the concept of maximum exposure is important with regard to estimating the exposure of the individual with the highest actual or possible exposure [45]. Therefore, EPA (US Environmental Protection Agency), has introduced the concept of maximum flux, which is stated to be an inherently more useful and practical parameter when evaluating the potential therapeutic benefit or toxicological risk of a topically or transdermally absorbed substance: $J_{\max} = k_p \times S$, where S is the solubility of the compound in the same vehicle used during the permeation studies determining k_p [46-50]. Since the dose solution applied to the skin should be the same (or a realistic surrogate) as that to which humans may be exposed, it was decided to use a more lipophilic ethanolic matrix instead of water, as it resembles more closely the real-life matrix where mycotoxins are also presented *e.g.* in fruit-waxes [32,51]. Assuming that ethanol (or the matrix in general) does not influence the skin barrier, the maximum flux can be calculated as follows: $J_{\max} = k_{p,v} \times S_v$, where both $k_{p,v}$ and S_v are experimentally determined. When applied in the risk assessment calculation, daily dermal exposure can be calculated according to [52,53]: $DDE_{\max} = (J_{\max} \times t_{\text{event}} \times SA \times ED \times EF \times EV) / (BW \times AT)$, giving a worst-case scenario. Table 2 gives available occurrence data. These indicate that real-life mycotoxin concentrations are much lower than the solubility concentrations in the “lipophilic” matrix (*i.e.* ethanol-water mimicking the real-life matrix). Therefore, the product of the experimentally obtained non-aqueous $k_{p,v}$ and the reported literature mycotoxin concentrations is considered a typical occupational exposure scenario: $DDE = (k_{p,v} \times [\text{mycotoxin}] \times t_{\text{event}} \times SA \times ED \times EF \times EV) / (BW \times AT)$. In these DDE calculations, the permeability coefficient for the investigated mycotoxins is obtained from our *ex vivo in vitro* transdermal FDC experiment (Table 3), [mycotoxin] is

the mycotoxin occurrence concentration and the event duration (t_{event}) is 8 h/event. The other exposure parameters are pre-defined as follows: a surface area (SA) of 0.08 m² was taken, considering only the hands are contacting fruits/nuts [54], exposure duration (ED) for industrial conditions is assumed to be 25 years, exposure frequency (EF) is supposed to be 250 days/year [53], event frequency (EV) is considered 1 event/day, the body weight (BW) was assumed to be 70 kg [53,55] and averaging times (AT) for non-carcinogenic chemical exposures are equivalent to the ED, *i.e.* 25 year (9125 days), whereas for carcinogenic chemical exposures, this is 70 year (25,550 days) [54]. Finally, the vehicle (matrix or medium) may alter the skin barrier functions as well. This additional effect is both compound and matrix (vehicle) dependent and still difficult to predict, but it is very likely that moderate ethanol concentrations, as well as waxes, will affect the skin [56-60].

Table 2: Occurrence data giving real concentrations of BEA and ENNs found in fruits/nuts (mean, mg/kg), obtained from Tolosa *et al.* [32].

Fruit/nut	ENN A	ENN A1	ENN B	ENN B1	BEA
Peanuts shell	7.972	0.523	14.61	_(¹)	_(¹)
Almonds shell	0.09	_(¹)	_(¹)	_(¹)	_(¹)
Pistachios shell	0.326	0.015	0.209	_(¹)	_(¹)
Walnuts shell	0.125	_(¹)	_(¹)	_(¹)	_(¹)
Hazelnuts shell	0.732	_(¹)	0.076	0.417	0.03
Sunflower seeds shell	2.62	0.026	0.047	0.22	_(¹)
Dates	0.666	0.025	0.49	_(¹)	0.006
Dried fruits	0.242	0.011	0.058	0.022	0.007
Median ⁽²⁾	0.4960	0.0250	0.1425	0.2200	0.0070

⁽¹⁾ Not detectable.

⁽²⁾ The median estimator is chosen because it is less influenced by outliers in comparison to the mean.

3. RESULTS

3.1. Human skin kinetics

For the first time, it is shown that the cyclic depsipeptide mycotoxins beauvericin and enniatins permeate the human skin (both intact as well as tape-stripped damaged skin) when applied in 60/40 (V/V) EtOH/H₂O. Only the amount of ENN C/F in the receptor fluid samples was too low to obtain useful cumulative amount versus time curves, but ENN C/F accounts for only 0.4% of the total amount of enniatins in the mixture and was therefore not taken into account. All other cyclic depsipeptide mycotoxins confirmed the unidirectional steady-state principle. After 24 hours, only 0.007 – 0.030% (intact skin) and 0.021 – 0.119% (damaged skin) of the dose applied, was cumulatively found in the receptor chamber. Figure 1 shows their mean cumulative amount (ng) versus time (h) plots for both intact, as well as stripped skin.

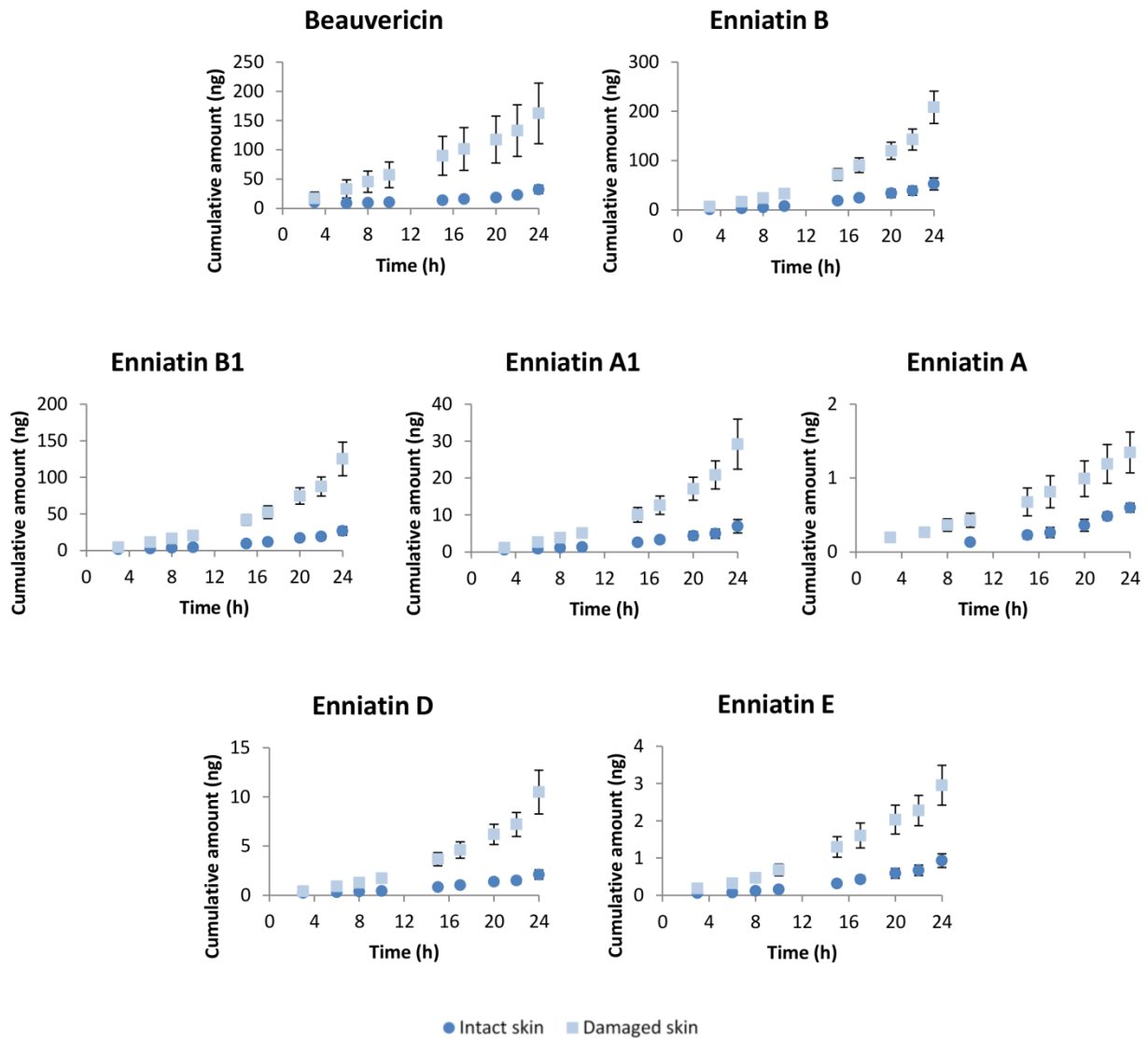


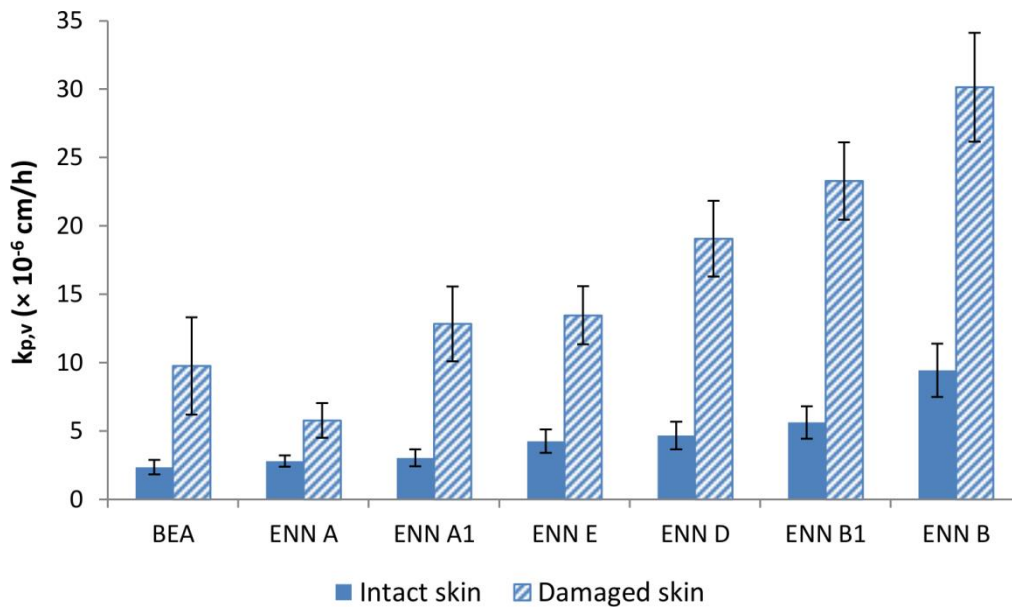
Figure 1: Individual cumulative amount (ng) versus time (h) curves of the investigated mycotoxins for both intact and damaged skin (mean \pm SEM, n = 3-11).

Linear regression of the individual curves was performed for each compound, in order to calculate the transdermal parameters, which are presented in Table 3. The steady-state apparent permeability ($k_{p,v}$) coefficients of the individual cyclic depsipeptide mycotoxins, ranked according to their log P values (BEA > ENN A > ENN A1 \sim ENN E > ENN B1 \sim ENN D > ENN B), are visualized in Figure 2 for both intact, as well as damaged skin.

Table 3: Transdermal parameters for cyclic depsipeptide mycotoxins obtained for intact and damaged skin after applying a 1 mg/mL 60/40 (V/V) EtOH/H₂O dose solution for 24h (mean ± SEM, n = 3 – 11).

Mycotoxin	J_{ss} (ng/(cm ² × h))		Q_{1d} (%)	
	Intact skin	Damaged skin	Intact skin	Damaged skin
BEA	2.65 ± 0.59	10.98 ± 4.00	0.007 ± 0.002	0.036 ± 0.011
ENN B	4.13 ± 0.85	13.18 ± 1.74	0.030 ± 0.007	0.119 ± 0.019
ENN B1	2.12 ± 0.45	8.78 ± 1.07	0.018 ± 0.004	0.084 ± 0.014
ENN A	0.050 ± 0.008	0.104 ± 0.023	0.008 ± 0.001	0.021 ± 0.004
ENN A1	0.44 ± 0.09	1.88 ± 0.40	0.010 ± 0.002	0.042 ± 0.008
ENN D	1.64 ± 0.36	6.68 ± 0.97	0.015 ± 0.003	0.075 ± 0.014
ENN E	0.073 ± 0.015	0.230 ± 0.036	0.014 ± 0.003	0.045 ± 0.007

Mycotoxin	Lag time (h)		$k_{p,v}$ (× 10 ⁻⁶ cm/h)	
	Intact skin	Damaged skin	Intact skin	Damaged skin
BEA	8.4 ± 0.7	2.0 ± 0.7	2.35 ± 0.52	9.76 ± 3.56
ENN B	8.5 ± 0.7	6.2 ± 0.6	9.44 ± 1.94	30.15 ± 3.99
ENN B1	8.0 ± 0.8	7.4 ± 0.7	5.62 ± 1.19	23.29 ± 2.83
ENN A	9.0 ± 1.1	4.9 ± 1.1	2.80 ± 0.42	5.78 ± 1.27
ENN A1	7.5 ± 0.7	7.0 ± 0.9	3.03 ± 0.63	12.83 ± 2.73
ENN D	7.3 ± 0.5	6.1 ± 0.5	4.67 ± 1.02	19.07 ± 0.28
ENN E	7.8 ± 1.0	6.5 ± 0.7	4.26 ± 0.86	13.46 ± 2.12

**Figure 2:** Mean permeability coefficient $k_{p,v}$ (10⁻⁶ × cm/h) of the different mycotoxins for both intact and damaged skin (mean ± SEM, n = 3-11).

Analysis of the skin, *i.e.* epidermis and dermis, after 24 hours resulted in dermis concentrations ranging from 0.10 – 2.65 µg/mL and 0.25 – 6.09 µg/mL for enniatins in intact and damaged skin, respectively. For beauvericin this is 13.00 µg/mL in intact and 25.86 µg/mL in damaged skin. The epidermal concentration of beauvericin was on average 302.32 µg/mL, while for enniatins this ranged from 3.87 µg/mL to 98.91 µg/mL. The individual skin concentrations for each compound, after application of the aforementioned dose solutions (Table 1), are given in Table 4. Normalised skin concentrations, to estimate the skin concentrations after application of 1 mg/mL of each cyclic depsipeptide mycotoxin, are presented in Figure 3.

Table 4: Experimentally determined concentrations of BEA and ENNs in different skin compartments (dermis and epidermis) after 24h (mean \pm SEM, n = 11 – 12).

Mycotoxin	Conc. applied DS (mg/mL) ⁽¹⁾	Dermis ($\mu\text{g/mL}$)		Epidermis ($\mu\text{g/mL}$)		$C_{\text{epidermis}}/C_{\text{vehiculum}}$		$C_{\text{dermis}}/C_{\text{epidermis}}$	
		Intact skin	Damaged skin	Intact skin	Damaged skin	Intact skin	Damaged skin	Intact skin	Damaged skin
BEA	1.13	13.00 \pm 1.85	25.86 \pm 4.72	275.64 \pm 23.59	329.00 \pm 27.04	0.245	0.293	0.047	0.079
ENN B	0.44	2.46 \pm 0.38	5.30 \pm 0.73	78.01 \pm 12.13	81.86 \pm 11.09	0.178	0.187	0.032	0.065
ENN B1	0.38	2.65 \pm 0.44	6.09 \pm 0.83	94.85 \pm 13.94	102.97 \pm 15.72	0.252	0.273	0.028	0.059
ENN A1	0.15	1.16 \pm 0.21	2.85 \pm 0.39	46.29 \pm 7.37	47.99 \pm 6.34	0.316	0.328	0.025	0.059
ENN A	1.80 $\times 10^{-2}$	0.15 \pm 0.03	0.40 \pm 0.05	7.08 \pm 1.20	8.07 \pm 1.08	0.394	0.450	0.022	0.050
ENN D	3.50 $\times 10^{-2}$	0.16 \pm 0.03	0.40 \pm 0.07	6.15 \pm 0.86	5.52 \pm 0.70	0.176	0.158	0.027	0.073
ENN E	1.71 $\times 10^{-2}$	0.10 \pm 0.02	0.25 \pm 0.05	3.96 \pm 0.63	3.78 \pm 0.50	0.232	0.222	0.025	0.067

(1) Experimentally determined; DS = dose solution.

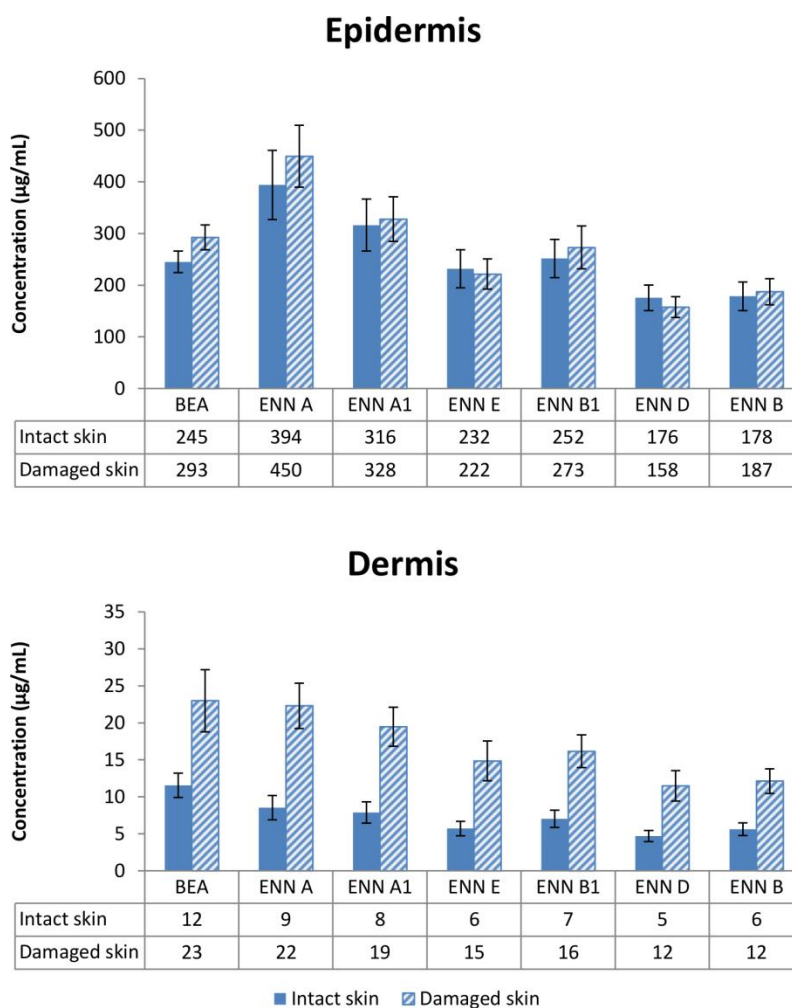


Figure 3: Normalised (to 1 mg/mL applied for each mycotoxin) concentration ($\mu\text{g/mL}$) of BEA and ENNs in the skin layers dermis and epidermis, for both intact and damaged skin after 24 h (mean \pm SEM, $n = 11-12$).

3.2. Solubility of BEA and ENNs

For BEA, average solubility values of 0.082, 0.069 and 7.151 mg/mL were obtained for respectively H_2O , 30/70 (V/V) EtOH/ H_2O and 60/40 (V/V) EtOH/ H_2O . For the enniatin mixture, the relative distribution of the different enniatins in the supernatans is calculated for each solvent, as well as for an analytical standard solution where the ENN mixture was completely dissolved, thus reflecting the relative composition (%) of the mixture. From the results it is concluded that there is no relevant difference in relative distribution between water as solvent compared to an analytical standard solution, and the EtOH/ H_2O mixtures in between the previous extremes confirm this. The fact that overall the same distribution proportions were found, indicated that the different enniatins have no relevant different solubility behaviour in our experimental set-up. Moreover, since we are working with a mixture and the structurally closely-related enniatins will influence each other's solubility, the true solubility of an enniatin (*i.e.* if it were a pure compound) approximately equals the solubility of

the enniatin complex. Although small solubility differences between the different enniatins may be expected from a theoretical point of view, these are thus negligibly small for our purposes. The average determined solubility concentrations for the enniatin mixture was 0.294 mg/mL in H₂O, 0.847 mg/mL in 30/70 (V/V) EtOH/H₂O and 36.918 mg/mL in 60/40 (V/V) EtOH/H₂O.

3.3. Risk assessment after dermal exposure

The obtained J_{\max} values for BEA and ENNs were also compared to the experimental values for some compounds from the EDETOX database determined by Guy [61] and are found to be in the range of estradiol and testosterone (Figure 4).

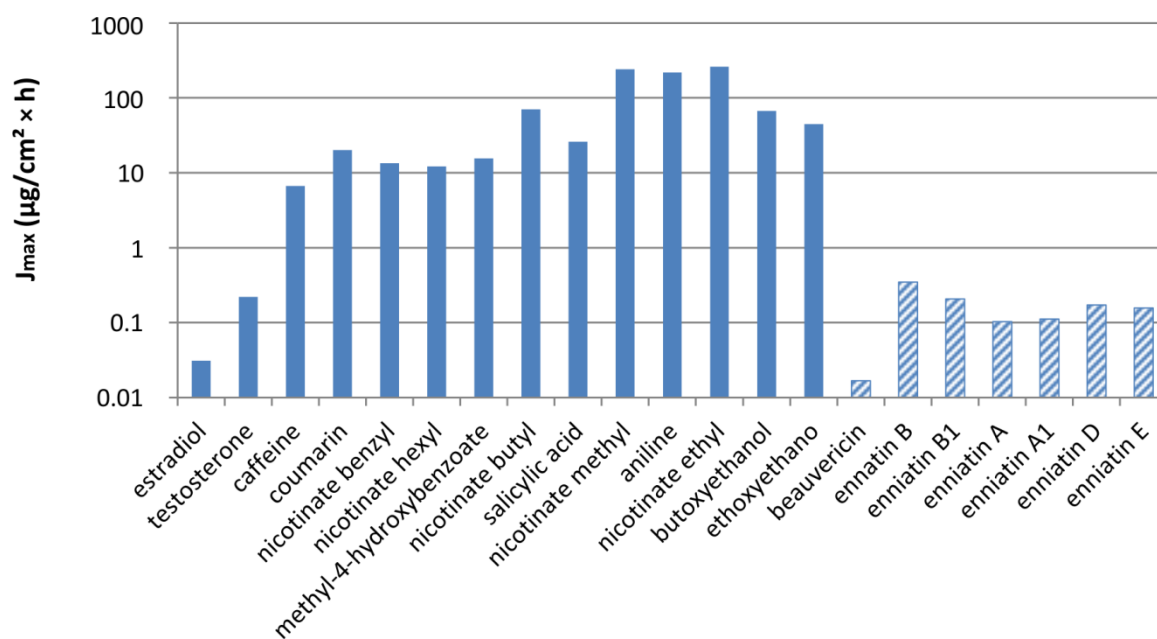


Figure 4: Comparison of calculated J_{\max} values ($\mu\text{g}/(\text{cm}^2 \times \text{h})$) for BEA and ENNs with the data obtained from Guy [61].

By calculating the dermal daily exposure, a first step was taken towards the exposure assessment of the cyclic depsipeptide mycotoxins BEA and ENNs. DDE_{\max} values were calculated as worst-case scenario, while on the other hand, DDE 's for a typical occupational scenario were calculated based on real-life mycotoxin concentrations for the industrial exposure of food related workers (Table 5). Due to a lack of appropriate data, other plausible scenarios were not yet explored, *e.g.* exposure of industrial workers to contaminated grain dust and residential exposure to mycotoxin-containing dust of moldy, water-damaged houses. Moreover, the absence of exposure data does not mean that the potential risk does not exist [33].

Table 5: Estimate of dermal daily exposure⁽¹⁾: genotoxic – non-genotoxic⁽²⁾.

DDE_{max}: worst-case scenario	BEA	ENN A	ENN A1	ENN B	ENN B1	ENN D	ENN E
Intact skin	0.376 – 1.05	2.31 – 6.47	2.50 – 7.01	7.79 – 21.8	4.64 – 13.0	3.86 – 10.8	3.52 – 9.85
Damaged skin	1.56 – 4.37	4.77 – 13.4	10.6 – 29.7	24.9 – 69.7	19.2 – 53.8	15.7 – 44.1	11.1 – 31.1
DDE: occupational scenario	BEA	ENN A	ENN A1	ENN B	ENN B1	ENN D	ENN E
Intact skin	0.368 – 1.03	31.1 – 87.0	1.69 – 4.74	30.1 – 84.2	27.7 – 77.4	_(3)	_(3)
Damaged skin	1.53 – 4.28	64.1 – 180	7.17 – 20.1	96.1 – 269	115 – 321	_(3)	_(3)

(1) DDE_{max} is expressed as $\mu\text{g}/(\text{kg BW} \times \text{day})$, while DDE is expressed as $(\mu\text{g} \times 10^{-6})/(\text{kg BW} \times \text{day})$.

(2) All exposure parameters are identical, except for the averaging time, which is 25 years versus 70 years for non-carcinogenic and carcinogenic chemical industrial exposures, respectively.

(3) For ENN D and ENN E no real-life exposure data was available (Table 2).

4. DISCUSSION

The skin is not only a protective barrier against many influences, it is also a popular target in therapeutic drug delivery, in which the stratum corneum is reputed to be the major barrier [62], thereby hindering the transdermal permeation of large molecules such as peptides, proteins and DNA. However, in the cosmetic field, peptides, *e.g.* derived from collagens and melanotropin, have been topically applied with functional claims [63,64]. Moreover, toxins, viruses and recombinant proteins have also been successfully delivered for skin immunisation purposes [65]. Most promising are cell penetrating peptides [66], such as SPACE-peptide [67,68] and Tat-peptide [69-73], which are not only able to cross the skin barrier, but allow transportation of a cargo as well. More specific for cyclic depsipeptides, it was found that romidepsin enhanced *in vitro* transfection of DNA complexes in Raji cells, indicating this compound can pass cellular membranes and therefore might also be able to cross the skin barrier [74]. Two cyclic lipodepsipeptides (fengycin and surfactin) increased acyclovir accumulation in the epidermis, most likely due to a combined interaction of the lipopeptides with the stratum corneum lipids on one side and acyclovir on the other [75].

In this study, quantitative transdermal parameters of the cyclic depsipeptide mycotoxins beauvericin and enniatins were obtained using human skin. Currently, the dermal route for these mycotoxins has not yet been explored. However, such quantitative information is important, not only within the context of risk assessment of these emerging mycotoxins, but also with respect to the development of topically applied new drugs with a similar cyclic depsipeptide structure, treating *e.g.* dermatological diseases like eczema, psoriasis and skin cancers or having systematic functions after transdermal permeation.

4.1. Permeability kinetics and the effect of skin damage

Since the outer most layer of the skin, the stratum corneum, serves as an important protective barrier, it is not surprising that superficial skin damage can influence transdermal kinetics. This effect was evaluated for the cyclic depsipeptide mycotoxins beauvericin and enniatins by comparing their intact and tape-stripped skin kinetics. Upon comparison of the $k_{p,v}$, J_{ss} and Q_{1d} of both damaged and intact skin for each compound separately, a significant 2 to 5 times increase for damaged skin was observed ($p < 0.10$ for BEA and $p < 0.05$ for ENNs) (Figure 2 and Table 3). This enhanced permeability was also confirmed by the increased dermis concentrations found at the end of the experiment (after 24h): a significant difference was observed between stripped and intact skin ($p < 0.05$), *i.e.* the concentration in the dermis after tape-stripping was increased by an overall mean factor of 2.4, which is in accordance with the increased $k_{p,v}$, Q_{1d} and flux (J_{ss}) values (Table S1, Supplementary information). While comparing the epidermis concentration of each compound after 24 hours, it was found that for tape-stripped skin this concentration was marginally higher than the concentration found in the epidermis of intact skin, however, this was not significant ($p > 0.15$). The K_{epi} ($C_{epidermis}/C_{vehicle}$) was also compared for all investigated compounds and the ratios $K_{epi,stripped}/K_{epi,intact}$ were indeed approximating 1 (Table S1, Supplementary Information).

Furthermore, an inverse relationship between $\log P$ and both $k_{p,v}$ values (intact and tape-stripped) was observed. Indeed, ENN B, with the lowest $\log P$ of 4.68 showed the highest permeability coefficients, whereas BEA and ENN A, having a $\log P$ of 7.13 and 5.87, respectively, had the lowest $k_{p,v}$'s. A significant difference in lag time was observed for BEA, ENNs A, D and B between damaged and intact skin ($p < 0.10$): for these ENNs the extrapolated lag time was approximately 1.5 times longer for intact skin, while for BEA this was 4.2 times (Table 3). This was not the case for the other ENNs A1, E and B1 (the obtained lag time for tape-stripped skin was similar to the lag time for intact skin, for each compound individually, $p > 0.33$). This effect could be linked to a difference in $\log P$: compounds with either a higher (BEA, ENN A) or lower (ENNs D, B) $\log P$ experience a significant effect on their lag time compared to compounds with a mid-range $\log P$ (ENNs A1, E, B1). This can be explained by the fact that for lipophilic cyclic depsipeptides the SC acts as skin reservoir, while more hydrophilic compounds do not diffuse as readily through the lipid layers of the SC. However, $\log P$ is probably not the only descriptor influencing these observed skin kinetics and concentrations, as binding to high amount of proteins present in the dermis, like collagen, is also possible [33].

For ENNs it is also noticed that, while the J_{ss} values are in line with the composition, differences between the ENNs are more explicitly reflected in the $k_{p,v}$ values: although they are all in the same order of magnitude, the relatively small differences observed are due to the different skin permeation characteristics of the ENNs.

4.2. Comparison with *in silico* permeability coefficients

Most current models, including Potts-Guy and variants, are derived from and thus strictly speaking only applicable to aqueous solutions. Therefore, we have used our experimentally determined solubility data to calculate aqueous $k_{p,w}$ values for BEA and ENNs, neglecting the possible skin-barrier-modulating properties of ethanol: $k_{p,w} = k_{p,v} \times (S_v/S_w)$, where $k_{p,v}$ is the experimentally obtained permeability coefficient of the compound in the vehicle (*i.e.* dose solution: 60/40 (V/V) EtOH/H₂O) and S_v and S_w are the saturated concentration in the vehicle and in water, respectively [76]. These are compared to the *in silico* predicted aqueous $k_{p,w}$'s determined using the Potts-Guy and Baert *et al.* models (Table 6) [50,77,78]. The predicted values from the Potts-Guy model are thus a very good approximation of the experimentally obtained $k_{p,w}$'s for these compounds, as the ratios of experimental to predicted values fall within 0.2 – 2.5, whereas in general the MLR1 model obtained from Baert *et al.* is less applicable to these compounds with ratios between 0.1 and 0.18.

Table 6: Comparison of the calculated $k_{p,w}$ values, with predicted $k_{p,w}$'s determined using *in silico* transdermal permeability models.

Mycotoxin	$k_{p,w}$ (cm/h) ⁽¹⁾	Potts-Guy $k_{p,w}$ (cm/h) ⁽²⁾	Baert <i>et al.</i> $k_{p,w}$ (cm/h) ⁽³⁾
BEA	2.06×10^{-4}	– ⁽⁴⁾	2.57×10^{-3}
ENN B	1.19×10^{-3}	4.74×10^{-4}	6.68×10^{-3}
ENN B1	7.06×10^{-4}	7.49×10^{-4}	7.97×10^{-3}
ENN A	3.52×10^{-4}	1.84×10^{-3}	4.07×10^{-2}
ENN A1	3.81×10^{-4}	1.18×10^{-3}	1.53×10^{-2}
ENN D	5.87×10^{-4}	6.68×10^{-4}	5.85×10^{-2}
ENN E	5.35×10^{-4}	1.04×10^{-3}	8.92×10^{-3}

(1) $k_{p,w} = k_{p,v} \times (S_v/S_w)$.

(2) $\log k_p = -6.3 + 0.71 \times \log P - 0.0061 \times MW$ [50,78].

(3) $\log k_p = -8.01 + 0.406 \times ALOGP + 0.606 \times Mor13v + 0.513 \times Jhetv - 1.40 \times Mor26v + 0.971 \times P2v - 0.0703 \times Mor11m - 0.484 \times MATS2e + 0.0809 \times Mor09u - 0.107 \times GATS4e$ [77].

(4) Log P is considered out of range.

4.3. Local skin concentrations and effects

Considering the amount applied on the skin is different for each individual mycotoxin (*i.e.* 1 mg/mL BEA versus 1 mg/mL total enniatins mixture), skin concentrations cannot be directly compared. Therefore the experimentally obtained skin concentrations were transformed through linear normalisation to represent skin concentrations after application of 1 mg/mL of each cyclic depsipeptide mycotoxin at 24 hours (Figure 3). From this, it was observed that the more lipophilic compounds (BEA, ENN A and ENN A1) resulted in higher dermis and epidermis skin concentrations in comparison to the less lipophilic. Also, for all cyclic depsipeptide mycotoxins, the obtained epidermis concentrations were 21 to 46 times higher than the dermis concentrations for intact skin, which can be partly attributed to the reservoir function of the protective stratum corneum barrier. This was only 13 to 20 times for stripped skin, which is due to the partial removal of the stratum corneum by

tape-stripping. For other mycotoxins, *i.e.* aflatoxin B1, ochratoxin A and T-2 toxin, such skin reservoir effects have also been observed and were ascribed to the higher log P of these compounds, suggesting a higher affinity and distribution for the upper skin layer *i.e.* the SC [33,79,80]. This is also in accordance with the obtained $k_{p,v}$ values, which are lower for more lipophilic compounds, and are thus at least partly due to these compounds being trapped in the skin.

The skin is an immunologically highly developed organ, containing Langerhans and T cells in the epidermis and macrophages, various dendritic cell and T cell subsets in the dermis [81,82]. This is important as it was shown that, besides their well-known cytotoxic properties [16,83-86], the cyclic depsipeptide mycotoxins ENNs and BEA also exert effects on the immune system in general. So have Gammelsrud *et al.* shown that ENN B en BEA influenced the expression of various co-stimulatory molecules [87], indicating that ENN B as well as BEA, could disturb dendritic cell migration and interfere with the macrophage differentiation process, inhibit the initiation of a specific immune response, modulate cytokine secretion and change the orientation of an immune response [83,88]. Moreover, Wu and co-workers have demonstrated that BEA decreased serum levels of TNF- α and IFN- γ in mice with experimental colitis and suppressed T-cell proliferation and activation, leading to apoptosis of activated T cells and making beauvericin a novel drug candidate for the treatment of colonic inflammation, such as Crohn's disease [89]. Immunological skin cells can thus be considered as possible targets for these cyclic depsipeptides. Our results showed that application of 1 mg/mL after 24h resulted in dermis concentrations up to 12.53 μ M for intact and 32.70 μ M for damaged skin, while for the epidermis this was 577.70 μ M and 659.96 μ M, respectively (ENN A). Moreover, instead of 1 mg/mL concentrations, which are high, real-life found concentrations are considered, namely up to 0.5 μ g/mL (Table 2). Assuming a linear relation, an epidermis concentration of 0.33 μ M and dermis concentrations of 0.016 μ M are calculated for real-life situations. Ficheux *et al.* noticed a decrease in macrophage and dendritic cell viability already starting from 0.1 μ M ENN B or BEA. Furthermore, effects on the dendritic cells maturation and monocytes differentiation process were seen at similar concentrations from 0.3 μ M BEA and 0.5 μ M ENN B [83], which are considered to be in the same order of magnitude as our extrapolated results. Persons both chronically and occasionally exposed to the investigated mycotoxins have to consider local skin effects, such as epidermal apoptosis and immunological disorders.

4.4. Risk assessment of mycotoxins after dermal exposure

A European Food Safety Authority (EFSA) request has been made on the risks to human and animal health related to beauvericin and enniatins in food and feed, which should address (in short): their co-occurrence with other *Fusarium* toxins, exposure of the EU population to these mycotoxins, evaluation of their toxicity and the determination of the daily exposure levels [90].

In order to investigate the safety concern of these mycotoxins after dermal exposure, the calculated human DDE's (Table 4) should be compared with risk assessment threshold limits, such as the negligible cancer risk intake (NCRI), no observed adverse effect level (NOAEL), lowest observed adverse effect level (LOAEL), benchmark dose (BMD) and tolerable daily intake (TDI). Only a few fragmentary *in vivo* toxicity studies have been reported concerning beauvericin and enniatins. The first ones date back to 1950, 1988 and 1989 and concern only the enniatins. These report that oral dosing of 0.5 – 1 mg/kg BW over 6 days in mice and single doses up to 50 mg/kg BW in rats did not produce toxic effects [91,92], that there is no transdermal lethality at 40 mg/kg for the subcutaneous route in guinea pig. A LD₅₀ of 20.6 mg/kg (early deaths in 2 – 10 minutes and later deaths at 1 – 4 days) by the intraperitoneal route in mice was also reported [93]. More recent studies are performed by McKee *et al.* [3] and Devreese *et al.* [94]. The former administered 1.25, 2.5, 5, 10, 20 and 40 mg/kg enniatin mixture (ENNs A1, B and B1) to mice at 8h intervals by means of intraperitoneal injection. They reported that the top three doses (10, 20 and 40 mg/kg) were toxic to the mice, with fatal outcome occurring between days 2 – 3 for the 40 mg/kg dose and between days 4 – 5 for both the 10 and 20 mg/kg dose [3]. The most recent study was a pilot toxicokinetic study focusing on enniatin B1 in pigs [94], without evaluation of toxicological end-points. Considering the very limited available data, only a first approximation of the risk assessment of beauvericin and enniatins after dermal exposure could be made, based upon various assumptions. From the limited data of McKee *et al.* [3], the NOAEL is fixed at 5 mg/kg BW. From this, the TDI can be estimated by dividing the NOAEL by some safety or uncertainty factors, generally applied to reflect limitations of the data used. A factor of 1000 (10 × 10 × 10) seems appropriate here, to account for (i) possible differences in responsiveness between humans and animals, (ii) variation in susceptibility among individuals in the population and (iii) for data bases which are less complete [95]. Therefore, the estimated TDI for enniatins is 5 µg/(kg BW × day). The non-genotoxic DDE_{max} for both intact and damaged skin exceeds this TDI for all ENNs, but this is worst-case scenario (J_{max}). DDE values for a more typical real-life situation are found to be much lower than the TDI. As these exposure data are only an estimation, they should, however, be interpreted with caution. Based on this approach and the limited available data used, industrial food related workers are potentially at risk to the cyclic depsipeptide mycotoxins beauvericin and enniatins after dermal exposure in the worst-case scenario, however in a typical real-life occupational scenario this is not the case. The latter is corroborated by the fact that, despite its proven cytotoxic effects, a mixture of enniatins has already been developed and is marketed as a pharmaceutical drug (fusafungine being its international non-proprietary name) for the treatment of local infections and inflammatory conditions of the nose and throat. Giving 500 µg per dose [96], this amounts to approximately 7 µg/(kg BW × day), assuming an average BW of 70 kg

[55], which is very similar to our derived TDI of $5 \mu\text{g}/(\text{kg BW} \times \text{day})$. However, more (reliable) *in vivo* toxicity data, leading to a proper hazard characterisation are still urgently needed.

5. CONCLUSIONS

Quantitative skin permeability data of the emerging cyclic depsipeptide mycotoxins beauvericin and enniatins were obtained by an *ex vivo in vitro* FDC approach, using dermatomed split-thickness intact human skin, as well as human skin with an impaired barrier. Using literature-based mycotoxin concentrations, dermal contact surface, exposure time and apparent $k_{p,v}$'s obtained in this study, the daily dermal exposure (DDE) was estimated for the industrial exposure of food related workers to contaminated fruits/nuts as a first approximation. Besides this typical occupational exposure scenario, J_{max} values calculated from experimentally determined $k_{p,v}$ and solubility values, were used to determine the DDE_{max} in a worst-case scenario as well. A TDI for enniatins of $5 \mu\text{g}/(\text{kg BW} \times \text{day})$ was estimated from available literature data and compared with our DDE and DDE_{max} values.

6. REFERENCES

- [1] Gäumann E, Naef-Roth S, Etlinger L, Plattner PA, Nager U. Enniatin, ein neues gegen mykobakterien wirksames antibiotikum. *Fusaria Experimentia* 1947; 3: 202-203.
- [2] Lin YC, Wang J, Wu XY, Zhou SN, Vrijmoed LLP, Jones EBG. A novel compound enniatin G from the mangrove fungus *Halosarpheia* sp. (strain 732) from the south China sea. *Aust J Chem* 2002; 55: 225-227.
- [3] McKee TC, Bokesch HR, McCormick JL, Rashid MA, Spielvogel D, Gustafson KR, Alavanja MM, Cardelline JH 2nd, Boyd MR. Isolation and characterization of new anti-HIV and cytotoxic leads from plants, marine and microbial origins. *J Nat Prod* 1997; 60: 431-438.
- [4] Nilanonta C, Isaka M, Chanphen R, Thong-Orn N, Tanticharoen M, Thebtaranonth Y. Unusual enniatins produced by the insect pathogenic fungus *Verticillium hemipterigenum*: isolation and studies on precursor-directed biosynthesis. *Tetrahedron* 2003; 59: 1015-1020.
- [5] Supothina S, Isaka M, Kirtikara K, Tanticharoen M, Thebtaranonth Y. Enniatin production by the entomopathogenic fungus *Verticillium hemipterigenum* BCC 1449. *J Antibiot* 2004; 57: 732-738.
- [6] Hamill RL, Higgins CE, Boaz HE, Gorman M. The structure of beauvericin, a new depsipeptide antibiotic toxic to *Artemia salina*. *Tetrahedron Lett* 1969; 49: 4255-4258.
- [7] Wang Q, Xu L. Beauvericin, a bioactive compound produced by fungi: a short review. *Molecules* 2012; 17: 2367-2377.
- [8] Andjelic CD, Planelles V, Barrows LR. Characterizing the Anti-HIV activity of papuamide A. *Mar Drugs* 2008; 6: 528-529.
- [9] Lemmens-Gruber R, Kamyar MR, Dornetshuber R. Cyclodepsipeptides - Potential drugs and lead compounds in the drug development process. *Curr Med Chem* 2009; 16: 1122-1137.
- [10] VanderMolen KM, McCulloh W, Pearce CJ, Oberlies NH. Romidepsin (Istodax, NSC 630176, FR901228, FK228, depsipeptide): a natural product recently approved for cutaneous T-cell lymphoma. *J Antibiot* 2011; 64: 525-531.
- [11] Dornetshuber R, Heffeter P, Kamyar MR, Peterbauer T, Berger W, Lemmens-Gruber R. Enniatin exerts p53-dependent cytostatic and p53-independent cytotoxic activities against human cancer cells. *Chem Res Toxicol* 2007; 20: 465-473.
- [12] Jestoi M. Emerging *Fusarium*-mycotoxins fusaproliferin, beauvericin, enniatins, and moniliformin - A review. *Crit Rev Food Sci Nutr* 2008; 48: 21-49.
- [13] Tomoda H, Nishida H, Huang XH, Masuma R, Kim YK, Omura S. New cyclodepsipeptides, enniatin-D, enniatin-E and enniatin-F produced by *Fusarium* sp. FO-1305. *J Antibiot* 1992; 45: 1207-1215.
- [14] Celik M, Aksoy H, Yilmaz S. Evaluation of beauvericin genotoxicity with the chromosomal aberrations, sister-chromatid exchanges and micronucleus assays. *Ecotox Environ Safety* 2010; 73: 1553-1557.

- [15] Ivanova L, Skjerve E, Eriksen GS, Uhlig S. Cytotoxicity of enniatins A, A1, B, B1, B2 and B3 from *Fusarium avenaceum*. *Toxicon* 2006; 47: 868-876.
- [16] Lee HS, Song HH, Jeong JH, Shin CG, Choi SU, Lee C. Cytotoxicities of enniatins H, I, and MK1688 from *Fusarium oxysporum* KFCC11363P. *Toxicon* 2008; 51: 1178-1185.
- [17] Macchia L, Di Paola R, Fornelli F, Nenna S, Moretti A, Napoletano R, Logrieco A, Caiaffa MF, Tursil MF, Bottalico A. Cytotoxicity of beauvericin to mammalian cells. Abstracts of the International Seminar on *Fusarium*, Martina Franca, Italy, 1995, 72-73.
- [18] Meca G, Font G, Ruiz MJ. Comparative cytotoxicity study of enniatins A, A(1), A(2), B, B-1, B-4 and J(3) on Caco-2 cells, Hep-G(2) and HT-29. *Food Chem Toxicol* 2011; 49: 2464-2469.
- [19] Nilanonta C, Isaka M, Kittakoop P, Trakulnaleamsai S, Tanticharoen M, Thebtaranonth Y. Precursor-directed biosynthesis of beauvericin analogs by the insect pathogenic fungus *Paecilomyces tenuipes* BCC 1614. *Tetrahedron* 2002; 58: 3355-3360.
- [20] Prosperini A, Meca G, Font G, Ruiz MJ. Study of the cytotoxic activity of beauvericin and fusaproliferin and bioavailability *in vitro* on Caco-2 cells. *Food Chem Toxicol* 2012; 50: 2356-2361.
- [21] Watjen W, Debbab A, Hohfeld A, Chovolou Y, Kampkotter A, Edrada RA, Ebel R, Hakiki A, Mosaddak M, Totzke F, Kubbutat MH, Proksch P. Enniatins A1, B and B1 from an endophytic strain of *Fusarium tricinctum* induce apoptotic cell death in H4IIE hepatoma cells accompanied by inhibition of ERK phosphorylation. *Mol Nutr Food Res* 2009; 53: 431-440.
- [22] Zahn JX, Burns AM, Liu MPX, Faeth SH, Gunatilaka AAL. Search for cell motility and angiogenesis inhibitors with potential anticancer activity: beauvericin and other constituents. *J Nat Prod* 2007; 70: 227-232.
- [23] Klaric MS, Darabos D, Rozgaj R, Kasuba V, Pepeljnjak S. Beauvericin and ochratoxin A genotoxicity evaluated using the alkaline comet assay: single and combined genotoxic action. *Arch Toxicol* 2010; 84: 641-650.
- [24] Fotso J, Smith JS. Evaluation of beauvericin toxicity with the bacterial bioluminescence assay and the Ames mutagenicity bioassay. *J Food Sci* 2003; 68: 1938-1941.
- [25] Behm C, Degen GH, Follmann W. The *Fusarium* toxin enniatin B exerts no genotoxic activity, but pronounced cytotoxicity *in vitro*. *Mol Nutr Food Res* 2009; 53: 423-430.
- [26] Tonshin AA, Teplova VV, Andersson MA, Salkinoja-Salonen MS. The *Fusarium* mycotoxins enniatins and beauvericin cause mitochondrial dysfunction by affecting the mitochondrial volume regulation, oxidative phosphorylation and ion homeostasis. *Toxicology* 2010; 276: 49-57.
- [27] Jestoi M, Rokka M, Jarvenpaa E, Peltonen K. Determination of *Fusarium* mycotoxins beauvericin and enniatins (A, A1, B, B1) in eggs of laying hens using liquid chromatography-tandem mass spectrometry (LC-MS/MS). *Food Chemistry* 2009; 115: 1120-1127.
- [28] Malachova A, Dzuman Z, Veprikova Z, Vaclavikova M, Zachariasova M, Hajslova J. Deoxynivalenol, deoxynivalenol-3-glucoside, and enniatins: the major mycotoxins found in cereal-based products on the Czech market. *J Agr Food Chem* 2011; 59: 12990-12997.

- [29] Santini A, Meca G, Uhlig S, Ritieni A. Fusaproliferin, beauvericin and enniatins: occurrence in food - a review. *World Mycotoxin J* 2012; 5: 71-81.
- [30] Sebastia N, Meca G, Soriano JM, Manes J. Presence of *Fusarium* emerging mycotoxins in tiger-nuts commercialized in Spain. *Food Control* 2012; 25: 631-635.
- [31] Serrano AB, Font G, Ruiz MJ, Ferrer E. Co-occurrence and risk assessment of mycotoxins in food and diet from Mediterranean area. *Food Chemistry* 2012; 135: 423-429.
- [32] Tolosa J, Font G, Manes F, Ferrer E. Nuts and dried fruits: natural occurrence of emerging *Fusarium* mycotoxins, *Food Control* 2013; 33: 215-220.
- [33] Boonen J, Malysheva SV, Taevernier L, Di Mavungu JD, De Saeger S, De Spiegeleer B. Human skin penetration of selected model mycotoxins. *Toxicology* 2012; 301: 21-32.
- [34] Hintikka EL, Holopainen R, Asola A, Jestoi M, Peitzsch M, Kalso S, Larsson L, Reijula K, Tuomi, T. Mycotoxins in the ventilation systems of four schools in Finland. *World Mycotoxin J* 2009; 2: 369-379.
- [35] Peitzsch M, Sulyok M, Taubel M, Vishwanath V, Krop E, Borrás-Santos A, Hyvärinen A, Nevalainen A, Krska R, Larsson L. Microbial secondary metabolites in school buildings inspected for moisture damage in Finland, The Netherlands and Spain. *J Env Monitoring* 2012; 14: 2044-2053.
- [36] Degen GH. Tools for investigating workplace-related risks from mycotoxin exposure. *World Mycotoxin J* 2011; 4: 315-327.
- [37] Cruz LJ, Lague-Ortega JR, Rivas L, Albericio F. Kahalalide F, an antitumor depsipeptide in clinical trials, and its analogues as effective antileishmanial agents. *Mol Pharmaceutics* 2009; 6: 813-824.
- [38] Chang J, Varghese DS, Gillam MC, Peyton M, Modi B, Schiltz R, Girard L, Martinez ED. Differential response of cancer cells to HDAC inhibitors trichostatin A and depsipeptide. *BJ Cancer* 2012; 106: 116-125.
- [39] US 2007/0060509. Endoparasitocidal compositions for topical application.
- [40] Baert B, Boonen J, Burvenich C, Roche N, Stillaert F, Blondeel P, Van Bocxlaer J, De Spiegeleer B. A new discriminative criterion for the development of Franz diffusion tests for transdermal pharmaceuticals. *J Pharm Pharmaceut Sci* 2010; 13: 218-230.
- [41] Organisation for Economic Co-operation and Development (OECD). Guidance document for the conduct of skin absorption studies. OECD series on testing and assessment, Paris, 2004, pp. 31.
- [42] De Spiegeleer B, Baert B, Vergote V, Van Dorpe S. Development of system suitability tests for *in vitro* skin integrity control: impedance and capacitance. The Eleventh International Perspectives in Percutaneous Penetration Conference, La Grande Motte, France, 2008; 43-43.
- [43] European Centre for Ecotoxicology and Toxicology of Chemicals (ECETOC). Monograph Report No 20 Percutaneous absorption. Brussels, 1993, pp. 90.

- [44] Taevernier L, Veyser L, Vandercruyssen K, D’Hondt M, Vansteelandt S, De Saeger S, De Spiegeleer B. Determination of the cyclic depsipeptide mycotoxins beauvericin and enniatins in in-vitro transdermal experiments. *J Pharm Biomed Anal* 2014; 100: 50-57.
- [45] U.S. Environmental Protection Agency (EPA). Guidelines for exposure assessment, Washington DC, 1992, pp. 139.
- [46] Organisation for Economic Co-operation and Development (OECD). Guidance notes on dermal absorption: Series on testing and assessment (No.156), Paris, 2011, pp. 72.
- [47] Jones AD, Dick IP, Cherrie JW, Cronin MTD, Van De Sandt JJM, Esdaile DJ, Iyengar S, ten Berge W, Wilkinson SC, Roper CS, Semple S, de Heer C, Williams FM. CEFIC workshop on methods to determine dermal penetration for human risk assessment. European Chemical Industry Council, December 2004, pp 88 (Research Report TM/04/07); http://www.iom-world.org/pubs/IOM_TM0407.pdf.
- [48] Magnusson BM, Anissimov YG, Cross SE, Roberts MS. Molecular size as the main determinant of solute maximum flux across skin. *J Invest Dermatol* 2004; 122: 993-999.
- [49] Kroes R, Renwick AG, Feron V, Galli CL, Gibney M, Greim H, Guy RH, Lhuguenot JC, van de Sandt JJ. Application of the threshold of toxicological concern (TTC) to the safety evaluation of cosmetic ingredients. *Food Chem Toxicol* 2007; 45: 2533-2562.
- [50] Mitragotri S, Anissimov YG, Bunge AL, Frasch F, Guy RH, Hadgraft J, Kasting GB, Lane ME, Roberts MS. Mathematical models of skin permeability: An overview. *International Journal of Pharmaceutics* 2011; 418: 115-129.
- [51] Riederer M, Schreiber L. Protecting against water loss: analysis of the barrier properties of plant cuticles. *Journal of Experimental Botany* 2001; 52: 2023-2032.
- [52] EPA. 2004. Risk assessment guidance for superfund volume I: human health evaluation manual – Part E, supplemental guidance for dermal risk assessment. Office of Superfund Remediation and Technology Innovation. U.S. Environmental Protection Agency (EPA), Washington, DC.
- [53] EPA. 2007. Dermal exposure assessment: a summary of EPA approaches. National Center for Environmental Assessment. U.S. Environmental Protection Agency (EPA), Washington, DC.
- [54] USEPA. 1997. Exposure factors handbook. U.S. Environmental Protection Agency (U.S. EPA), Washington, DC.
- [55] CDER. 2005. Guidance for industry estimating the maximum safe starting dose in initial clinical trials for therapeutics in adult healthy volunteers. U.S. Department of Health and Human Services. Food and Drug Administration (FDA). Center for Drug Evaluation and Research (CDER), Rockville, MD.
- [56] Zhang Q, Li P, Roberts MS. Maximum transepidermal flux for similar size phenolic compounds is enhanced by solvent uptake into the skin. *Journal of Controlled Release* 2011; 154: 50-57.
- [57] Zhang Q, Peng L, Liu D, Roberts MS. Effect of vehicles on the maximum transepidermal flux of similar size phenolic compounds. *Pharmaceutical Research* 2013; 30: 32-40.

- [58] Pershing LK, Parry GE, Lambert LD. Disparity of in-vitro and in-vivo oleic acid-enhanced beta-estradiol percutaneous-absorption across human skin. *Pharmaceutical Research* 1993; 10: 1745-1750.
- [59] Pirot F, Kalia YN, Stinchcomb AL, Keatings G, Bunge A. Characterization of the permeability barrier of human skin *in vivo*. *Proc Natl Acad Sci* 1997; 94: 1562-1567.
- [60] Bommannan O, Potts RO, Guy RH. Examination of stratum corneum barrier function *in vivo* by infrared spectroscopy. *The Journal of Investigative Dermatology* 1990; 95: 403-408.
- [61] Guy RH. Predicting the rate and extent of fragrance chemical absorption into and through the skin. *Chem Res Toxicol* 2010; 23: 864-870.
- [62] Nasrollahi SA, Taghibiglou C, Azizi E, Farboud ES. Cell-penetrating peptides as novel transdermal drug delivery system. *Chem Biol Drug Des* 2012; 80: 693-646.
- [63] Chai HJ, Li JH, Huang HN, Li TL, Chan YL, Wu CJ. Effects of sizes and conformation of fish-scale collagen peptides on facial skin qualities and transdermal penetration efficiency. *J Biomed Biotech* 2010; doi:10.1155/2010/757301.
- [64] Dawson BV, Hadley ME, Levine N, Kreutzfeld KL, Don S, Eytan BST, Hruby VJ. *In vitro* transdermal delivery of a melanotropic peptide through human skin. *The Society for Investigative Dermatology* 1990; 94: 432-435.
- [65] Partidos CD, Beignon A-S, Brown F, Kramer E, Briand J-P, Muller S. Applying peptide antigens onto bare skin: induction of humoral and cellular immune responses and potential for vaccination. *J Control Rel* 2002; 85: 27-34.
- [66] Stalmans S, Wynendaele E, Bracke N, Gevaert B, D'Hondt M, Peremans K. Chemical-functional diversity in cell-penetrating peptides. *PLoS ONE* 2013; 8: e71752.
- [67] Chen M, Zakrewsky M, Gupta V, Anselmo AC, Slee DH, Muraski JA, Mitragotri S. Topical delivery of siRNA into skin using SPACE-peptide carriers. *J Control Rel* 2014; 179: 33-41.
- [68] Hsu T, Mitragotri S. Delivery of siRNA and other macromolecules into skin and cells using a peptide enhancer. *PNAS* 2011; 108: 15816-15821.
- [69] Lopes LB, Brophy CM, Furnisch E, Flynn CR, Sparks O, Komalavilas P, Joshi L, Panitch A, Bentley MV. Comparative study of the skin penetration of protein transduction domains and a conjugated peptide. *Pharm Res* 2005; 22: 750-757.
- [70] Manosroi J, Lohcharoenkal W, Gotz F, Werner RG, Manosroi W, Manosroi A. Transdermal absorption and stability enhancement of salmon calcitonin by tat peptide. *Drug Development and Industrial Pharmacy* 2013; 39: 520-525.
- [71] Manosroi J, Khositsuntiwong N, Manosroi W, Gotz F, Werner RG, Manosroi A. Potent enhancement of transdermal absorption and stability of human tyrosinase plasmid by tat peptide and an entrapment in elastic cationic niosomes. *Drug Delivery* 2013; 20: 10-18.
- [72] Patlolla RR, Desai PR, Belay K, Singh MS. Translocation of cell penetrating peptide grafted nanoparticles across skin layers. *Biomaterials* 2010; 31: 5598-5607.

- [73] Uchida T, Kanazawa T, Takashima Y, Okada H. Development of an efficient transdermal delivery system of small interfering RNA using functional peptides, tat and AT-1002. *Chem Pharm Bull* 2011; 59: 196-201.
- [74] Weecharangsan W, Opanasopit P, Lee RJ. Effect of depsipeptide on *in vitro* transfection efficiency of PEI/DNA complexes. *Anticancer Research* 2008; 28: 793-798.
- [75] Nicoli S, Eeman M, Deleu M, Bresciani E, Padula C, Santi P. Effect of lipopeptides and iontophoresis on aciclovir skin delivery, *J Pharm Pharmacol* 2010; 62: 702-708.
- [76] Cleek RL, Bunge AL. A new method for estimating dermal absorption from chemical exposure. 1. General approach. *Pharm Res* 1993; 10: 497-506.
- [77] Baert B, Deconinck E, Van Gele M, Slodicka M, Stoppie P, Bodé S, Slegers G, Vander Heyden Y, Lambert J, Beetens J, De Spiegeleer B. Transdermal penetration behaviour of drugs: CART-clustering, QSPR and selection of model compounds. *Bioorg Med Chem* 2007; 15: 6943-6955.
- [78] Potts RO, Guy RH. Predicting skin permeability. *Pharm Res* 1992; 9: 663-669; <http://www.cdc.gov/niosh/topics/skin/skinpermcalf.html>.
- [79] Bunner BL, Wannemacher RW, Dinterman RE, Broski FH. Cutaneous absorption and decontamination of [H-3] T-2 toxin in the rat model. *J Toxicol Env Health* 1989; 26: 413-423.
- [80] Pang VF, Swanson SP, Beasley VR, Buck WB, Haschek WM. The toxicity of T-2 toxin in swine following topical application. 1. Clinical signs, pathology, and residue concentrations. *Fundam Appl Toxicol* 1987 9: 41-49.
- [81] Heath WR, Carbone, FR. The skin-resident and migratory immune system in steady state and memory: innate lymphocytes, dendritic cells and T cells. *Nature Immunology* 2013; 14: 978-985.
- [82] Nestle FO, Di Meglio P, Qin JZ, Nickoloff BJ. Skin immune sentinels in health and disease. *Nature Reviews Immunology* 2009; 9: 679-691.
- [83] Ficheux AS, Sibiril Y, Parent-Massin D. Effects of beauvericin, enniatin b and moniliformin on human dendritic cells and macrophages: an *in vitro* study. *Toxicon* 2013; 71: 1-10.
- [84] Ivanova L, Egge-Jacobsen MW, Solhaug A, Thoen E, Faeste CK. Lysosomes as a possible target of enniatin B-induced toxicity in Caco-2 cells. *Chem Res Toxicol* 2012; 25: 1662-1674.
- [85] Macchia L, Caiaffa MF, Fornelli F, Calo L, Nenna S, Moretti A, Logrieco A, Tursi A. Apoptosis induced by the Fusarium mycotoxin beauvericin in mammalian cells. *J Appl Genet* 2002; 43: 363-371.
- [86] Ojcius DM, Zychlinsky A, Li MZ, Young JDE. Ionophore-induced apoptosis – Role of DNA fragmentation and calcium fluxes. *Exp Cell Res* 1991; 197: 43-49.
- [87] Gammelsrud A, Solhaug A, Dendele B, Sandberg WJ, Ivanova L, Kocbach Bølling A, Lagadic-Gossmann D, Refsnes M, Becher R, Eriksen G. Enniatin B-induced cell death and inflammatory responses in RAW 267.4 murine macrophages. *Toxicol Appl Pharmacol* 2012; 261: 74-87.
- [88] Schaeuble K, Hauser MA, Rippl AV, Bruderer R, Otero C, Groettrup M, Legler DF. Ubiquitylation of the chemokine receptor CCR7 enables efficient receptor recycling and cell migration. *J Cell Sci* 2012; 125: 4463-4474.

-
- [89] Wu XF, Xu R, Ouyang ZJ, Qian C, Shen Y, Wu WD, Gu YH, Xu Q, Sun Y. 2013. Beauvericin ameliorates experimental colitis by inhibiting activated T cells via downregulation of the PI3K/Akt signaling pathway. *PLoS ONE*. 8:e83013.
- [90] EFSA. question number: EFSA-Q-2010-00999; mandate number: M-2010-0305; <http://registerofquestions.efsa.europa.eu/raw-war/login>.
- [91] Bosch U, Mirocha CJ, Abbas HK, Dimenna M. Toxicity and toxin production by *Fusarium* isolates from New Zealand. *Mycopathologia* 1989; 108: 73-79.
- [92] Gäumann E, Naef-Roth S, Ettlinger L. Zur gewinnung von enniatinen aus dem myzel verschiedener Fusarien. *J Phytopathol* 1950; 16: 289-299.
- [93] Wannemacher RW, Bunner DL, Dinterman RE. Parenteral, dermal, and transdermal toxicity of depsipeptide ionophores, enniatin and valinomycin. *FASEB J* 1988; 2: A1351-A1351
- [94] Devreese M, Broekaert N, De Mil T, Fraeyman S, De Backer P, Croubels S. Pilot toxicokinetic study and absolute oral bioavailability of the *Fusarium* mycotoxin enniatin B1 in pigs. *Food Chem Toxicol* 2014; 63: 161-165.
- [95] IRIS. 1993. Reference Dose (RfD): Description and use in health risk assessment. Integrated Risk Information System (IRIS); <http://www.epa.gov/iris/rfd.htm>.
- [96] Locabiotol®, patient information leaflet.

CHAPTER VI

BLOOD-BRAIN BARRIER TRANSPORT KINETICS OF BEAUVERICIN AND ENNIATINS

“I not only use all the brains that I have, but all I can borrow.”

Woodrow Wilson

(^o1856 - †1924, American president, Nobel Peace Prize winner)

Parts of this chapter were published:

Taevernier L, Wynendaele E, D’Hondt M, De Spiegeleer B. Analytical quality-by-design approach for sample treatment of BSA-containing solutions. *Journal of Pharmaceutical Analysis*. 2015; **5**: 27-32, doi: 10.1016/j.jpha.2014.06.001

Taevernier L, Bracke N, Veryser L, Wynendaele E, Gevaert B, Peremans K, De Spiegeleer, B. Blood-brain barrier transport kinetics of the cyclic depsipeptide mycotoxins beauvericin and enniatins. *Toxicology Letters*. 2016; **258**: 175-184, doi: 10.1016/j.toxlet.2016.06.1741.

ABSTRACT

The cyclic depsipeptide mycotoxins beauvericin and enniatins are capable of reaching the systemic circulation through various routes of exposure and are hence capable of exerting central nervous system (CNS) effects, if they are able to pass the blood-brain barrier (BBB), which was the main objective of this study.

Quantification of the mycotoxins was performed using an in-house developed and verified bio-analytical UHPLC-MS/MS method. Prior to the BBB experiments, the metabolic stability of the mycotoxins was evaluated *in vitro* in mouse serum and brain homogenate. The BBB permeation kinetics of beauvericin and enniatins were studied using an *in vivo* mouse model, applying multiple time regression for studying the blood-to-brain influx. Additionally, capillary depletion was applied to obtain the fraction of the peptides really entering the brain parenchyma and the fraction loosely adhered to the brain capillary wall. Finally, also the brain-to-blood efflux transport kinetics was studied.

Metabolic stability data indicated that the investigated mycotoxins were stable during the duration of the *in vivo* study. The brain influx study showed that beauvericin and enniatins are able to cross the blood-brain barrier in mice: using the Gjedde-Patlak biphasic model, it was shown that all investigated mycotoxins exert a high initial influx rate into the brain (K_1 ranging from 11 to 53 $\mu\text{L}/(\text{g}\times\text{min})$), rapidly reaching a plateau. After penetration, the mycotoxins reached the brain parenchyma (95%) with only a limited amount residing in the capillaries (5%). No statistically significant efflux out of the brain was observed.

CHAPTER VI

BLOOD-BRAIN BARRIER TRANSPORT

KINETICS OF BEAUVERICIN AND ENNIATINS

Main focus in this chapter:

- Quantitative determination of BEA and ENNs BBB transport kinetics in an *in vivo* mouse model:
 - blood-to-brain (multiple time regression influx);
 - brain distribution, *i.e.* parenchyma vs. capillaries (capillary depletion);
 - brain-to-blood (efflux).

1. INTRODUCTION

Cyclic depsipeptides are a large group of nonribosomal peptides from natural origin, synthesised by *i.a.* bacteria, fungi and marine sponges, possessing a wide range of bioactivities [1]. A well-known example is romidepsin, an FDA approved medicine used in the treatment of cutaneous T-cell lymphoma. The cyclic hexadepsipeptides enniatins (ENNs) and beauvericin (BEA) are considered as mycotoxins, posing a potential health hazard [2]. They are non-ionised molecules which are further characterised by their ionophoric and lipophilic properties. Both ENNs and BEA are produced by *i.a.* *Fusarium* fungi, known to frequently infest crops and be the cause of mold in water-damaged houses in milder climate regions such as North America and Western Europe [3]. Indeed, in a recent study ENN B1 was detected in 92% of all investigated feed and feed ingredient samples [4]. Animals and humans may thus come in contact with these mycotoxins through different routes of exposure like inhalation [5] or ingestion of contaminated feed and food [3]. Moreover, it was recently demonstrated that these mycotoxins are capable of reaching systemic circulation after dermal and mucosal exposure as well [2,6]. Besides their well-known antibiotic and insecticidal activities, *in vitro* cytotoxicity and genotoxicity has been evidenced for BEA and ENNs [7-17].

Zhang and colleagues demonstrated in an *in vivo* immunocompromised mouse model that BEA in combination with ketoconazole prolonged survival of the host infected with *Candida parapsilosis* and reduced fungal colony counts in animal organs such as the brains, which could not be achieved with ketoconazole alone [18]. Moreover, Zahn *et al.* determined that BEA was cytotoxic against SF-268

(human CNS cancer glioma) cells with an IC_{50} of 2.29 μ M [17]. Entry of such xenobiotics in the brain is strictly regulated by the blood-brain-barrier (BBB), which is an anatomical defence barrier characterised by extensive tight junctions and energy-dependent efflux transporters. The BBB is important for protecting the central nervous system from toxic substances and serving to maintain brain homeostasis [19,20]. However, it has already been shown that peptides can cross the BBB, either by direct membrane permeation (*i.e.* passive diffusion) or by a saturable, active or facilitated, transport mechanism, or both [21-23]. Moreover, the BBB is an important biological barrier with declining functionality in ageing [24].

Moreover, it was demonstrated *in vitro* by Weidner *et al.* that both T-2 toxin and its main metabolite HT-2 toxin have the ability to enter the brain via the BBB. The same research group also recently investigated the BBB effects of the *Fusarium* mycotoxins deoxynivalenol, 3-acetyldeoxynivalenol, and moniliformin. All were shown to be permeable mycotoxins and possess the ability to reduce BBB integrity. Currently, however, there is no data available about the transport kinetics through the blood-brain barrier of BEA and ENNs, nor about cyclic depsipeptides in general. However, this information is highly wanted within the context of risk assessment, since these mycotoxins might cause local central nervous system (CNS) effects once they pass the BBB. Therefore, it was our objective to quantitatively determine the BBB transport kinetics of BEA and ENNs in an *in vivo* mouse model, encompassing the blood-to-brain (multiple time regression influx) as well as a brain-to-blood (efflux) transport. Moreover, their distribution, *i.e.* the fraction transported into the brain parenchyma and the fraction trapped by the endothelial cells lining the BBB (the capillaries) is also investigated by capillary depletion. Quantification of the mycotoxins is done using an in-house developed bio-analytical UHPLC-MS/MS method.

2. MATERIALS

2.1. Chemicals and reagents

Mycotoxins BEA, ENN B and the enniatin mixture (ENNs) were supplied by Bioaustralis (Smithfield, NSW, Australia). For the latter, no formal ENN composition was supplied by the manufacturer (only e-mail correspondence), therefore the composition was experimentally determined by our group, assuming a relative response factor (RRF) = 1 for the individual constituents: 43.8% ENN B, 34.4% ENN B1, 14.0% ENN A1, 3.6% ENN D, 1.8% ENN A, 1.8% ENN E and 0.4% ENN C or F [1]. Ultrapure water (H_2O) with a quality of 18.2 M Ω .cm was produced by an Arium 611 purification system (Sartorius, Göttingen, Germany). Disodium hydrogen phosphate dihydrate ($Na_2HPO_4 \cdot 2H_2O$) was purchased at VWR (Leuven, Belgium). Potassium chloride (KCl), dimethylsulfoxide (DMSO), sodium chloride (NaCl), calcium dichloride dihydrate ($CaCl_2 \cdot 2H_2O$), sodium lactate, magnesium sulphate

(MgSO₄), hydrated sodium dihydrogen phosphate (NaH₂PO₄·H₂O), Krebs-Henseleit buffer and urethane were purchased from Sigma-Aldrich (Diegem, Belgium), while bovine serum albumin (BSA) was obtained from Merck KGaA (Darmstadt, Germany). Absolute ethanol came from Fisher Scientific (Erembodegem, Belgium). Dextran was obtained from AppliChem GmbH (Darmstadt, Germany). UHPLC-MS grade formic acid (FA), acetonitrile (ACN), trifluoroacetic acid (TFA) and 2-propanol came from Biosolve (Valkenswaard, The Netherlands) and D-glucose, sodium hydroxide (NaOH) and HEPES (N-2-hydroxyethylpiperazine-N-2-ethane sulfonic acid) were purchased at Fluka (Diegem, Belgium). The BBB-positive control dermorphin was obtained from Bachem (Bubendorf, Switzerland). For the radiolabeling, Iodo-Gen® coated tubes were purchased from Thermo Scientific (Erembodegem, Belgium) and the radioactive sodium iodide solution (Na¹²⁵I) from Perkin Elmer (Zaventem, Belgium).

2.1. Animals

Female, Institute for Cancer Research, Caesarean Derived-1 (ICR-CD-1) mice of age 7-10 weeks and weighing 29-32 g, were obtained from Harlan Laboratories (Venray, Netherlands). All animal experiments were performed according to the Ethical Committee principles of laboratory animal welfare and approved by our institute (Ghent University, Faculty of Veterinary Medicine, no. EC2014/128).

3. METHODS

3.1. *In vitro* metabolic stability

The *in vitro* metabolic stability of BEA and ENNs in mouse brain homogenate and mouse serum was evaluated as previously described [25,26]. The protein content of the brain homogenate was determined using the Pierce Modified Lowry Protein Assay method (Thermo Scientific), in order to prepare a stock solution containing a 0.6 mg/mL protein concentration in Krebs-Henseleit buffer (pH 7.4). To 75 µL of a 1 mg/mL peptide solution (BEA, respectively ENN mixture in 2% (V/V) ACN in Krebs-Henseleit buffer pH 7.4), 375 µL of serum/brain homogenate and 300 µL of Krebs-Henseleit buffer pH 7.4 was added. This mixture was incubated at 37 °C while shaking at 750 rpm. After 0, 5, 10, 15 and 60 min, 100 µL aliquots were taken and transferred into LoBind Eppendorf tubes containing 100 µL of 1:99, TFA:H₂O (V/V). Then, the samples were heated at 95 °C for 5 min and subsequently cooled on ice for 30 min. After centrifugation (20 000 g, 5 °C, 30 min) an aliquot of the clear supernatant was taken and analysed using HPLC-UV, as described below. Beside these test samples, control solutions were also prepared and analysed at t = 60 min: ‘placebo’ solutions (without peptide) to exclude matrix inferences, ‘stability’ solutions (peptide without serum/brain homogenate) to correct for chemical degradation and adsorption and ‘inactivated enzyme’ solutions

(heat inactivation prior to peptide addition) to determine if the enzyme inactivation process is able to completely inactivate the enzyme. We previously reported that these peptides are prone to adsorption [1], therefore during the metabolic stability study the necessary precautions were taken to minimise this adsorption phenomena (*i.e.* prior stock solutions were prepared immediately before use and containing at least 50% ACN).

An Acquity UHPLC equipped with a temperature controlled autosampler tray and column oven was used, thermostated at respectively 5 °C and 45 °C (Waters, Milford, MA, USA). Chromatographic separation was achieved on an Acquity UHPLC charged surface hybrid (CSH) C18 column (1.7 µm, 150 mm × 2.1 mm, 130 Å), attached to an Acquity UHPLC VanGuard pre-column (1.7 µm, 5 mm × 2.1 mm, 130 Å), both obtained from Waters. The dwell volume of the system was 525 µL. A gradient mobile phase system consisting of (A) 5:95 ACN:H₂O (V/V) containing 0.1% FA and 0.1% 2-propanol and (B) 95:5 ACN:H₂O (V/V) containing 0.1% FA and 0.1% 2-propanol was used. The gradient profile was as follows: 0-16 min, 65-79% B; 16-16.5 min, 79-100% B; 16.5-18.5 min, 100% B; 18.5-19 min, 100-65% B; 19-22 min, 65% B. The flow rate was set to 0.6 mL/min and 10 µL was injected. As needle wash 10:10:80 DMSO:2-propanol:ACN (V/V/V) was used (for 6 s post-injection). The UHPLC system was coupled to a PDA detector, operated from 190 nm to 300 nm, with quantification at 205 nm (Waters, Milford, MA, USA). For ENN C/F data was below the limit of detection (0.3 µg/mL) and therefore not taken into account.

3.2. *In vivo* blood-brain barrier experiments with mice

Blood-to-brain transport

An *in vivo* multiple time regression (MTR) analysis was performed to investigate if BEA and/or ENNs are able to enter the brain from the blood. A dose solution of BEA, respectively ENNs, with a final concentration of 33.2 µg/mL in 6:94 EtOH:Lactated Ringer's solution containing 1% BSA (V/V) was prepared, corresponding to a dose of 0.2 mg/kg. This dose resembles a feed contamination of 1 mg/kg, which is included in a broad range of contamination levels that have been detected in feed (\pm 10 µg/kg to \geq 5 mg/kg) [3,4,10], assuming the feed intake of a 30 g weighing mouse is approximately 5 g/day [27].

The ICR-CD-1 mice were anesthetized by intraperitoneal injection with a 40% (w/V) urethane solution (3 g/kg), the jugular internalis vein and carotid artery were isolated and 200 µL of the dose solution was injected into the jugular vein. Blood was obtained from the carotid artery at regular time points after injection (1, 3, 5, 10, 12.5 and 15 min, with first and last in duplicate), thereafter the mice were immediately decapitated. Next, the brains were collected and the blood collected from the carotid artery was centrifuged at 10 000 g for 15 min at 21 °C. The serum and brain samples were analysed according to the described bioanalytical method (see section 3.3.).

As negative and positive control, ^{125}I labelled BSA and dermorphin were used, respectively, to assure the overall validity of the experiment [28]. Furthermore, the influence of the ethanol-containing dose formulations on the BBB integrity was also investigated in a radioactive MTR influx study with ^{125}I radiolabelled BSA.

In order to determine the BBB permeability of BEA/ENN, the ratio of its brain and serum concentration ($\mu\text{L/g}$) was plotted versus a derived time variable, *i.e.* the exposure time (Θ) [29,30]. The exposure time is defined as the integral of the concentration of BEA/ENN in the serum from start ($t=0$ min) to time T, divided by the concentration of BEA/ENN in serum at time T: $\Theta = \int_0^T \frac{C_s(t) \cdot dt}{C_s(T)}$. The area under the curve until time T is given by the integral of the concentration of BEA/ENN in serum from zero to time T. A biphasic model of blood-brain transfer was used to fit the uptake, as elaborated by Wong *et al.* [31]:

$$\frac{C_{\text{brain}}(T)}{C_s(T)} = K \times \Theta + V_g \times \left(1 - e^{\left(-\Theta \times \left(\frac{K_1 - K}{V_g} \right) \right)} \right) + V_0 \cong \underset{K=0}{V_g} \times \left(1 - e^{\left(-\Theta \times \left(\frac{K_1}{V_g} \right) \right)} \right) + V_0$$

where $C_{\text{brain}}(T)$ is the concentration of cyclic depsipeptide mycotoxin in the brain at time T (ng/g), $C_s(T)$ is the concentration of peptide in serum at time T ($\text{ng}/\mu\text{L}$), K is the net clearance ($\mu\text{L}/(\text{g} \times \text{min})$), K_1 is the unidirectional clearance ($\mu\text{L}/(\text{g} \times \text{min})$), V_g is the brain tissue distribution volume ($\mu\text{L/g}$), and V_0 is the vascular brain distribution volume, experimentally determined as the brain distribution volume of radioiodinated BSA ($14.8 \mu\text{L/g}$) [28].

The obtained serum concentrations (ng/mL) were first plotted in function of time (min) semi-logarithmically in order to determine whether the compounds exhibit a mono- or multi-exponential decay. Then, a two-compartment model was fitted [32]:

$$C(t) = A \times e^{-\alpha t} + B \times e^{-\beta t}$$

where $C(t)$ is the serum concentration of cyclic depsipeptide mycotoxin at time t (ng/mL) and where A, B, α and β are obtained from the intercepts and slopes of the serum concentration versus time curve by curve fitting using nonlinear regression analysis (GraphPad®, La Jolla, USA). The half-lives were calculated as $t_{1/2} = \ln(2)/k$, where k is the rate constant of the distribution (α), respectively elimination (β) phase.

Capillary depletion

To investigate the distribution of BEA/ENNs in the capillaries (fraction trapped by the endothelial cells lining the BBB) and parenchyma (the fraction transported into the brain) of the brain, a capillary depletion experiment was performed. The method of Triguero *et al.* [33], as modified by Gutierrez *et al.* [34], was used [35]. Briefly, after anesthetizing the mice intraperitoneally with 40% (w/v) urethane solution (3 g/kg), 200 μL of the 33.2 $\mu\text{g/mL}$ BEA/ENNs dose solution as used for the blood-

to-brain influx experiment was injected into the jugular vein. Blood was collected from the abdominal aorta 10 min after injection (in duplicate) and serum was obtained by centrifuging the blood at 10 000 g during 15 min at 21 °C. Immediately thereafter, the skin of the mice's chest was removed and the aorta was clamped so that perfusion occurs only in the direction of the brains and not through the whole body. Next, the brain was perfused manually with 20 mL of Lactated Ringer's solution. Immediately after perfusion, the mice were decapitated and brain was collected. The brains were transferred into an Eppendorf tube and weighed to which 525 µL ice-cold capillary buffer (10 mM HEPES, 141 mM NaCl, 4 mM KCl, 2.8 mM CaCl₂, 1 mM MgSO₄, 1 mM NaH₂PO₄ and 10 mM D-glucose adjusted to pH 7.4) was added and homogenized. Then, 1000 µL of ice-cold 26% dextrane solution in capillary buffer was added and vortexed. The tubes were centrifuged at 20 000 g for 60 min at 4 °C to separate pellet (capillaries) and supernatant (parenchyma and fat tissues). These were collected into separate Eppendorf tubes and weighed. For the pellet, the sample preparation as applied for mice brains was used, while for the supernatant the mice serum sample preparation method was used (see section 3.3.).

The capillary depletion (CD) fractions taken up by the capillaries or present in the parenchyma are normalized to the total brain weight and the serum concentration as follows: $CD_{tissue} (\mu L/g) = M_{tissue}/W_{brain}/C_s$, where M_{tissue} represents the amount of peptide in the capillaries, respectively parenchyma, W_{brain} is the total brain weight and C_s is the concentration of peptide in serum. The distribution was then calculated as follows:

$$\text{Fraction (\%)} = \frac{CD_{tissue}}{CD_{capillaries} + CD_{parenchyma}} \times 100.$$

Brain-to-blood transport

The BEA/ENN efflux out of the brain was evaluated using an *in vivo* method previously described [35]. First, the ICR-CD-1 mice were anesthetised using a 40% (w/V) urethane solution (3 g/kg), after which the skin of the skull was removed. Then, a hole was made in the skull above the lateral ventricle using a 22 G needle at a depth of 2 mm at the following coordinates: 1 mm lateral and 0.34 mm posterior to the bregma. Next, 1 µL of a 6 mg/mL BEA/ENNs in 50:50 EtOH:Lactate Ringer's solution (V/V), also corresponding to a dose of 0.2 mg/kg, was injected intracerebroventricularly (ICV) using a syringe pump (KDS100, KR analytical, Cheshire, UK) at a speed of 360 µL/h for 10 s. At specified time points post-injection (1, 3, 5, 10, 12.5 and 15 min), blood was obtained from the abdominal aorta, thereafter the mice were immediately decapitated. Serum was obtained by centrifuging the blood at 10 000 g during 15 min at 21 °C and brains were collected.

The brain efflux was determined from the linear regression of the natural logarithm of the peptide concentration in brain (ng/g) versus time (min), where k_{out} (min⁻¹) is defined as the efflux rate constant calculated as the negative value of the slope of the linear regression.

3.3. Bio-analytics

Sample preparation

The sample preparation of the mice serum and brain samples was based on the method of Devreese *et al.*, taking into account our results obtained from a quality-by-design Derringer desirability (D) study, where bovine serum albumin (BSA) loss, dilution factor and variability were combined [36]. In this approach we constructed an optimal working space for sample preparation of samples containing BSA, with the edge of failure defined as $D < 0.9$, indicating at least 80% ACN and 0.75% FA is required for a sufficient and robust protein precipitation [37].

As an internal standard (IS) ENN B (pure) was used for the determination of BEA, while BEA was used as IS for the different enniatins present in the enniatin mixture.

To 50 μL serum, 200 μL IS in 1:99 FA:ACN (V/V) was added, followed by vortex mixing for 15 s and centrifugation (20 000 g, 15 min, room temperature). Then, 200 μL supernatans was transferred to another container and evaporated to dryness (N_2 , 45 $^\circ\text{C}$, 5.1 torr). Next, the residue was reconstituted in 150 μL 70:30 ACN:H₂O (V/V). After vortex mixing (15 s), the sample was transferred into an autosampler vial for UHPLC-MS/MS analysis.

Isolated mice brains were transferred into a Eppendorf tube and weighed, after which 1.0 mL IS in ACN was added. Next, the brains were squashed and sliced, each time using a fresh scalpel knife. After vortex mixing (15 s), the samples were incubated for 30 min (300 rpm, room temperature) and centrifuged (20 000 g, 15 min, room temperature). Then, 800 μL supernatans was transferred to another container and evaporated to dryness (N_2 , 45 $^\circ\text{C}$, 5.1 torr). Next, the residue was reconstituted in 150 μL 70:30 ACN:H₂O (V/V). After vortex mixing (15 s), the sample was transferred into an autosampler vial for UHPLC-MS/MS analysis.

UHPLC-MS²

In **Chapter IV**, the previously developed bioanalytical high-throughput UHPLC-MS/MS method for the sensitive, specific and simultaneous determination and quantification of cyclic depsipeptide mycotoxins beauvericin and enniatins (A, A1, B, B1, D, E, C/F) was already presented. Briefly, an Acquity UHPLC equipped with a temperature controlled autosampler tray and column oven, thermostated at respectively 25 \pm 5 $^\circ\text{C}$ and 45 \pm 5 $^\circ\text{C}$, was used (Waters, Milford, MA, USA). Chromatographic separation was achieved on an Acquity UHPLC charged surface hybrid (CSH) C18 column (1.7 μm , 100 mm \times 2.1 mm, 130 \AA), attached to an Acquity UHPLC VanGuard pre-column (1.7 μm , 5 mm \times 2.1 mm, 130 \AA), both obtained from Waters. The mobile phase consisted of 30:70 ACN:H₂O (V/V) containing 0.1% FA and 0.1% 2-propanol and the flow rate was set to 0.6 mL/min. From the samples a 10 μL aliquot was injected. 10:10:80 DMSO:2-propanol:ACN (V/V/V) was used as

needle wash (during 6 s post-injection). The total run time was 4.5 min, of which the first 1.5 min was diverted to the waste.

The UHPLC system was coupled to a Xevo TQ-S detector, operated in the positive electrospray ionisation mode (ESI+) (Waters, Milford, MA, USA). An optimised capillary voltage of 3.50 kV, a cone voltage of 50 V and a source offset of 60 V was used. Desolvation and source temperatures were set at 600 and 150 °C, respectively, while desolvation and cone gas flows were 1000 and 150 L/h, respectively. Acquisition was done in the multiple reaction monitoring (MRM) mode. Optimised collision energies are given between brackets. The selected precursor ion for ENN B was m/z 639.91 with two selected product ions at m/z 196.08 (25 V) as quantifier and m/z 527.26 (22 V) as qualifier, for ENN D and B1 the precursor ion was m/z 653.99 while m/z 196.09 (23 V) and m/z 541.05 (21 V) were the product ions (quantifier and qualifier, respectively). For ENN E and A1, m/z 668.07 was the precursor ion and m/z 209.99 (24 V) and m/z 555.29 (21 V) were its product ions (quantifier and qualifier, respectively). ENNs A and C/F have a precursor ion of m/z 682.47 with product ions m/z 209.93 (26 V) as quantifier and m/z 555.01 (23 V) as qualifier. Lastly, BEA has a precursor ion at m/z 783.94, with m/z 244.01 (24 V) and m/z 623.23 (23 V) as its product ions (quantifier and qualifier, respectively). Data were acquired using Masslynx software (V4.1 SCN 843, Waters, Milford, MA, USA).

Method verification

To verify the bioanalytical method, pre-spiked and post-spiked matrix calibration curves were constructed for both matrices (brain and serum), as well as a standard calibration curve in diluent, *i.e.* 70:30 ACN:H₂O (V/V). For the ENNs mixture, this was done in duplicate for each of the three different concentration levels 10 ng/mL (low), 50 ng/mL (mid) and 100 ng/mL (high), with pre-spiked quality control (QC) samples in duplicate at two concentration levels 25 ng/mL (low-mid) and 75 ng/mL (mid-high), for determination of the method accuracy. For BEA, additional concentration levels (1 ng/mL and 5 ng/mL) are added.

The recoveries ($\text{response}_{\text{pre-spiked}}/\text{response}_{\text{post-spiked}} \times 100\%$) in serum were 100.6% for BEA and between 92.5% and 101.6% for the ENNs, while in mouse brain this was 99.5% for BEA and between 85.1% and 93.6% for the ENNs. The IS corrected matrix effect, determined as $\text{response}_{\text{post-spiked}}/\text{response}_{\text{diluent}} \times 100\%$, was 108.6% and 110.5% for BEA in serum and brain respectively, and for the ENNs, between 99.1% and 108.1% in serum and between 98.5% and 112.3% in mouse brain. The accuracy ($\text{concentration}_{\text{back calculated}}/\text{concentration}_{\text{nominal}} \times 100\%$ using the QC samples) was determined to be 100.2% (5 ng/mL), 103.4% (25 ng/mL) and 98.8% (75 ng/mL) for BEA in mouse serum, while for brain matrix this was 101.4, 99.9 and 96.8%, respectively. For ENNs, accuracies were 88.1-97.3% (25 ng/mL) and 96.3-103.1% (75 ng/mL) in serum, and 104.0-109.9% (25 ng/mL) and 93.2-98.9% (75

ng/mL) in brain. For ENN A and ENN C/F accuracy at 25 ng/mL in mouse brain was slightly higher: 136.5% and 115.9%, respectively. The precision of the method, determined on the duplicates, ranged from 0.2% to 10.9% RSD for all samples.

4. RESULTS

4.1. *In vitro* metabolic stability

In mouse serum, metabolic stability could only be unambiguously concluded for BEA, ENN B and ENN B1 due to co-eluting endogenous compounds with the other ENNs. However, considering their chemical resemblance, a similar metabolic stability behaviour is expected for all enniatins. The percentage of the amount at the start of the incubation, *i.e.* $t = 0$ min, versus $t = 60$ min was found to be between 90 – 110%. Moreover, the 95% confidence interval of the slope of the percentage versus time curves contains zero, which indicates no significant serum degradation under our analytical conditions.

In the brain homogenate, these percentages were within 80 – 120% for all investigated peptides, once corrected for the controls to take into account adsorption and other analytical phenomena. Moreover, no additional degradation peaks were observed (reporting threshold 2%).

Overall the results of this study indicate that these peptides are highly stable in serum and brain during the duration of the *in vivo* study under our operational conditions.

4.2. Blood-to-brain transport kinetics

The BBB transport kinetics of BEA and ENNs were investigated using the MTR method. The negative and the positive control confirmed the validity of the executed BBB experiments. The K_1 value of the positive control dermorphin was $0.26 \mu\text{L}/(\text{g}\times\text{min})$, while for the negative control BSA this was $0.12 \mu\text{L}/(\text{g}\times\text{min})$, both consistent with previous data [35,38]. The blank formulation did not influence the BBB functionality as no difference in BSA BBB influx was observed between the ethanol-containing formulation (Figure 1), *i.e.* Lactated Ringer's solution containing 1% ^{125}I BSA (m/V) and 6% EtOH (V/V), and the formulation without ethanol, *i.e.* Lactated Ringer's solution containing 1% ^{125}I BSA (m/V) only (Figure 1).

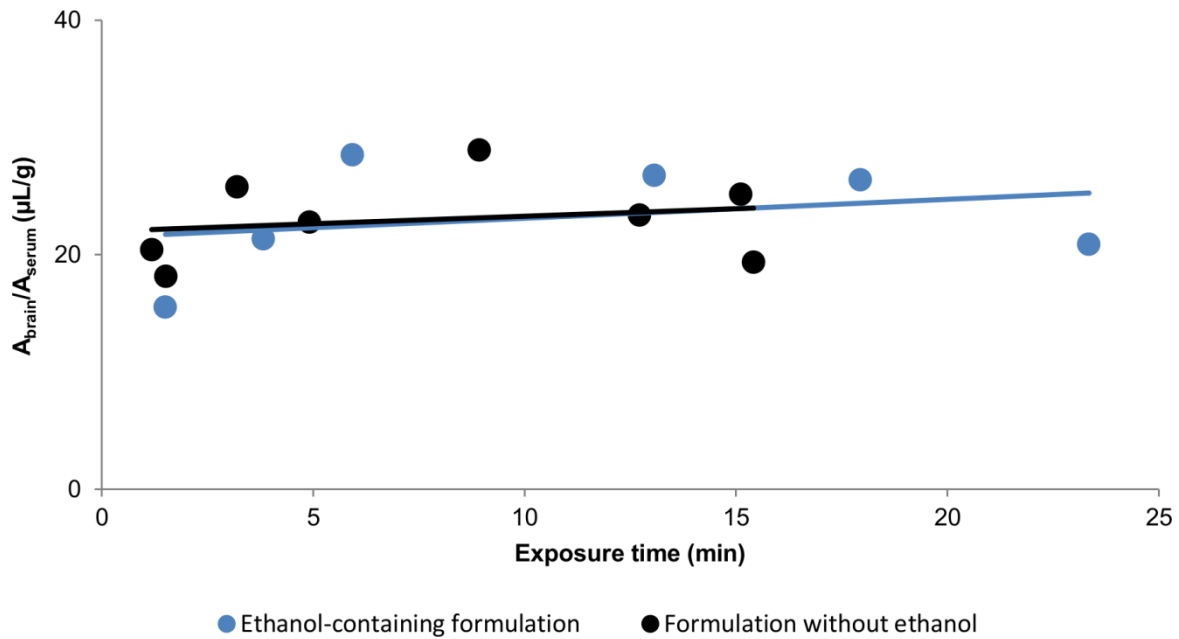


Figure 1: Multiple time regression influx study of ^{125}I BSA using linear regression. Brain/serum activity ratio ($\mu\text{L/g}$) in function of exposure time (min) of both the ethanol-containing formulation (blue) and the formulation without ethanol control (black).

In Figure 2, the ratio of the concentration of peptide in brain and serum is plotted versus the exposure time. These data indicate that the cyclic depsipeptide mycotoxins BEA and ENNs cross the blood-brain barrier: a significant influx into the mouse brain was observed.

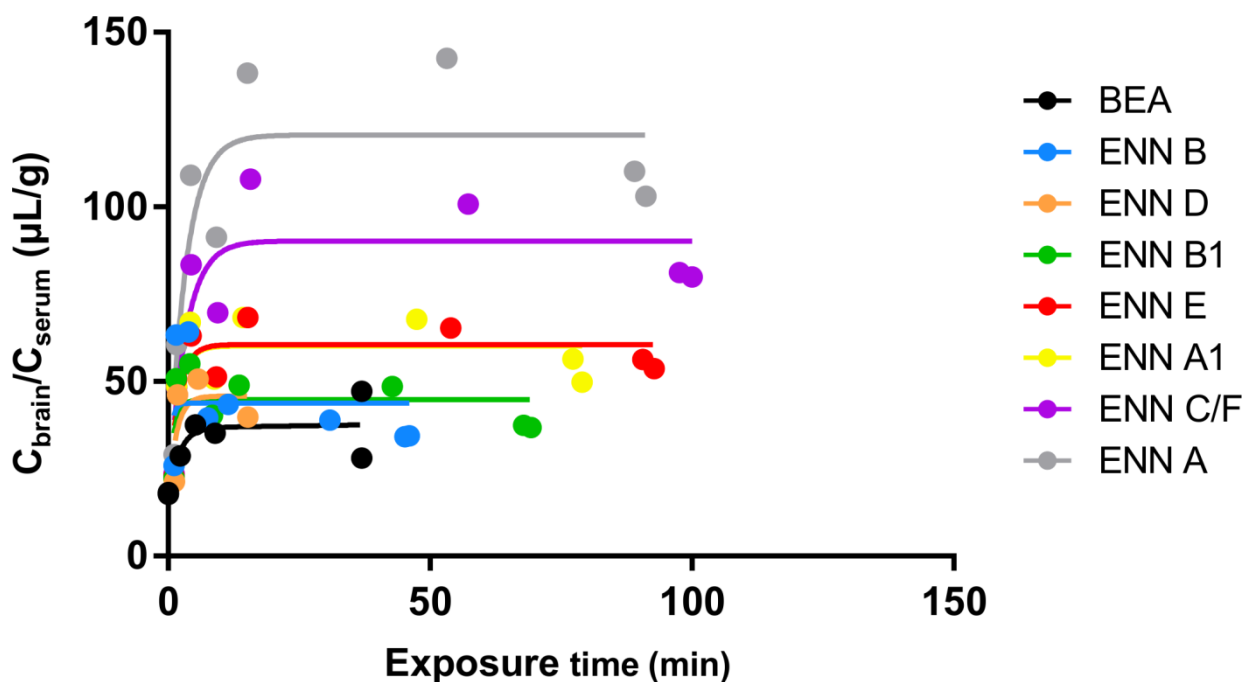


Figure 2: Brain influx results of beauvericin and enniatins (MTR in mice). The ratio of the brain-to-serum activity is plotted versus the exposure time, fitted using the biphasic Gjedde-Patlak model.

All mycotoxins thus showed a high initial influx rate into the brain with K_1 values ranging between 11 and 53 $\mu\text{L}/(\text{g}\times\text{min})$, followed by a plateau phase characterised by negligible net brain clearance (very low K-values). Moreover, the brain tissue distribution volumes (V_g) ranges between 22 and 106 $\mu\text{L}/\text{g}$. These data are presented in Table 1.

The serum concentrations obtained during these experiments are shown in Figure 3. From the semi-logarithmic plots, *i.e.* In of serum concentration (ng/mL) in function of time (min), a clear biphasic decline was noticed, indicating thus a two compartment model characterised by a very fast transfer from the central to the peripheral compartment (distribution phase), followed by a second, much longer and slower phase (elimination phase). The model parameters obtained for each of the cyclic depsipeptide mycotoxins and the calculated half-lives are given in Table 2.

Table 1: Summary of the BBB data obtained for all investigated cyclic depsipeptide mycotoxins (mean \pm SE).

Cyclic depsipeptide		MTR blood-to-brain influx ⁽¹⁾			Capillary depletion		Efflux
		K ($\mu\text{L}/(\text{g}\times\text{min})$)	V _g ($\mu\text{L}/\text{g}$)	K ₁ ($\mu\text{L}/(\text{g}\times\text{min})$)	Parenchymal fraction (%)	Capillary fraction (%)	Slope (min^{-1})
Beauvericin	(BEA)	0.02272 \pm 0.3153	21.91 \pm 9.664	11.15 \pm 11.42	91.92 \pm 1.41	8.08 \pm 1.41	-0.1205 \pm 0.04218
Enniatin B	(ENN B)	$\approx 2.071 \times 10^{-16}$	28.97 \pm 11.07	52.95 \pm 108.4	96.03 \pm 0.19	3.97 \pm 0.19	-0.08802 \pm 0.06985
Enniatin D	(ENN D)	0.001640 \pm 0.09873	34.39 \pm 6.588	21.66 \pm 11.43	96.71 \pm 0.15	3.29 \pm 0.15	0.005063 \pm 0.003091
Enniatin B1	(ENN B1)	$\approx 1.444 \times 10^{-16}$	29.94 \pm 7.594	30.03 \pm 24.19	96.10 \pm 0.00	3.90 \pm 0.00	0.002408 \pm 0.002707
Enniatin E	(ENN E)	$\approx 9.769 \times 10^{-13}$	45.77 \pm 5.795	25.08 \pm 10.86	96.20 \pm 0.36	3.80 \pm 0.36	-0.005929 \pm 0.003019
Enniatin A1	(ENN A1)	$\approx 2.185 \times 10^{-16}$	45.38 \pm 9.303	25.38 \pm 13.12	95.70 \pm 0.10	4.30 \pm 0.10	-0.01277 \pm 0.005588
Enniatin C/F	(ENN C/F)	$\approx 1.845 \times 10^{-16}$	75.43 \pm 15.39	23.53 \pm 10.22	95.30 ⁽²⁾	4.70 ⁽²⁾	-0.02976 \pm 0.009449
Enniatin A	(ENN A)	$\approx 1.840 \times 10^{-16}$	105.8 \pm 21.95	32.41 \pm 13.76	94.20 \pm 0.71	5.80 \pm 0.71	-0.04421 \pm 0.02059

(1) V₀ = 14.8 $\mu\text{L}/\text{g}$ of BSA.

(2) n = 1 (the other sample was < limit of detection).

Table 2: Serum kinetics of all investigated cyclic depsipeptide mycotoxins, following a two compartment model.

Cyclic depsipeptide		Two compartment model				R ²	Distribution half-life (min^{-1})	Elimination half-life (min^{-1})
		A	B	α	β			
Beauvericin	(BEA)	3772000	307	6.709	0.02129	0.9993	0.10	32.6
Enniatin B	(ENN B)	222536	124	6.405	0.09259	0.9983	0.11	7.49
Enniatin D	(ENN D)	103128	18.1	7.831	0.2119	0.9990	0.09	3.27
Enniatin B1	(ENN B1)	255568	161	6.315	0.1449	0.9985	0.11	4.78
Enniatin E	(ENN E)	6358	7.29	5.742	0.1936	0.9988	0.12	3.58
Enniatin A1	(ENN A1)	35133	56.79	5.198	0.1539	0.9989	0.13	4.50
Enniatin C/F	(ENN C/F)	425.6	1.25	4.550	0.1972	0.9989	0.15	3.51
Enniatin A	(ENN A)	1952	5.58	4.370	0.1624	0.9991	0.16	4.27

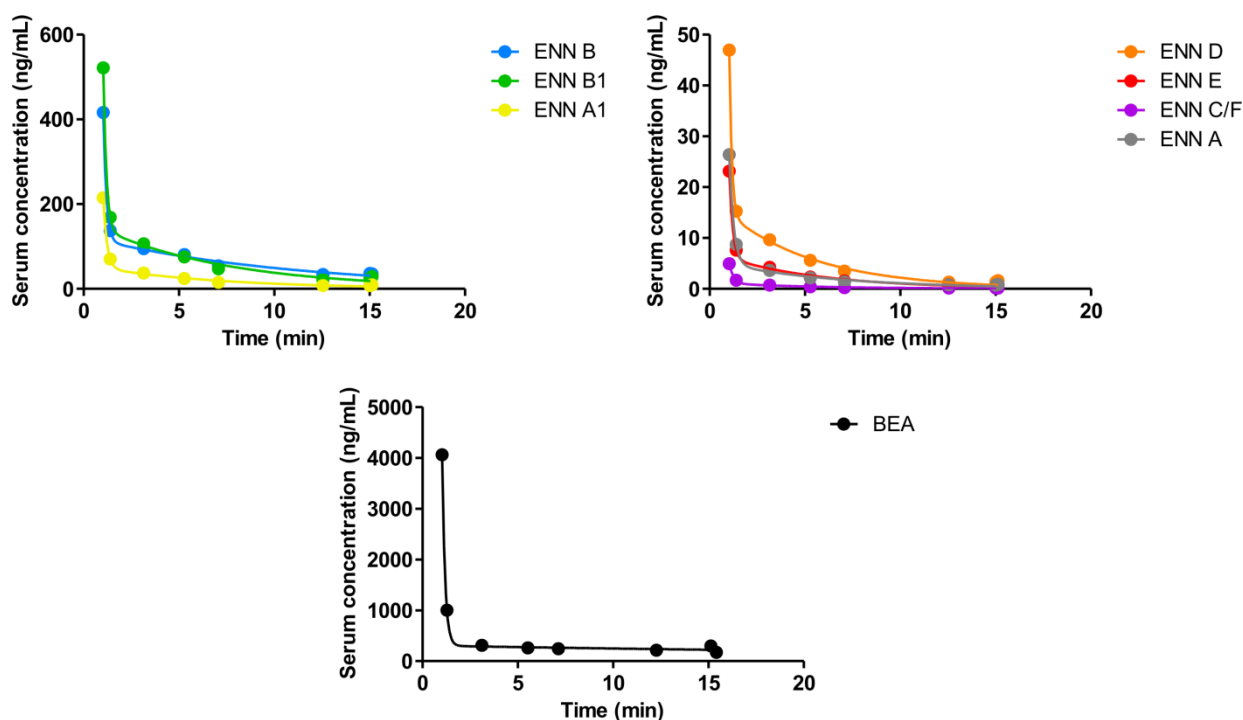


Figure 3: Serum concentrations (ng/mL) of BEA and ENNS in function of time (min), as obtained during the MTR experiments. Data were fitted using a two compartment model.

4.3. Capillary depletion

The distribution of the peptides in the brain (at 10 minutes after injection) is expressed as fraction (%) with respect to the total brain homogenate (*i.e.* the sum of brain capillaries and parenchyma) and are presented in Figure 4. A very high brain penetration of all cyclic depsipeptide mycotoxins was found. Overall, approximately 95% of the total quantity retained by the brain was found in the brain parenchyma and only approximately 5% of the mycotoxins remained in the brain capillaries (Table 1). Moreover, when comparing the $C_{\text{brain}}/C_{\text{serum}}$ ratios ($\mu\text{L/g}$) at 10 min post-injection obtained from both the MTR and CD study, these data were found to be in the same order of magnitude, indicating the overall validity and consistency of the experiments.

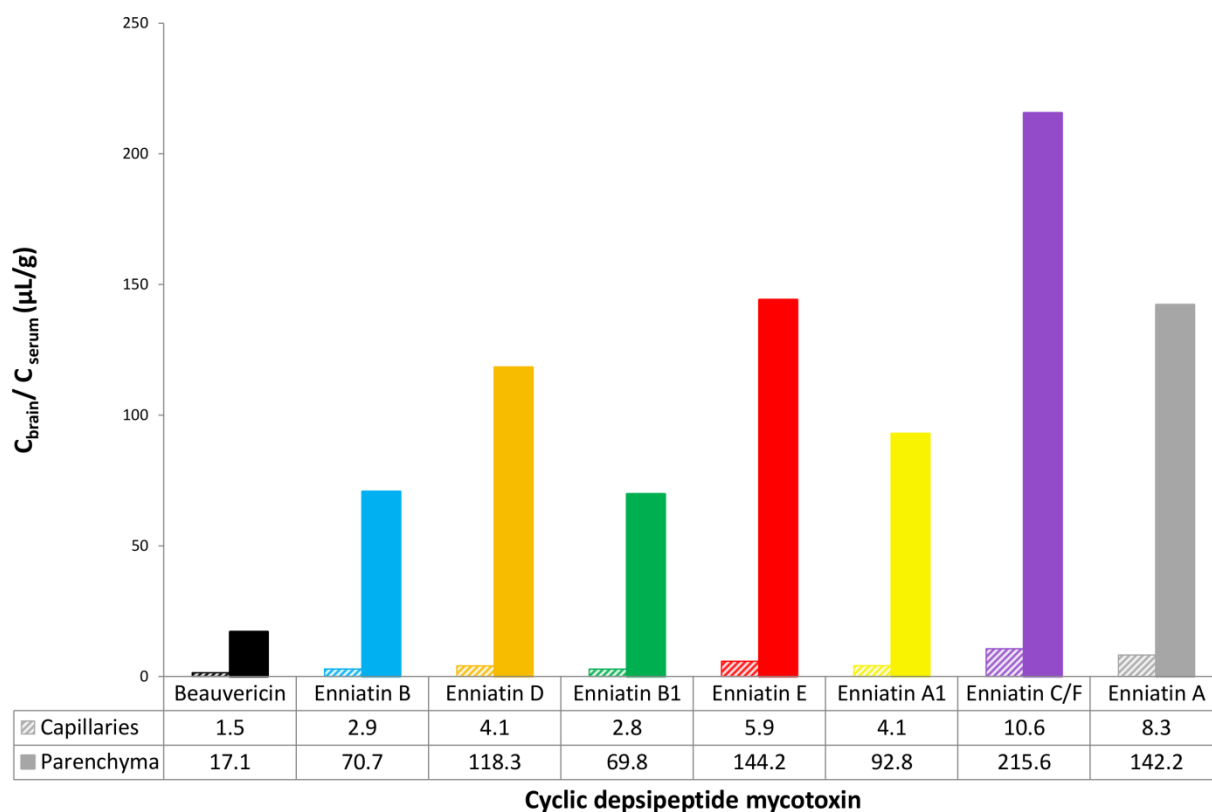


Figure 4: Compartmental distribution by capillary depletion at 10 min post-injection (mean absolute amounts in $\mu\text{L/g}$), showing a very high brain parenchyma penetration for all investigated cyclic depsipeptide mycotoxins.

4.4. Brain-to-blood transport kinetics

The efflux properties of BEA and ENNs out of the brain were investigated by quantifying their concentration in the brain after intracerebroventricular injection of the dose solution and deriving the efflux transfer constant k_{out} , which is the negative value of the slope of the natural logarithm of the concentration of BEA/ENNs in the brain (ng/g) versus the experimental time curve (min), as presented in Figure 5 and Table 1. It is concluded that there is no significant efflux out of the brain observed for each of the investigated cyclic depsipeptides (k_{out} is less than 0.005 min^{-1}).

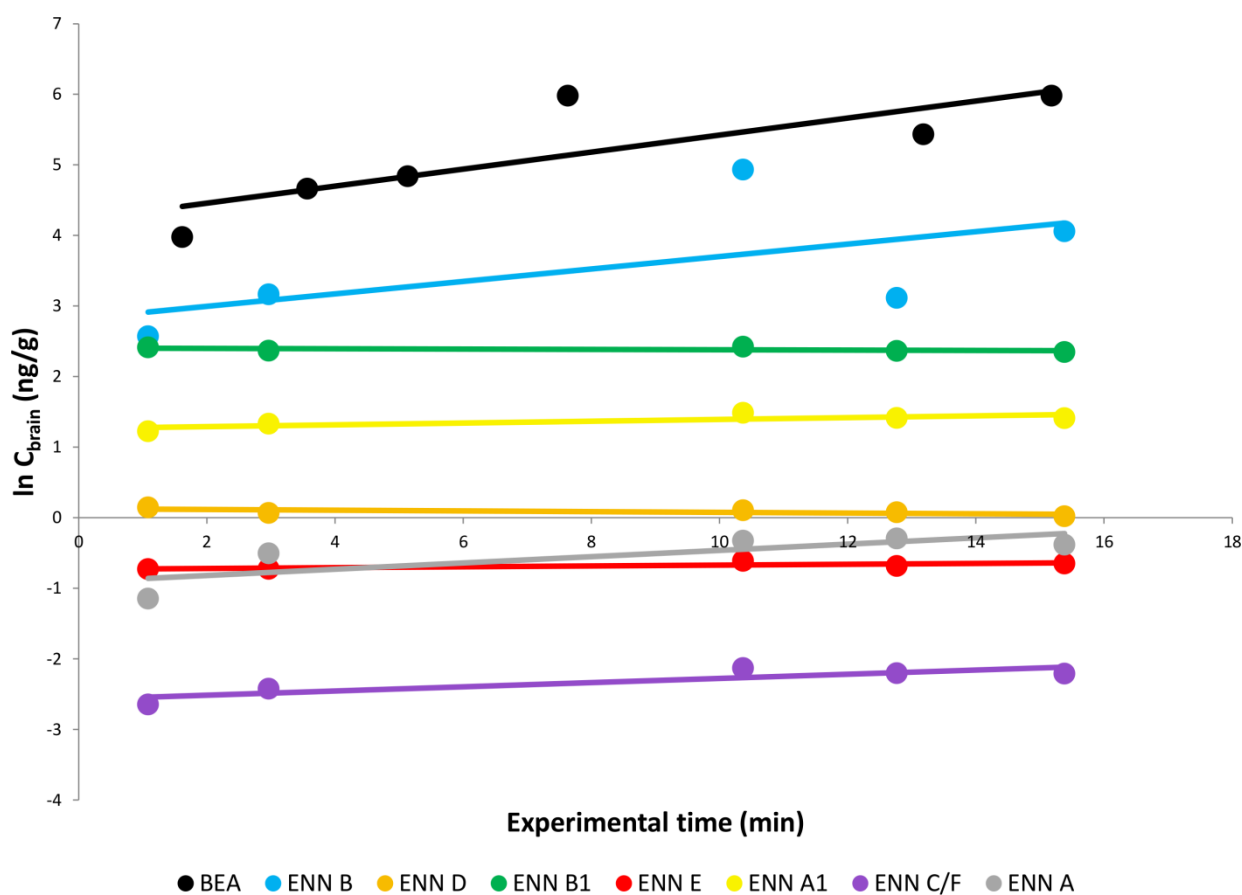


Figure 5: Brain efflux of beauvericin and enniatins, fitted using linear regression of the natural logarithm of the peptide concentration in brain (ng/g) versus time (min).

5. DISCUSSION

In the present study, we investigated the blood-brain barrier transport kinetics of the cyclic depsipeptide mycotoxins BEA and ENNs in an *in vivo* mice experiment with a dose corresponding to 0.2 mg/kg, resembling a real-life feed contamination. Our results clearly show that these peptides rapidly permeate the BBB after intravenous administration: applying a biphasic process model, high initial influx rates varying from 11.15 up to 52.95 $\mu\text{L}/(\text{g}\times\text{min})$ were observed, after which a plateau is reached. These K_1 values indicate significantly higher initial influx rates into the brains compared to the negative control ^{125}I BSA (0.12 $\mu\text{L}/(\text{g}\times\text{min})$) and positive control ^{125}I dermorphin (0.26 $\mu\text{L}/(\text{g}\times\text{min})$), also included in this study. Moreover, the capillary depletion results indicated a brain tissue distribution of 95% peptides in the brain parenchyma, whereas only 5% remained trapped in the capillaries. Comparable $C_{\text{brain}}/C_{\text{serum}}$ ratios ($\mu\text{L}/\text{g}$) at 10 min post-injection were obtained from both the MTR and CD study, indicating that for ENNs C/F and A there is a higher brain influx, for ENNs B, B1 and BEA the lowest influx is noticed, while the other ENNs (ENN A1, E and D) range in between. Furthermore, only for ENN D a minor efflux was observed ($k_{\text{out}} = 0.005 \text{ min}^{-1}$), which is biologically

negligible within the experimental time frame of 15 minutes, while for the others no statistically significant efflux out of the brain into the blood was observed.

Our *in vivo* experimentally obtained BBB permeability results were compared with two *in silico* computational models as proposed by Suenderhauf *et al.* [39]. For the first model using CHAID (chi-squared automatic interaction detector), conflicting results were obtained due to the rotatable bonds cut-off splitting criterion: for BEA, ENN A, ENN A1 and ENN C/F (> 7) a weak BBB permeation is expected, while for ENN B, ENN B1 and ENN D (≤ 7) a strong permeation is predicted. However, for the second model using CART (classification and regression tree), a strong BBB permeation is expected for all our investigated cyclic depsipeptides, which is in accordance with the results obtained in this study. The values for the molecular descriptors of BEA/ENNs used to calculate their *in silico* BBB permeability are given in Table 3.

Table 3: Molecular descriptors of BEA and ENNs used for the *in silico* prediction of their BBB permeability.

Compound	Molecular descriptor ⁽¹⁾		
	aLogP	tPSA	Number of rotatable bonds
Beauvericin	7.661	139.83	9
Enniatin A	6.890	139.83	9
Enniatin A1	6.434	139.83	8
Enniatin B	5.522	139.83	6
Enniatin B1	5.978	139.83	7
Enniatin C	6.688	139.83	9
Enniatin D	5.910	139.83	7

(1) Calculated using Dragon 5.5 (Talete, Milan, Italy).

The BBB-influx classification system for peptides as proposed by Stalmans *et al.* indicated that BEA and ENNs are located in class 5, corresponding to a very high brain influx, which was also confirmed by comparing our obtained influx data of BEA/ENNs with those of other peptides [28,40].

The pharmacokinetic biphasic behaviour observed in the MTR study (Figure 2) demonstrates a bidirectional transport mechanism with transition from a phase with an initial sharp increase to a steady-state condition. These observations can be explained by a number of concurrent pharmacokinetic mechanisms. Indeed, taking into account the two compartment serum kinetics (Figure 3 and Table 2), a very fast distribution phase is noticed with a corresponding rapid decrease in serum concentration (half-lives ranging from 0.09 to 0.16 min⁻¹ for the different compounds), due to a transfer from the central to the peripheral compartment, represented by the different tissues. A second elimination phase is much slower, with half-lives ranging from 3.27 to 7.49 min⁻¹ for the different ENNs and 32.6 min⁻¹ for BEA, indicating a slower diffusion back from the peripheral compartment to the central compartment. Considering their lipophilicity, bioaccumulation or sequestration of these mycotoxins seems plausible and has been numerously suggested [10,41-44]. In an earlier study with tritiated ENN B, bioaccumulation in liver, kidney and brain was indeed observed [44,45]. During a recent *in vivo* pilot toxicokinetic study in pigs, Devreese *et al.*

demonstrated rapid distribution (0.15h) and elimination (1.13h) half-lives for ENN B1 after intravenous administration [3]. In another *in vivo* study in rats, an elimination half-life of 3.2h was obtained for beauvericin after oral administration [46].

Although in this study, no significant serum and brain metabolisation was observed *in vitro*, this should not be ruled out. Extensive metabolisation has been demonstrated *in vitro* by incubation of ENN B in human, dog and rat liver microsomes, indicating that oxidative phase I reactions (N-demethylation and isopropyl oxidation of N-methyl-L-valine and D-2-hydroxyisovaleric acid) by CYP3A and CYP1A play an important role in the metabolism of this mycotoxin [44,47]. These CYP enzymes are not only active in the liver, but also occur in extrahepatic regions [48,49].

Both ENNs and BEA have been previously described to interact with proteins involved in efflux transport, where they either act as efflux pump inhibitors, inhibiting the ABCG2- and ABCB1-mediated efflux of specific fluorescent substrates in human cell lines [50,51], or as efflux pump substrates, *i.e.* ENN B1 was found to be a substrate of intestinal P-glycoprotein in the human intestinal Caco-2 cell line, with the basolateral (blood) to apical (intestine) direction being 6.7× higher as compared to the permeability in the opposite direction, indicating significant efflux activity [52].

6. CONCLUSIONS

This study evaluated the quantitative BBB transport kinetics of the cyclic depsipeptide mycotoxins BEA and ENNs. The results indicate a very high influx rate into the brain, with a significant distribution in the brain parenchyma. No significant serum or brain metabolisation, nor significant brain efflux to the blood was observed. Our results thus highly increases the possibility of these cyclic depsipeptide mycotoxins to exert local central nervous system (CNS) effects once present in the systemic circulation.

7. REFERENCES

- [1] Taevernier L, Veryser L, Vandercruyssen K, D'Hondt M, Vansteelandt S, De Saeger S, De Spiegeleer B. UHPLC-MS/MS method for the determination of the cyclic depsipeptide mycotoxins beauvericin and enniatins in *in vitro* transdermal experiments. *Journal of Pharmaceutical and Biomedical Analysis* (2014); 100: 50-57.
- [2] Taevernier L, Veryser L, Roche N, Peremans K, Burvenich C, Delesalle C, De Spiegeleer B. Human skin permeation of emerging mycotoxins (beauvericin and enniatins). *Journal of Exposure Science and Environmental Epidemiology* 2016; 26: 277-287.
- [3] Devreese M, Broekaert N, De Mil T, Fraeyman S, De Backer P, Croubels S. Pilot toxicokinetic study and absolute oral bioavailability of the *Fusarium* mycotoxin enniatin B1 in pigs. *Food and Chemical Toxicology* 2014; 63: 161-165.
- [4] Streit E, Schwab C, Sulyok M, Naehrer K, Krska R, Schatzmayr R. Multimycotoxin screening reveals the occurrence of 139 different secondary metabolites in feed and feed ingredients. *Toxins* 2013; 5: 504-523.
- [5] Peitzsch M, Sulyok M, Taubel M, Vishwanath V, Krop E, Borrás-Santos A, Hyvärinen A, Nevalainen A, Krska R, Larsson L. Microbial secondary metabolites in school buildings inspected for moisture damage in Finland, The Netherlands and Spain. *Journal of Environmental Monitoring* 2012; 14: 2044-2053.
- [6] Taevernier L, Detroyer S, Veryser L, De Spiegeleer B. Enniatin-containing solutions for oromucosal use: quality-by-design ex-vivo transmucosal risk assessment of composition variability. *International Journal of Pharmaceutics* 2015; 491: 144-151.
- [7] Celik M, Aksoy H, Yilmaz S. Evaluation of beauvericin genotoxicity with chromosomal aberrations, sister-chromatid exchanges and micronucleus assays. *Ecotoxicology and Environmental Safety* 2010; 73: 1553-1557.
- [8] Dornetshuber R, Heffeter P, Kamyar MR, Peterbauer T, Berger W, Lemmens-Gruber R. Enniatin exerts p53-dependent cytostatic and p53-independent cytotoxic activities against human cancer cells. *Chem Res Toxicol* 2007; 20: 465-473.
- [9] Ivanova L, Skjerve E, Eriksen GS, Uhlig S. Cytotoxicity of enniatins A, A1, B, B1, B2 and B3 from *Fusarium avenaceum*. *Toxicon* 2006; 47: 868-876.
- [10] Jestoi M. Emerging *Fusarium*-mycotoxins fusaproliferin, beauvericin, enniatins, and moniliformin - A review. *Crit Rev Food Sci Nutr* 2008; 48: 21-49.
- [11] Klaric MS, Pepeljnjak S, Rozgaj R. Genotoxicity of fumonisin B1, beauvericin and ochratoxin A in porcine kidney PK15 cells: effects on individual and combined treatment. *Croatica Chemica Acta* 2008; 81: 139-146.
- [12] Klaric MS, Darabos D, Rozgaj R, Kasuba V, Pepeljnjak S. Beauvericin and ochratoxin A genotoxicity evaluated using the alkaline comet assay: single and combined genotoxic action. *Arch Toxicol* 2010; 84: 641-650.
- [13] Lee HS, Song HH, Jeong JH, Shin CG, Choi SU, Lee C. Cytotoxicities of enniatins H, I, and MK1688 from *Fusarium oxysporum* KFCC11363P. *Toxicon* 2008; 51: 1178-1185.

- [14] Meca G, Font G, Ruiz MJ. Comparative cytotoxicity study of enniatins A, A(1), A(2), B, B-1, B-4 and J(3) on Caco-2 cells, Hep-G(2) and HT-29. *Food Chem Toxicol* 2011; 49: 2464-2469.
- [15] Prosperini A, Meca G, Font G, Ruiz MJ. Study of the cytotoxic activity of beauvericin and fusaproliferin and bioavailability *in vitro* on Caco-2 cells. *Food Chem Toxicol* 2012; 50: 2356-2361.
- [16] Watjen W, Debbab A, Hohfeld A, Chovolou Y, Kampkotter A, Edrada RA *et al.* Enniatins A1, B and B1 from an endophytic strain of *Fusarium tricinctum* induce apoptotic cell death in H4IIE hepatoma cells accompanied by inhibition of ERK phosphorylation. *Mol Nutr Food Res* 2009; 53: 431-440.
- [17] Zahn JX, Burns AM, Liu MPX, Faeth SH, Gunatilaka AAL. Search for cell motility and angiogenesis inhibitors with potential anticancer activity: beauvericin and other constituents. *J Nat Prod* 2007; 70: 227-232.
- [18] Zhang L, Yan K, Zhang Y, Huang R, Bian J, Zheng C, Sun H, Chen Z, Sun N, An R, Min F, Zhao W, Zhuo Y, You J, Song Y, Yu Z, Lio Z, Yang K, Gao H, Dai H, Zhang X, Wang J, Fu C, Pei G, Liu J, Zhang S, Goodfellow M, Jiang Y, Kuai J, Zhou G, Chen X. High-throughput synergy screening identifies microbial metabolites as combination agents for the treatment of fungal infections. *PNAS* 2007; 104: 4606-4611.
- [19] Abbott NJ, Patabendige AAK, Dolman DEM, Yusof SR, Begley DJ. Structure and function of the blood–brain barrier. *Neurobiology of Disease* 2010; 37: 13-25.
- [20] Ballabh P, Braun A, Nedergaard M. The blood–brain barrier: an overview: structure, regulation, and clinical implications. *Neurobiology of Disease* 2004; 16: 1-13.
- [21] Banks WA, Kastin AJ. Interactions between the blood–brain barrier and endogenous peptides: emerging clinical implications. *Am J Med Sci* 1988; 295: 459-465.
- [22] Verbeke M, Wynendaele E, Mauchauffée E, Bracke N, Stalmans S, Bojnik E, Benyhe S, Peremans K, Polis I, Burvenich C, Gjedde A, Hernandez J-F, De Spiegeleer B. Blood–brain transfer and antinociception of linear and cyclic N-methyl-guanidine and thiourea-enkephalins. *Peptides* 2015; 63: 10-21.
- [23] Wynendaele E, Verbeke F, Stalmans S, Gevaert B, Janssens Y, Van De Wiele C, Peremans K, Burvenich C, De Spiegeleer B. Quorum sensing peptides selectively penetrate the blood-brain barrier. *PLOS ONE* 2015; 10(11): e0142071.
- [24] De Spiegeleer B, Wynendaele E, Bracke N, Veryser L, Taevernier L, Degroote A, Stalmans S. Regulatory development of geriatric medicines: To GIP or not to GIP? *Ageing Res Rev* 2016; 27: 23-36.
- [25] Stalmans S, Bracke N, Wynendaele E, Gevaert B, Peremans K, Burvenich C, Polis I, De Spiegeleer B. Cell-Penetrating peptides selectively cross the blood-brain barrier *in vivo*. *PLOS ONE* 2015; 10: e0139652.
- [26] Vergote V, Van Dorpe S, Peremans K, Burvenich C, De Spiegeleer B. *In vitro* metabolic stability of obestatin: Kinetics and identification of cleavage products. *Peptides* 2008; 29: 1740-1748.

- [27] Research Diets Inc., Typical food intake: <http://www.researchdiets.com/resource-center-page/typical-food-intake> (consulted 17/12/2015).
- [28] Stalmans S, Gevaert B, Wynendaele E, Nielandt J, De Tré G, Peremans K, Burvenich C, De Spiegeleer B. Classification of peptides according to their blood-brain barrier influx. *Protein Pept Lett* 2015; 22: 768-775.
- [29] Gjedde A. High-affinity and low-affinity transport of D-glucose from blood to brain. *J Neurochem* 1981; 36: 1463-1471.
- [30] Patlak CS, Blasberg RG, Fenstermacher JD. Graphical evaluation of blood-to-brain transfer constants from multiple-time uptake data. *J Cerebr Blood F Met* 1983; 3: 1-7.
- [31] Wong DF, Gjedde A, Wagner Jr HN. Quantification of neuroreceptors in the living human brain I. Irreversible binding of ligands. *J Cerebr Blood Flow Metab* 1986; 6: 137-146.
- [32] Fan J, de Lannoy IAM. Pharmacokinetics. *Biochem Pharmacol* 2014; 87: 93-120.
- [33] Triguero D, Buciak J, Pardridge WM. Capillary depletion method for quantification of blood–brain barrier transport of circulating peptides and plasma proteins. *J Neurochem* 1990; 54: 1882-1888.
- [34] Gutierrez EG, Banks WA, Kastin AJ. Murine tumor necrosis factor alpha is transported from blood to brain in the mouse. *J Neuroimmunol* 1993; 47: 169-176.
- [35] Stalmans S, Wynendaele E, Bracke N, Knappe D, Hoffman R, Peremans K, Polis I, Burvenich C, De Spiegeleer B. The blood-brain barrier transport of short proline-rich antimicrobial peptides. *Protein Pept Lett* 2014; 21: 399-406.
- [36] Devreese M, De Baere S, De Backer P, Croubels S. Quantitative determination of the *Fusarium* mycotoxins beauvericin, enniatin A, A1, B and B1 in pig plasma using high performance liquid chromatography–tandem mass spectrometry. *Talanta* 2013, 106: 212-219.
- [37] Taevernier L, Wynendaele E, D’Hondt M, De Spiegeleer B. Analytical quality-by-design approach for sample treatment of BSA-containing solutions. *Journal of Pharmaceutical Analysis*. 2015; 5: 27-32.
- [38] Kastin AJ, Akerstrom V. Entry of exendin-4 into brain is rapid but may be limited at high doses. *Int J Obes* 2003; 27: 313-318.
- [39] Suenderhauf C, Hammann F, Huwyler J. Computational prediction of blood-brain barrier permeability using decision tree induction. *Molecules* 2012; 17: 10429-10445.
- [40] Van Dorpe S, Bronselaer A, Nielandt J, Stalmans S, Wynendaele E, Audenaert K, Van De Wiele C, Burvenich C, Peremans K, Hsuchou H, De Tré G, De Spiegeleer B. Brainpeps: the blood–brain barrier peptide database. *Brain structure and function* 2012; 217: 687-718 (<http://brainpeps.ugent.be/>).
- [41] Jestoi M, Rokka M, Peltonen, K. Residues of emerging *Fusarium* – mycotoxins and coccidiostats in Finnish poultry tissues. *Molecular Nutrition and Food Research* 2007; 51: 625-637.

- [42] Jestoi M, Rokka M, Järvenpää E, Peltonen K. Determination of *Fusarium* mycotoxins beauvericin and enniatins (A, A1, B, B1) in eggs of laying hens using liquid chromatography-tandem mass spectrometry (LC-MS/MS). *Food Chem* 2009; 115: 1120-1127.
- [43] Thakur RA, Smith JS. Liquid chromatography/thermospray/mass spectrometry analysis of beauvericin. *J Agric Food Chem* 1997; 45: 1234-1239.
- [44] Faeste C, Ivanova L, Uhlig S. *In vitro* metabolism of the mycotoxin enniatin B in different species and cytochrome P450 enzyme phenotyping by chemical inhibitors. *Drug Metabol Dispos* 2011; 39: 1768-1776.
- [45] Lohmann A. Analytische, pharmakologische und mikrobiologische untersuchungen des ionophoren antibiotikums fusafungin. Westfälische Wilhelms Universität, Münster, 1988, pp. 294.
- [46] Mei L, Zhang L, Dai R. An inhibition study of beauvericin on human and rat cytochrome P450 enzymes and its pharmacokinetics in rats. *J. Enzyme Inhib Med Chem* 2009; 24: 753-762.
- [47] Ivanova L, Faeste CK, Uhlig S. *In vitro* phase I metabolism of the depsipeptide enniatin B. *Anal Bioanal Chem* 2011; 400: 2889-2901.
- [48] Miksys S, Hoffmann E, Tyndale RF. Regional and cellular induction of nicotine-metabolizing CYP2B1 in rat brain by chronic nicotine treatment. *Biochem Pharmacol* 2000; 59: 1501-1511.
- [49] Miksys S, Tyndale RF. Cytochrome P450-mediated drug metabolism in the brain. *J Psychiatry Neurosci* 2013; 38: 152-163.
- [50] Tedjitsop Feudjio F, Dornetshuber R, Lemmens M, Hoffmann O, Lemmens-Gruber R, Berger W. Beauvericin and enniatin: emerging toxins and/or remedies? *World Mycotoxin J* 2010. 3: 415-430.
- [51] Dornetshuber R, Heffeter P, Sulyok M, Schumacher R, Chiba P, Kopp S, Koellensperger G, Micksche M, Lemmens-Gruber R, Berger W. Interactions between ABC-transport proteins and the secondary *Fusarium* metabolites enniatin and beauvericin. *Mol Nutr Food Res* 2009; 53: 904-920.
- [52] Ivanova L, Uhlig S, Eriksen GS, Johannessen LE. Enniatin B-1 is a substrate of intestinal P-glycoprotein, multidrug resistance-associated protein 2 and breast cancer resistance protein. *World Mycotoxin Journal* 2010; 3: 271-281.

CHAPTER VII

QUALITY-BY-DESIGN RISK ASSESSMENT OF ENNIATIN-CONTAINING SOLUTIONS FOR OROMUCOSAL USE

“Quality begins on the inside... then works its way out.”

Robert ‘Bob’ Moawad

(°1941 - †2007, American teacher, coach, author, innovator and benefactor)

Parts of this chapter were published:

Taevernier L, Detroyer S, Veryser L, De Spiegeleer B. Enniatin-containing solutions for oromucosal use: Quality-by-design *ex-vivo* transmucosal risk assessment of composition variability. *International Journal of Pharmaceutics*. 2015; **491**: 144-151, doi: 10.1016/j.ijpharm.2015.06.029.

ABSTRACT

Fusafungine, a mixture of the cyclic hexadepsipeptides enniatins, is currently on the market for the treatment of upper respiratory tract diseases because of its bacteriostatic and anti-inflammatory effects.

In this study, a quality-by-design risk assessment was performed with two objectives: (i) investigate whether enniatins are able to permeate the mucosa and reach blood circulation, as the summary of product characteristics indicates this is not the case, and if so, to quantify their transmucosal kinetics and (ii) study the influence of excipient concentration variability on mucosal permeation.

First, the concentration of the two main excipients isopropyl myristate and ethanol, known penetration enhancers, in several marketed samples was determined using GC-FID. Then, the transmucosal kinetics of the enniatins were quantitatively evaluated for different dose solutions, using buccal porcine mucosa in an *ex vivo in vitro* Franz diffusion cell set-up, with UHPLC-MS/MS bioanalytics.

This study demonstrated that enniatins are capable of permeating the mucosa. However, no risk of a significant different transmucosal permeability with varying excipient concentrations was detected. Moreover, steady-state plasma concentrations after buccal application were estimated up to 1.3 mg/L, or 13 mg/L for the marketed preparations, which contain up to a 10 times higher enniatin dosage and assuming linear extrapolation. These results indicate that enniatin-based therapies for treatment of upper respiratory tract infections should be questioned, because of the possibly negative benefit-risk ratio.

CHAPTER VII

QUALITY-BY-DESIGN RISK ASSESSMENT OF ENNIATIN-CONTAINING SOLUTIONS FOR OROMUCOSAL USE

Main focus in this chapter:

- To evaluate if fusafungine ENNs are able to permeate the mucosa and reach blood circulation.
- To determine the influence of the excipient concentration variability on ENNs bioavailability.

1. INFLUENCE OF EXCIPIENTS

Fusafungine, a mixture of the cyclic hexadepsipeptides enniatins (ENNs) produced by *Fusarium lateritium* strains, is a medicinal product, originally patented in 1953 (FR1021824) and marketed under the trade names Locabiotal[®], Bioparox[®], Locabiosol[®] and Fusaloyos[®] [1]. It is claimed to have clinically relevant bacteriostatic and anti-inflammatory effects [2,3] and is used topically to treat upper respiratory tract diseases [4-6].

The summary of product characteristics (SmPC) indicates that no systemic absorption of fusafungine has been shown. However, no data substantiating this claim could be found in literature, questioning its validity. It is likely to assume that enniatins might pass the mucosa, since (i) it was recently demonstrated in an *ex vivo in vitro* Franz diffusion cell (FDC) experiment that enniatins are in fact capable of crossing the human skin barrier [7], (ii) it is generally accepted that mucosal permeation is significantly higher than skin permeation [8-13] (iii) enniatins in pharmaceutical preparations are mainly formulated in ethanol (EtOH) and isopropyl myristate (IPM), which are both chemical skin and mucosal penetration enhancers [14-23] and (iv) a considerable total water solubility of 0.3 mg/mL has been demonstrated for enniatins [7].

On the other hand, as EtOH and IPM were previously mentioned to be chemical penetration enhancers, their presence in topical formulations might thus play a key role in the bioavailability of enniatins after administration. According to the European Medicines Agency (EMA) guideline on

'specification and control tests on the finished product', excipients which affect the bioavailability of active substances must be subjected to a quantitative determination in each batch [24].

Therefore, the overall objective of this study was to quantitatively evaluate the transmucosal kinetics of enniatins, using excised buccal porcine mucosa in an *ex vivo in vitro* FDC set-up with the application of a quality-by-design (QbD) risk assessment of the quantitative excipient composition variability. This is of pivotal importance, since enniatins have recently been identified as mycotoxins, which are secondary metabolites produced by fungi, posing a health hazard by exerting a toxic activity on human or animal cells *in vitro* with 50% effect levels < 1000 µM [7,25-30]. The European Food and Safety Authority (EFSA) recently published their "scientific opinion on the risks to human and animal health related to the presence of beauvericin and enniatins in food and feed". Therein, it is concluded that for the moment, based on the limited data available, human health is considered not at risk after acute exposure to these mycotoxins, however, with regard to chronic exposure no such conclusions could be drawn. Insufficient data also did not allow for the calculation of risk assessment threshold limits (such as tolerable daily intake), so relevant *in vivo* toxicokinetic data are urgently needed [1]. Moreover, one study where mice were topically treated with fusafungine 1% for 10 days with two sprays daily showed histopathological changes, such as hyperplasia, low-grade dysplasia, congestion or oedema. Consequently, the authors already suggested a change or withdrawal of such locally applied agents [31].

The two main objectives of this study were (i) to investigate whether ENNs permeate the mucosa and reach the systemic circulation after oral application of fusafungine formulated preparations (such as Locabital®), and if so, their transmucosal kinetics will be quantified and (ii) to study the influence of excipient content variability on the ENNs penetration/permeation.

2. MATERIALS AND METHODS

2.1. Chemicals and reagents

The mycotoxin beauvericin (BEA), which was used as an internal standard, was supplied by BioAustralis (Smithfield NSW, Australia), while the enniatin mixture (ENNs) was obtained from Cfm Oscar Tropitzsch (Marktredwitz, Germany). As no formal ENN composition was supplied by the manufacturer (only e-mail correspondence), we experimentally determined the relative composition, assuming a relative response factor (RRF) = 1 for the individual constituents: 43.8% ENN B, 34.4% ENN B1, 14.0% ENN A1, 3.6% ENN D, 1.8% ENN A, 1.8% ENN E and 0.4% ENN C or F. These data were obtained by UHPLC-MS and UHPLC-UV (205 nm) normalised areas. For Locabiotol[®], a very similar relative composition was found by our group [32]. Five different batches of the finished pharmaceutical product Locabiotol[®] were purchased from different Belgian pharmacies. Ultrapure water (H₂O) was produced by an Arium pro VF TOC water purification system (Sartorius, Göttingen, Germany), resulting in ultrapure water of 18.2 MΩ × cm quality. ULC-MS grade formic acid (FA), 2-propanol and acetonitrile (ACN), used for preparation of the mobile phase, were purchased from Biosolve (Valkenswaard, The Netherlands). Sigma-Aldrich (St. Louis, MO, USA) supplied dimethyl sulfoxide (DMSO), isopropyl myristate (IPM) and 0.01 M phosphate buffered saline (PBS). Ethanol (EtOH) was purchased from Fisher Scientific (Waltham, MA, USA), who also supplied UHPLC grade ACN, HPLC grade methanol (MeOH) and acetone. Dimethylacetamide (DMA) was obtained from Janssen Chimica (Geel, Belgium). Cerestar (Mechelen, Belgium) supplied pharma grade hydroxypropyl-β-cyclodextrin (HPBCD), used as a solubilising modifier to the receptor fluid (PBS), to assure sink conditions of the hydrophobic cyclic depsipeptides throughout the experiment [33].

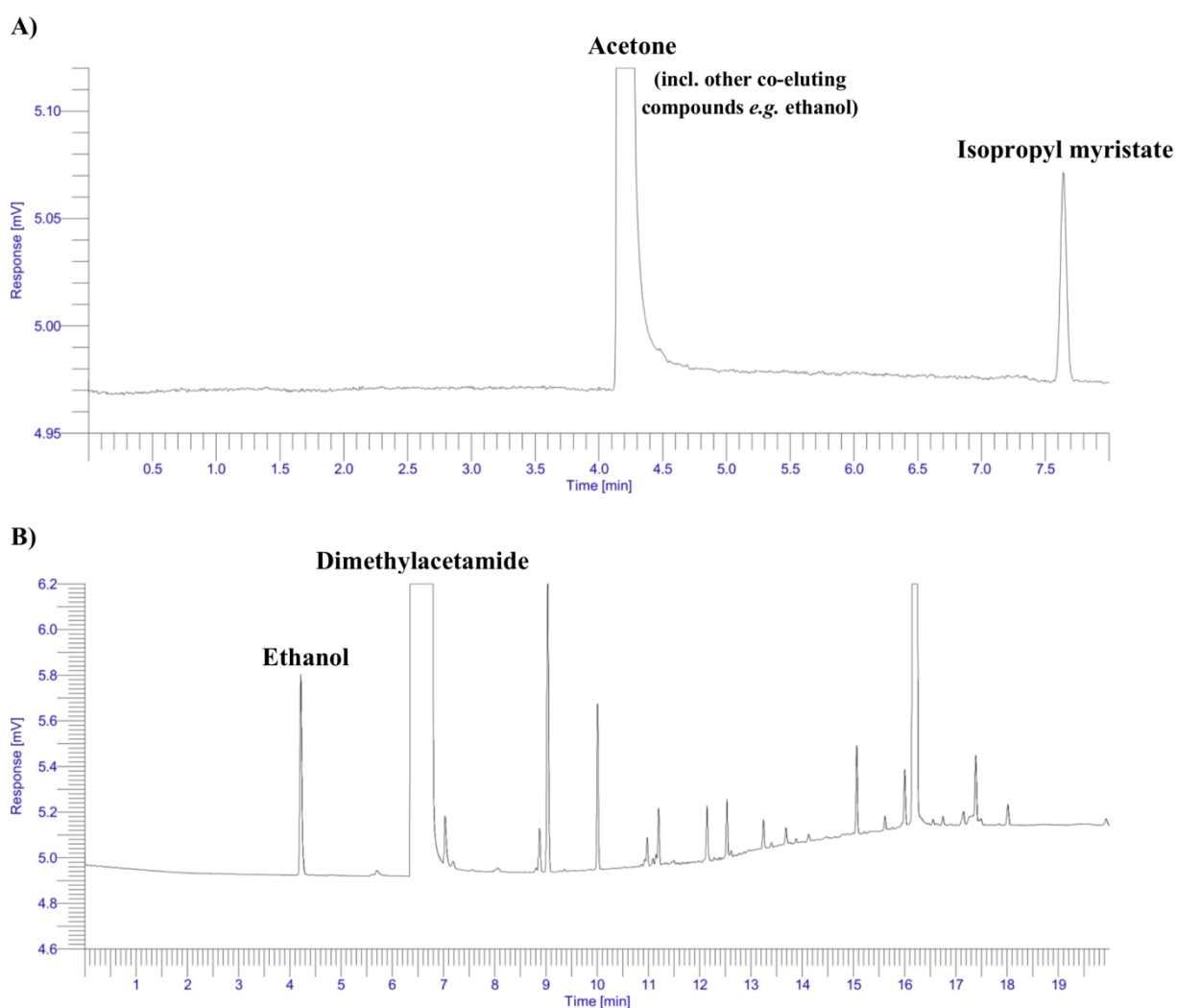
2.2. Analytical methods

GC-FID determination of EtOH and IPM

Because no quantitative excipient composition of Locabiotol[®] is given (in SmPC nor in the patient information leaflet (PIL)), the amount EtOH and IPM was first quantitatively determined using an in-house developed GC-FID method. This platform consisted of a Clarus 600 GC equipped with a liquid autosampler and a programmable split/splitless capillary injector, coupled to a FID detector and operated by TotalChrom V6.3.2 software (Perkin Elmer, Waltham, Massachusetts, USA). Chromatographic separation was achieved on a SE-54 (5%-phenyl)(1%-vinyl)-methylpolysiloxane column (30 m × 0.32 mm × 0.25 μm) obtained from Agilent (Santa Clara, CA, USA), with N₂ as carrier gas. A method summary for both compounds, including the GC temperature gradient and sample information, is given in Table 1. Typical GC-FID chromatograms for EtOH and IPM in Locabiotol[®] are shown in Figure 1.

Table 1: GC-FID method for the quantitative determination of EtOH and IPM in Locabital®.

Parameter	General settings	
N ₂ linear velocity	12.0 cm/s	
H ₂ supply detector	40 mL/min	
Air supply detector	400 mL/min	
Injection volume	1 µL	
Split ratio	50:1	
Injection temperature	250°C	
Detector temperature	250°C	
Compound	EtOH	IPM
Oven temperature programme	0 – 7.5 min: 100°C 7.5 – 13 min: 30°C/min 13 – 20 min: 265°C	0 – 8 min: 223°C (isothermal)
Retention time	4.2 min	7.7 min
Target concentration	1000 ppm (V/V)	100 ppm (V/V)
Solvent	dimethylacetamide (DMA)	acetone

**Figure 1:** Typical GC-FID chromatograms of Locabital® for the assay of IPM (A) and EtOH (B).

These methods were in-house verified for their linearity, limit of detection (LoD), specificity, accuracy, repeatability and robustness. Linearity was determined using five concentrations, each in triplicate (50, 75, 100, 125 and 150 ppm (V/V) for IPM and 500, 750, 1000, 1250 and 1500 ppm (V/V) for EtOH). Repeatability and accuracy were determined using the 75 – 125 ppm (V/V) solutions for

IPM and the 750 – 1250 ppm (V/V) solutions for EtOH. Specificity was assessed using MeOH as a closely related structure. LoD was determined using the signal-to-noise approach, where LoD corresponds to a signal-to-noise ratio of 3:1. Robustness was assessed using the response factors and retention times as system suitability tests, performed at the start of each analysis.

For the determination of IPM, Locabital® samples were prepared by appropriate dilution in acetone (target concentration = 100 ppm V/V) and reference solutions of 50, 75, 100, 125 and 150 ppm (V/V) IPM in acetone were prepared starting from a 1% (V/V) IPM in acetone stock solution. For the determination of EtOH in the Locabital® samples, these were appropriately diluted in DMA (target concentration = 1000 ppm (V/V)), with reference solutions of 500, 750, 1000, 1250 and 1500 ppm (V/V) EtOH in DMA, prepared from a 10% V/V EtOH in DMA stock solution.

UHPLC-MS/MS determination of ENNs

Previously, a sensitive, specific and high-throughput bioanalytical ultra high performance liquid chromatography tandem mass spectrometry (UHPLC-MS/MS) method was developed for the quantitative and simultaneous determination of cyclic depsipeptide mycotoxins beauvericin and enniatins (A, A1, B, B1, D, E, C/F) in human skin Franz diffusion cell samples (**Chapter IV**). Briefly, the UHPLC-MS/MS platform consisted of an Acquity UHPLC equipped with a Xevo TQ-S MS detector (Waters, Milford, MA, USA). For chromatographic separation, an Acquity UHPLC CSH C18 column (1.7 μm , 100 \times 2.1 mm, 130Å), attached to an Acquity UHPLC VanGuard pre-column (1.7 μm , 5 \times 2.1 mm, 130Å), thermostated at 45°C, was used (Waters, Milford, MA, USA). The needle wash consisted of 10/10/80 (V/V/V) DMSO/2-propanol/ACN. The isocratic flow rate was set to 0.6 mL/min, using 70/30 (V/V) ACN/H₂O with 0.1% FA and 0.1% 2-propanol as mobile phase. The run time was 4.5 min and the injection volume was 10 μL . The mass spectrometer was operated in the positive electrospray ionization mode (ESI+), with a cone voltage of 50 V and a capillary voltage of 3.50 kV. Cone and desolvation gas flows were respectively 150 and 1000 L/h, while source and desolvation temperatures were set at 150 °C and 600 °C, respectively. Data were acquired using Masslynx software (V4.1 SCN 843, Waters, Milford, MA, USA). BEA was used as an internal standard for the enniatin mixture. The selected precursor and product ions, with the applied collision energies between brackets, are given. The selected precursor ion for ENN B was m/z 639.91 with two selected product ions at m/z 196.08 (25 V) and m/z 527.26 (22 V), for ENN D and B1 the precursor ion was m/z 653.99 and m/z 196.09 (23 V) and m/z 541.05 (21 V) were the product ions. For ENN E and A1, m/z 668.07 was the precursor ion and m/z 209.99 (24 V) and m/z 555.29 (21 V) were its product ions. ENNs A and C or F have a precursor ion of m/z 682.47 with product ions m/z 209.93 (26 V) and m/z 555.01 (23 V). Lastly BEA has a precursor ion at m/z 783.94, with m/z 244.01 (24 V) and m/z 623.23 (23 V) as its product ions. This method has also been successfully verified. It was demonstrated that

beauvericin and enniatins are stable for at least 7 days when formulated in different organic or aqueous mixtures and under different storage conditions. Additional attention was paid to the investigation of analyte losses due to adsorption issues. It was shown that at least 50% organic solvent is required to prevent significant adsorption to glass. The limits of detection were 17 pg/mL for BEA and ENN B, 14 pg/mL for ENN D and ENN B1, 15 pg/mL for ENN E, ENN A1 and ENN A and 10 pg/mL for ENN C/F. More details about the development and verification of the applied bioanalytical method are given in **Chapter IV**.

2.3. In vitro FDC study using buccal porcine mucosa

The set-up consisted of static Franz diffusion cells with a receptor compartment of 5 mL and an available diffusion area of 0.64 cm² (Logan Instruments Corp., New Jersey, USA). Buccal porcine mucosa were collected from freshly slaughtered pigs (Porc Meat Zele NV, Zele, Belgium). Immediately thereafter, the mucosa samples were cleaned with 0.01 M PBS pH 7.4, wrapped in aluminium foil and stored at -35 °C. Just before the start of the experiments, the mucosa was thawed, mounted on a template and dermatomed using an electrically powered dermatome set at 0.64 mm (Integra Life Sciences, New Jersey, USA). The experimentally obtained overall thickness of the mucosa, determined with a micrometer (Mitutoyo, Tokyo, Japan), was 524 ± 11 µm (mean ± SEM, n = 48). The samples were visually inspected for damage and were then sandwiched between the donor and acceptor chambers, with the epithelial layer facing upwards, making sure all air underneath is removed. The whole assembly was fixed on a magnetic stirrer and the receptor fluid was continuously stirred using a Teflon coated magnetic stirring bar (600 rpm). Before starting the experiments, the integrity was checked by measuring the impedance using an automatic micro-processor controlled LCR impedance bridge (Tinsley, Croydon, UK). Mucosa pieces with an impedance value < 10 kΩ, a system-suitability cut-off, were discarded and replaced by a new piece [34]. Then, the dose solutions were topically applied (400 µL), the donor chamber was covered with parafilm and the temperature of the receptor compartment was kept at 37 ± 1 °C. Samples (200 µL) were drawn at regular time intervals (0.5, 1, 2, 3, 4, 6 and 8h) from the sampling port and were immediately replaced by 200 µL fresh receptor solution. The analytically determined assay values in the FDC samples were correspondingly corrected for these replenishments. At the end of the experiment (*i.e.* after 8h), the remaining donor solution was removed from the mucosa surfaces by swabbing with cotton wool, which was extracted overnight with 70:30 ACN:H₂O (V/V) at 40 °C by mild shaking (150 rpm), using a Thermo max Q400 incubator shaker (Thermo Scientific, Waltham, MA, USA). The exposed mucosa were carefully cut out using a scalpel and extracted with 1 mL 95:5 ACN:H₂O (V/V) overnight at 25 °C with mild shaking at 750 rpm using a Thermomixer comfort (Eppendorf, Hamburg, Germany). These were all analysed and used to construct a mass balance: the

recovery of each enniatin was between $80.3 \pm 1.3\%$ and $101.9 \pm 1.4\%$ (mean \pm SEM, $n = 24$), confirming the quantitative validity of our data.

For the preparation of the dose solutions the following rationale is applied. According to the PIL/SmPC, Locabiotol® is composed of IPM as main solvent, as well as ethanol as most important ingredient, next to an aromatic mixture and the sweetener saccharine. Therefore, the concentration of both IPM and EtOH in Locabiotol® was determined by GC-FID. Based on this information, the dose solutions for investigation of composition variability within the context of a quality-by-design risk assessment are investigated for varying EtOH concentrations with matching IPM concentrations: 1/99, 3/97, 5/95, 10/90 (V/V) EtOH/IPM, while maintaining a constant total enniatin concentration of 1 mg/mL.

2.4. Kinetic data analysis

The mucosa permeation parameters were calculated from the individual curves of the cumulative amount of each enniatin permeated as a function of time. Steady-state flux (J_{ss}) was derived from the slope of the linear portion of the curve divided by 0.64 cm^2 to correct for the exposed mucosal area. The lag time (t_{lag}) was estimated by extrapolating the linear portion of the curve to the time-axis. From these experimentally determined secondary kinetic parameters, the apparent primary parameters could be calculated [35]. The permeability coefficient $k_{p,v}$ was obtained using the following equation: $k_{p,v} = J_{ss}/C_v$, where C_v is the experimentally determined concentration of each enniatin in the vehicle (dose formulation). From the mucosa extractions, the enniatin concentrations within the mucosa were also determined, taking the respective mucosa volumes into account: mucosa volume (cm^3) = mucosa thickness (cm) \times mucosa surface (0.64 cm^2).

To determine statistically significant differences at a 95% confidence level, one-way analyses of variances (ANOVA), incl. homogeneity of variances (Levene's test), were performed. If these ANOVA analyses demonstrated a significant difference, a post hoc analysis was performed as well. In the case of equal variances, a Bonferroni test was used. When the assumption of equal variances was violated, a post hoc Games-Howell test (for unequal variances) was applied.

2.5. Calculation of steady-state plasma concentration after buccal application

For a clinical interpretation of these results, the steady-state plasma concentration after buccal application is calculated as well, using the following equation: $C_{pl,ss,buccal} = (A \times k_{p,v} \times C_v)/Cl$, where A is the exposed mucosal area, C_v is the compound concentration in the vehicle, Cl is the plasma clearance of the compound and $k_{p,v}$ is the permeability coefficient for the investigated mycotoxins, obtained from our *ex vivo in vitro* transmucosal FDC experiment [36]. For ENN B1, an average plasma clearance of 1.96 L/h/kg was previously reported [29]. For the other enniatins, a similar plasma

clearance was assumed. An average body weight of 70 kg and total surface area of 100 cm² for the oral mucosa was considered for the calculations [37].

3. RESULTS AND DISCUSSION

3.1. GC-FID determination of EtOH and IPM

During the method evaluation, a linear range was established between 50 – 150 ppm (V/V) for IPM and 500 – 1500 ppm (V/V) for EtOH, confirmed by a coefficient of determination (R^2) of respectively 0.995 and 0.999 and the lack-of-fit F-test ($\alpha = 0.05$). For accuracy, the bias ranged between -1.68 – 0.59% for IPM and between 0.28 – 2.92% for EtOH, which comply with the previously set criteria (< 3%) [38]. For repeatability, relative standard deviations (RSD) of 1.86 – 4.15% were obtained for IPM, while this was 1.52 – 5.28% for EtOH, which are slightly higher than the pre-set limit of 3% [39], however considered still acceptable for our purposes. Limit of detection was found to be 3.0 ppm (V/V) for IPM and 4.2 ppm (V/V) for EtOH. As discrimination between EtOH and MeOH was achieved by visual examination of the chromatograms, the method specificity was considered acceptable. Concerning robustness, the method was considered sufficiently robust: retention times remained unchanged and response factors were in agreement with the repeatability (2.3% RSD for IPM and 3% RSD for EtOH) during the analytical experiments.

Experimental determination of the amount of IPM and EtOH in the different batches of Locabiotol® revealed an overall average content of $91.60 \pm 2.02\%$ (V/V) IPM and $1.67 \pm 0.03\%$ (V/V) EtOH after analysis (mean \pm SEM, $n = 5$). No statistically significant differences were found between the batches ($p > 0.10$).

3.2. Franz diffusion cell experiments using buccal porcine mucosa

Our results demonstrate that ENNs are able to diffuse through buccal porcine mucosa skin when applied in an EtOH/IPM solution. Figure 2 shows the mean cumulative amount (ng) versus time (h) plots for the different enniatins applied on buccal porcine mucosa in the four varying EtOH/IPM dose formulations. Only the amount of ENN A and ENN C/F in the receptor fluid samples was too low to obtain useful cumulative amount versus time curves and were therefore not taken into account. All other ENNs confirmed the unidirectional steady-state principle. Linear regression of the individual curves was performed for each compound between 2 – 8h ($R^2 \geq 0.96$), in order to calculate the transmucosal parameters, which are presented in Table 2.

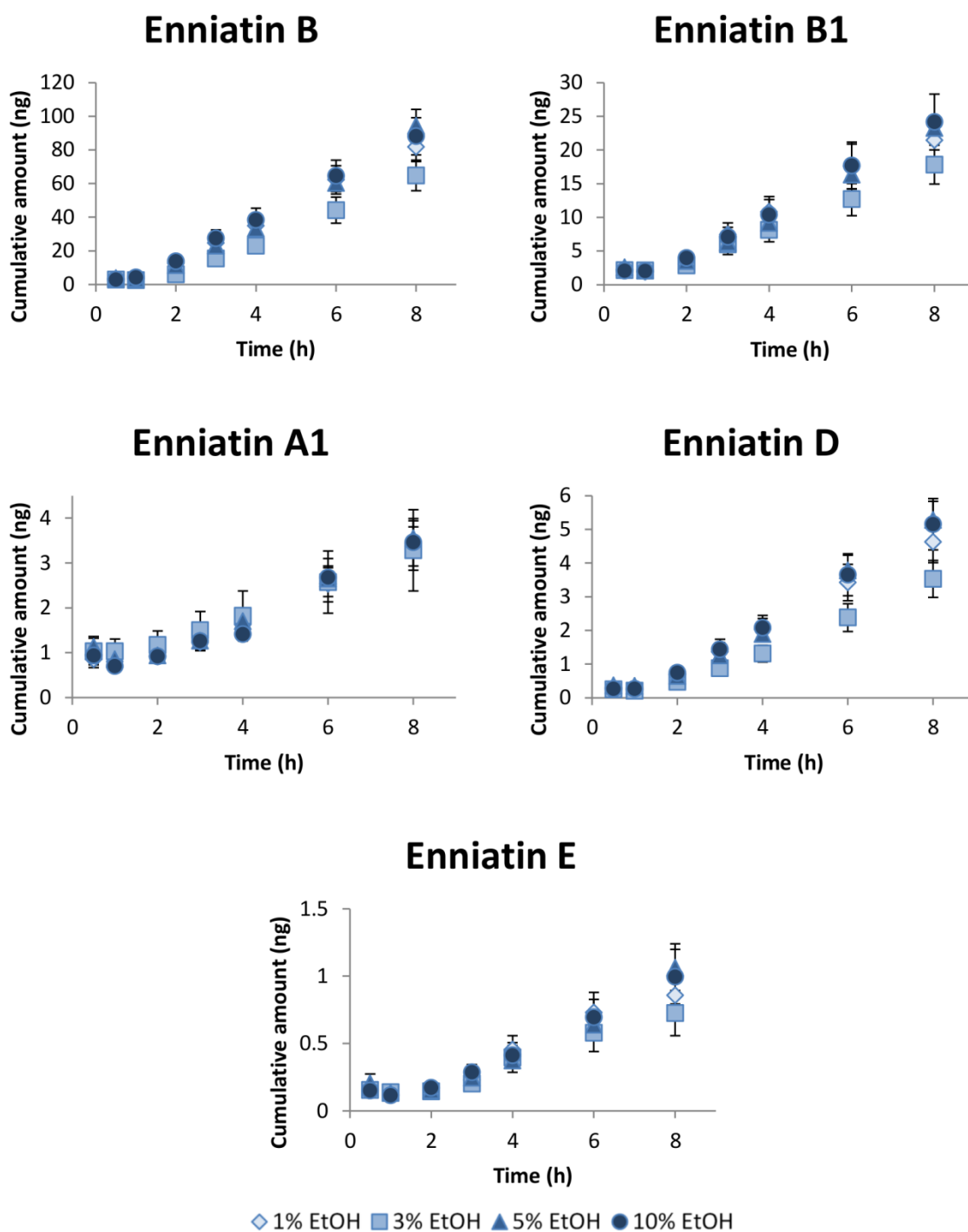


Figure 2: Individual cumulative amount (ng) versus time (h) curves of the investigated enniatins for buccal porcine mucosa when exposed to dose solutions containing 1 mg/mL total enniatin mixture in varying EtOH/IPM concentrations (1/99, 3/97, 5/95 and 10/90, V/V) (mean \pm SEM, n = 2 – 6).

Table 2: Transmucosal parameters for enniatins obtained through buccal pig mucosa after applying 1 mg/mL dose solutions with varying EtOH/IPM (V/V) concentrations (mean \pm SEM, n = 2 – 6).

EtOH/IPM (V/V)	J_{ss} (ng/(cm ² × h))				Q_{8h} (%) ⁽¹⁾			
	1/99	3/97	5/95	10/90	1/99	3/97	5/95	10/90
ENN B	20.11 \pm 2.00	15.16 \pm 1.98	21.24 \pm 1.76	19.43 \pm 2.13	0.048 \pm 0.006	0.035 \pm 0.005	0.053 \pm 0.005	0.053 \pm 0.007
ENN B1	5.54 \pm 0.79	3.45 \pm 0.62	5.96 \pm 0.73	5.36 \pm 0.93	0.018 \pm 0.003	0.014 \pm 0.002	0.020 \pm 0.003	0.021 \pm 0.004
ENN A1	0.68 \pm 0.12	0.56 \pm 0.16	0.90 \pm 0.19	0.81 \pm 0.12	0.006 \pm 0.001	0.006 \pm 0.002	0.008 \pm 0.002	0.008 \pm 0.001
ENN D	1.13 \pm 0.14	6.79 \pm 0.12	1.18 \pm 0.10	1.16 \pm 0.16	0.034 \pm 0.005	0.024 \pm 0.004	0.033 \pm 0.004	0.038 \pm 0.006
ENN E	0.22 \pm 0.04	0.14 \pm 0.02	0.24 \pm 0.04	0.22 \pm 0.04	0.014 \pm 0.003	0.011 \pm 0.002	0.015 \pm 0.003	0.014 \pm 0.002

EtOH/IPM (V/V)	$k_{p,v}$ ($\times 10^{-5}$ cm/h)				Lag time (h)			
	1/99	3/97	5/95	10/90	1/99	3/97	5/95	10/90
ENN B	4.36 \pm 0.43	3.25 \pm 0.43	4.75 \pm 0.40	4.68 \pm 0.51	1.24 \pm 0.22	1.56 \pm 0.16	0.93 \pm 0.20	0.94 \pm 0.19
ENN B1	1.62 \pm 0.23	1.06 \pm 0.19	1.79 \pm 0.22	1.87 \pm 0.32	1.16 \pm 0.24	0.73 \pm 0.21	1.13 \pm 0.05	0.93 \pm 0.08
ENN A1	0.50 \pm 0.08	0.43 \pm 0.12	0.67 \pm 0.14	0.70 \pm 0.11	0.67 \pm 0.38	– ⁽²⁾	0.53 \pm 0.20	0.68 \pm 0.21
ENN D	3.04 \pm 0.39	2.14 \pm 0.33	2.95 \pm 0.25	3.47 \pm 0.48	1.20 \pm 0.14	1.31 \pm 0.09	0.94 \pm 0.18	1.16 \pm 0.13
ENN E	1.20 \pm 0.22	0.80 \pm 0.14	1.36 \pm 0.21	1.45 \pm 0.30	0.86 \pm 0.12	0.50 \pm 0.11	0.92 \pm 0.05	0.86 \pm 0.12

(1) Q_{8h} = the cumulative quantity, expressed as percentage of the effective dose applied, obtained after one day.

(2) Lag time could not be calculated due to a positive intercept in the linear regression.

Table 3: Local buccal pig mucosa concentrations for enniatins obtained after applying in 1 mg/mL total enniatins dose solutions with varying EtOH/IPM (V/V) concentrations for 8h (mean \pm SEM, n = 6).

EtOH/IPM (V/V)	Local mucosa concentrations (μ M)							
	ENN B	ENN B1	ENN A1	ENN D	ENN A	ENN E	ENN C/F	Total ENNs
1/99	13.23 \pm 2.24	5.67 \pm 2.00	1.62 \pm 0.48	0.56 \pm 0.13	0.16 \pm 0.05	0.22 \pm 0.06	0.04 \pm 0.01	21.49 \pm 4.84
3/97	18.96 \pm 2.16	9.78 \pm 2.24	2.41 \pm 0.43	0.82 \pm 0.13	0.24 \pm 0.05	0.32 \pm 0.05	0.06 \pm 0.01	32.59 \pm 5.00
5/95	15.06 \pm 3.09	6.31 \pm 2.51	1.63 \pm 0.48	0.57 \pm 0.15	0.16 \pm 0.05	0.22 \pm 0.06	0.04 \pm 0.01	23.98 \pm 6.34
10/90	11.00 \pm 1.54	3.81 \pm 0.97	1.08 \pm 0.22	0.44 \pm 0.09	0.10 \pm 0.02	0.16 \pm 0.03	0.03 \pm 0.01	16.62 \pm 2.86

Upon comparison of the $k_{p,v}$, J_{ss} , t_{lag} and Q_{8h} of the four different dose solutions, containing a fixed concentration of enniatins and a varying amount of EtOH/IPM (V/V), for each compound separately, no statistically significant differences were observed ($p > 0.05$).

Figure 3 presents a distribution overview of the ENN B (*i.e.* the most abundant ENN present in Locabiotol®) concentrations in the different compartments (dose solution, mucosa and receptor fluid) obtained under our experimental conditions, applying dose solutions of 1 mg/mL total enniatin mixture. The obtained distribution pattern is comparable for the four different dose solutions: a decreasing concentration gradient is observed, however, with relatively high local mucosal concentrations. For the other investigated enniatins, a similar distribution was obtained (data not shown).

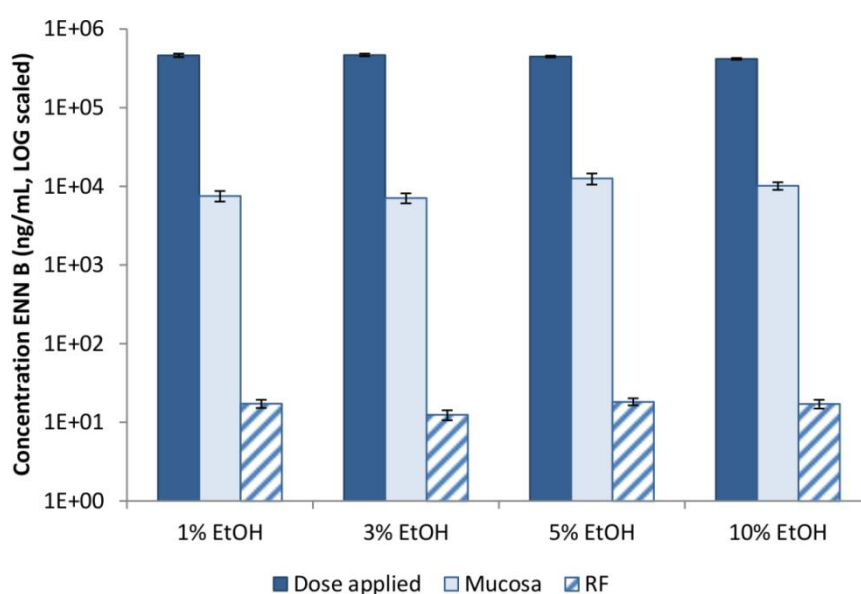


Figure 3: Distribution overview of the ENN B concentrations in the different compartments (dose solution, mucosa and receptor fluid) obtained under our experimental conditions, applying dose solutions of 1 mg/mL total enniatin mixture.

Local mucosa concentration for each enniatin is given in Table 3. After 8h exposure under our operational conditions, a total enniatin concentration up to 33 μ M was found. No statistically significant difference in mucosa concentration was found between the different dose solutions for each investigated enniatin ($p > 0.05$).

From this QbD approach, it is concluded that the transmucosal permeability of the enniatins through buccal porcine mucosa is not affected with varying concentrations of the excipients EtOH and IPM within the investigated range. There is thus no risk of a significantly different (*i.e.* increased/decreased) systemic enniatin availability in terms of composition variability within the currently tested EtOH/IPM range (1/99 – 10/90, V/V). This is also confirmed by the enniatin amount

penetrated into the mucosa, for which no significant difference was found between the different dose solutions, investigated for each enniatin separately.

After 8 hours, 0.006 – 0.053% of the dose applied was cumulatively found in the receptor chamber (Q_{8h}), depending on the enniatin. Overall average permeability coefficients were determined to be between 0.60×10^{-5} and 4.26×10^{-5} cm/h, while for J_{ss} this was between 0.21 and 18.99 ng/(cm² × h). Overall average lag times ranged from 0.63 – 1.17h for ENN A1 and ENN B, respectively. These are considerably shorter than the lag times reported for transdermal permeation through intact (\pm 8h) and even damaged (\pm 6h) human skin, when applied in a dose formulation with up to 60% EtOH [7]. This confirms previous observations, explained by the difference in anatomy between skin and mucosa: the skin has an extensive barrier function exerted by the stratum corneum, which the mucosa is lacking. This also explains the higher $k_{p,v}$ and J_{ss} values obtained in this mucosa study.

Furthermore, an inverse relationship between log P on the one hand and average $k_{p,v}$, t_{lag} and Q_{8h} values on the other hand was observed. Indeed, ENN B, with the lowest log P of 4.68 showed the highest permeability coefficients, lag times and Q_{8h} values, whereas ENN A1, having a log P of 5.48, respectively, had the lowest $k_{p,v}$'s, t_{lag} 's and Q_{8h} 's.

Taking into account that the marketed preparations contain up to a 10 times higher enniatin dosage than the dose experimentally applied in this study and assuming linear extrapolation, local mucosa concentrations up to 330 μ M and transmucosal steady-state fluxes as high as 0.2 μ g/(cm² × h) might be expected.

3.3. Clinical interpretation

This study proved that enniatins dissolved in IPM/EtOH mixtures are indeed capable of permeating the mucosa, at least questioning current SmPC information. Our *ex vivo in vitro* study neglects the *in vivo* situation where continuous saliva production and flow is present, metabolism might occur, as well as GI absorption of the swallowed ENNs. Moreover, in these calculations a constant exposure to the fusafungine solution is assumed. Indeed, a clear systemic exposure can be expected, since it was already shown by Devreese *et al.* that ENN B1 is rapidly absorbed after oral administration ($T_{1/2}$ = 0.15h, T_{max} = 0.24h) and that a high absolute oral bioavailability (90.9%) is reached [29]. As such, our study can be considered as a “worst-case” situation. The calculated steady-state plasma concentrations after buccal application for the different enniatins, given in Table 4, range from 0.026 mg/L for ENN E to 1.339 mg/L for ENN B. Taking into account that the marketed preparations contain up to a 10 times higher enniatin dosage than the dose experimentally applied in this study and assuming linear extrapolation, steady-state plasma concentrations after buccal application up to 13.39 mg/L might be expected. Moreover, according to the patient information given for these products (Locabiotol[®], patient information leaflet), the spray should be applied every 4h, likely

causing local built-up, which might eventually lead to a mucosal enniatin sink reservoir, from which enniatins can slowly diffuse into the blood circulation and result in undesired chronic exposure to these mycotoxins. It is therefore recommended in the treatment of minor, rather innocent, upper respiratory infections, to question enniatin-based preparations, since for the mycotoxins present in the formulation local and systemic toxic effects cannot be excluded [7].

Table 4: Estimated enniatin steady-state plasma concentrations $C_{pl,ss,buccal}$ (mg/L) after buccal application.

Compound	$k_{p,v}$ ($\times 10^{-5}$ cm/h) ⁽¹⁾	C_v (mg/mL) ⁽²⁾	Cl (L/h) ⁽³⁾	A (cm ²) ⁽⁴⁾	$C_{pl,ss,buccal}$ (mg/L) ⁽⁵⁾
ENN B	4.26	0.43	136.85	100	1.339
ENN B1	1.58	0.31	136.85	100	0.358
ENN A1	0.61	0.15	136.85	100	0.067
ENN D	2.90	0.04	136.85	100	0.085
ENN E	1.20	0.03	136.85	100	0.026

(1) Overall mean $k_{p,v}$ values obtained from our *ex-vivo in-vitro* transmucosal FDC experiment.

(2) The label claim of Locabiotol® is 10 mg/mL fusafungine. The quantitative composition of the enniatins in this formulation was previously determined (D'Hondt *et al.*, 2014). Enniatins C/F and A were not taken into account (due to $k_{p,v}$ unavailable).

(3) For ENN B1 a mean plasma clearance of 1.96 L/h/kg was previously reported [29]. For the other enniatins, a similar plasma clearance was assumed and an average body weight of 70 kg was taken into account.

(4) The total surface area of the oral mucosa was assumed to be 100 cm² [37].

(5) Steady-state plasma concentration after buccal application: $C_{pl,ss,buccal} = (A \times k_{p,v} \times C_v) / Cl$.

Interestingly, approximately one year after our group published these results, the European Medicines Agency (EMA) Pharmacovigilance Risk Assessment Committee (PRAC) advised to withdraw nasal and mouth sprays containing fusafungine from the market because of its negative risk-benefit ratio, particularly the risk for serious allergic reactions and antibiotic resistance (EMEA/H/A-31/1420, February 12th, 2016). This negative advice was followed by the CMDh (Coordination Group for Mutual Recognition and Decentralised Procedures – Human), which has endorsed by consensus the revocation of marketing authorisations for fusafungine sprays in the EU. Member States will implement this decision and start revoking the medicinal products affected by the procedure in their territories, according to an agreed timetable (EMEA/H/A-31/1420, April 1st, 2016). For example, in Belgium the Federal Agency for Medicines and Health Products (FAMHP) has issued the revocation of Locabiotol (May 4th, 2016) [40].

4. CONCLUSIONS

It was demonstrated in this study that enniatins in topical medicines are capable of permeating the mucosa barrier. Furthermore, it is also proven that the transmucosal permeability of the enniatins through buccal porcine mucosa is not affected with varying concentrations of the penetration enhancers EtOH and IPM, present in marketed fusafungine preparations.

Up to 0.05% of the dose applied was cumulatively detected in the receptor fluid after 8h exposure and high local mucosa concentrations were found as well. Moreover, steady-state plasma

concentrations after buccal application were estimated to reach up to 1.3 mg/L, or 13 mg/L for the marketed preparations, which contain up to a 10 times higher enniatin dosage and assuming linear extrapolation. Bearing in mind that this *in vitro* study represents a worst-case approach, neglecting the saliva flow, enniatin-based therapies should be questioned in the treatment of innocent upper respiratory tract infections, because of the negative benefit-risk ratio, as long-term chronic effects of these mycotoxins have not yet been thoroughly investigated.

5. REFERENCES

- [1] European Food Safety Authority (EFSA). Scientific opinion on the risks to human and animal health related to the presence of beauvericin and enniatins in food and feed. *EFSA Journal*, 2014; 12(8): 3802, pp. 174.
- [2] German-Fattal M. Fusafungine an antimicrobial agent for the local treatment of respiratory tract infections, *Clinical Drug Investigation* 1996; 12(6): 308-317.
- [3] Krosiak M. Efficacy and acceptability of fusafungine, a local treatment for both nose and throat infections, in adult patients with upper respiratory tract infections. *Current Medical Research and Opinion* 2002; 18(4): 194-200.
- [4] Hamann KF. Fusafungin therapy of acute laryngitis – A phase IV study. *HNO* 1994; 42(2): 113-118.
- [5] German-Fattal M. Fusafungine, an antimicrobial with anti-inflammatory properties in respiratory tract infections: Review, and recent advances in cellular and molecular activity, *Clinical Drug Investigation* 2001; 21(9): 653-670.
- [6] Lund VJ, Grouin JM, Eccles R, Bouter C, Chabolle F. Efficacy of fusafungine in acute rhinopharyngitis: a pooled analysis. *Rhinology* 2004; 42(4): 207-212.
- [7] Taevernier L, Veryser L, Roche N, Peremans K, Burvenich C, Delesalle C, De Spiegeleer B. Human skin permeation of emerging mycotoxins (beauvericin and enniatins). *Journal Of Exposure Science And Environmental Epidemiology* 2016; 26: 277-287.
- [8] Amores S, Lauroba J, Calpena AC, Colom H, Gimeno A, Domenech J. A comparative *ex vivo* drug permeation study of beta-blockers through porcine buccal mucosa. *International Journal of Pharmaceutics* 2014; 468: 50-54.
- [9] Boonen J, Baert B, Roche N, Burvenich C, De Spiegeleer B. Transdermal behaviour of the N-alkylamide spilanthol (affinin) from *Spilanthes acmella* (Compositae) extracts. *Journal of Ethnopharmacology* 2010; 127: 77-84.
- [10] Boonen J, Baert B, Burvenich C, Blondeel P, De Saeger S, De Spiegeleer B. LC–MS profiling of N-alkylamides in *Spilanthes acmella* extract and the transmucosal behaviour of its main bio-active spilanthol. *Journal of Pharmaceutical and Biomedical Analysis* 2010; 53: 243-249.
- [11] Galey WR, Lonsdale HK, Nacht S. The *in vitro* permeability of skin and buccal mucosa to selected drugs and tritiated water. *Journal of Investigative Dermatology* 1976; 67: 713-717.
- [12] Hu L, Silva SMC, Damai BB, Martin R, Michniak-Kohna BB. Transdermal and transbuccal drug delivery systems: Enhancement using iontophoretic and chemical approaches. *International Journal of Pharmaceutics* 2011; 421: 53-62.
- [13] Squier CA, Johnson NW, Hopps RM. Human Oral Mucosa: Development structure and function. Blackwell Scientific Publications, Oxford, 1976, pp. 176.
- [14] Squier CA, Cox P, Hall BK. Enhanced penetration of nitrosonornicotine across oral mucosa in the presence of ethanol. *Journal of Oral Pathology & Medicine* 1986; 15(5): 276-279.

- [15] Kai T, Mak VHW, Potts RO, Guy RH. Mechanism of percutaneous penetration enhancement: Effect of n-alkanols on the permeability barrier of hairless mouse skin. *Journal of Controlled Release* 1990; 12(2): 103-112.
- [16] Coutel-Egros A, Maitani Y, Veillard M, Machida Y, Nagai T. Combined effects of pH, cosolvent and penetration enhancers on the *in vitro* buccal absorption of propranolol through excised hamster cheek pouch. *International Journal of Pharmaceutics* 1992; 84: 117-128.
- [17] Obata Y, Takayama K, Maitani Y, Machida Y, Nagai T. Effect of ethanol on skin permeation of nonionized and ionized diclofenac. *International Journal of Pharmaceutics* 1993; 89(3): 191-198.
- [18] Turunen TM, Urtti A, Paronen P, Audus KL, Rytting JH. Effect of some penetration enhancers on epithelial membrane lipid domains: evidence from fluorescence spectroscopy studies. *Pharmaceutical Research* 1994; 11(2): 288-294.
- [19] Brinkmann I, Muller-Goymann CC. An attempt to clarify the influence of glycerol, propylene glycol, isopropyl myristate and a combination of propylene glycol and isopropyl myristate on human stratum corneum. *Pharmazie* 2003; 60(3): 215-220.
- [20] Williams AC, Barry BW. Penetration enhancers. *Advanced Drug Delivery Reviews* 2004; 56(5): 603-618.
- [21] Nicolazzo JA, Reed BL, Finnin BC. Modification of buccal drug delivery following pretreatment with skin penetration enhancers. *Journal of Pharmaceutical Sciences* 2004; 93(8): 2054-2063.
- [22] Engelbrecht TN, Demé B, Dobner B, Neubert RH. Study of the influence of the penetration enhancer isopropyl myristate on the nanostructure of stratum corneum lipid model membranes using neutron diffraction and deuterium labelling. *Skin Pharmacology and Physiology* 2012; 25(4): 200-207.
- [23] Santos P, Watkinson AC, Hadgraft J, Lane ME. Influence of penetration enhancer on drug permeation from volatile formulations. *International Journal of Pharmaceutics* 2012; 439: 260-268.
- [24] European Medicines Agency (EMA). Specifications and control tests on the finished product. Directive 75/318/EEC: 83-94, 1992, pp. 12.
- [25] Jestoi M. Emerging *Fusarium*-mycotoxins fusaproliferin, beauvericin, enniatins, and moniliformin - A review. *Critical Reviews in Food Science and Nutrition* 2008; 48: 21-49.
- [26] Tedjiotsop Feudjio F, Dornetshuber R, Hoffmann O, Lemmens-Gruber R, Berger W. Beauvericin and enniatin: Emerging toxins and/or remedies? *World Mycotoxin Journal* 2010; 3: 415-430.
- [27] Faeste CK, Ivanova L, Uhlig S. *In vitro* metabolism of the mycotoxin enniatin B in different species and cytochrome p450 enzyme phenotyping by chemical inhibitors. *Drug Metabolism and Disposition* 2011; 39(9): 1768-1776.
- [28] Kolf-Clauw M, Sassahara M, Luciola J, Rubira-Gerez J, Alassan-Kpembi I, Lyazhri F, Borin C, Oswald IP. The emerging mycotoxin, enniatin B1, down-modulates the gastrointestinal toxicity of T-2 toxin *in vitro* on intestinal epithelial cells and *ex vivo* on intestinal explants. *Archives of Toxicology* 2013; 87(12): 2233-2241.

- [29] Devreese M, Broekaert N, De Mil T, Fraeyman S, De Backer P, Croubels S. Pilot toxicokinetic study and absolute oral bioavailability of the *Fusarium* mycotoxin enniatin B1 in pigs. *Food and Chemical Toxicology* 2014; 63: 161-165.
- [30] Taevernier L, Wynendaele E, De Vreese L, Burvenich C, De Spiegeleer B. The mycotoxin definition reconsidered towards fungal cyclic depsipeptides. *Journal of Environmental Science and Health, Part C* 2016; 34: 114-135.
- [31] Yuca K, Çankaya H, Bayram I, Özbek H, Kiris M. Local irritant effects of topical oral sprays on oral mucosa in mice. *Advances in Therapy* 2006; 23(1): 98-106.
- [32] D'Hondt M, Bracke N, Taevernier L, Gevaert B, Verbeke F, Wynendaele E, De Spiegeleer B. Related impurities in peptide medicines. *Journal of Pharmaceutical and Biomedical Analysis* 2014; 101: 2-30.
- [33] Baert B, Boonen J, Burvenich C, Roche N, Stillaert F, Blondeel P, Van Boxlaer J, De Spiegeleer B. A new discriminative criterion for the development of Franz diffusion tests for transdermal pharmaceuticals. *Journal of Pharmaceutical Sciences* 2010; 13: 218-230.
- [34] De Spiegeleer B, Baert B, Vergote V, Van Dorpe S. Development of system suitability tests for *in vitro* skin integrity control: impedance and capacitance. *The Eleventh International Perspectives in Percutaneous Penetration Conference, La Grande Motte, France, 2008*, pp. 43.
- [35] European Centre for Ecotoxicology and Toxicology of Chemicals (ECETOC). Monograph Report No 20 Percutaneous absorption. European Centre for Ecotoxicology and Toxicology of Chemicals, Brussels, 1993, pp. 90.
- [36] Veryser L, Taevernier L, Roche N, Peremans L, Burvenich C, De Spiegeleer B. Quantitative transdermal behavior of pellitorine from *Anacyclus pyrethrum* extract. *Phytomedicine* 2014; 21: 1801-1807.
- [37] Smart JD. Drug delivery using buccal-adhesive systems. *Advanced Drug Delivery Reviews* 1993; 11: 253-270.
- [38] Food and Drug Administration (FDA), Office of Regulatory Affairs (ORA). Laboratory procedure: Methods, method verification and validation, Appendix 1 Validation and Verification Guidance for Human Drug Analytical Methods (ORALAB.5.4.5), 2014, pp. 19.
- [39] European Directorate for the Quality of Medicines and Healthcare (EDQM). Qualification of Equipment, Annex 2: Qualification of GC Equipment, 2006, pp. 11.
- [40] http://www.fagg-afmps.be/nl/news/intrekking_geneesmiddelen_met_fusafungine_locabiotol.

BROADER INTERNATIONAL CONTEXT, RELEVANCE & FUTURE PERSPECTIVES

“The journey of a thousand miles begins with a single step”

*Laozi
(°604 BC - †531 BC, Chinese philosopher)*

BROADER INTERNATIONAL CONTEXT, RELEVANCE & FUTURE PERSPECTIVES

1. BROADER INTERNATIONAL CONTEXT AND RELEVANCE

Overall, this multidisciplinary work contributed to human health by means of an innovative blend of medicinal chemistry, philosophy, toxicology, pharmacokinetics and regulatory fields. This chapter will discuss our findings in a broader research field and highlight the relevance for improvement of human health, concluding with some interesting future research perspectives.

Cyclic depsipeptides as drug leads of the future

Within the pharmaceutical industry, peptides have certainly conquered their place next to traditional small molecules, with over a hundred peptides already authorised or currently used in (pre)clinical studies, displaying a wide array of interesting biological activities [1]. Today, nature still serves as an important factory for the discovery of new drug leads, with evolution as driving-force to create an enormous biodiversity of peptide-related compounds. Among these are also the cyclic depsipeptides, isolated from a variety of (micro)organisms, found all over the planet. As disparate as their presence is, are also their diverse chemical structures. Although in violation with many “drug-likeness” predictors and bioavailability rules, such as Lipinski’s “Rule of Five”, they offer a huge potential to the medicinal chemistry and pharmaceutical industry field for the development of new medicines. In recent years, technological advances have guided researchers towards further elucidation of disease targets, gaining insight in protein-protein or protein-DNA interactions. Naturally occurring cyclic peptides display a wide variety of unusual and potent biological activities, and they can be considered as a new generation drugs that are able to modify this large macromolecular target space, which lies beyond that of the enzyme active sites and receptors. Cyclic depsipeptides, and cyclic peptides in general, are characterised by larger molecular weights and more polar group counts, yet retaining membrane permeability, metabolic stability and oral bioavailability [2][3][4][5]. This was also demonstrated in this research for the cyclic depsipeptides (CDPs) beauvericin and enniatins. They are capable of crossing different important biological barrier systems and are able to reach blood circulation and accumulate to significant local skin, oromucosal and brain concentrations. CDPs should thus indeed be considered as promising drug leads of the future. Some CDPs have already proven their potential as medicines: daptomycin (Cubicin®) is celebrating its 10th anniversary on the European market as an agent against several bacterial infections, while

tacrolimus (Protopic® and Protopy®) has been authorised in 2002 by EMA as a therapy for atopic dermatitis. Another immunosuppressive compound is rapamycin (also known as sirolimus, Rapamune®), given as an oral solution or tablet and used to prevent the body from rejecting a newly transplanted kidney. In 2009, FDA has approved Istodax® (romidepsin), a histone deacetylase (HDAC) inhibitor, and granted it the orphan drug status for treatment of patients with cutaneous T-cell lymphoma [6][7].

Currently, several other compounds with CDP structure are being evaluated in (pre)clinical trials, either naturally occurring secondary metabolites or synthetic derivatives thereof [8]. Kahalalide F, for example, is tested for its anticancer activity against prostate tumours. Although the mode of action has not been completely determined, it is known to target lysosomes. More recently, it was also investigated as an anti-Leishmania lead with a new mode of action [8][9]. Another investigational anticancer agent is dehydrodidemnin B or plitidepsin (Aplidin®), at the moment undergoing clinical development for treatment of diverse haematological cancers [8][10].

However, CDPs may not only be useful in our fight against cancer, but also in the cure of infectious diseases, in particular when caused by antibiotic resistant bacteria. Antibiotic resistance is a growing concern in the 21st century, as we are currently running out of last resort antibiotics. Fortunately, CDPs like katanosin B and plusbacin A3 offer a promising and viable alternative in treatment of the feared MRSA (methicillin resistant *Staphylococcus aureus*) infection, due to blocking of transglycosylation and other steps prior in peptidoglycan cell wall synthesis via a mechanism different from that of other antibiotics such as vancomycin [11]. Recently, CDPs with quorum sensing inhibitory effects were also identified: solonomides, ngercheumicins, arthroamide and turnagainolide A [12][13][14]. It has been suggested that such an inhibition of virulence factor production and activity could also serve as new therapeutic approach to treat infections caused by antibiotic resistant pathogens [15].

Many more CDPs are still being discovered, and are awaiting investigation of their biological activities and potential drug use. CDP data is found widely scattered over literature, resulting in a daunting task for many researchers to get a complete overview and understanding of this group of natural peptides as a whole. Therefore, we presented a broad evaluation of different CDP structures and proposed a new straightforward classification system, whereby a total of 1348 naturally occurring CDPs were included. This tool allows natural product and peptide scientists to study the wide diversity in CDP structures, their chemical interrelationships and identification of existing and newly found CDPs. CDPs have a lot to offer to the medical world and they should not get lost in the huge pile of data available nowadays. Moreover, we would like to invite medicinal chemists, leading the drug discovery of the future, not to be fixated on conventional drug-likeness and bioavailability

rules, but rather encourage them to enter and further unravel the wonderful world of cyclic depsipeptides.

Mycotoxins: the importance of risk prioritization

We should, however, not only look at these CDPs from a pharmacological point of view as interesting bioactive lead compounds improving our health, but also from a toxicological point of view as hazards that are reasonably likely to cause harm or damage to humans, other organisms or the environment [16]. Indeed, the organisms that produce these CDPs are sometimes more closely in contact with us than we might originally suspect. They can, for example, be infecting our drinking water, feed and food [17][18][19], harbouring within the house dust mite, which are common on human skin and in house dusts [20], and can be widely distributed throughout the environment, *i.e.* present on plant debris, soil, wood, textiles and shower curtains [21][22][23].

Authorities seem overwhelmed by the idea that hundreds to thousands potentially toxic fungal metabolites exist. In their best efforts to control these hazards, multiple expert groups bend over the huge pile of research investigations available concerning mycotoxins and actions are taken to propose measures, guidelines, regulations and limits for these toxins. However, the struggle cannot be concealed: there should be no more mycotoxins identified, simply because we just cannot handle it...

On no account must we gloss over this by avoiding the discussion: we believe this is hardly the right approach. While recognizing the limited resources available and understanding that not every single compound can be fully investigated, it seems to us that careful risk prioritization is a justifiable way to appropriately handle the large amount of potentially toxic fungal metabolites. Risk assessment is therefore a valuable method that is widely integrated in today's society and applied in the fields of pharmaceutical health-care, ecological environment and the food industry, but also in other areas such as socio-economics and the financial world. Within the context of straightforward risk prioritization, clear definitions are indispensable. In this work, we highlighted the inconsistency, leading to confusion about what compounds should be called mycotoxin. Therefore, in an attempt to aid researchers as well as health authorities and tackle this problem, we have proposed a new mycotoxin definition in order to ease the risk prioritization process concerning mycotoxins in a global, objective and scientific way. While causing quite a stir, we certainly succeeded in bringing the topic under the attention. Although likely no consensus is reached (yet), the exact numbers are open for discussion and can be modified and supplemented, depending on the context, in order to achieve a future global risk prioritization plan for mycotoxins.

Beyond the oral exposure route

For some mycotoxins, there are already regulations available and specific limitations are set for food, feed and medicines, in order to guarantee the safety of the consumer and patient. However, for the cyclic depsipeptide mycotoxins beauvericin and enniatins, investigated in this work, no regulations are set (yet). Therefore, in 2010 the European Commission requested the European Food Safety Authority (EFSA) for their scientific opinion concerning the risk to human and animal health related to the presence of beauvericin and enniatins in food and feed.

EFSA is a European agency funded by the European Union that operates apart from the European legislative and its executive institutions and EU Member States. Following a series of food crises in the late 1990s, it was set up as an independent source of scientific advice and communication on risks associated with the food chain [24]. EFSA is working to keep food safe for the consumer, but it largely ignores other routes, such as respiration and dermal exposure, although it is widely recognised that inhalation of spore-borne toxins and skin contact with mould-infested substrates are also important sources of exposure [25]. In the case of industrial workers exposed to contaminated (natural) fruit waxes, grain dust and residential exposure to mycotoxin-containing dust of mouldy, water-damaged houses, these routes should thus certainly not be neglected.

There are, however, agencies responsible for occupational safety and health, *i.e.* Occupational Safety and Health Administration (OSHA) of the US Department of Labour and the European Agency for Safety and Health at Work (EU-OSHA). These set out minimum requirements and lay out fundamental principles, as well as the responsibilities of employers and employees, aiming to facilitate the implementation of legislation and providing a safe and healthy workplace.

These instances do recognize the intrinsic hazard and possible negative effects of moulds and their produced mycotoxins, which are an increasing risk at workplaces where workers may be exposed (*e.g.* bulk handling of agricultural foodstuffs (nuts, grain, maize, coffee), animal-feed production, brewing/malting, waste management, composting, food production, working with indoor moulds), and therefore give guidance information regarding recognition, prevention, detection and precautionary measures. It is, however, stated that the effects on human health are still controversial and more research has to be carried out on mycotoxins. Moreover, a detailed assessment of dermal and respiratory exposure to mycotoxins is currently lacking [26][27][28].

In this research, we tackled the missing risk assessment of the emerging mycotoxins beauvericin and enniatins via dermal exposure, by quantitatively investigating their transdermal kinetics. By demonstrating that these CDP mycotoxins are able to cross the skin barrier and reach the systemic circulation, we underlined that topical exposure should not be forgotten as an important route next to ingestion and respiration.

European regulatory recall of enniatin medicines

In the final chapter of this work, fusafungine medicines for topical treatment of upper respiratory tract infections were examined. These medicines contain a mixture of enniatins formulated in the known penetration-enhancing ethanol and isopropyl myristate, and, like many other traditional medicines, have been available on the market in several European countries for over 50 years [29][30][31][32]. Its summary of product characteristics (SmPC) explicitly mentioned no systemic absorption of the active compound; however, today newer techniques have become available and no data substantiating this claim could be found in literature, which made us question the validity of this statement. Therefore, the mucosal permeation of enniatins was investigated and it was concluded to question the use of fusafungine nasal-oral solutions in the treatment of innocent upper respiratory infections due to a negative risk-benefit ratio. It should be noted that only recently, approximately one year after our work was published, the European Medicines Agency (EMA) started to revoke the marketing authorizations of fusafungine medicines, through national procedures of the concerned member states, due to a negative risk-benefit balance [32]. This fusafungine case is thus a nice illustration that stresses the importance of continuous monitoring and quality-by-design risk assessment in both the pre- and post-market evaluation of topical products.

Here, the spatio-temporal character of any published data is also emphasised, meaning that nothing is truly fixed, but it is rather a snapshot taken at a certain moment in time, at a certain place in space. In 1966, fusafungine was first introduced as topical antibiotic spray for improvement of human health, and has been marketed so for 50 years, while now in 2016 it is recalled from the market due to the fact that current information indicates that it does more bad than good. Changes in technology, our growing knowledge, evolution of economic standards, increasing concern for human health, etc. are continuously forcing us to both expand and re-evaluate our research.

2. FUTURE PERSPECTIVES

As it was previously mentioned that CDPs display a large variety of biological activities, including quorum sensing inhibitory effects, one of the next burning questions is if these CDPs are not **quorum sensing molecules** themselves? Could they be produced by bacteria and/or fungi present as commensals in and on our human bodies, as many of these CDPs are isolated from *i.a.* *Bacillus*, *Fusarium* and *Alternaria* sp., which are organisms of the oral [33] and gut microbiome [34]? As such, these CDPs could possibly influence our microbiome, or even our own cells, and thereby have a continuous impact on our health status, especially since it was demonstrated in this thesis that they are able to cross different important human barriers.

A chemical classification system for cyclic depsipeptides was proposed, based on apparent chemical characteristics. However, a more objective and automatic system would be of additional value. While we initially investigated the use of traditional descriptors used for small molecules, these were found inadequate for clustering/classification of the very diverse members of the CDP family. A current lack of obvious, useful **chemical molecular descriptors** available for peptide (related) products stimulates future on-going research to propose new relevant, mathematically calculated descriptors for peptides, allowing clustering of these peptide compounds from a chemometric point of view.

In Chapter V of this work we investigated the quantitative transdermal kinetics of emerging mycotoxins BEA and ENNs, serving as model CDPs. We demonstrated that these are indeed capable of crossing the human skin barrier, leading us towards additional interesting research questions certainly worth investigating. In the skin, do CDPs BEA and ENNs use the transcellular or intercellular (paracellular) route or rather take advantage of shunt pathways, or in other words, what is their **transdermal mechanistic transportation pathway** and how can we map this? What is the affinity of BEA and ENNs for the different skin cell layers and cell types? Can we identify potential targets related to *e.g.* immune (*e.g.* mast and Langerhans cells) or malignant skin cells, which may reveal the potential use of these compounds as therapeutics in immunological skin diseases and skin cancers? In order to answer the first question, at this very moment, we are developing a method to determine BEA and ENNs in *ex vivo* human skin samples, using state-of-the-art MALDI-MS imaging. Recently, the scientific community has put forward imaging mass spectrometry techniques as a new powerful tool and as a viable alternative to microscopy and autoradiography, for mapping biological molecules in tissue samples [35][36][37][38][39][40], more specifically in skin tissue sections [41][42][43]. Our pilot data look at least promising and Figure 1 gives a flavour of what can be expected.

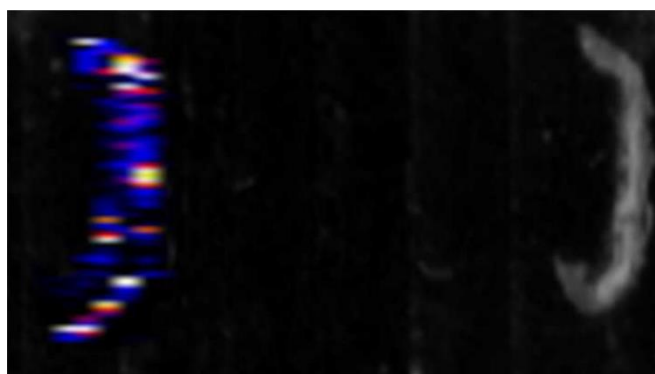


Figure 1: Cross section of BEA-spiked skin tissue. Left: MALDI-MS image showing the intensity distribution of BEA as sodium adduct at m/z 806. Right: non-analysed sample, real image in grey scale taken with CCD camera.

We previously demonstrated that BEA and ENNs are able to pass the BBB, with a very high influx rate into the brain and a significant distribution in the brain parenchyma. The time has come now to look

beyond their pharmacokinetics and further investigate their effects on a **pharmacodynamics** level. As their ability to enter the brain increases the possibility of these compounds to exert local CNS effects once present in the systemic circulation. Therefore, we are currently investigating the effects of BEA and ENNs on **different brain cell types**. Pilot experiments have been launched on BV-2 microglial cells. In the CNS, microglia are the principal resident immune cells, which undergo morphological and functional activation once they receive signals of damage, stress or other pathogenic danger-associated molecular patterns, giving rise to their name as “sensors of pathology”. Activated microglia will secrete a number of pro-inflammatory factors, such as tumour necrosis factor- α (TNF- α) and nitric oxide (NO), representing an acute inflammatory reaction that promotes neuronal recovery. A chronic neuroinflammatory reaction, however, leads to persistent microglial overactivation eventually causing slow neurodegeneration. Although still a controversial research area, microglial cells are said to underlie many neurological disorders or at least play a role in their pathology, *e.g.* Parkinson’s and Alzheimer’s disease, amyotrophic lateral sclerosis, multiple sclerosis, neuropathic pain and brain tumours [44][45][46][47]. Our group developed a protocol to evaluate the effect on immortalized BV-2 microglia on three levels: morphological, NO and cytokines (IL-6/TNF- α). Awaiting future experiments, a glimpse of the preliminary results already reveals a significant increase of TNF- α , and IL-6 to a lesser extent, compared to the controls, when exposed to submicromolar BEA concentrations. Also under investigation is the PC-12 rat pheochromocytoma cell line. PC-12 cells respond reversibly to neural growth factor (NGF) by induction of the neuronal phenotype and have been widely used as a model for neural differentiation [48][49]. At this very moment, the neurotrophic (induction of neurite outgrowth) and neurotoxic (inhibition of neurite outgrowth) properties of BEA and ENNs are being investigated.

In conclusion, our research is only the start of exploring the intriguing world of cyclic depsipeptides.

3. REFERENCES

- [1] Gevaert B, Stalmans S, Wynendaele E, Taevernier L, Bracke N, D'Hondt M, De Spiegeleer B. Exploration of the medicinal peptide space. *Protein & Peptide Letters* 2016; 23(4): 324-335.
- [2] Bockus AT, McEwen CM, Lokey RS. Form and function in cyclic peptide natural products: A pharmacokinetic perspective. *Curr Top Med Chem* 2013; 13: 821-836.
- [3] Yu X, Sun D. Macrocyclic drugs and synthetic methodologies towards macrocycles. *Molecules* 2013; 18: 6230-6268.
- [4] Driggers EM, Hale SP, Lee J, Terre, NK. The exploration of macrocycles for drug discovery — an underexploited structural class. *Nature Reviews Drug Discovery* 2008; 7: 608-624.
- [5] Luo B, Cheung HW, Subramanian A, Sharifnia T, Okamoto M, Yang X, Hinkle G, Boehm JS, Beroukhim R, Weir BA, Mermel C, Barbie DA, Awad T, Zhou X, Nguyen T, Piqani B, Li C, Golub TR, Meyerson M, Hacohen N, Hahn WC, Lander ES, Sabatini DM, Root DE. Highly parallel identification of essential genes in cancer cells. *Proc Natl Acad Sci USA* 2008; 105(51): 20380-20385.
- [6] <http://www.ema.europa.eu/> (consulted 19th of August, 2016)
- [7] <http://www.accessdata.fda.gov/scripts/cder/drugsatfda/index.cfm> (consulted 19th of August, 2016)
- [8] Newman DJ, Cragg GM. Marine natural products and related compounds in clinical and advanced preclinical trials. *J Nat Prod* 2004; 67:1216-1238.
- [9] Cruz LJ, Luque-Ortega JR, Rivas L, Albericio F. Kahalalide F, an antitumor depsipeptide in clinical trials, and its analogues as effective antileishmanial agents. *Mol Pharm* 2009; 6(3):813-824.
- [10] <https://www.pharmamar.com/2016/03/31/aplidin-shows-positive-results-in-pivotal-phase-iii-clinical-trial-for-multiple-myeloma/> (consulted 19th of August, 2016)
- [11] Maki,H, Miura K, Yamano, Y. Katanosin B and plusbacin A(3), inhibitors of peptidoglycan synthesis in methicillin-resistant *Staphylococcus aureus*. *Antimicrob Agents Chemother* 2001; 45(6): 1823-1827.
- [12] Mansson M, Nielsen A, Kjærulff L, Gotfredsen CH, Wietz M, Ingmer H, Gram L, Larsen TO. Inhibition of virulence gene expression in *Staphylococcus aureus* by novel depsipeptides from a marine Photobacterium. *Mar Drugs* 2011; 9: 2537-2552.
- [13] Igarashi Y, Yamamoto K, Fukuda T, Shojima A, Nakayama J, Carro L, Trujillo ME. Arthroamide, a cyclic depsipeptide with quorum sensing inhibitory activity from *Arthrobacter* sp. *J Nat Prod* 2015; 78(11): 2827-2831.
- [14] Kjaerulff L, Nielsen A, Mansson M, Gram L, Larsen TO, Ingmer H, Gotfredsen CH. Identification of four new agr quorum sensing-interfering cyclodepsipeptides from a marine Photobacterium. *Mar Drugs* 2013; 11(12): 5051-5062.
- [15] Rasko DA, Sperandio V. Anti-virulence strategies to combat bacteria-mediated disease. *Nat. Rev. Drug Discov* 2010; 9: 117-128.

- [16] Sperber WH. Hazard identification: from a quantitative to a qualitative approach. *Food Control* 2001; 12(4): 223-228.
- [17] Bober B, Lechowski Z, Bialczyk J. Determination of some cyanopeptides synthesized by *Woronichinia naegeliana* (Chroococcales, Cyanophyceae). *Phycological Research* 2011; 59: 286-294
- [18] Hautala H, Lamminmäki U, Spoo L, Nybom S, Meriluoto J, Vehniäinen M. Quantitative PCR detection and improved sample preparation of microcystin-producing *Anabaena*, *Microcystis* and *Planktothrix*. *Ecotoxicol Environ Saf* 2013; 87: 49-56.
- [19] Streit E, Schatzmayr G, Tassis P, Tzika E, Marin D, Taranu I, Tabuc C, Nicolau A, Aprodu I, Puel O, Oswald IP. Current situation of mycotoxin contamination and co-occurrence in animal feed - focus on Europe. *Toxins (Basel)* 2012; 4(10): 788-809.
- [20] Tang VH, Chang BJ, Srinivasan A, Mathaba LT, Harnett GB, Stewart GA. Skin-associated *Bacillus*, staphylococcal and micrococcal species from the house dust mite, *Dermatophagoides pteronyssinus* and bacteriolytic enzymes. *Exp Appl Acarol* 2013; 61(4): 431-447.
- [21] Hawkes M, Rennie R, Sand C, Vaudry W. *Aureobasidium pullulans* infection: fungemia in an infant and a review of human cases. *Diagn Microbiol Infect Dis* 2005; 51(3): 209-213.
- [22] Girardi LS, Malowitz R, Tortora GT, Spitzer ED. *Aureobasidium pullulans* septicemia. *Clin Infect Dis* 1993; 16(2): 338-339.
- [23] Miller JD, McMullin DR. Fungal secondary metabolites as harmful indoor air contaminants: 10 years on. *Appl Microbiol Biotechnol* 2014; 98(24): 9953-9966.
- [24] <https://www.efsa.europa.eu/en/aboutefsa> (consulted 20th of August, 2016)
- [25] Bennet JW, Klich M. Mycotoxins. *Clin Microbiol Rev* 2003; 16(3): 497-516.
- [26] <https://www.osha.gov/SLTC/molds/> (consulted 21th of August, 2016)
- [27] European Agency for Safety and Health at Work. European risk observatory report: Expert forecast on emerging biological risks related to occupational safety and health. 2007.
- [28] European Agency for Safety and Health at Work. European risk observatory report: Exposure to carcinogens and work-related cancer: A review of assessment methods. 2014.
- [29] Hamann KF, 1994, Fusafungin therapy of acute laryngitis – A phase IV study, *HNO*, 42(2): 113-118.
- [30] German-Fattal M. Fusafungine, an antimicrobial with anti-inflammatory properties in respiratory tract infections, *Clinical Drug Investigation* 2001, 21(9): 653-670.
- [31] Lund VJ, Grouin JM, Eccles R, Bouter C, Chabolle F. Efficacy of fusafungine in acute rhinopharyngitis: a pooled analysis, *Rhinology* 2004, 42(4): 207-212.
- [32] http://www.ema.europa.eu/ema/index.jsp?curl=pages/medicines/human/referrals/Fusafungine_for_omucosal_and_nasal_use/human_referral_prac_000054.jsp&mid=WC0b01ac05805c516f (consulted 21th of August, 2016).

- [33] Ghannoum MA, Jurevic RJ, Mukherjee PK, Cui F, Sikaroodi M, Naqvi A, Gillevet PM. Characterization of the oral fungal microbiome (mycobiome) in healthy individuals. *PLoS Pathog* 2010; 6(1): e1000713.
- [34] Samb-Ba B, Mazonot C, Gassama-Sow A, Dubourg G, Richet H, Hugon P, Lagier J, Raoult D, Fenollar F. MALDI-TOF Identification of the human gut microbiome in people with and without diarrhea in Senegal. *PLoS One* 2014; 9(5): e87419.
- [35] Chaurand P. Imaging mass spectrometry of thin tissue sections: a decade of collective efforts. *J Proteomics* 2012; 75(16): 4883-4892.
- [36] Seeley EH, Schwamborn K, Caprioli RM. Imaging of intact tissue sections: moving beyond the microscope. *J Biol Chem* 2011; 286(29): 25459-25466.
- [37] Nimesh S, Mohottalage S, Vincent R, Kumarathasan P. Current status and future perspectives of mass spectrometry imaging. *Int J Mol Sci* 2013; 14(6): 11277-11301.
- [38] Pirman DA, Yost RA. Quantitative tandem mass spectrometric imaging of endogenous acetyl-L-carnitine from piglet brain tissue using an internal standard. *Anal Chem* 2011; 83(22): 8575-8581.
- [39] Pirman DA, Reich RF, Kiss A, Heeren RM, Yost RA. Quantitative MALDI tandem mass spectrometric imaging of cocaine from brain tissue with a deuterated internal standard. *Anal Chem* 2013; 85(2): 1081-1089.
- [40] Hamm G, Bonnel D, Legouffe R, Pamelard F, Delbos JM, Bouzom F, Stauber J. Quantitative mass spectrometry imaging of propranolol and olanzapine using tissue extinction calculation as normalization factor. *J Proteomics* 2012; 75(16): 4952-4961.
- [41] Enthaler B, Trusch M, Fischer M, Rapp C, Pruns JK, Vietzke JP. MALDI imaging in human skin tissue sections: focus on various matrices and enzymes. *Anal Bioanal Chem* 2013; 405(4): 1159-1170.
- [42] Hart PJ, Francese S, Claude E, Woodroffe MN, Clench MR. MALDI-MS imaging of lipids in ex vivo human skin. *Anal Bioanal Chem* 2011; 401(1): 115-125.
- [43] Enthaler B, Pruns JK, Wessel S, Rapp C, Fischer M, Wittern KP. Improved sample preparation for MALDI-MSI of endogenous compounds in skin tissue sections and mapping of exogenous active compounds subsequent to ex-vivo skin penetration. *Anal Bioanal Chem* 2012; 402(3): 1159-1167.
- [44] Gertig U, Hanisch UK. Microglial diversity by responses and responders. *Front Cell Neurosci* 2014; 8: 101.
- [45] Kreutzberg GW. Microglia: a sensor for pathological events in the CNS. *Trends Neurosci* 1996; 19: 312-318.
- [46] Graeber MB, Streit WJ. Microglia: biology and pathology. *Acta Neuropathol* 2010; 119(1): 89-105.
- [47] Bozic I, Savic D, Jovanovic M, Bjelobaba I, Laketa D, Nedeljkovic N, Stojiljkovic M, Pekovic S, Lavrnja I. Low-dose ribavirin treatments attenuate neuroinflammatory activation of BV-2 cells by interfering with inducible nitric oxide synthase. *Analytical Cellular Pathology* 2015; 2015: 923614.

- [48] Westerink RHS, Ewing AG. The PC12 cell as model for neurosecretion. *Acta Physiol (Oxf)* 2008; 192(2): 273-285.
- [49] Greene LA, Tischler AS. Establishment of a noradrenergic clonal line of rat adrenal pheochromocytoma cells which respond to nerve growth factor. *Proc Natl Acad Sci USA* 1976; 73(7): 2424-2428

SUMMARY & GENERAL CONCLUSIONS

“One should use common words to say uncommon things”

*Arthur Schopenhauer
(°1788 - †1860, German philosopher)*

SUMMARY & GENERAL CONCLUSIONS

Chapter I, provides an introduction to the fascinating and chemically diverse world of the natural cyclic depsipeptides (CDPs), isolated from various organisms found all over the world and displaying a wide range of interesting biological activities. In **Chapter II** of this work, we exposed the need for a uniform and straightforward classification system for these cyclic depsipeptides. Up till now, there was only scattered data available in literature, making it hard for natural product and peptide scientists to get a clear overview of this group of compounds as a whole. Although some groups have published different reviews discussing this family of compounds, they all had rather limited scopes. As these CDPs display a wide variety of biological activities, their biomedical potential and potential uses should not get lost in the huge pile of data available today. Therefore, we proposed a chemical classification system, using apparent chemical characteristics based on different structures of 1348 naturally occurring CDPs. Moreover, it is demonstrated that traditional CDP subfamilies are named arbitrarily, which might be misleading from a chemical point of view. Overall, this tool allows researchers working in the field to get a better global understanding of the wide diversity in CDP structures, their chemical interrelationships and identification of existing and newly found CDPs. In this way, we contributed in a positive way to the appreciation of all efforts related to these CDPs and are looking forward to the new CDP (derived) molecules that will enrich our current array of medicinal treatments.

As indicated in this classification system, the cyclic hexadepsipeptides beauvericin (BEA) and enniatins (ENNs) are members of an important group of CDPs. Moreover, these compounds are currently increasingly investigated as emerging mycotoxins. However, as there are hundreds more fungal CDPs already identified, the question rose if these should not be considered as mycotoxins as well? A literature study revealed that a lot of information about mycotoxins is already available, but the scientific community is not unanimous about what should be called a mycotoxin, revealing a lack of consistency in the definition, leading to confusion. Therefore, in **Chapter III**, we presented a clear, unambiguous and quantitatively expressed 'mycotoxin' definition, which is of pivotal importance in risk assessment prioritization and allows more awareness of the now underestimated potential hazard of some of these fungal metabolites. Moreover, this definition was also applied to a set of fungal CDPs to determine whether or not these metabolites should be classified as mycotoxins, which ultimately indicated that for some CDPs, this should indeed be the case.

Further focus was laid on BEA and ENNs as model cyclic depsipeptide mycotoxins, as it was previously demonstrated in this thesis that exposure to these emerging mycotoxins should not be considered trivial, seen their possible biological effects and presence as common contaminants in

food and feed. Moreover, it was indicated that in order to better understand and appreciate their biological role, their kinetic interaction with some of the most important and relevant biological barrier systems should be investigated. This knowledge is not only required for the urgently needed global risk assessment, but also in the development of new therapeutics with similar CDP structure.

Therefore, in **Chapter IV** we developed a selective and high throughput bioanalytical method that empowered us to quantitatively determine BEA and ENNs in diverse biological matrices. The method was successfully validated, whereby special attention was paid to analytical stability and adsorption to glass. Both phenomena can possibly lead to loss of the analyte and increased analytical variability. We found that adsorption losses could be as high as 45%, an effect often overlooked by many researchers in the field but should certainly not be neglected.

The transdermal kinetics of BEA and ENNs were quantitatively determined in **Chapter V**, using excised human skin in an *ex vivo in vitro* Franz diffusion cell (FDC) set-up. It was demonstrated for the first time that these CDPs mycotoxins are able to cross the human skin barrier and reach the systemic circulation, with significant concentrations residing in the skin (μM range). The calculated maximal fluxes of these CDPs are in the range of testosterone and estradiol. Furthermore, the daily dermal exposure was calculated for both a typical occupational, as well as worst-case scenario, emphasising the importance of the transdermal path as route of exposure, next to ingestion and respiration.

In **Chapter VII**, the ENNs were viewed from a regulatory perspective, as they were first patented in 1953 under the international nonproprietary name of fusafungine. Formulated in the known penetration-enhancing excipients ethanol and isopropyl myristate, it is used in the topical treatment of upper respiratory tract infections. Like many other traditional medicines, it has been available on the market under different trade names in several European countries for over 50 years. Its summary of product characteristics (SmPC) explicitly mentioned no systemic absorption of the active compound. Today however, newer techniques have become available that made us question the validity of this statement. Moreover, we also investigated the variability in mucosal permeation of ENNs due to a difference in excipient composition. It was demonstrated that ENNs are in fact capable of permeating the oral mucosa. However, no significant different transmucosal permeability with varying excipient concentrations was detected. In this study, we already questioned the use of enniatin-based therapies in the treatment of innocent upper respiratory tract infections, because of the possibly negative benefit-risk ratio. It should be noted that very recently, for the same reasons, the European Medicines Agency (EMA) started to revoke the marketing authorizations of these fusafungine medicines. This fusafungine case is a seminal example to illustrate the importance of a careful evaluation of pre- and post-market data of topical products, stressing the importance of continuous monitoring and quality-by-design risk assessment.

After it was demonstrated that the CDP mycotoxins BEA and ENNs are able to reach the blood stream, in **Chapter VI** it was investigated in a quantitative manner if they could also cross the blood-brain-barrier and thus enter the CNS. By the use of *in vivo* mice studies, it was shown that BEA and ENNs are able to pass the BBB with a very high influx rate into the brain and a significant distribution in the brain parenchyma. This clearly indicates the possibility of these compounds to exert local CNS effects once present in the systemic circulation.

Finally, in the last chapter, we discussed the **broader international context, relevance and future perspectives** related to this research. Interesting new research questions were revealed and we lifted a tip of the veil of currently on-going research in our group. In the future, we want to focus more on the pharmacodynamics part and study for example the effects of BEA and ENNs in different brain cells. Moreover, we are also developing a MALDI-MS imaging method to map more in detail the transdermal transportation of these compounds in the different human skin layers, which can help in elucidating the mechanistic pathway.

Overall, this research contributed to the urgently needed global risk assessment of the emerging mycotoxins BEA and ENNs by quantitatively investigating their skin, mucosal and BBB kinetics, knowledge that is also highly appreciated in the drug development of new medicines with similar CDPs structures.

SAMENVATTING & ALGEMENE CONCLUSIES

*“Weten wat men weet en weten wat men niet weet,
dat is het ware weten.”*

*Confucius
(°551 BC - †479 BC, Chinees filosoof)*

SAMENVATTING & ALGEMENE CONCLUSIES

Hoofdstuk I, geeft een inleiding tot de wondere wereld van de chemisch erg diverse cyclische depsipeptiden (CDPs). Deze moleculen worden gesynthetiseerd door een enorme variëteit aan in de natuur voorkomende organismen, die men kan vinden in alle uithoeken van de wereld. CDPs vertonen tal van biologische activiteiten, die interessante mogelijkheden bieden voor het ontwikkelen van nieuwe geneesmiddelen. In **Hoofdstuk II** van dit werk, toonden we aan dat er nood is aan een uniforme en eenduidige classificatiemethode voor CDPs. Tot op heden, was alle CDP-data echter verspreid over de literatuur, wat het voor onderzoekers in het veld erg moeilijk maakt om een duidelijk beeld te krijgen van deze groep componenten in zijn geheel. Bovendien handelen re reviews die al gepubliceerd zijn, slechts over een bepaald en nauw gebied. Gezien deze CDPs erg interessante biologische activiteiten vertonen mag hun biomedisch potentiaal dus niet verloren gaan in de gigantische berg aan data die vandaag de dag beschikbaar is. Daarom hebben wij een chemisch classificatiesysteem voor CDPs voorgesteld, dat gebaseerd is op duidelijk structurele aspecten van 1348 verschillende CDPs. Daarnaast werd ook aangetoond dat nomenclatuur van traditionele CDP subfamilies zeer arbitrair gebeurt, wat misleidend kan zijn vanuit chemisch oogpunt. Deze classificatiemethode laat wetenschappers toe een globaal beeld te krijgen van de grote diversiteit aan CDP structuren, de chemische onderlinge verbanden beter te begrijpen en kan hen helpen bij het identificeren van zowel bestaande, als nieuw ontdekte CDPs. Op deze manier heeft dit onderzoek op een positieve manier bijgedragen tot de appreciatie van de CDP-familie, en wordt verder uitgekeken naar nieuwe CDP (afgeleide) moleculen, die onze huidig repertorium aan geneesmiddelen kunnen verrijken.

Zoals werd aangetoond door middel van dit classificatiesysteem, maken de cyclische hexadepsipeptiden beauvericin (BEA) en enniatins (ENNs) deel uit van een belangrijke klasse aan CDPs. Daarenboven worden zij tegenwoordig naar voren geschoven als opkomende (*'emerging'*) mycotoxines. Nochtans zijn er op vandaag nog veel meer CDPs die door schimmels worden aangemaakt geïdentificeerd, moeten deze dan ook niet als mycotoxines worden beschouwd? Een literatuurstudie heeft aangetoond dat er tegenwoordig heel wat informatie over mycotoxines beschikbaar is, maar dat niet iedereen het helemaal eens is over wat men al dan niet een mycotoxine noemt. Er is dus nood aan een duidelijke en consistente mycotoxine-definitie. Daarom hebben wij in **Hoofdstuk III** een ondubbelzinnige en kwantitatieve definitie voorgesteld, wat van centraal belang binnen risicoanalyse. Op deze manier werd ook de bewustwording gestimuleerd betreffende het soms nog onderschatte gevaar dat deze moleculen met zich mee kunnen brengen. Tot slot werd een

selectie aan fungale CDPs afgetoetst aan deze definitie en kon besloten worden dat sommige CDPs inderdaad als mycotoxines beschouwd kunnen worden.

Verder werd de focus gelegd op BEA en ENNs als model CDP mycotoxines, waarbij eerder in deze thesis al werd aangetoond dat blootstelling aan deze opkomende mycotoxines niet als onbelangrijk beschouwd mag worden, gezien hun mogelijke biologische effecten en hun voorkomen als contaminanten in ons voedsel. Om hun biologische rol en invloed beter te begrijpen en waarderen, werd hun kinetische interactie met enkele van de belangrijkste biologische barrières in het menselijk lichaam bestudeerd. Deze kennis is niet alleen belangrijk bij het inschatten van hun globale risico, maar ook bij de ontwikkeling van nieuwe geneesmiddelen met gelijkaardige CDP structuur.

Daarom ontwikkelden we in **Hoofdstuk IV** een selectieve en '*high throughput*' bioanalytische methode die ons toelaat BEA en ENNs kwantitatief te bepalen in diverse biologische matrices. Deze methode werd succesvol gevalideerd, waarbij eveneens de analytische stabiliteit en adsorptie aan glas onderzocht werd. Deze twee fenomenen kunnen namelijk leiden tot verlies van de analyte en zo een hoge analytische variabiliteit tot gevolg hebben. Zo werd aangetoond dat adsorptieverliezen kunnen oplopen tot 45%, een effect waar vele onderzoekers vaak geen aandacht aan besteden, maar dat zeker niet genegeerd zou mogen worden.

De transdermale kinetiek van BEA en ENNs werd kwantitatief bepaald in **Hoofdstuk V**, gebruik makende van *ex vivo in vivo* humane huid in een Franz diffusie cel (FDC) set-up. Voor de eerste keer werd aangetoond dat deze CDP mycotoxines de humane huid barrière kunnen doorkruisen en de systemische circulatie kunnen bereiken, met significante concentraties in de huid zelf (μM gebied). De berekende maximale fluxen van deze CDPs liggen in de range van testosteron en estradiol. Verder, werd de dagelijkse dermale blootstelling berekend voor zowel een typische beroeps-, als worst-case situatie. Hierdoor benadrukten we het belang van de transdermale weg als blootstellingsroute, naast die van orale inname en inhalatie.

In **Hoofdstuk VII**, werden de ENNs vanuit een regulatorisch perspectief benaderd. Deze werden namelijk voor het eerst gepatenteerd in 1953 met als '*international nonproprietary name*' fusafungine. Geformuleerd in de gekende penetratiebevorderende excipiënten ethanol en isopropylmyristaat, werd het gebruikt in de topische behandeling van infecties van de bovenste luchtwegen. Zoals zo vele andere traditionele geneesmiddelen, was het meer dan 50 jaar verkrijgbaar in verschillende Europese landen. De samenvatting van de kenmerken van het product (SKP) vermeldde expliciet dat de actieve component niet kon worden aangetoond in het plasma, echter vandaag de dag zijn er echter nieuwe technieken beschikbaar die deze claim in vraag stellen. Daarenboven onderzochten we eveneens de variabiliteit in mucosale permeatie van ENNs bij een verschil in samenstelling van de hulpstoffen. Er werd aangetoond dat ENNs wel degelijk in staat zijn doorheen de orale mucosa te dringen. Echter, er werd geen significant verschil in transmucosale permeabiliteit vastgesteld bij een

verschil in excipiënt concentratie. Door de resultaten van deze studie werd het gebruik van enniatin-gebaseerde behandelingen van onschuldige infecties van de bovenste luchtwegen in vraag gesteld, door de mogelijk negatieve risico-baten verhouding. Er dient opgemerkt te worden dat, om diezelfde reden, het Europees Geneesmiddelen Agentschap (EMA) heel recent de terugtrekking van fusafungine bevattende geneesmiddelen heeft bekrachtigd. Het fusafungine verhaal is een kritisch voorbeeld dat het belang aantoont van een voorzichtige evaluatie van pre- en post marketing data van topische producten en van een continue monitoring en *'quality-by-design'* risicoanalyse.

Nadat werd aangetoond dat de CDP mycotoxines BEA en ENNs in staat zijn om de bloedbaan te bereiken, werd in **Hoofdstuk VI** kwantitatief onderzocht of ze eveneens de bloedhersenbarrière (BHB) kunnen doorkruisen en dus het centraal zenuwstelsel (CZS) bereiken. Aan de hand van *in vivo* muisstudies, werd vastgesteld dat BEA en ENNs de BHB doorkruisen met een hoge influx snelheid en een significante distributie in het hersenparenchym. Dit vergroot de mogelijkheid dat deze componenten lokale effecten kunnen uitoefenen in het CZS, eens ze de systemische circulatie bereiken.

Tot slot werd in het laatste hoofdstuk de **breder internationale context, de relevantie en de toekomstperspectieven** van dit onderzoek toegelicht. Interessante nieuwe onderzoeksvragen werden vooropgesteld en we lichtten reeds een tipje van de sluier op omtrent het onderzoek dat momenteel verder gevoerd wordt binnen onze groep. In de toekomst, willen we ons meer toespitsen op het farmacodynamische aspect en bijvoorbeeld de effecten van BEA en ENNs in de verschillende hersencellen bestuderen. Daarnaast, wordt op dit ogenblik ook een MALDI-MS beeldvormingsmethode ontwikkeld om nog meer in detail de transdermale route van deze moleculen in de verschillende lagen van de huid in kaart te kunnen brengen.

We kunnen besluiten dat dit onderzoek heeft bijgedragen tot de globale risicoanalyse van deze *'emerging'* mycotoxines BEA en ENNs, door kwantitatief hun huid, mucosa en BHB kinetiek te onderzoeken. Deze kennis is zeker ook van belang binnen het gebied van de geneesmiddelenontwikkeling, waarbij men zoek gaat naar nieuwe geneesmiddelen met gelijkaardige CDP structuur.

CURRICULUM VITAE

"There is no real ending. It's just the place where you stop the story."

*Frank Herbert
(°1920 - †1986, American science fiction writer)*

CURRICULUM VITAE**LIEN TAEVERNIER****PERSONALIA**

Surname: Taevernier
First name: Lien
Nationality: Belgian
Place & date of birth: Waregem
February 17th, 1989
Private address: Gentse Heerweg 41
8790 Waregem
Professional address: Drug Quality & Registration (DruQuaR) laboratory
Department of Pharmaceutical Analysis
Faculty of Pharmaceutical Sciences
Ghent University
Ottergemsesteenweg 460
9000 Ghent
Phone: (+32) 9 264 81 01
E-mail: Lien.Taevernier@UGent.be
URL: <http://www.ugent.be/fw/en/research/pharmaceutical-analysis/druquar>

EDUCATION

2001 – 2007: Latin-Sciences at OLVH Institute (Waregem)
2007 – 2010: Bachelor of Pharmaceutical Sciences at Ghent University
2010 – 2012: Master of Science in Drug Development at Ghent University
2012: Multivariate Data Analysis at Ghent University
Design of Experiments at Ghent University
2013: Doctoral Schools: Leadership Foundation Course at Ghent University
2014: Doctoral Schools: Introduction Day new PhD students at Ghent University
2015: Economic Evaluations of Medical Interventions (Leuven)
2016: Doctoral Schools: Job Market for Young Researchers at Ghent University

PROFESSIONAL EXPERIENCE

- August 2012 – present: Staff scientist at DruQuaR:
- Research in drug development
 - Supporting bachelor/master theses and practical courses
 - Servicing activities and analyses
- September 2015 – present: Quality Assurance manager at DruQuaR, Ghent University

PUBLICATIONS IN JOURNALS WITH PEER REVIEW

PUBLISHED AND/OR ACCEPTED

Boonen J, Malysheva S, Taeavernier L, Diana Di Mavungu J, De Saeger S, De Spiegeleer B. Human skin penetration of selected model mycotoxins. *Toxicology*. 2012; **301**: 21-32, doi.org/10.1016/j.tox.2012.06.012.

De Spiegeleer B, Boonen J, Veryser L, Taeavernier L, Malysheva S, Diana Di Mavungu J, De Saeger S, Roche N, Blondeel P. Skin penetration enhancing properties of the plant N-alkylamide spilanthol. *Journal of Ethnopharmacology*. 2013; **148**: 117-125, doi.org/10.1016/j.jep.2013.03.076.

Boonen J, Veryser L, Taeavernier L, Roche N, Peremans K, Burvenich C, De Spiegeleer B. Risk evaluation of impurities in topical excipients: the acetol case. *Journal of Pharmaceutical Analysis*. 2014; **4**: 303-315, doi.org/10.1016/j.jpha.2013.12.006.

D'Hondt M, Fedorova M, Peng C-Y, Gevaert B, Taeavernier L, Hoffmann Ralf, De Spiegeleer B. Dry heat forced degradation of busserelin peptide: kinetics and degradant profiling. *International Journal of Pharmaceutics*. 2014; **467**: 48-59, doi.org/10.1016/j.ijpharm.2014.03.043.

D'Hondt M, Bracke N, Taeavernier L, Gevaert B, Verbeke F, Wynendaele E, De Spiegeleer B. Related impurities in peptide medicines. *Journal of Pharmaceutical and Biomedical Analysis*. 2014; **101**: 2-30, doi.org/10.1016/j.jpba.2014.06.012.

Taeavernier L, Veryser L, Vandercruyssen K, D'Hondt M, Vansteelandt S, De Saeger S, De Spiegeleer B. UHPLC-MS/MS method for the determination of the cyclic depsipeptide mycotoxins beauvericin and enniatins in in-vitro transdermal experiments. *Journal of Pharmaceutical and Biomedical Analysis*. 2014; **100**: 50-57, doi.org/10.1016/j.jpba.2014.07.021.

Veryser L, Taeavernier L, Roche N, Peremans K, Burvenich C, De Spiegeleer B. Quantitative transdermal behavior of pellitorine from *Anacyclus pyrethrum*. *Phytomedicine*. 2014; **21**: 1801-1807, doi.org/10.1016/j.phymed.2014.08.015.

Veryser L, Wynendaele E, Taeavernier L, Verbeke F, Joshi T, Takte P, De Spiegeleer. N-alkylamides: from plant to brain. *Journal of Functional Foods in Health and Disease*. 2014; **4**: 264-275.

Taevernier L, Wynendaele E, D'Hondt M, De Spiegeleer B. Analytical quality-by-design approach for sample treatment of albumin containing solutions. *Journal of Pharmaceutical Analysis*. 2015; **5**: 27-32, doi.org/10.1016/j.jpha.2014.06.001.

Taevernier L, Detroyer S, Veryser L, De Spiegeleer B. Enniatin-containing solutions for oromucosal use: quality-by-design ex-vivo transmucosal risk assessment of composition variability. *International Journal of Pharmaceutics*. 2015; **491**: 144-151, doi.org/10.1016/j.ijpharm.2015.06.029.

Veryser L, Taevernier L, Roche N, Blondeel P, De Spiegeleer B. Implementation of a single quad MS detector in high-throughput transdermal research of plant extracts. *Journal of Pharmaceutical and Biomedical Analysis*. 2015; **115**: 594-602, doi.org/10.1016/j.jpba.2015.08.016.

Veryser L, Boonen J, Taevernier L, Guillaume J, Risseeuw M, Hussain Shah SN, Roche N, Van Calenberg S, De Spiegeleer B. The influence of the acyl chain on the transdermal penetration enhancing effect of synthetic phytoceramides. *Skin Pharmacology and Physiology*. 2015; **28**: 124-136, doi.org/10.1159/000365730.

Taevernier L, Veryser L, Roche N, Peremans K, Burvenich C, Delesalle C, De Spiegeleer B. Human skin permeation of emerging mycotoxins (beauvericin and enniatins). *Journal of Exposure Science and Environmental Epidemiology*. 2016; **26**: 277-287, doi.org/10.1038/jes.2015.10.

Taevernier L, Wynendaele E, De Vreese L, Burvenich C, De Spiegeleer B. The mycotoxin definition reconsidered towards fungal cyclic depsipeptides. *Journal of Environmental Science and Health, Part C*. 2016; **34**: 114-135, doi.org/10.1080/10590501.2016.1164561.

Taevernier L, Bracke N, Veryser L, Wynendaele E, Gevaert B, Peremans K, De Spiegeleer, B. Blood-brain barrier transport kinetics of the cyclic depsipeptide mycotoxins beauvericin and enniatins. *Toxicology Letters*. 2016; **258**: 175-184, doi: 10.1016/j.toxlet.2016.06.1741.

Desmet E, Bracke S, Forier K, Taevernier L, Stuart M, De Spiegeleer B, Raemdonck K, Van Gele M, Lambert J. An elastic liposomal formulation for RNAi-based topical treatment of skin disorders: proof-of-concept in the treatment of psoriasis. *International Journal of Pharmaceutics*. 2016; **500**: 268-274, doi.org/10.1016/j.ijpharm.2016.01.042.

De Spiegeleer, Wynendaele E, Bracke N, Veryser L, Taevernier L, Degroote A, Stalmans S. Regulatory development of geriatric medicines: To GIP or not to GIP? *Ageing Research Reviews*. 2016; **27**: 23-36, doi.org/10.1016/j.arr.2016.02.004.

Gevaert B, Stalmans S, Wynendaele E, Taevernier L, Bracke N, D'Hondt M, De Spiegeleer B. Exploration of the medicinal peptide space. *Protein & Peptide Letters*. 2016; **23**: 324-335, doi.org/10.2174/0929866523666160215162326.

Haspelslagh M, Taevernier L, Maes A, Vlaminck L, De Spiegeleer B, Croubels S, Martens A. Topical distribution of acyclovir in normal equine skin and equine sarcoids: an in vitro study. *The Veterinary Journal*. 2016; **106**: 107-111, doi.org/10.1016/j.rvsc.2016.03.021.

Veryser L, Taevernier L, Joshi T, Tatke P, Wynendaele E, Bracke N, Stalmans S, Peremans K, Burvenich C, Risseeuw M, De Spiegeleer B. Mucosal and blood-brain barrier transport kinetics of the plant N-alkylamide spilanthol using in vitro and in vivo models. *BMC Complementary and Alternative Medicine*. 2016; **16**:177, doi.org/10.1186/s12906-016-1159-0.

Veryser L, Bracke N, Wynendaele E, Joshi T, Tatke P, Taevernier L, De Spiegeleer B. Quantitative in vitro and in vivo evaluation of intestinal and blood-brain barrier transport kinetics of the plant N-alkylamide pellitorine. *BioMed Research International*. 2016; **2016**: 5497402, doi.org/10.1155/2016/5497402.

SUBMITTED/IN PREPARATION

Taevernier L, Wynendaele E, Gevaert B, De Spiegeleer B. Chemical classification of cyclic depsipeptides. **Submitted (under revision at Current Protein and Peptide Science).**

De Spiegeleer B, Taevernier L, Gevaert B, Janssens Y, Wynendaele E, Verbeke F, Peremans K. Interaction of beauvericin and enniatins with brain cells. **In preparation.**

PRESENTATIONS AT (INTER)NATIONAL CONFERENCES

Boonen J, Veryser L, Taevernier L, Roche N, De Spiegeleer B. Transdermal penetration enhancing effect of the N-alkylamide spilanthol. Scientific Afternoon of the Faculty of Pharmaceutical Sciences, Ghent University, 16 May 2012, Ghent, Belgium.

Poster presentation

De Spiegeleer B, Boonen J, Veryser L, Taevernier L, Malysheva S, Diana Di Mavungu J, De Saeger S. Skin penetration enhancing effect of the plant N-alkylamide spilanthol. Stratum Corneum VII conference, 10 – 12 September 2012, Cardiff, Wales, UK.

Poster presentation

Veryser L, Wynendaele E, Taevernier L, Verbeke F, Joshi T, Tatke P, De Spiegeleer B. Are plant N-alkylamide cosmenutriceuticals also active in the central nervous system? 15th International Conference of Functional Food Center, 10 – 14 May 2014, Regensburg, Germany.

Oral presentation

Taevernier L, Vansteelandt S, De Spiegeleer B. Adsorption of cyclic depsipeptide mycotoxins to glass. Drug Analysis and Pharmaceutical and Biomedical Analysis Symposium, 22 – 25 June 2014, Liège, Belgium.

Poster presentation

Taevernier L, Veryser L, Roche N, De Spiegeleer B. Human skin kinetics of cyclic depsipeptide mycotoxins. 33rd European Peptide Symposium, 31 August – 5 September 2014, Sofia, Bulgaria.

Poster presentation

Stalmans S, Wynendaele E, Bracke N, Veryser L, Taevernier L, De Spiegeleer B. Euthanasia for geriatric medicines? 5th Studenten Onderzoekssymposium (SOS) of the Faculty of Pharmaceutical Sciences, Ghent University, 4 May 2015, Ghent, Belgium.

Poster presentation

Taevernier L, Detroyer S, Veryser L, De Spiegeleer B. Quality-by-design risk assessment of topical formulation variability. 26th International Pharmaceutical and Biomedical Analysis Symposium, 5 – 9 July 2015, Tbilisi, Georgia.

Poster presentation

Veryser L, Taevernier L, Roche N, De Spiegeleer B. The use of UHPLC coupled to single quad MS detection in Franz diffusion cell methodologies. 26th International Pharmaceutical and Biomedical Analysis Symposium, 5 – 9 July 2015, Tbilisi, Georgia.

Poster presentation

Taevernier L, Veryser L, Wynendaele E, De Spiegeleer B. Ex-vivo in-vitro skin/mucosal permeability kinetics: Tool in modeling and product classification. 6th Studenten Onderzoekssymposium (SOS) of the Faculty of Pharmaceutical Sciences, Ghent University, 26 April 2016, Ghent, Belgium.

Poster presentation

Taevernier L, Bracke N, Veryser L, Wynendaele E, De Spiegeleer B. Do cyclic depsipeptide mycotoxins beauvericin and enniatins cross the blood-brain barrier? 9th World Mycotoxin Forum and 14th IUPAC International Symposium on Mycotoxins, 6 – 9 June 2016, Winnipeg, Canada.

Poster presentation

